MECHANISMS BY WHICH SLE-ASSOCIATED GENETIC VARIANTS CONTRIBUTE TO SLE PATHOGENESIS

EDITED BY: José Carlos Crispín and Laurence Morel
PUBLISHED IN: Frontiers in Immunology

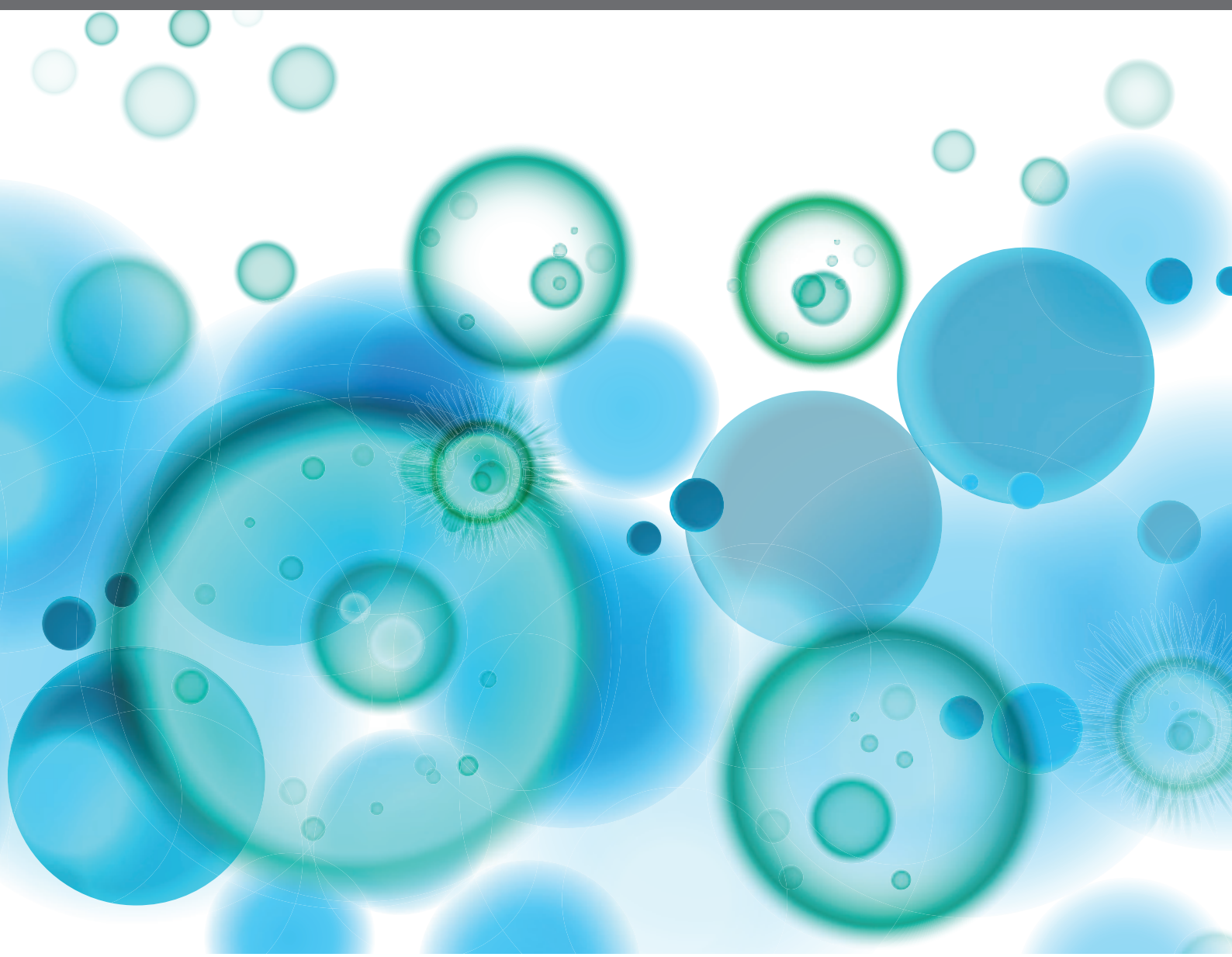

frontiers Research Topics

frontiers

ISSN 1664-8714
ISBN 978-2-88963-370-8
DOI 10.3389/978-2-88963-370-8

About Frontiers

Frontiers is more than just an open-access publisher of scholarly articles: it is a pioneering approach to the world of academia, radically improving the way scholarly research is managed. The grand vision of Frontiers is a world where all people have an equal opportunity to seek, share and generate knowledge. Frontiers provides immediate and permanent online open access to all its publications, but this alone is not enough to realize our grand goals.

Frontiers Journal Series

The Frontiers Journal Series is a multi-tier and interdisciplinary set of open-access, online journals, promising a paradigm shift from the current review, selection and dissemination processes in academic publishing. All Frontiers journals are driven by researchers for researchers; therefore, they constitute a service to the scholarly community. At the same time, the Frontiers Journal Series operates on a revolutionary invention, the tiered publishing system, initially addressing specific communities of scholars, and gradually climbing up to broader public understanding, thus serving the interests of the lay society, too.

Dedication to Quality

Each Frontiers article is a landmark of the highest quality, thanks to genuinely collaborative interactions between authors and review editors, who include some of the world's best academicians. Research must be certified by peers before entering a stream of knowledge that may eventually reach the public - and shape society; therefore, Frontiers only applies the most rigorous and unbiased reviews.
Frontiers revolutionizes research publishing by freely delivering the most outstanding research, evaluated with no bias from both the academic and social point of view. By applying the most advanced information technologies, Frontiers is catapulting scholarly publishing into a new generation.

What are Frontiers Research Topics?

Frontiers Research Topics are very popular trademarks of the Frontiers Journals Series: they are collections of at least ten articles, all centered on a particular subject. With their unique mix of varied contributions from Original Research to Review Articles, Frontiers Research Topics unify the most influential researchers, the latest key findings and historical advances in a hot research area! Find out more on how to host your own Frontiers Research Topic or contribute to one as an author by contacting the Frontiers Editorial Office: researchtopics@frontiersin.org

MECHANISMS BY WHICH SLE-ASSOCIATED GENETIC VARIANTS CONTRIBUTE TO SLE PATHOGENESIS

Topic Editors:
José Carlos Crispín, Instituto Nacional de Ciencias Médicas y Nutrición Salvador Zubirán (INCMNSZ) and Tecnológico de Monterrey, Mexico
Laurence Morel, University of Florida, United States

Citation: Crispín, J. C., Morel, L., eds. (2020). Mechanisms by Which SLE-Associated Genetic Variants Contribute to SLE Pathogenesis. Lausanne: Frontiers Media SA. doi: 10.3389/978-2-88963-370-8

Table of Contents

frontiers in Immunology

EDITORIAL
published: 03 December 2019
doi: 10.3389/fimmu.2019.02808

Editorial: Mechanisms by Which SLE-Associated Genetic Variants Contribute to SLE Pathogenesis

José C. Crispín[1,2]* *and Laurence Morel*[3]*

[1] Department of Immunology and Rheumatology, Instituto Nacional de Ciencias Médicas y Nutrición Salvador Zubirán, Mexico City, Mexico, [2] Tecnológico de Monterrey, Escuela de Medicina y Ciencias de la Salud, Mexico City, Mexico, [3] Department of Pathology, Immunology, and Laboratory Medicine, University of Florida, Gainesville, FL, United States

Keywords: lupus (SLE), SNP, genetic variant, pathogenesis, autoimmunity

Editorial on the Research Topic

Mechanisms by Which SLE-Associated Genetic Variants Contribute to SLE Pathogenesis

Systemic lupus erythematosus (SLE) is a complex disease strongly influenced by genetic factors (1). Through their effects on gene expression and function, genetic variants may modify disease manifestation and outcomes by facilitating certain cellular behaviors (2). This Research Topic brings together original and review papers that explore how individual genes and their variants may affect SLE development, pathogenesis, and therapeutics. Alperin et al. present a review article that describes monogenic syndromes that share clinical and pathological similarities with SLE. The extreme phenotypes associated with the genetic deficiencies that cause these syndromes demonstrate the role of individual genes in the immune system. Martínez-Bueno and Alarcón-Riquelme present a bioinformatics imputation analysis that identifies 98 candidate genes that may contribute to SLE through rare variants that cannot be detected in conventional genetic association studies.

Transcription of the long non-coding RNA Linc00513 is shown by Xue et al. to be affected by an SLE-associated single-nucleotide polymorphism (SNP). Cells bearing the risk allele have increased levels of Linc00513 because the SLE-associated variant promotes its transcription in response to type I IFN. This lncRNA facilitates the expression of a relatively large number of IFN-induced genes. Therefore, the presence of the risk allele could amplify the signal conveyed by type I IFN.

The paper by Ju et al. describes a previously unknown variant of the *Nasp* gene identified as a pathogenic element located in the *Slec1* sublocus of the NZM2410 mouse (3, 4). The lupus-associated variant modified the sNASP protein resulting in an increased capacity to bind histones. Importantly, in the presence of the lpr mutation (Fas^{lpr}), the risk variant of *Nasp* increased lymphoproliferation and tissue inflammation (lung and kidney), suggesting that it may possess a pathogenic capacity.

Gorman et al. present a thorough analysis of the functional effects of the $TYK2^{P1104A}$ variant that protects against multiple autoimmune diseases, including SLE (5). They show that healthy humans carrying the protective allele have a lower number of circulating follicular helper T cells (T_{FH}) and switched memory B cells. Moreover, the amino acid substitution decreased the response of CD4 T cells to IL-12, IL-23, and IFN-α, confirming that it represents a hypomorphic allele. *In vivo*, the $Tyk2^{P1104A}$ variant protected mice from experimental autoimmune encephalomyelitis (EAE), although it did not show any effects in two models of murine lupus-like disease.

Molineros et al. conducted a detailed study that identified a SNP (rs11631591) that facilitates binding of hnRNP-K. Because it is located in an enhancer region, the risk allele increases the expression of *RASGRP1* and, consequently, MAP kinase signaling. Calcium/Calmodulin Kinase IV

OPEN ACCESS

Edited and reviewed by:
Betty Diamond,
Feinstein Institute for Medical Research, United States

***Correspondence:**
José C. Crispín
carlos.crispina@incmnsz.mx
Laurence Morel
morel@ufl.edu

Specialty section:
This article was submitted to Autoimmune and Autoinflammatory Disorders, a section of the journal Frontiers in Immunology

Received: *04 November 2019*
Accepted: *15 November 2019*
Published: *03 December 2019*

Citation:
Crispín JC and Morel L (2019) Editorial: Mechanisms by Which SLE-Associated Genetic Variants Contribute to SLE Pathogenesis. Front. Immunol. 10:2808. doi: 10.3389/fimmu.2019.02808

(CaMK4) is a serine/threonine kinase that regulates cell signaling and gene expression in a variety of cells that includes T cells, podocytes, and mesangial cells. Expression levels and activity of CaMK4 are abnormally increased in T cells from patients with SLE (6) and in renal cells in a variety of immune and non-immune conditions (7). The review by Ferretti et al. describes the role of CaMK4 in human disease and mouse models and discusses strategies to block the activity of this kinase as interesting and novel therapies.

Two of the papers explore the effects that sex, either through chromosomal or hormonal differences, imposes on gene expression and function (Harris et al.) and disease phenotype (Savelli et al.). Finally, the review by Vukelic et al. discusses novel therapeutic strategies in SLE.

The papers included in this Research Topic illustrate the complex relationship between genetic variants, environmental stimuli, and immune function, and offer a glance into how individual variants may affect the behavior of specific types of cells in manners that may promote or avoid autoimmune and/or inflammatory organ damage. We believe that understanding how genetic variants affect immune function in the steady state and in the setting of chronic inflammation will improve our capacity to predict disease phenotypes, including prognosis and response to therapy of individual patients.

AUTHOR CONTRIBUTIONS

JC and LM: conceptualization and writing.

FUNDING

LM supported by a grant from the NIH RO1 AI045050.

REFERENCES

1. Tsokos GC. Systemic lupus erythematosus. *N Engl J Med.* (2011) 365:2110–21. doi: 10.1056/NEJMra1100359
2. Rosetti F, de la Cruz A, Crispín JC. Gene-function studies in systemic lupus erythematosus. *Curr Opin Rheumatol.* (2019) 31:185–92. doi: 10.1097/BOR.0000000000000572
3. Morel L, Croker BP, Blenman KR, Mohan C, Huang G, Gilkeson G, et al. Genetic reconstitution of systemic lupus erythematosus immunopathology with polycongenic murine strains. *Proc Natl Acad Sci USA.* (2000) 97:6670–5. doi: 10.1073/pnas.97.12.6670
4. Morel L, Blenman KR, Croker BP, Wakeland EK. The major murine systemic lupus erythematosus susceptibility locus, Sle1, is a cluster of functionally related genes. *Proc Natl Acad Sci USA.* (2001) 98:1787–92. doi: 10.1073/pnas.031336098
5. Cunninghame Graham DS, Morris DL, Bhangale TR, Criswell LA, Syvänen A-C, Rönnblom L, et al. Association of NCF2, IKZF1, IRF8, IFIH1, and TYK2 with systemic lupus erythematosus. *PLoS Genet.* (2011) 7:e1002341. doi: 10.1371/journal.pgen.1002341
6. Juang Y-T, Wang Y, Solomou EE, Li Y, Mawrin C, Tenbrock K, et al. Systemic lupus erythematosus serum IgG increases CREM binding to the IL-2 promoter and suppresses IL-2 production through CaMKIV. *J Clin Invest.* (2005) 115:996–1005. doi: 10.1172/JCI22854
7. Maeda K, Otomo K, Yoshida N, Abu-Asab MS, Ichinose K, Nishino T, et al. CaMK4 compromises podocyte function in autoimmune and nonautoimmune kidney disease. *J Clin Invest.* (2018) 128:3445–59. doi: 10.1172/JCI99507

Conflict of Interest: The authors declare that the research was conducted in the absence of any commercial or financial relationships that could be construed as a potential conflict of interest.

frontiers in Immunology

MINI REVIEW
published: 01 October 2018
doi: 10.3389/fimmu.2018.02113

Calcium/Calmodulin Kinase IV Controls the Function of Both T Cells and Kidney Resident Cells

Andrew P. Ferretti, Rhea Bhargava, Shani Dahan, Maria G. Tsokos and George C. Tsokos*

Department of Medicine, Beth Israel Deaconess Medical Center, Harvard Medical School, Boston, MA, United States

Calcium calmodulin kinase IV (CaMK4) regulates multiple processes that significantly contribute to the lupus-related pathology by controlling the production of IL-2 and IL-17 by T cells, the proliferation of mesangial cells, and the function and structure of podocytes. CaMK4 is also upregulated in podocytes from patients with focal segmental glomerulosclerosis (FSGS). In both immune and non-immune podocytopathies, CaMK4 disrupts the structure and function of podocytes. In lupus-prone mice, targeted delivery of a CaMK4 inhibitor to $CD4^+$ T cells suppresses both autoimmunity and the development of nephritis. Targeted delivery though to podocytes averts the deposition of immune complexes without affecting autoimmunity in lupus-prone mice and averts pathology induced by adriamycin in normal mice. Therefore, targeted delivery of a CaMK4 inhibitor to podocytes holds high therapeutic promise for both immune (lupus nephritis) and non-immune (FSGS) podocytopathies.

Keywords: calcium/calmodulin kinase IV, CaMK4, IL-2 deprivation, Treg deficiency, IL-17, podocyte dysfunction

OPEN ACCESS

Edited by:
Laurence Morel,
University of Florida, United States

Reviewed by:
Antonio La Cava,
University of California, Los Angeles, United States
Amr Sawalha,
University of Michigan, United States

****Correspondence:***
Andrew P. Ferretti
aferrett@bidmc.harvard.edu

Specialty section:
This article was submitted to Autoimmune and Autoinflammatory Disorders, a section of the journal Frontiers in Immunology

Received: *30 July 2018*
Accepted: *28 August 2018*
Published: *01 October 2018*

Citation:
Ferretti AP, Bhargava R, Dahan S, Tsokos MG and Tsokos GC (2018) Calcium/Calmodulin Kinase IV Controls the Function of Both T Cells and Kidney Resident Cells. Front. Immunol. 9:2113. doi: 10.3389/fimmu.2018.02113

INTRODUCTION

Calcium/calmodulin-dependent kinase IV (CaMK4) is a serine threonine kinase important for activating transcription factors downstream of T cell receptor (TCR) signaling. Aberrant activation of CaMK4 contributes to T cell abnormalities in systemic lupus erythematosus (SLE), a chronic systemic autoimmune disease presenting with diverse clinical manifestations (1). Immunologic abnormalities are a hallmark in the pathogenesis of SLE including altered antigen receptor–mediated activation and signaling in both T and B cells, defective clearance of immune complexes, neutrophil extracellular traps formation, auto-antibody production, and complement activation (2). Importantly, a multitude of pathways contribute to the expression of SLE pathology and this complicates the identification of a single specific molecule that will result in a successful treatment for all or the majority of the patients. However, many studies suggest that CaMK4 is a central molecule contributing to multiple pathological pathways in T cells from patients with SLE including suppression of IL-2, increased production of IL-17, and imbalance between regulatory and Th17 cells.

Ca^{2+}/CALMODULIN DEPENDENT PROTEIN KINASES (CaMKs)

Calcium (Ca^{2+}) is a ubiquitous universal intracellular second messenger, responsible for the control of numerous cellular processes (3). It exerts its functions by forming a complex with calmodulin (CaM), a 148-amino acid key protein that transduces signals in response to elevation of intracellular Ca^{2+} (4). Ca^{2+} binding to CaM induces conformational changes, leading to increased affinity

of the complex for its targets. One such target is CaMK4 (4, 5). The multifunctional CaMK4 has been isolated and localized in the nucleus, with a rather limited normal tissue distribution in discrete regions of the brain, T-lymphocytes, and post-meiotic germ cells (6–8). CaMK4 is activated by the binding of Ca^{2+}/CaM causing a structural modification by removing the auto-inhibitory domain exposing the catalytic pocket and enabling substrate access. To be fully activated and gain independent activity, CaMK4 requires phosphorylation on a threonine residue in the activation loop. This is generated by the upstream Ca^{2+}/CaM-dependent kinase kinases (CaMKKs) (9).

Upon activation, the autonomous CaMK4 is translocated into the nucleus, where it regulates the activity of several transcription-related components, including cyclic-AMP-response-element-binding protein (CREB), CREB-binding protein, cyclic-AMP response element modulator α (CREMα), histone deacetylase 4, monocyte enhancer factor 2A (MEF2), and retinoid orphan receptor (ROR) (4, 10–16). These factors play a key role in immune system development and function, including regulation of T cell differentiation, cytokines secretion and cell signaling (13, 17–19).

CONTRIBUTION OF CaMK4 TO THE SUPPRESSION OF IL-2 PRODUCTION IN SLE

Reduced IL-2 is a fundamental immunologic abnormality of T lymphocytes from patients with SLE and mice prone to lupus (20, 21). Since regulatory T (Treg) cells depend highly on IL-2 and IL-2 is diminished in patients with SLE, the number and function of Treg cells is also reduced in SLE patients (22). This skewed cytokine production in SLE also leads to impaired T cell regulation of B cell immunoglobulin production and poor activity of cytotoxic T cells. As a result, SLE patients are predisposed to severe life-threatening infections (23).

CaMK4 is a key molecule contributing to reduced IL-2 production in SLE T cells because it controls the ratio of phosphorylated CREB (pCREB) and phosphorylated CREM (pCREM). Activation of the transcription factor CREB by phosphorylation induces IL-2 transcription while activation of CREM by phosphorylation represses IL-2 transcription (24). In T cells from patients with SLE, translocation of CaMKIV to the nucleus is increased. In the nucleus, CaMK4 phosphorylates CREMα, promotes the binding of CREMα to the IL-2 promoter and represses IL-2 transcription (**Figure 1**) (14). Mechanistically, CREMα recruits DNMT3a and HDAC1 which promote hypermethylation and silencing of gene transcription (25, 26). This mechanism likely contributes to reduced levels of IL-2 in patients with SLE because deletion of CaMK4 reduces pCREMα binding to the IL-2 promoter, restores production of IL-2, and improves *in vitro* polarization of Treg cells. In the MRL/*lpr* lupus-prone mouse, depletion of CaMK4 restores serum levels of IL-2 as well as Treg cell numbers and function (16).

The specific mechanism leading to increased CaMK4 activity in T cells remains nebulous. One potential cause may be the increased calcium signaling in T cells from patients with SLE. Extensive evidence suggests that the CD3 complex in T cells from patients with SLE is rewired to produce an aberrantly enhanced TCR signal (27). Normally, TCR stimulation signals through immune receptor tyrosine-based motifs (ITAM) containing CD3ζ. CD3ζ associates with ZAP70 to propagate the signal. In contrast, T cells from patients with SLE have reduced CD3ζ and the Fc receptor common γ chain (FcRγ) associates with the TCR. Instead of associating with ZAP70, FcRγ associates with spleen tyrosine kinase (Syk) (28). Signaling through FcRγ-Syk in comparison to CD3ζ-ZAP70 transmits a stronger signal leading to enhanced intracellular Ca^{2+} concentration (29, 30). Thus, this enhanced intracellular calcium flux may lead to enhanced CaMK4 activation. Interestingly, in T cells from healthy patients, CaMK4 is activated in response to exposure to IgG isolated from sera from patients with SLE (14). The induction of CaMK4 is attributed to anti-TCR/CD3 antibodies because absorption of serum on TCR/CD3 positive cells but not TCR/CD3 negative cells diminishes CREM binding to the IL-2 promoter. Therefore, in addition to antigen specific activation, activation of the TCR by IgG from patients with SLE potentially contributes to a non-specific activation of T cells.

ABERRANT CaMK4 ACTIVATION DISRUPTS THE BALANCE OF TREG AND Th17 CELLS IN SLE

At the single cell level, the differentiation into either Treg or Th17 cell lineage appears reciprocal in nature (31). For example, upon TCR stimulation, the addition of TGFβ drives naïve T cells to express FoxP3 and differentiate into Treg cells. However, the addition of IL-6 to TGFβ promotes RORγt expression, steers cells toward Th17 differentiation and inhibits FoxP3 and Treg cell differentiation. The reciprocal nature of Treg and Th17 cells is also apparent in SLE where numbers and activity of anti-inflammatory Treg cells are reduced while proinflammatory Th17 cells are increased (32). CaMK4 plays a central role in the imbalance of Treg and Th17 cells. As noted above, CaMK4 contributes to the reduction of IL-2 and limits Treg cells in patients with SLE. Since IL-2 is known to inhibit Th17 differentiation (33), inhibition of IL-2 by CaMK4 likely also promotes Th17 differentiation indirectly.

Furthermore, our lab has established a direct mechanism whereby CaMK4 promotes the polarization of Th17 cells. Increased CaMK4 activity causes increased expression and activity of CREMα in T cells from patients with SLE and lupus-prone mice. Activated CREMα binds to CRE sites in the proximal IL-17 promoter (**Figure 1**) (34). In contrast to the IL-2 promoter discussed above, CREM binding to the IL-17 promoter facilitates the transcription of IL-17 in T cells from SLE patients (25). An additional pathway whereby CaMK4 promotes Th17 differentiation is through the activation

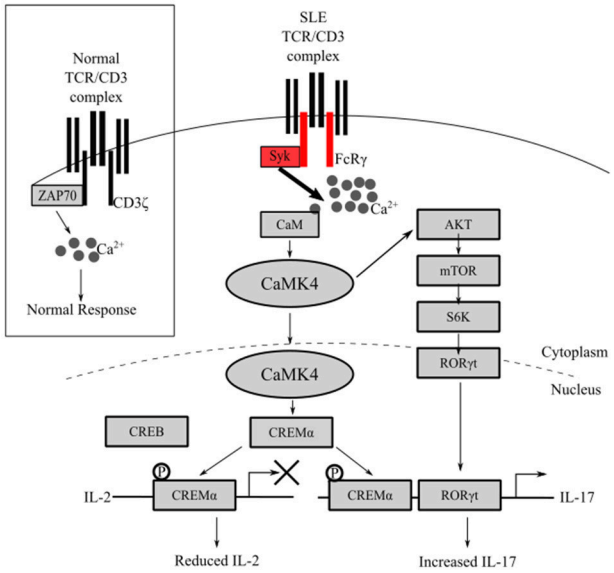

FIGURE 1 | Overactive CaMK4 in T cells signals to reduce IL-2 and increase IL-17 production. In patients with SLE, FcRγ, instead of CD3ζ, associates with the TCR complex and signals through Syk generating a stronger calcium signal. Overactive CaMK4 phosphorylates CREMα and mitigates IL-2 transcription. Concomitantly, CaMK4 promotes IL-17 production through activation of RORγt by phosphorylating AKT.

of RORγt (**Figure 1**). RORγt is a key transcription factor for Th17 differentiation and IL-17 production (13). In T cells from MRL/*lpr* mice, CaMK4 binds to and activates AKT activating the mTOR/S6K pathway (15), a pathway known to activate RORγt. Thus, CaMK4 promotes the differentiation of Th17 cells indirectly by inhibiting IL-2 transcription and directly by promoting IL-17 transcription through CREMα and by activating RORγt through the AKT/mTOR/S6K pathway.

This mechanism is supported by *in vitro* and *in vivo* evidence that suggests CaMK4 promotes Th17 differentiation. In normal T cells, overexpression of CaMK4 increases differentiation of Th17 cells *in vitro* and genetic depletion of CaMK4 disrupts Th17 cell differentiation in T cells derived from normal or autoimmune prone MRL/*lpr* mice (15). Moreover, mice lacking CaMK4 or mice subject to pharmacological inhibition of CaMK4 are resistant to experimental autoimmune encephalomyelitis (EAE), which has been well established that it depends on Th17 cells (15, 35). Thus, ample evidence suggests CaMK4 is a key contributor to IL-17 production and Th17 cell differentiation.

Further evidence suggests CaMK4 activation alters the balance of Treg and Th17 cells in patients with SLE. Activation of CaMK4 is increased in T cells from patients with SLE (14) and lupus-prone MRL/*lpr* mice (16). In T cells from autoimmune-prone MRL/lpr mice, CaMK4 is induced the most after stimulating naïve T cells under Th17 but not Th1, Th2, or Treg polarizing conditions (15). Importantly, depletion of CaMK4 restores IL-2 production (16) and improves Treg cell number and function in MRL/*lpr* mice (36). At the same time, depletion of CaMK4 inhibits Th17 development in SLE T cells (15) and prevents infiltration of IL-17 producing cells in the kidney (35). In sum, increased activation of CaMK4 directs T cells toward Th17 differentiation and away from Treg cell differentiation. Inhibition of CaMKIV restores the Treg/Th17 imbalance, limits lymphocyte proliferation and activation, suppresses nephritis and skin disease, and improves survival in lupus-prone mice (16, 35, 37).

CaMK4 IN RESIDENT KIDNEY CELLS

Lupus nephritis is a major manifestation of SLE occurring in more than 50% of SLE patients and is characterized by immune complex deposition and cell proliferation (38). Resident kidney cells including mesangial cells and podocytes have been implicated in the expression of nephritis in patients with SLE. Interestingly, CaMK4 also plays a role in resident kidney cells and contributes to the pathogenesis of lupus nephritis by promoting mesangial cell proliferation through IL-6 production. Mesangial cells in the glomerulus are known to produce IL-6 when exposed to dsDNA antibodies (39), and in an autocrine fashion, IL-6 stimulates mesangial cell proliferation (40, 41). This is thought to contribute to the pathogenesis of lupus nephritis since blockade of IL-6 or the IL-6 receptor ameliorates kidney disease in lupus-prone mice (42–44). In MRL/*lpr* mice, IL-6 production by mesangial cells in increased, especially upon stimulation with platelet-derived growth factor (PDGF). This increased production is reversed when mice are treated with a CaMK4 inhibitor or genetic depletion of *CaMK4*. Moreover, global depletion of CaMK4 reduces mesangial cell proliferation, and greatly reduces kidney damage (45).

CaMK4 appears to contribute to podocyte disfunction in autoimmune kidney disease. Podocytes from lupus nephritis patients exhibit elevated levels of CaMK4. While the exact mechanism responsible for CaMK4 upregulation is unknown, autoantibodies likely play a role because podocytes exposed to IgG from patients with lupus nephritis display increased CaMK4 and alter the expression of proteins known to be important for the structure and function of podocytes including podocin and nephrin, respectively (46). Also, exposure of podocytes to IgG from patients with SLE causes an increase in the expression of the costimulatory molecules CD80 and CD86 on the surface membrane (46, 47). Global genetic ablation of CaMK4 in MRL.*lpr* mice greatly reduces proteinuria (45).

Podocytes from patients with FSGS also express increased levels of CaMK4 suggesting that this kinase may represent a shared molecule in the expression of immune and non-immune podocytopathies. At the biochemical level, increased levels of CaMK4 disrupt the maintenance of the slit diaphragm by phosphorylating the adaptor molecule 14-3-3β. 14-3-3β stabilizes synaptopodin, an actin binding molecule that is critical for the maintenance of normal actin fiber dynamics. Therefore, phosphorylation of 14-3-3β by

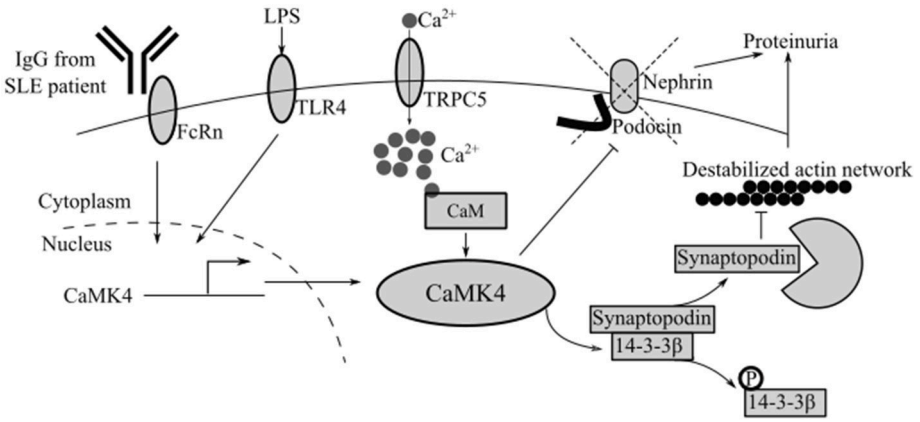

FIGURE 2 | CaMK4 contributes to podocyte dysfunction in autoimmune and non-autoimmune kidney disease. Multiple stimuli including IgG from SLE patients or LPS upregulate CaMK4 leading to destabilization of the actin network and downregulation of nephrin and podocin. TRPC5, short transient receptor potential channel 5.

CaMK4 causes the release and degradation of synaptopodin leading to destabilization of the actin fiber network (**Figure 2**) (48).

TARGETING CaMK4 IN LUPUS

To address potential off target concerns of systematic delivery of CaMK4 inhibitors, our lab has explored nanolipogel-based delivery of the CAMK4 inhibitor KN-93 to target CaMK4 specifically in T cells or podocytes. Use of KN-93 packaged nanolipogels coated with an antibody recognizing CD4 targeted KN-93 specifically to CD4 T cells without increasing cell death. Delivery of KN-93 targeted to CD4 T cells to lupus-prone MRL/*lpr* mice increased IL-2 levels in the serum, reduced IL-17 producing infiltrating cells in the kidneys and improved kidney function as measured by proteinuria. Importantly, the effective dose of KN-93 delivered by nanolipogels was 10% of the dose necessary to warrant an effect from systemically delivered KN-93 (35).

Using the same delivery approach, KN-93 targeted to podocytes MRL.*lpr* mice at the beginning of their clinical disease surprisingly never developed proteinuria and immune complexes never deposited despite the fact that humoral and cellular elements of autoimmunity were rampant in these mice. This observation suggests that immune complexes do not deposit if the structure and the function of the podocytes is kept intact. Interestingly, the treated mice did not develop crescents which have been claimed to originate from podocytes (48). Pharmacologic inhibition or silencing of CaMK4 in cultured podocytes subjected to scratch injury did not move to fill up the inflicted empty space.

TARGETING CaMKIV IN FSGS

Focal segmental glomerulosclerosis (FSGS) is the most common primary glomerular disease which results in end-stage renal disease. It is a heterogeneous clinical entity characterized by a characteristic histologic pattern. The origin of FSGS is diverse and genetic, metabolic, infectious, and unknown factors have been claimed to be involved in its expression. Proteinuria is the typical clinical finding of FSGS (49). The podocyte is the target cell for injury in FSGS and a growing list of disease-causing gene mutations encoding proteins that regulate podocyte survival and homeostasis has been identified in FSGS patients (50).

Adriamycin has been used extensively to study aspects of FSGS (51). Injection of adriamycin into mice increases the expression of CaMK4 in podocytes. Targeted delivery of a CaMK4 inhibitor to podocytes at the time of injection of adriamycin prevented the development of glomerular damage and more importantly, delivery of the CaMK4 inhibitor 7 days later reversed all damage (48). This evidence strongly urges the consideration of novel approaches to limit FSGS which, through the invariable need of kidney dialysis and transplantation, is responsible for major taxation of the health system expenses.

In summary, CaMK4 is a central molecule that regulates multiple processes that significantly contribute to the pathology of SLE by controlling the production of IL-2 and IL-17 by T cells, the proliferation of mesangial cells and the function and structure of podocytes. CaMK4 is also upregulated in podocytes from patients with FSGS. In both immune and non-immune podocytopathies, CaMK4 disrupts the structure and function of podocytes. It is not known at this point whether CaMK4 is increased in the podocytes from patients with other glomerular diseases and whether it represents a common molecular link for several kidney diseases. It is also not known whether CaMK4 is increased in renal tubular cells in patients with immune and non-immune kidney injury. Although in lupus nephritis it appears that IgG that enters podocytes elicits an increase in the expression of CaMK4, the involved mechanism is still at large. Similarly, we have no insight in to the causes of increased expression of CaMK4 in patients with FSGS although the known increased calcium flux certainly contributes (52). In lupus-prone mice, targeted delivery of a CaMK4 inhibitor suppresses

both autoimmunity and the development of nephritis. Yet, targeted delivery to podocytes averts the deposition of immune complexes without affecting autoimmunity. This observation strongly suggests that immune complexes may deposit after podocytes have been injured and changes the approach we should take to prevent kidney damage. It appears that delivery of a CaMK4 inhibitor to podocytes holds high therapeutic promise for both immune (lupus nephritis) and non-immune (FSGS) podocytopathies.

AUTHOR CONTRIBUTIONS

AF and GT wrote and edited the review. RB, SD, and MT edited the review and aided with review content.

ACKNOWLEDGMENTS

AF was supported by NIH grant T32AI007512. We also acknowledge support from NIH grant R01AR064350.

REFERENCES

1. Tsokos GC. Systemic lupus erythematosus. *N Engl J Med.* (2011) 365:2110–21. doi: 10.1056/NEJMra1100359
2. Tsokos GC, Lo MS, Reis PC, Sullivan KE. New insights into the immunopathogenesis of systemic lupus erythematosus. *Nat Rev Rheumatol.* (2016) 12:716–30. doi: 10.1038/nrrheum.2016.186
3. Berridge MJ, Lipp P, Bootman MD. The versatility and universality of calcium signalling. *Nat Rev Mol Cell Biol.* (2000) 1:11–21. doi: 10.1038/35036035
4. Racioppi L, Means AR. Calcium/calmodulin-dependent kinase IV in immune and inflammatory responses: novel routes for an ancient traveller. *Trends Immunol.* (2008) 29:600–7. doi: 10.1016/j.it.2008.08.005
5. Hook SS, Means AR. Ca^{2+}/CaM-dependent kinases: from activation to function. *Annu Rev Pharmacol Toxicol.* (2001) 41:471–505. doi: 10.1146/annurev.pharmtox.41.1.471
6. Frangakis MV, Ohmstede CA, Sahyoun N. A brain-specific Ca^{2+}/calmodulin-dependent protein kinase (CaM kinase-Gr) is regulated by autophosphorylation. Relevance to neuronal Ca^{2+} signaling. *J Biol Chem.* (1991) 266:11309–16.
7. Jensen KF, Ohmstede CA, Fisher RS, Sahyoun, N. Nuclear and axonal localization of Ca^{2+}/calmodulin-dependent protein kinase type Gr in rat cerebellar cortex. *Proc Natl Acad Sci USA.* (1991) 88:2850–3. doi: 10.1073/pnas.88.7.2850
8. Ohmstede CA, Jensen KF, Sahyoun NE. Ca^{2+}/calmodulin-dependent protein kinase enriched in cerebellar granule cells. Identification of a novel neuronal calmodulin-dependent protein kinase *J Biol Chem.* (1989) 264:5866–75.
9. Soderling TR. The Ca-calmodulin-dependent protein kinase cascade. *Trends Biochem Sci.* (1999) 24:232–6. doi: 10.1016/S0968-0004(99)01383-3
10. Chow FA, Anderson KA, Noeldner PK, Means AR. The autonomous activity of calcium/calmodulin-dependent protein kinase IV is required for its role in transcription. *J Biol Chem.* (2005) 280:20530–8. doi: 10.1074/jbc.M500067200
11. Impey S, Fong AL, Wang Y, Cardinaux JR, Fass DM, Obrietan K, et al. Phosphorylation of CBP mediates transcriptional activation by neural activity and CaM kinase IV. *Neuron* (2002) 34:235–44. doi: 10.1016/S0896-6273(02)00654-2
12. Youn HD, Sun L, Prywes R, Liu JO. Apoptosis of T cells mediated by Ca^{2+}-induced release of the transcription factor MEF2. *Science* (1999) 286:790–3. doi: 10.1126/science.286.5440.790
13. Ivanov II, McKenzie BS, Zhou L, Tadokoro CE, Lepelley A, Lafaille JJ, et al. The orphan nuclear receptor RORgammat directs the differentiation program of proinflammatory IL-17+ T helper cells. *Cell* (2006) 126:1121–33. doi: 10.1016/j.cell.2006.07.035
14. Juang YT, Wang Y, Solomou EE, Li Y, Mawrin C, Tenbrock K, et al. Systemic lupus erythematosus serum IgG increases CREM binding to the IL-2 promoter and suppresses IL-2 production through CaMKIV. *J Clin Invest.* (2005) 115:996–1005. doi: 10.1172/JCI22854
15. Koga T, Hedrich CM, Mizui M, Yoshida N, Otomo K, Lieberman LA, et al. CaMK4-dependent activation of AKT/mTOR and CREM-alpha underlies autoimmunity-associated Th17 imbalance. *J Clin Invest.* (2014) 124:2234–45. doi: 10.1172/JCI73411
16. Koga T, Ichinose K, Mizui M, Crispin JC, Tsokos GC. Calcium/calmodulin-dependent protein kinase IV suppresses IL-2 production and regulatory T cell activity in lupus. *J Immunol.* (2012) 189:3490–6. doi: 10.4049/jimmunol.1201785
17. Hammerich L, Warzecha KT, Stefkova M, Bartneck M, Ohl K, Gassler N, et al. Cyclic adenosine monophosphate-responsive element modulator alpha overexpression impairs function of hepatic myeloid-derived suppressor cells and aggravates immune-mediated hepatitis in mice. *Hepatology* (2015) 61:990–1002. doi: 10.1002/hep.27571
18. Kim HP, Leonard WJ. CREB/ATF-dependent T cell receptor-induced FoxP3 gene expression: a role for DNA methylation. *J Exp Med.* (2007) 204:1543–51. doi: 10.1084/jem.20070109
19. Ohl K, Wiener A, Schippers A, Wagner N, Tenbrock K. Interleukin-2 treatment reverses effects of cAMP-responsive element modulator alpha-over-expressing T cells in autoimmune-prone mice. *Clin Exp Immunol.* (2015) 181:76–86. doi: 10.1111/cei.12629
20. Linker-Israeli M, Bakke AC, Kitridou RC, Gendler S, Gillis S, Horwitz DA. Defective production of interleukin 1 and interleukin 2 in patients with systemic lupus erythematosus (SLE). *J Immunol.* (1983) 130:2651–5.
21. Theofilopoulos AN, Dixon FJ. Murine models of systemic lupus erythematosus. *Adv Immunol.* (1985) 37:269–390. doi: 10.1016/S0065-2776(08)60342-9
22. Mizui M, Tsokos GC. Targeting regulatory T cells to treat patients with systemic lupus erythematosus. *Front Immunol.* (2018) 9:786. doi: 10.3389/fimmu.2018.00786
23. Iliopoulos A, Tsokos G. Immunopathogenesis and spectrum of infections in systemiclupus erythematosus. *Semin Arthritis Rheum.* (1996) 25:318–36.
24. Solomou EE, Juang YT, Gourley MF, Kammer GM, Tsokos GC. Molecular basis of deficient IL-2 production in T cells from patients with systemic lupus erythematosus. *J Immunol.* (2001) 166:4216–22. doi: 10.4049/jimmunol.166.6.4216
25. Hedrich CM, Crispin JC, Rauen T, Ioannidis C, Apostolidis SA, Lo MS, et al. cAMP response element modulator alpha controls IL2 and IL17A expression during CD4 lineage commitment and subset distribution in lupus. *Proc Natl Acad Sci USA.* (2012) 109:16606–11. doi: 10.1073/pnas.1210129109
26. Hedrich CM, Rauen T, Tsokos GC. cAMP-responsive element modulator (CREM)alpha protein signaling mediates epigenetic remodeling of the human interleukin-2 gene: implications in systemic lupus erythematosus. *J Biol Chem.* (2011) 286:43429–36. doi: 10.1074/jbc.M111.299339
27. Krishnan S, Farber DL, Tsokos GC. T cell rewiring in differentiation and disease. *J Immunol.* (2003) 171:3325–31. doi: 10.4049/jimmunol.171.7.3325
28. Enyedy EJ, Nambiar MP, Liossis SN, Dennis G, Kammer GM, Tsokos GC. Fc epsilon receptor type I gamma chain replaces the deficient T cell receptor zeta chain in T cells of patients with systemic lupus erythematosus. *Arthritis Rheum* (2001) 44:1114–21. doi: 10.1002/1529-0131(200105)44:5<1114::AID-ANR192>3.0.CO;2-B
29. Vassilopoulos D, Kovacs B, Tsokos GC. TCR/CD3 complex-mediated signal transduction pathway in T cells and T cell lines from patients with systemic lupus erythematosus. *J Immunol.* (1995) 155:2269–81.
30. Crispin JC, Kyttaris VC, Juang YT, Tsokos GC. How signaling and gene transcription aberrations dictate the systemic lupus erythematosus T cell phenotype. *Trends Immunol.* (2008) 29:110–5. doi: 10.1016/j.it.2007.12.003
31. Korn T, Bettelli E, Oukka M, Kuchroo VK. IL-17 and Th17 Cells. *Annu Rev Immunol.* (2009) 27:485–517. doi: 10.1146/annurev.immunol.021908.132710
32. Moulton VR, Tsokos GC. T cell signaling abnormalities contribute to aberrant immune cell function and autoimmunity. *J Clin Invest.* (2015) 125:2220–7. doi: 10.1172/JCI78087

33. Laurence A, Tato CM, Davidson TS, Kanno Y, Chen Z, Yao Z, et al. Interleukin-2 signaling via STAT5 constrains T helper 17 cell generation. *Immunity* (2007) 26:371–81. doi: 10.1016/j.immuni.2007.02.009
34. Rauen T, Hedrich CM, Juang YT, Tenbrock K, Tsokos GC. cAMP-responsive element modulator (CREM)alpha protein induces interleukin 17A expression and mediates epigenetic alterations at the interleukin-17A gene locus in patients with systemic lupus erythematosus. *J Biol Chem.* (2011) 286:43437–46. doi: 10.1074/jbc.M111.299313
35. Otomo K, Koga T, Mizui M, Yoshida N, Kriegel C, Bickerton S, et al. Cutting edge: nanogel-based delivery of an inhibitor of CaMK4 to $CD4^+$ T cells suppresses experimental autoimmune encephalomyelitis and lupus-like disease in mice. *J Immunol.* (2015) 195:5533–7. doi: 10.4049/jimmunol.1501603
36. Koga T, Mizui M, Yoshida N, Otomo K, Lieberman LA, Crispin JC, et al. KN-93, an inhibitor of calcium/calmodulin-dependent protein kinase IV, promotes generation and function of Foxp3(+) regulatory T cells in MRL/lpr mice. *Autoimmunity* (2014) 47:445–50. doi: 10.3109/08916934.2014.915954
37. Ichinose K, Juang YT, Crispin JC, Kis-Toth K, Tsokos GC. Suppression of autoimmunity and organ pathology in lupus-prone mice upon inhibition of calcium/calmodulin-dependent protein kinase type IV. *Arthritis Rheum* (2011) 63:523–9. doi: 10.1002/art.30085
38. Tsokos GC. Systemic lupus erythematosus in 2015: cellular and metabolic requirements of effector T cells. *Nat Rev Rheumatol.* (2016) 12:74–6. doi: 10.1038/nrrheum.2015.178
39. Yung S, Cheung KF, Zhang Q, Chan TM. Anti-dsDNA antibodies bind to mesangial annexin II in lupus nephritis. *J Am Soc Nephrol.* (2010) 21:1912–27. doi: 10.1681/ASN.2009080805
40. Ruef C, Budde K, Lacy J, Northemann W, Baumann M, Sterzel RB, et al. Interleukin 6 is an autocrine growth factor for mesangial cells. *Kidney Int.* (1990) 38:249–57. doi: 10.1038/ki.1990.193
41. Suematsu S, Matsusaka T, Matsuda T, Ohno S, Miyazaki J, Yamamura K, et al. Generation of plasmacytomas with the chromosomal translocation t(12;15) in interleukin 6 transgenic mice. *Proc Natl Acad Sci USA.* (1992) 89:232–5. doi: 10.1073/pnas.89.1.232
42. Cash H, Relle M, Menke J, Brochhausen C, Jones SA, Topley N, et al. Interleukin 6 (IL-6) deficiency delays lupus nephritis in MRL-Faslpr mice: the IL-6 pathway as a new therapeutic target in treatment of autoimmune kidney disease in systemic lupus erythematosus. *J Rheumatol.* (2010) 37:60–70. doi: 10.3899/jrheum.090194
43. Liang B, Gardner DB, Griswold DE, Bugelski PJ, Song XY. Anti-interleukin-6 monoclonal antibody inhibits autoimmune responses in a murine model of systemic lupus erythematosus. *Immunology* (2006) 119:296–305. doi: 10.1111/j.1365-2567.2006.02433.x
44. Kiberd BA. Interleukin-6 receptor blockage ameliorates murine lupus nephritis. *J Am Soc Nephrol.* (1993) 4:58–61.
45. Ichinose K, Rauen T, Juang YT, Kis-Toth K, Mizui M, Koga T, et al. Cutting edge: Calcium/Calmodulin-dependent protein kinase type IV is essential for mesangial cell proliferation and lupus nephritis. *J Immunol.* (2011) 187:5500–4. doi: 10.4049/jimmunol.1102357
46. Ichinose K, Ushigusa T, Nishino A, Nakashima Y, Suzuki T, Horai Y, et al. Lupus nephritis IgG induction of calcium/calmodulin-dependent protein kinase iv expression in podocytes and alteration of their function. *Arthritis Rheumatol.* (2016) 68:944–52. doi: 10.1002/art.39499
47. Reiser J, von Gersdorff G, Loos M, Oh J, Asanuma K, Giardino L, et al. Induction of B7-1 in podocytes is associated with nephrotic syndrome. *J Clin Invest.* (2004) 113:1390–7. doi: 10.1172/JCI20402
48. Maeda K, Otomo K, Yoshida N, Abu-Asab MS, Ichinose K, Nishino T, et al. CaMK4 compromises podocyte function in autoimmune and nonautoimmune kidney disease. *J Clin Invest.* (2018) 128:3445–59. doi: 10.1172/JCI99507
49. Wen Y, Shah S, Campbell KN. Molecular mechanisms of proteinuria in focal segmental glomerulosclerosis. *Front Med.* (2018) 5:98. doi: 10.3389/fmed.2018.00098
50. Sampson MG, Pollak MR. Opportunities and challenges of genotyping patients with nephrotic syndrome in the genomic era. *Semin Nephrol.* (2015) 35:212–21. doi: 10.1016/j.semnephrol.2015.04.002
51. Fogo AB. Animal models of FSGS: lessons for pathogenesis and treatment. *Semin Nephrol.* (2003) 23:161–71. doi: 10.1053/snep.2003.50015
52. Greka A, Mundel P. Balancing calcium signals through TRPC5 and TRPC6 in podocytes. *J Am Soc Nephrol.* (2011) 22:1969–80. doi: 10.1681/ASN.2011040370

Conflict of Interest Statement: The authors declare that the research was conducted in the absence of any commercial or financial relationships that could be construed as a potential conflict of interest.

frontiers in Immunology

REVIEW
published: 30 October 2018
doi: 10.3389/fimmu.2018.02496

Monogenic Lupus: A Developing Paradigm of Disease

Jessie M. Alperin[1], *Lourdes Ortiz-Fernández*[1] *and Amr H. Sawalha*[1,2]*

[1] Division of Rheumatology, Department of Internal Medicine, University of Michigan, Ann Arbor, MI, United States, [2] Center for Computational Medicine and Bioinformatics, University of Michigan, Ann Arbor, MI, United States

Monogenic lupus is a form of systemic lupus erythematosus (SLE) that occurs in patients with a single gene defect. This rare variant of lupus generally presents with early onset severe disease, especially affecting the kidneys and central nervous system. To date, a significant number of genes have been implicated in monogenic lupus, providing valuable insights into a very complex disease process. Throughout this review, we will summarize the genes reported to be associated with monogenic lupus or lupus-like diseases, and the pathogenic mechanisms affected by the mutations involved upon inducing autoimmunity.

Keywords: lupus, monogenic, familial, genetic, mendelian

OPEN ACCESS

Edited by:
José Carlos Crispín, Instituto Nacional de Ciencias Médicas y Nutrición Salvador Zubirán, Mexico

Reviewed by:
Christian Michael Hedrich, University of Liverpool, United Kingdom
Mindy S. Lo, Boston Children's Hospital, Harvard Medical School, United States

***Correspondence:**
Amr H. Sawalha
asawalha@umich.edu

Specialty section:
This article was submitted to Autoimmune and Autoinflammatory Disorders, a section of the journal Frontiers in Immunology

Received: *28 July 2018*
Accepted: *09 October 2018*
Published: *30 October 2018*

Citation:
Alperin JM, Ortiz-Fernández L and Sawalha AH (2018) Monogenic Lupus: A Developing Paradigm of Disease. Front. Immunol. 9:2496. doi: 10.3389/fimmu.2018.02496

INTRODUCTION

Systemic lupus erythematosus (SLE or lupus) is a complex multisystem disease whose underlying disease mechanism continues to be a topic of intense research. SLE can affect many organs including the kidneys, skin, joints, lungs, cardiovascular system, central nervous system, and hematopoietic system. As with most complex diseases, the etiology of SLE is incompletely understood, however, cumulative evidence has pointed to the involvement of both genetic and epigenetic mechanisms (1, 2). Multiple genetic variants associated with lupus susceptibility have been identified through genome-wide association studies (GWAS). Support for a genetic component of lupus can be realized from twin studies. Concordance rate of lupus in monozygotic and dizygotic twins has been reported to be 24 and 2%, respectively, demonstrating a role for genetic susceptibility in lupus (3). In parallel, monozygotic twin studies have also provided evidence highlighting the relevance of DNA methylation changes (4). At the same time, non-genetic factors such as viral infections or exposure to ultraviolet (UV) light among others are clearly involved, as suggested by incomplete concordance in monozygotic twins.

Patients with childhood onset SLE usually present with a more severe phenotype and have an increased frequency of glomerulonephritis, cytopenias, neuropsychiatric disease, cutaneous manifestations, anti-dsDNA antibodies, and hemolytic anemia (5). It can be presumed that in early onset disease, genetic factors may play a more important role than environmental and hormonal factors (5). Monogenic lupus is a form of SLE that typically presents early in life, usually at <5 years of age, with severe disease manifestations. This form of lupus is caused directly by a genetic variant in a specific gene. Monogenic lupus represents a collection of distinct genetic abnormalities causing similar clinical features and resulting in autoantibody production. In particular, consanguinity presents a significant increased risk for monogenic lupus and should prompt consideration in patients with familial SLE. Though monogenic lupus accounts for only a small subset of lupus patients, it provides significant insight into the cause and mechanisms of lupus, and potential treatment strategies.

In the last years, large achievements understanding the genetic component of SLE have been accomplished. More than 80 loci have been reported to be associated with susceptibility in polygenic lupus, and a considerable number of monogenic causes of SLE and lupus-like syndromes are emerging due to the evolution of new sequencing techniques that can identify rare genetic variations across the entire genome. Through this review, we will explore the implications on the disease pathogenesis of the genes that have been found to cause monogenic lupus or lupus-like phenotype (**Figure 1**, **Table 1**).

INTERFERONOPATHIES

Although the clinical manifestations and severity observed are different among patients, the interferonopathies are a wide group of complex genetic disorders with a common pathogenic mechanism characterized by imbalance of interferon (IFN) mediated immune responses. Given that studies have repeatedly identified an increased blood IFN signature in SLE patients (35, 36), it is not surprising that clinical features of some of the diseases classified as interferonopathies overlap with systemic lupus erythematosus. Consequently, some of these diseases, such as Aicardi-Goutières Syndrome (AGS) and Spondyloenchondrodysplasia (SPENCD) can also be considered as forms of monogenic lupus or lupus-like syndromes.

Aicardi-Goutières Syndrome

Aicardi-Goutières Syndrome is a genetic syndrome caused by multiple genetic defects. The disease phenotype resembles a congenital viral infection and many patients develop lupus as a feature of the syndrome. AGS develops in young patients, typically before 6 months of age and is characterized by encephalopathy that is usually associated with calcification of the basal ganglia and white matter changes on brain imaging (37). Frequently, there is cutaneous involvement and, in particular, chilblains. Patients with AGS have been shown to have multiple IgG autoantibodies particularly directed against nuclear antigens, basement membrane components, gliadin, and brain endothelial cells and astrocytes. Patient with AGS develop elevated type I IFN levels in both serum and cerebral spinal fluid (7). These observations suggest that genetic defects in RNA or DNA clearance result in increased type I IFN production and interferon stimulated genes (ISGs), and then lead to autoimmunity. AGS is associated with mutations in multiples genes and many of these overlap with various forms of monogenic lupus, suggesting a spectrum of disease likely influenced by the location of the mutation as well as environmental factors (7).

Mutations of *TREX1* gene have been identified in AGS. Approximately 25% of AGS patients have a *TREX1* mutation. Patients with AGS due to a *TREX1* mutation have a prototypical disease phenotype. A review of autoimmune features in AGS patients showed that approximately 60% of patients with a *TREX1* variant had at least one autoimmune feature: thrombocytopenia, leukopenia, antinuclear antibodies (ANA), skin lesions, oral ulceration, arthritis, anti-dsDNA antibodies, or antibodies to extractable nuclear antigens (ENA) (34). Persisting severe physical and intellectual disability is frequent. In the large majority, patients will have no purposeful gross motor, hand or communication function. About a third of patients with a *TREX1*-related AGS present in the neonatal period with thrombocytopenia, hepatosplenomegaly, and a transaminitis in addition to neurological disease (7). For reasons that are not understood, these extra-neurological features often resolve within the first year of life. A broad spectrum of mutations across *TREX1* have been associated with different immune-mediated diseases. Most patients with AGS show biallelic mutations within *TREX1* with autosomal recessive inheritance, which usually causes a complete loss of protein function. However, some heterozygous mutations have also been identified in individuals diagnosed with AGS (34). Early-onset familial chilblain lupus (FCL) is a rare form of cutaneous lupus which results in cold-induced severe discoloration of hands, feet, and ears, where the lesions frequently ulcerate. Most of these patients have heterozygous mutations with autosomal dominant inheritance (34). In addition, heterozygous mutations in *TREX1* with autosomal dominant inheritance has been linked to retinal vasculopathy with cerebral leukodystrophy (RVCL) (38). Interestingly, a deleterious homozygous variant of this gene has been recently identified in a patient with cerebral SLE (39), and, it is worth noting that several single nucleotides polymorphisms (SNPs) in *TREX1* have been found associated with common forms of SLE in different populations (40–42). This gene, located on chromosome 3, encodes a protein with exonuclease activity which is an IFN-inducible protein responsible for degradation of genomic DNA in response to DNA damage. Therefore, it plays an important role in the immune response to single-stranded (ss)-DNA and dsDNA (43), and maintains immune tolerance to cytosolic self-DNA (44). When TREX1 is dysfunctional, the cytosolic DNA does not get degraded which constitutes a damage-associated molecular pattern (DAMP). This activates the cGAS-STING-mediated type I IFN response and systemic inflammation (44). TREX1 deficiency is thought to trigger autoimmunity through the accumulation of self DNA in the cytosol. These are sensed by cyclic GMP-AMP (cGAMP) synthase (cGAS). cGAMP is a ligand for stimulator of IFN genes protein (STING), which leads to the production of type I IFN (43). On the other hand, TREX1 is a DNase component of the SET complex which is involved, among other mechanisms, in apoptosis (45). Altogether, these data provide different pathomechanisms for the involvement of TREX1 dysfunction in SLE.

Patients with *IFIH1* (interferon induced with helicase C domain 1) gain of function mutations can develop early onset SLE and AGS-like disease, including musculoskeletal involvement and Jaccoud's arthropathy (46). *IFIH1* gene, which encodes MDA5 (melanoma differentiation-associated protein 5), is a cytoplasmic RNA receptor that binds cytoplasmic double-stranded RNA. IFIH1 belongs to the RIG-I–like family which is part of the pathway responsible for activating type I interferon signaling (19). The gain of function mutation in *IFIH1* gene leads to activated dendritic cells and macrophages, which are the primary producers of IFN-alpha in response to nucleic acid (47). This leads to the activation of T cells and production of

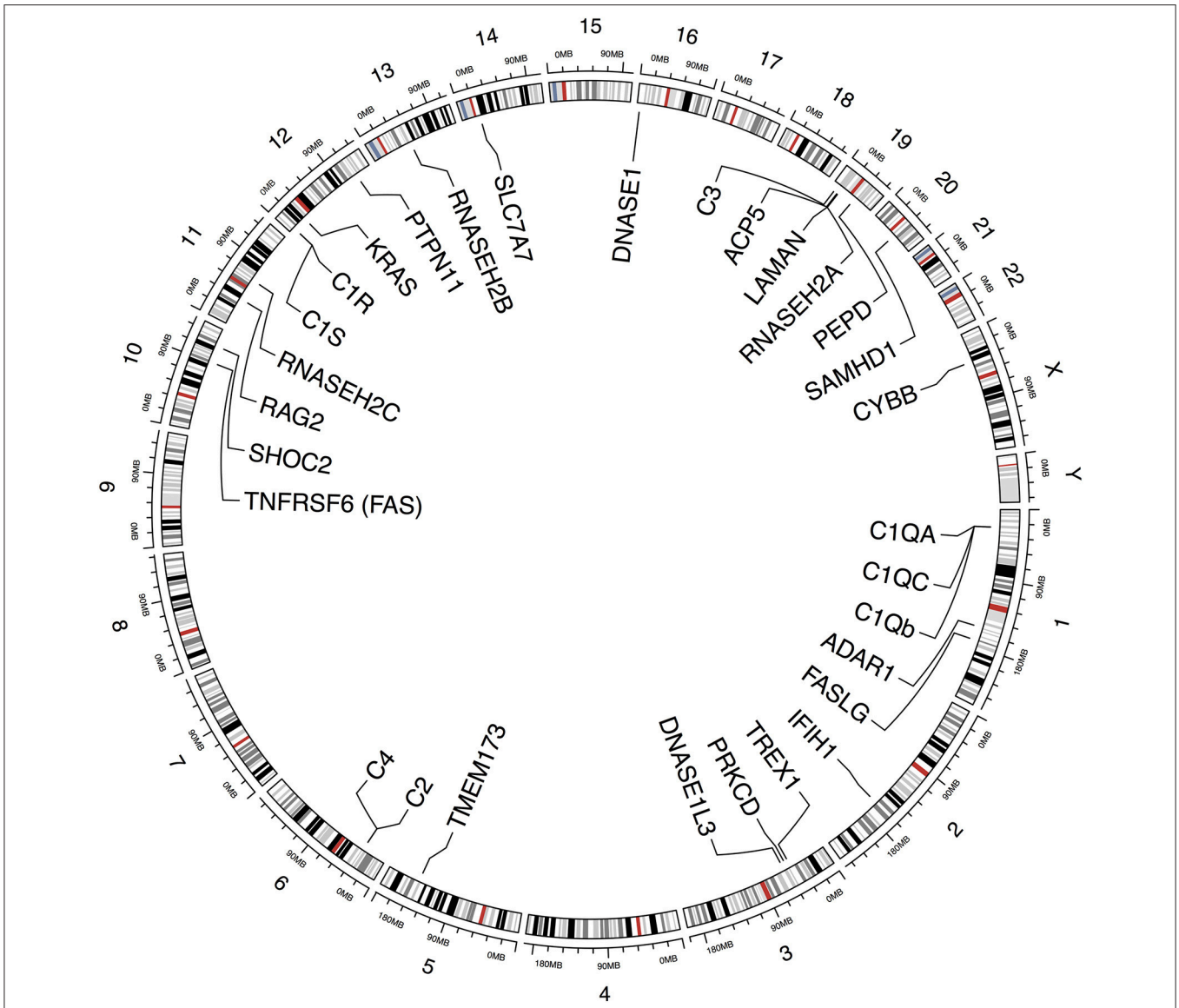

FIGURE 1 | Schematic representation depicting genes and chromosomal locations previously identified to be implicated in monogenic lupus. This figure was produced using 'circlize' in R (http://cran.r-project.org/web/packages/circlize/).

autoantibodies (48). It is interesting to note that polymorphisms in *IFIH1* have been reported in patients with inflammatory myopathies and anti-MDA5 antibodies are seen in some patients with amyopathic dermatomyositis (49). Remarkably, a recent study revealed that these patients showed a high activity of type I IFN system. Although the mechanisms are still unclear, the study detected high levels of transcripts of IFN-associated sensors and several IFN-inducible genes were up-regulated in these patients (50).

SAMHD1 (SAM domain and HD domain-containing protein 1) is a dGTP-dependent triphosphohydrolase responsible for the regulation of intracellular levels of deoxynucleoside triphosphates (dNTPs), the building blocks of DNA synthesis (51, 52). In unaffected individuals, SAMHD1 promotes cell stability and prevents reverse transcription of retroviruses. Deficiency of SAMHD1 results in unbalanced pools of dNTPs. This leads to loss of DNA replication and repair, DNA damage, and apoptosis leading to a sustained IFN production (53). SAMHD1 is upregulated in response to viral infections. It plays a role in the antiviral immune response through initiation of the interferon pathway (51). *SAMHD1* disease-causing variants can present with AGS, SLE, and chilblain lupus (29, 30). SAMHD1 has been shown to be reduced or absent in the cells of patients with AGS (54). Cells from patients with *SAMHD1* mutations exhibited increased dNTP pools and DNA damage resulting in a failure of the cell cycle and cellular senescence. Increased DNA damage leads to upregulation in IFN-stimulated genes by activation of the innate immune system (53).

TABLE 1 | List of genes identified to cause monogenic lupus or lupus-like diseases.

Locus	Gene name	Gene Location	Protein	Inheritance	Pathway	Phenotype	References
ACP5	Acid phosphatase 5, tartrate resistant	19p13.2	TRAP	AR	Nucleic acid sensing and degradation Type I IFN	SPENCD SLE	(6)
ADAR1	Adenosine deaminase, RNA specific	1q21.3	Adenosine deaminase, RNA specific	AR/AD	Type I IFN	AGS SLE	(7, 8)
C1QA	Complement C1q A chain	1p36.12	C1q	AR	Complement	Complement deficiencies SLE	(9)
C1QB	Complement C1q B chain	1p36.12	C1q	AR	Complement	Complement deficiencies SLE	(9)
C1QC	Complement C1q C chain	1p36.12	C1q	AR	Complement	Complement deficiencies SLE	(9)
C1R	Complement C1r	12p13.31	C1r	AR	Complement	Complement deficiencies SLE	(10)
C1S	Complement C1s	12p13.31	C1s	AR	Complement	Complement deficiencies SLE	(11)
C2	Complement C2	6p21.33	C2	AR	Complement	Complement deficiencies SLE	(12)
C4A	complement C4A	6p21.33	C4	AR	Complement	Complement deficiencies SLE	(13)
C4B	complement C4B	6p21.33	C4	AR	Complement	Complement deficiencies SLE	(13)
CYBB	Cytochrome b-245 beta chain	Xp21.1-p11.4	NADPH oxidase 2	X-linked	Phagocytosis	Chronic granulomatous disease	(14)
DNASE1	Deoxyribonuclease 1	16p13.3	DNASE1	AD	Nucleic acid sensing and degradation	SLE	(15)
DNASE1L3	Deoxyribonuclease 1 like 3	3p14.3	DNASE1L3	AR	Nucleic acid sensing and degradation	SLE	(16)
FAS or TNFRSF6	Fas cell surface death receptor	10q23.31	FAS	AD	Apoptosis	ALPS	(17)
FASL	Fas ligand	1q24.3	FASL	AD	Apoptosis	ALPS	(18)
IFIH1	Interferon induced with helicase C domain 1	2q24.2	IFIH1	AD	Type I IFN	AGS SLE	(19)
ISG15	ISG15 ubiquitin-like modifier	1p36.33	ISG15	AR	Type I IFN	AGS	(20)
KRAS	KRAS proto-oncogene, GTPase	12p12.1	KRAS	AD	RAS-MAPK signaling	Noonan syndrome	(21)
LAMAN or MAN2B1	Mannosidase alpha class 2B member 1	19p13.13	Lysosomal Alpha-mannosidase	AR	Metabolism of carbohydrates	Alpha-mannosidosis	(22)
PEPD	Peptidase D	19q13.11	PEPD	AR	Aminopeptidase activity	Prolidase defiency	(23)
PRKCD	Protein kinase C delta	3p21.1	PRKCD	AR	Self-tolerance	SLE	(24)
PSMA3	Proteasome subunit alpha 3	14q23.1	PSMA3	AD	Proteasome	CANDLE	(25)
PSMB4	Proteasome subunit beta 4	1q21.3	PSMB4	AD	Proteasome	CANDLE	(25)
PSMB8	Proteasome subunit beta 8	6p21.32	PSMB8	AD	Proteasome	CANDLE	(25)
PTPN11	Protein tyrosine phosphatase, non-receptor type 11	12q24.13	PTPN11	AD	RAS-MAPK signaling	Noonan syndrome	(26)
RAG2	Recombination activating 2	11p12	RAG2	AR/AD	Self-tolerance	SLE	(27)
RNASEH2A	Ribonuclease H2 subunit A	19p13.13	RNASEH2 Complex	AR	Nucleic acid sensing and degradation	AGS	(28)
RNASEH2B	Ribonuclease H2 subunit B	13q14.3	RNASEH2 Complex	AR	Nucleic acid sensing and degradation	AGS	(28)

(Continued)

TABLE 1 | Continued

Locus	Gene name	Gene Location	Protein	Inheritance	Pathway	Phenotype	References
RNASEH2C	Ribonuclease H2 subunit C	11q13.1	RNASEH2 Complex	AR	Nucleic acid sensing and degradation	AGS	(28)
SAMHD1	SAM and HD domain containing deoxynucleoside triphosphate triphosphohydrolase 1	20q11.23	SAMHD1	AR	Type I IFN	AGS SLE FCL	(29, 30)
SHOC2	SHOC2, leucine rich repeat scaffold protein	10q25.2	SHOC2	AD	RAS-MAPK signaling	Noonan syndrome	(31)
SLC7A7	Solute carrier family 7 member 7	14q11.2	SLC7A7	AR	Amino acid transporter	Lysinuric protein intolerance	(32)
TMEM173	transmembrane protein 173	5q31.2	STING	AD	Type I IFN	SAVI	(33)
TREX1	three prime repair exonuclease 1	3p21.31	TREX1	AD	Nucleic acid sensing and degradation	AGS FCL	(34)

AGS, Aicardi-Goutières Syndrome; AD, autosomal dominant; ALPS, autoimmune lymphoproliferative syndrome; AR, autosomal recessive; CANDLE, chronic atypical neutrophilic dermatosis with lipodystrophy and elevated temperature; FCL, familial chilblain lupus; SAVI, STING-associated vasculopathy with onset in infancy; SLE, systemic lupus erythematosus; SPENCD, Spondyloenchondrodysplasia.

RNaseH2 (Ribonuclease H2) is a nucleic acid repair surveillance enzyme expressed in all cells and functions to remove ribonucleotides from DNA hybrid complexes. Three different genes encode the three protein components of the RNaseH2 complex, *RNASEH2A*, *RNASEH2B* and *RNASEH2C*. Mutations in all three genes have been associated with AGS and SLE. A recent study established mice models in which mutations in *RNASEH2B* trigger an increase of the expression levels of ISGs. The results of this work also proposed that this inflammatory response is dependent upon the cGAS/STING pathway (28). The findings of another study described that these mutations result in accumulation of ribonucleotides in genomic DNA placed during replication, which causes chronic DNA damage triggering the p53 pathway and type I IFN production (55). It has also been reported that fibroblasts from patients with SLE and AGS secondary to RNaseH2 mutations, as well as RNaseH2 deficient mice have significant accumulation of ribonucleotides and increased DNA in the cytoplasm. Furthermore, patient fibroblasts revealed an upregulation in IFN stimulated genes, which was enhanced, among other factors, by UV light exposure. UV light is a major trigger of SLE symptoms and it is thought that UV can raise apoptotic debris containing nucleic acids. Therefore, a deficiency in RNAseH2 in individuals exposed to UV light could be a possible link between genetic and environmental factors in the pathogenesis of SLE (55). Approximately one-third of AGS patients with variants in the RNaseH2 complex have positive ANA. Sequencing of the genes encoding the RNaseH2 complex in 600 SLE subjects identified 18 rare variants. Clinically, these patients mainly showed cutaneous involvement, photosensitivity, arthritis, lymphopenia, and autoantibody formation; internal organ involvement was less frequent (41).

ADAR1 (adenosine deaminase, RNA specific) gene, located on chromosome 1, encodes a widely expressed enzyme which is involved in the editing of long double strand RNA. Mutations in this gene have been reported to cause AGS and SLE (7, 8). A proinflammatory signal upon recognition of viral or cellular dsRNA unedited due to loss of function mutations in *ADAR1* has been described (56). Interestingly, mutations in this gene also cause Dyscrhromatosus Symmetrica Hereditaria (DSH1), a rare skin condition which has been associated with SLE (57).

ISG15 is transcriptionally regulated by IFN-alpha and beta. Patients with ISG15 deficiency have increased risk of viral infection. Mutations in *ISG15* are associated with central nervous system (CNS) disease including intracranial calcifications and seizures (20). Patients show immunological and clinical signs of enhanced IFN-alpha/beta immunity. Interestingly, mutations in *ISG15* have been found in AGS and, in addition, a higher expression of this gene in SLE patients has been reported in several studies (58–60) ISG15 negatively regulates IFN-alpha and beta production (58), and is known as an activator of natural killer (NK) cells and a driver of IFNγ secretion (61). Therefore, ISG15 has emerged as a potentially critical bridge between type I and type II IFN immune responses.

Spondyloenchondrodysplasia

Spondyloenchondrodysplasia (SPENCD) is a rare immuno-osseous disorder which causes skeletal dysplasia as well as variable neurologic manifestations (spacticity, developmental delay, intracranial calcification). In addition, it has been reported that SPENCD patients also may show overlapping features of lupus such as nephritis, thrombocytopenia, and dsDNA antibodies amongst others. Indeed, some of these patients fulfilled the American College of Rheumatology classification criteria for lupus (6, 62). The *ACP5* gene encodes tartrate-resistant acid phosphate (TRAP) protein which is mostly expressed in monocytic cells including osteoclasts, macrophages, and dendritic cells (63). Several different biallelic null mutations in *ACP5* distributed throughout the protein

have been identified in individuals diagnosed with SPENCD-associated lupus. All mutations identified to date, cause a complete loss of enzymatic function. TRAP regulates the phosphorylation levels of osteopontin (OPN) which is a cytokine required for the production of type I IFN by plasmacytoid dendritic cells in response to TLR9 stimulation (64). It has been described that decreased expression of TRAP triggers increased phosphorylation of OPN leading to overproduction of type I interferon (6, 62). In addition, after TLR9 stimulation, a reduced expression of TRAP provokes higher levels of IFN-alpha, interleukin-6, ISGs, and tumor necrosis factor (TNF) (65). It is worth to note that in a recent study *ACP5* was sequenced in nearly 1,000 SLE patients and more than 500 healthy controls. The results of this study showed a significant increase in heterozygous *ACP5* missense variants in SLE patients compared to healthy individuals (65).

COMPLEMENT DEFICIENCIES

The classical complement pathway begins with C1, which consists of C1q, two C1r molecules, and two C1s molecules. C1 binds to the Fc portion of IgG or IgM antibody which complexes to antigens. The binding results in the activation of C1q which activates C1r, and then activates C1s. C1s cleaves C4 (to C4a and C4b) and C2 (to C2a and C2b). C4b and C2b combine and cleave C3 which is added to the complex resulting in C4bC2bC3b (also known as C5 convertase). This complex will cleave C5 resulting in the assembly of the membrane attack complex (C5bC6C7C8C9). The alternative complement pathway begins with the hydrolysis of C3 to C3(H2O). C3(H2O) is always present to a small degree but is maintained in homeostasis. The alternate pathway is initiated when C3(H2O) binds to factor Bb (factor B having been cleaved by factor D to form factor Ba and Bb) which forms C3b(H2O)Bb. The C3b(H2O)Bb is an alternative C3 convertase (66). Any defect in these complement components might prevent or hinder the removal or clearance of apoptotic cells or immune complexes, thus allowing these potential autoantigens to activate the immune system and lead to a loss of tolerance. Therefore, deficiencies of C1q, C1r, C1s, C2, or C4 have been strongly associated with both immunodeficiency as well as autoimmunity, including lupus-like phenotype (67).

Approximately 90% of people with C1q deficiency develop lupus like-phenotype (9, 68) including clinical characteristics such as photosensitive skin rash, nephritis, oral ulceration, and arthritis. Most of these patients have early onset disease with an age range from 6 months to 42 years, and a median age of onset of 6 years (69). Interestingly, patients with C1q deficiency have normal complement C3 and C4 levels with low total hemolytic complement levels which can be a helpful tool in diagnosis (70). Of interest, there are case reports of treatment with plasma transfusion, which restores C1q levels, leading to resolution of symptoms (71). Another small case series reported successful cure of patients with a C1q deficiency with bone marrow transplantation (72). C1q is encoded by three genes (*C1QA*, *C1QB,* and *C1QC*) which are closely linked on chromosome 1p34-1p36 (69). Multiple causal mutations, in the three genes, resulting in the deficiency of C1q have been identified in individuals with SLE-like phenotype. C1q is directly responsible for identification and opsonization of apoptotic cells which stimulates phagocytosis and activates the classical complement pathway. Apoptosis generates cellular debris, which if not properly cleared, can promote autoimmunity. Thus, deficiency of C1q results in autoantigen presentation with subsequent loss of tolerance (44). In addition, C1q suppresses IFN alpha production by interacting with leucocyte associated Ig-like receptor (LAIR)1 on plasmacytoid dendritic cells, and indirectly through uptake of C1q containing immune complexes by monocytes rather than plasmacytoid dendritic cells which are the primary producers of IFN alpha (68). Furthermore, C1q can inhibit TLR7 and TLR9 induced IFN-alpha production. Consequently, it has been described that patients with C1q deficiency develop increased levels of IFN alpha (9, 68). Taken into consideration the IFN-signature found in these patients, complement deficiencies could be also considered as secondary interferonopathies.

Deficiencies in C1r and C1s are rare and these patients usually die at a young age due to recurrent and severe infections. However, more than a half of these patients develop a lupus-like disease, with skin involvement and ANA positivity being the most noticeable features (73). Both genes encoding C1s and C1r are located on the short arm of chromosome 12 and several deleterious mutations, resulting in no detectable protein in the serum, have been identified in patients with lupus-like phenotype. Remarkably, consistent reduction in the serum protein levels of C1s in patients with C1r deficiency and low levels of C1r in patients with C1s deficiency have been observed (10, 11, 74).

C2 is the most common complement deficiency, occurring in about 1 in 20,000 individuals of European descent, however lupus develops only in about 10% of patients with C2 deficiency (73). This is likely due to the fact that C2 can be bypassed by the alternative complement pathway and is therefore not required for activation of the complement system (12). Patients with SLE secondary to C2 deficiency are similar in presentation and severity to the general SLE population, with a mean age of onset of 39 years. These patients will typically develop multiple infections at an early age, but are otherwise phenotypically similar to other patients with SLE (75).

C4 is a key component of the classical complement pathway. Homozygous deficiency of C4 results in a dysfunctional immune response which can cause lupus with >75% of penetrance (76). This protein is encoded by two genes, *C4A* and *C4B*, closely located within the human major histocompatibility complex (MHC) on chromosome 6. There is a complex pattern of variation in this region and duplications of C4 genes are common. The copy number variation (CNV) of these genes range from two to eight copies (13). Interestingly, the relationship of C4 gene copy number with non-Mendelian SLE has been repeatedly analyzed in different populations and the results of

these studies consistently reported that the fewer the number of gene copies the higher the risk of lupus. Conversely, an increased number of C4 gene numbers is protective (77, 78). A deficiency in C4 in mice alters B cell tolerance by increasing the number of self-reactive B cells. These mice develop lupus-like features like glomerulonephritis and high levels of autoantibodies (79).

AUTOIMMUNE LYMPHOPROLIFERATIVE SYNDROME

Autoimmune lymphoproliferative syndrome (ALPS) is a rare autoimmune disease mainly caused by mutations in FAS-mediated apoptotic pathway genes (17, 18). ALPS patients present with clinical features similar to SLE and mutations in these genes have been associated with both diseases (17, 18). The fas cell surface death receptor (FAS) is a protein in the TNF receptor superfamily. It plays a key role in programmed cell death; the binding of this receptor with its ligand results in signaling complex that includes Fas-associated death domain protein (FADD), caspase 8, and caspase 10 (17). Apoptosis is of particular interest in lupus as abnormalities in this process provide a source of autoantigens which are thought to drive the autoimmune response in this disease. Apoptotic cell death results in increased DNA fragments, which if not properly processed can accumulate and result in autoimmunity. *FAS* gene polymorphisms have been shown to be associated with SLE (80) and variants in the *FASL* gene have been related to increase apoptosis (81). In this context, it is noteworthy that mice with deficiencies in Fas and FasL develop clinical features similar to SLE and ALPS, thus represent useful murine models to study the pathophysiology of both diseases. Specifically, MRL/*lpr* mice have been widely used to investigate lupus and these studies significantly contributed to our current knowledge of the pathogenesis of SLE (82, 83).

OTHER GENES INVOLVED IN MONOGENIC LUPUS

PRKCD (protein kinase c delta) is a signaling kinase with multiple downstream target proteins which plays a role in

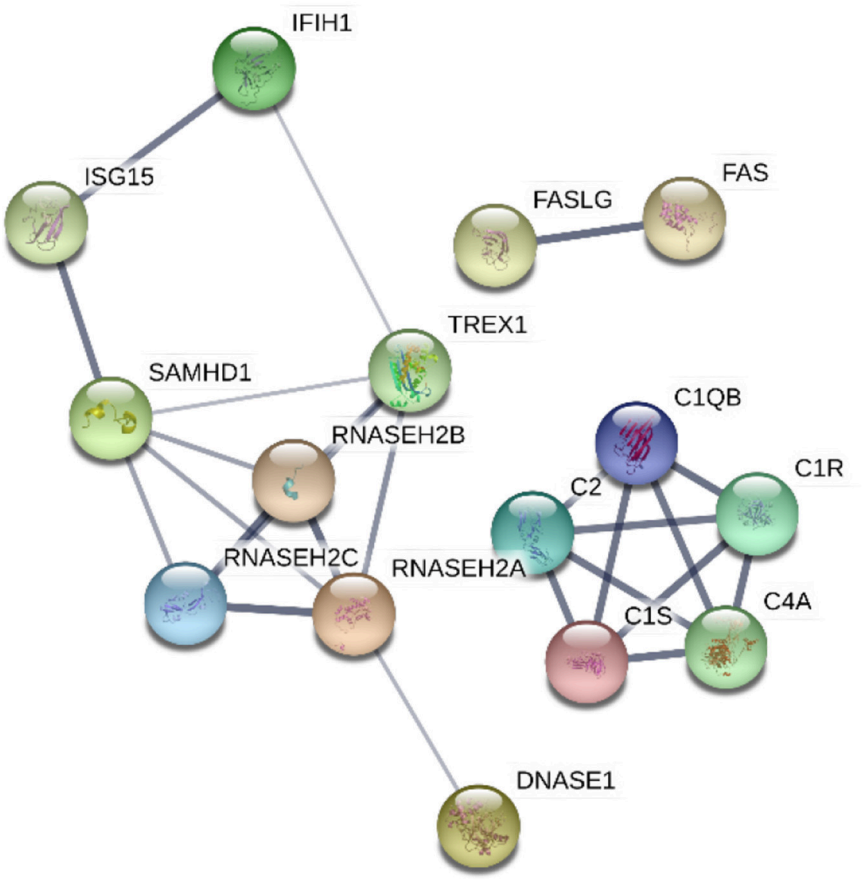

FIGURE 2 | Protein-protein interaction network of proteins encoded by genes found to cause monogenic lupus. The confidence of data supporting these interactions are represented by the thickness of the lines. The analysis was performed using STRING V10.0 (STRING https://string-db.org/).

regulating B cell development, proliferation, and apoptosis (84). The absence of PRKCD results in chronic B cell receptor signaling, decreased apoptosis, and increased response to stimulation. Conversely, overexpression of PRKCD results in inhibition of cell growth (85). A mutation in the *PRKCD* gene has been identified in a family with monogenic SLE, and is associated with loss of B cell tolerance and an increased number of immature B cells even in family members heterozygous for the mutation (24). In addition, PRKCD has a negative role in T cell proliferation and a deficiency in PRKCD results in increased T cell activation contributing to T cell autoimmunity (84). Patients with SLE secondary to *PRKCD* mutation demonstrate typical features of lupus including autoantibody production as well as increased incidence of glomerulonephritis.

Both *DNASE1* (deoxyribonuclease 1) and *DNASE1L3* (deoxyribonuclease 1 like 3) genes encode proteins involved in the nucleic acid degradation pathway. DNASE1L3 enzyme plays an important role in the clearance of DNA debris from apoptotic cells and exogenous DNA. A loss of function variant in this gene has been identified as the cause of a monogenic form of lupus. Positive ANA, anti-dsDNA, and hypocomplementemia among other features were present in all lupus patients harboring this variant (16). DNASE1L3 variations have also been reported in patients with hypocomplementemic urticarial vasculitis syndrome (86). A heterozygous null allele in *DNASE1*, which encodes for an endonuclease with certain degree of homology to DNASE1L3, has also been identified in individuals diagnosed with a monogenic form of SLE (15). Further studies have also reported the association of polymorphisms in *DNASE1* with non-Mendelian SLE (87). All these findings are consistent with the demonstration that mice deficient in DNASE1 develop a lupus-like phenotype (88). Interestingly, mutations in *DNASE2*, which encodes another member of the DNAse family, have been identified in three children presenting with severe autoimmune features. Although these patients did not fulfill criteria for a classification of SLE, all of them showed high levels of anti-DNA antibodies among others lupus-like symptoms (89).

Others monogenic disorders presenting rare cases of lupus-like phenotype have been reported. Although in most of them the mechanism causing autoimmunity is unclear, several causal genes have been described (**Table 1**), including *CYBB* gene causing chronic granulomatous disease, *PTPN11* and *SHOC2* genes associated with Noonan Syndrome, among others. Further studies focused on understanding the role of these genes in autoimmunity will help to better understand the pathogenesis of SLE.

FINAL CONSIDERATIONS

Understanding the implications of the genes identified to cause monogenic lupus have enhanced our knowledge of pathways and molecular mechanisms involved in the pathogenesis of SLE. As it has been explored through this review, monogenic lupus results from mutations in genes related to the immune response, either in the innate or in the adaptive immune system. Furthermore, protein-protein interaction analysis suggests that these genes encode proteins with related functions, creating molecular networks (**Figure 2**). Specifically, these genes are primarily involved in pathways including the complement system, nucleic acid repair, nucleic acid degradation and sensing, apoptosis, and type I interferon regulation. Although we do not yet know the full extent of monogenic lupus, the study of this type of lupus has provided new areas of investigation applicable to non-Mendelian SLE. Many genes have been identified as causes of monogenic lupus and at the same time have been associated with common forms of SLE, such as C4 number variation and polymorphisms in *TREX1*, among others. Besides, a recent study proposes that a set of rare variants across *PRKCD* play a role in a wider context of SLE susceptibility (90). Altogether, these findings reinforce the idea of analyzing the genetics of complex diseases by taking into consideration their Mendelian forms, and highlight the potential contribution of rare variants to the heritability of SLE.

The molecular complexity of autoimmune diseases and the clinical overlap among them makes accurate diagnosis and specific targeted therapy more challenging. In this context, a better knowledge of the genetic bases may generate insights into biomarker development and new drug targets.

AUTHOR CONTRIBUTIONS

All authors listed have made a substantial, direct and intellectual contribution to the work, and approved it for publication.

FUNDING

This work was supported by the National Institute of Allergy and Infectious Diseases of the National Institutes of Health grants number R01AI097134 and U19AI110502, the National Institute of Arthritis and Musculoskeletal and Skin Diseases of the National Institutes of Health grant number R01AR070148, and the Lupus Research Alliance.

ACKNOWLEDGMENTS

We would like to thank Patrick Coit for graphical support.

REFERENCES

1. Wu H, Zhao M, Tan L, Lu Q. The key culprit in the pathogenesis of systemic lupus erythematosus: Aberrant DNA methylation. *Autoimmun Rev.* (2016) 15:684–9. doi: 10.1016/j.autrev.2016.03.002
2. Mohan C, Putterman C. Genetics and pathogenesis of systemic lupus erythematosus and lupus nephritis. *Nat Rev Nephrol.* (2015) 11:329–41. doi: 10.1038/nrneph.2015.33
3. Deapen D, Escalante A, Weinrib L, Horwitz D, Bachman B, Roy-Burman P, Walker A, et al. A revised estimate of twin concordance

in systemic lupus erythematosus. *Arthritis Rheum.* (1992) 35:311–8. doi: 10.1002/art.1780350310
4. Javierre BM, Fernandez AF, Richter J, Al-Shahrour F, Martin-Subero JI, Rodriguez-Ubreva J, et al. Changes in the pattern of DNA methylation associate with twin discordance in systemic lupus erythematosus. *Genome Res.* (2010) 20:170–9. doi: 10.1101/gr.100289.109
5. Webb R, Kelly JA, Somers EC, Hughes T, Kaufman KM, Sanchez E, et al. Early disease onset is predicted by a higher genetic risk for lupus and is associated with a more severe phenotype in lupus patients. *Ann Rheum Dis.* (2011) 70:151–6. doi: 10.1136/ard.2010.141697
6. Briggs TA, Rice GI, Daly S, Urquhart J, Gornall H, Bader-Meunier B, et al. Tartrate-resistant acid phosphatase deficiency causes a bone dysplasia with autoimmunity and a type I interferon expression signature. *Nat Genet.* (2011) 43:127–31. doi: 10.1038/ng.748
7. Crow YJ, Chase DS, Lowenstein Schmidt J, Szynkiewicz M, Forte GM, Gornall HL, et al. Characterization of human disease phenotypes associated with mutations in TREX1, RNASEH2A, RNASEH2B, RNASEH2C, SAMHD1, ADAR, and IFIH1. *Am J Med Genet A* (2015) 167A:296–312. doi: 10.1002/ajmg.a.36887
8. Rice GI, Kasher PR, Forte GM, Mannion NM, Greenwood SM, Szynkiewicz M, et al. Mutations in ADAR1 cause Aicardi-Goutieres syndrome associated with a type I interferon signature. *Nat Genet.* (2012) 44:1243–48. doi: 10.1038/ng.2414
9. Lood C, Gullstrand B, Truedsson L, Olin AI, Alm GV, Ronnblom L, et al. C1q inhibits immune complex-induced interferon-alpha production in plasmacytoid dendritic cells: a novel link between C1q deficiency and systemic lupus erythematosus pathogenesis. *Arthritis Rheum.* (2009) 60:3081–90. doi: 10.1002/art.24852
10. Demirkaya E, Zhou Q, Smith CK, Ombrello MJ, Deuitch N, Tsai WL, et al. Brief report: deficiency of complement 1r subcomponent in early-onset systemic lupus erythematosus: the role of disease-modifying alleles in a monogenic disease. *Arthritis Rheumatol.* (2017) 69:1832–39. doi: 10.1002/art.40158
11. Bienaime F, Quartier P, Dragon-Durey MA, Fremeaux-Bacchi V, Bader-Meunier B, Patey N, et al. Lupus nephritis associated with complete C1s deficiency efficiently treated with rituximab: a case report. *Arthritis Care Res.* (2010) 62:1346–50. doi: 10.1002/acr.20163
12. Miller EC, Atkinson JP. Overcoming C2 deficiency. *Clin Immunol.* (2012) 144:269–71. doi: 10.1016/j.clim.2012.07.005
13. Blanchong CA, Chung EK, Rupert KL, Yang Y, Yang Z, Zhou B, Moulds JM, Yu CY. Genetic, structural and functional diversities of human complement components C4A and C4B and their mouse homologues, Slp and C4. *Int Immunopharmacol.* (2001) 1:365–92. doi: 10.1016/S1567-5769(01)00019-4
14. Battersby AC, Cale AM, Goldblatt D, Gennery AR. Clinical manifestations of disease in X-linked carriers of chronic granulomatous disease. *J Clin Immunol.* (2013) 33:1276–84. doi: 10.1007/s10875-013-9939-5
15. Yasutomo K, Horiuchi T, Kagami S, Tsukamoto H, Hashimura C, Urushihara M, et al. Mutation of DNASE1 in people with systemic lupus erythematosus. *Nat Genet.* (2001) 28:313–4. doi: 10.1038/91070
16. Al-Mayouf SM, Sunker A, Abdwani R, Abrawi SA, Almurshedi F, Alhashmi N, et al. Loss-of-function variant in DNASE1L3 causes a familial form of systemic lupus erythematosus. *Nat Genet.* (2011) 43:1186–8. doi: 10.1038/ng.975
17. Agrebi N, Ben-Mustapha I, Matoussi N, Dhouib N, Ben-Ali M, Mekki N, et al. Rare splicing defects of FAS underly severe recessive autoimmune lymphoproliferative syndrome. *Clin Immunol.* (2017) 183:17–23. doi: 10.1016/j.clim.2017.06.009
18. Wu J, Wilson J, He J, Xiang L, Schur PH, Mountz JD. Fas ligand mutation in a patient with systemic lupus erythematosus and lymphoproliferative disease. *J Clin Invest.* (1996) 98:1107–13. doi: 10.1172/JCI118892
19. Rice GI, Del Toro Duany Y, Jenkinson EM, Forte GM, Anderson BH, Ariaudo G, et al. Gain-of-function mutations in IFIH1 cause a spectrum of human disease phenotypes associated with upregulated type I interferon signaling. *Nat Genet.* (2014) 46:503–9. doi: 10.1038/ng.2933
20. Hermann M, Bogunovic D. ISG15: In Sickness and in Health. *Trends Immunol.* (2017) 38:79–93. doi: 10.1016/j.it.2016.11.001
21. Leventopoulos G, Denayer E, Makrythanasis P, Papapolychroniou C, Fryssira H. Noonan syndrome and systemic lupus erythematosus in a patient with a novel KRAS mutation. *Clin Exp Rheumatol.* (2010) 28:556–7.
22. Urushihara M, Kagami S, Yasutomo K, Ito M, Kondo S, Kitamura A., Sisters with alpha-mannosidosis and systemic lupus erythematosus. *Eur J Pediatr.* (2004) 163:192–5. doi: 10.1007/s00431-004-1404-2
23. Klar A, Navon-Elkan P, Rubinow A, Branski D, Hurvitz H, Christensen E, et al. Prolidase deficiency: it looks like systemic lupus erythematosus but it is not. *Eur J Pediatr.* (2010) 169:727–32. doi: 10.1007/s00431-009-1102-1
24. Belot A, Kasher PR, Trotter EW, Foray AP, Debaud AL, Rice GI, S et al. Protein kinase cdelta deficiency causes mendelian systemic lupus erythematosus with B cell-defective apoptosis and hyperproliferation. *Arthritis Rheum.* (2013) 65:2161–71. doi: 10.1002/art.38008
25. Al-Mayouf SM, AlSaleem A, AlMutairi N, AlSonbul A, Alzaid T, Alazami AM, et al. Monogenic interferonopathies: Phenotypic and genotypic findings of CANDLE syndrome and its overlap with C1q deficient SLE. *Int J Rheum Dis.* (2018) 21:208–13. doi: 10.1111/1756-185X.13228
26. Quaio CR, Carvalho JF, da Silva CA, Bueno C, Brasil AS, Pereira AC, et al. Autoimmune disease and multiple autoantibodies in 42 patients with RASopathies. *Am J Med Genet A* (2012) 158A:1077–82. doi: 10.1002/ajmg.a.35290
27. Walter JE, Lo MS, Kis-Toth K, Tirosh I, Frugoni F, Lee YN, et al. Impaired receptor editing and heterozygous RAG2 mutation in a patient with systemic lupus erythematosus and erosive arthritis. *J Allergy Clin Immunol.* (2015) 135:272–3. doi: 10.1016/j.jaci.2014.07.063
28. Mackenzie KJ, Carroll P, Lettice L, Tarnauskaite Z, Reddy K, Dix F, et al. Ribonuclease H2 mutations induce a cGAS/STING-dependent innate immune response. *EMBO J.* (2016) 35:831–44. doi: 10.15252/embj.201593339
29. Abdel-Salam GM, El-Kamah GY, Rice GI, El-Darouti M, Gornall H, Szynkiewicz M, et al. Chilblains as a diagnostic sign of aicardi-goutieres syndrome. *Neuropediatrics* (2010) 41:18–23. doi: 10.1055/s-0030-1255059
30. Ravenscroft JC, Suri M, Rice GI, Szynkiewicz M, Crow YJ. Autosomal dominant inheritance of a heterozygous mutation in SAMHD1 causing familial chilblain lupus. *Am J Med Genet A* (2011) 155A:235–7. doi: 10.1002/ajmg.a.33778
31. Bader-Meunier B, Cave H, Jeremiah N, Magerus A, Lanzarotti N, Rieux-Laucat F, et al. Are RASopathies new monogenic predisposing conditions to the development of systemic lupus erythematosus? Case report and systematic review of the literature. *Semin Arthritis Rheum.* (2013) 43:217–9. doi: 10.1016/j.semarthrit.2013.04.009
32. Esteve E, Krug P, Hummel A, Arnoux JB, Boyer O, Brassier A, et al. Renal involvement in lysinuric protein intolerance: contribution of pathology to assessment of heterogeneity of renal lesions. *Hum Pathol.* (2017) 62:160–9. doi: 10.1016/j.humpath.2016.12.021
33. Liu Y, Jesus AA, Marrero B, Yang D, Ramsey SE, Sanchez GAM, et al. Activated STING in a vascular and pulmonary syndrome. *N Engl J Med.* (2014) 371:507–18. doi: 10.1056/NEJMoa1312625
34. Rice GI, Rodero MP, Crow YJ. Human disease phenotypes associated with mutations in TREX1. *J Clin Immunol.* (2015) 35:235–43. doi: 10.1007/s10875-015-0147-3
35. Baechler EC, Batliwalla FM, Karypis G, Gaffney PM, Ortmann WA, Espe KJ, et al. Interferon-inducible gene expression signature in peripheral blood cells of patients with severe lupus. *Proc Natl Acad Sci USA.* (2003) 100:2610–5. doi: 10.1073/pnas.0337679100
36. Reynier F, Petit F, Paye M, Turrel-Davin F, Imbert PE, Hot A, et al. Importance of correlation between gene expression levels: application to the type I interferon signature in rheumatoid arthritis. *PLoS ONE* (2011) 6:e24828. doi: 10.1371/journal.pone.0024828
37. Crow YJ. Aicardi-Goutieres Syndrome. In: Adam MP, Ardinger HH, Pagon RA, Wallace SE, Bean LJH, Stephens K, Amemiya A, editors *GeneReviews((R))*. Seattle, WA (1993).
38. DiFrancesco JC, Novara F, Zuffardi O, Forlino A, Gioia R, Cossu F, et al. TREX1 C-terminal frameshift mutations in the systemic variant of retinal vasculopathy with cerebral leukodystrophy. *Neurol Sci.* (2015) 36:323–30. doi: 10.1007/s10072-014-1944-9
39. Ellyard JI, Jerjen R, Martin JL, Lee AY, Field MA, Jiang SH, et al. Identification of a pathogenic variant in TREX1 in early-onset cerebral systemic lupus

erythematosus by Whole-exome sequencing. *Arthritis Rheumatol.* (2014) 66:3382–6. doi: 10.1002/art.38824
40. Lee-Kirsch MA, Gong M, Chowdhury D, Senenko L, Engel K, Lee YA, et al. Mutations in the gene encoding the 3'-5' DNA exonuclease TREX1 are associated with systemic lupus erythematosus. *Nat Genet.* (2007) 39:1065–7. doi: 10.1038/ng2091
41. Barizzone N, Monti S, Mellone S, Godi M, Marchini M, Scorza R, et al. Rare variants in the TREX1 gene and susceptibility to autoimmune diseases. *Biomed Res Int.* (2013) 2013:471703. doi: 10.1155/2013/471703
42. Namjou B, Kothari PH, Kelly JA, Glenn SB, Ojwang JO, Adler A, et al. Evaluation of the TREX1 gene in a large multi-ancestral lupus cohort. *Genes Immun.* (2011) 12:270–9. doi: 10.1038/gene.2010.73
43. Hiraki LT, Silverman ED. Genomics of systemic lupus erythematosus: insights gained by studying monogenic young-onset systemic lupus erythematosus. *Rheum Dis Clin North Am.* (2017) 43:415–34. doi: 10.1016/j.rdc.2017.04.005
44. Costa-Reis P, Sullivan KE. Monogenic lupus: it's all new! *Curr Opin Immunol.* (2017) 49:87–95. doi: 10.1016/j.coi.2017.10.008
45. Chowdhury D, Beresford PJ, Zhu P, Zhang D, Sung JS, Demple B, et al. The exonuclease TREX1 is in the SET complex and acts in concert with NM23-H1 to degrade DNA during granzyme A-mediated cell death. *Mol Cell* (2006) 23:133–42. doi: 10.1016/j.molcel.2006.06.005
46. de Carvalho LM, Ngoumou G, Park JW, Ehmke N, Deigendesch N, Kitabayashi N, et al. Musculoskeletal disease in MDA5-related type I interferonopathy: a mendelian mimic of Jaccoud's arthropathy. *Arthritis Rheumatol.* (2017) 69:2081–91. doi: 10.1002/art.40179
47. Lo MS, Tsokos GC. Recent developments in systemic lupus erythematosus pathogenesis and applications for therapy. *Curr Opin Rheumatol.* (2018) 30:222–8. doi: 10.1097/BOR.0000000000000474
48. Funabiki M, Kato H, Miyachi Y, Toki H, Motegi H, Inoue M, et al. Autoimmune disorders associated with gain of function of the intracellular sensor MDA5. *Immunity* (2014) 40:199–212. doi: 10.1016/j.immuni.2013.12.014
49. Gono T, Kawaguchi Y, Sugiura T, Furuya T, Kawamoto M, Hanaoka M, et al. Interferon-induced helicase (IFIH1) polymorphism with systemic lupus erythematosus and dermatomyositis/polymyositis. *Mod Rheumatol.* (2010) 20:466–70. doi: 10.3109/s10165-010-0311-9
50. Zhang SH, Zhao Y, Xie QB, Jiang Y, Wu YK, Yan B. Aberrant activation of type I interferon system may contribute to the pathogenesis of anti-MDA5 dermatomyositis. *Br J Dermatol.* (2018). doi: 10.1111/bjd.16917. [Epub ahead of print].
51. Ballana E, Este JA. SAMHD1: at the crossroads of cell proliferation, immune responses, and virus restriction. *Trends Microbiol.* (2015) 23:680–92. doi: 10.1016/j.tim.2015.08.002
52. Rehwinkel J, Maelfait J, Bridgeman A, Rigby R, Hayward B, Liberatore RA, et al. SAMHD1-dependent retroviral control and escape in mice. *EMBO J.* (2013) 32:2454–62. doi: 10.1038/emboj.2013.163
53. Kretschmer S, Wolf C, Konig N, Staroske W, Guck J, Hausler M, et al. SAMHD1 prevents autoimmunity by maintaining genome stability. *Ann Rheum Dis.* (2015) 74:e17. doi: 10.1136/annrheumdis-2013-204845
54. Tungler V, Staroske W, Kind B, Dobrick M, Kretschmer S, Schmidt F, et al. Single-stranded nucleic acids promote SAMHD1 complex formation. *J Mol Med.* (2013) 91:759–70. doi: 10.1007/s00109-013-0995-3
55. Gunther C, Kind B, Reijns MA, Berndt N, Martinez-Bueno M, Wolf C, et al. Defective removal of ribonucleotides from DNA promotes systemic autoimmunity. *J Clin Invest.* (2015) 125:413–24. doi: 10.1172/JCI78001
56. Gallo A, Vukic D, Michalik D, O'Connell MA, Keegan LP. ADAR RNA editing in human disease; more to it than meets the I. *Hum Genet.* (2017) 136:1265–78. doi: 10.1007/s00439-017-1837-0
57. Al-Saif F, Alhumidi A, Alhallaf RA. Dyschromatosis symmetrica hereditaria with cutaneous lupus erythematosus and hyperthyroidism. *Int Med Case Rep J.* (2017) 10:149–52. doi: 10.2147/IMCRJ.S132489
58. Yuan Y, Ma H, Ye Z, Jing W, Jiang Z. Interferon-stimulated gene 15 expression in systemic lupus erythematosus : Diagnostic value and association with lymphocytopenia. *Z Rheumatol.* (2017) 77:256–62. doi: 10.1007/s00393-017-0274-8.
59. Feng X, Huang J, Liu Y, Xiao L, Wang D, Hua B, et al. Identification of interferon-inducible genes as diagnostic biomarker for systemic lupus erythematosus. *Clin Rheumatol.* (2015) 34:71–9. doi: 10.1007/s10067-014-2799-4
60. Zhang X, Bogunovic D, Payelle-Brogard B, Francois-Newton V, Speer SD, Yuan C, et al. Human intracellular ISG15 prevents interferon-alpha/beta over-amplification and auto-inflammation. *Nature* (2015) 517:89–93. doi: 10.1038/nature13801
61. D'Cunha J, Knight E Jr, Haas AL, Truitt RL, Borden EC. Immunoregulatory properties of ISG15, an interferon-induced cytokine. *Proc Natl Acad Sci USA.* (1996) 93:211–5. doi: 10.1073/pnas.93.1.211
62. Lausch E, Janecke A, Bros M, Trojandt S, Alanay Y, De Laet C, et al. Genetic deficiency of tartrate-resistant acid phosphatase associated with skeletal dysplasia, cerebral calcifications and autoimmunity. *Nat Genet.* (2011) 43:132–7. doi: 10.1038/ng.749
63. Oddie GW, Schenk G, Angel NZ, Walsh N, Guddat LW, de Jersey J, et al. Structure, function, and regulation of tartrate-resistant acid phosphatase. *Bone* (2000) 27:575–84. doi: 10.1016/S8756-3282(00)00368-9
64. Shinohara ML, Lu L, Bu J, Werneck MB, Kobayashi KS, Glimcher LH, et al. Osteopontin expression is essential for interferon-alpha production by plasmacytoid dendritic cells. *Nat Immunol.* (2006) 7:498–506. doi: 10.1038/ni1327
65. An J, Briggs TA, Dumax-Vorzet A, Alarcon-Riquelme ME, Belot A, Beresford M, et al. Tartrate-resistant acid phosphatase deficiency in the predisposition to systemic lupus erythematosus. *Arthritis Rheumatol.* (2017) 69:131–42. doi: 10.1002/art.39810
66. Hochberg MC, Silman AJ, Smolen JS, Weinblatt ME, Weisman MH. *Rheumatology E-Book.* Elsevier Health Sciences (2014).
67. Chen M, Daha MR, Kallenberg CG. The complement system in systemic autoimmune disease. *J Autoimmun.* (2010) 34:J276–86. doi: 10.1016/j.jaut.2009.11.014
68. Hagberg N, Rönnblom L. Systemic lupus erythematosus–a disease with a dysregulated type i interferon system. *Scandinav J Immunol.* (2015) 82:199–207. doi: 10.1111/sji.12330
69. Lipsker D, Hauptmann G. Cutaneous manifestations of complement deficiencies. *Lupus* (2010) 19:1096–106. doi: 10.1177/0961203310373370
70. Lintner KE, Wu YL, Yang Y, Spencer CH, Hauptmann G, Hebert LA, et al. Early components of the complement classical activation pathway in human systemic autoimmune diseases. *Front Immunol.* (2016) 7:36. doi: 10.3389/fimmu.2016.00036
71. Mehta P, Norsworthy PJ, Hall AE, Kelly SJ, Walport MJ, Botto M, et al. SLE with C1q deficiency treated with fresh frozen plasma: a 10-year experience. *Rheumatology* (2010) 49:823–4. doi: 10.1093/rheumatology/kep387
72. Arkwright PD, Riley P, Hughes SM, Alachkar H, Wynn RF. Successful cure of C1q deficiency in human subjects treated with hematopoietic stem cell transplantation. *J Allergy Clin Immunol.* (2014) 133:265–7. doi: 10.1016/j.jaci.2013.07.035
73. Pickering MC, Botto M, Taylor PR, Lachmann PJ, Walport MJ. Systemic lupus erythematosus, complement deficiency, and apoptosis. *Adv Immunol.* (2000) 76:227–324. doi: 10.1016/S0065-2776(01)76021-X
74. Wu YL, Brookshire BP, Verani RR, Arnett FC, Yu CY. Clinical presentations and molecular basis of complement C1r deficiency in a male African-American patient with systemic lupus erythematosus. *Lupus* (2011) 20:1126–34. doi: 10.1177/0961203311404914
75. Jönsson G, Sjöholm AG, Truedsson L, Bengtsson AA, Braconier JH, Sturfelt G. Rheumatological manifestations, organ damage and autoimmunity in hereditary C2 deficiency. *Rheumatology* (2007) 46:1133–9. doi: 10.1093/rheumatology/kem023
76. Macedo ACL, Isaac L. Systemic lupus erythematosus and deficiencies of early components of the complement classical pathway. *Front Immunol.* (2016) 7:55. doi: 10.3389/fimmu.2016.00055
77. Yang Y, Chung EK, Wu YL, Savelli SL, Nagaraja HN, Zhou B, et al. Gene copy-number variation and associated polymorphisms of complement component C4 in human systemic lupus erythematosus (SLE): low copy number is a risk factor for and high copy number is a protective factor against SLE susceptibility in European Americans. *Am J Hum Genet.* (2007) 80:1037–54. doi: 10.1086/518257

78. Chen JY, Wu YL, Mok MY, Wu YJ, Lintner KE, Wang CM, et al. Effects of complement C4 gene copy number variations, size dichotomy, and C4A deficiency on genetic risk and clinical presentation of systemic lupus erythematosus in east asian populations. *Arthritis Rheumatol.* (2016) 68:1442–53. doi: 10.1002/art.39589
79. Prodeus AP, Goerg S, Shen LM, Pozdnyakova OO, Chu L, Alicot EM, et al. A critical role for complement in maintenance of self-tolerance. *Immunity* (1998) 9:721–31. doi: 10.1016/S1074-7613(00)80669-X
80. Xiang N, Li XM, Wang GS, Tao JH, Li XP. Association of Fas gene polymorphisms with systemic lupus erythematosus: a meta-analysis. *Mol Biol Rep.* (2013) 40:407–15. doi: 10.1007/s11033-012-2075-0
81. Glesse N, Vianna P, Paim LMG, Matte MCC, Aguiar AKK, Palhano PL, et al. Evaluation of polymorphic variants in apoptotic genes and their role in susceptibility and clinical progression to systemic lupus erythematosus. *Lupus* (2017) 26:746–55. doi: 10.1177/0961203316678671
82. Nickerson KM, Christensen SR, Shupe J, Kashgarian M, Kim D, Elkon K, et al. TLR9 regulates TLR7- and MyD88-dependent autoantibody production and disease in a murine model of lupus. *J Immunol.* (2010) 184:1840–8. doi: 10.4049/jimmunol.0902592
83. Tilstra JS, Avery L, Menk AV, Gordon RA, Smita S, Kane LP, et al. Kidney-infiltrating T cells in murine lupus nephritis are metabolically and functionally exhausted. *J Clin Invest.* (2018) 120859. doi: 10.1172/JCI120859. [Epub ahead of print].
84. Salzer E, Santos-Valente E, Keller B, Warnatz K, Boztug K. Protein Kinase C delta: a Gatekeeper of Immune Homeostasis. *J Clin Immunol.* (2016) 36:631–40. doi: 10.1007/s10875-016-0323-0
85. Miyamoto A, Nakayama K, Imaki H, Hirose S, Jiang Y, Abe M, et al. Increased proliferation of B cells and auto-immunity in mice lacking protein kinase Cδ. *Nature* (2002) 416:865. doi: 10.1038/416865a
86. Ozcakar ZB, Foster J II, Diaz-Horta O, Kasapcopur O, Fan YS, Yalcinkaya F, et al. DNASE1L3 mutations in hypocomplementemic urticarial vasculitis syndrome. *Arthritis Rheum.* (2013) 65:2183–9. doi: 10.1002/art.38010
87. Bodano A, Gonzalez A, Ferreiros-Vidal I, Balada E, Ordi J, Carreira P, et al. Association of a non-synonymous single-nucleotide polymorphism of DNASEI with SLE susceptibility. *Rheumatology* (2006) 45:819–23. doi: 10.1093/rheumatology/kel019
88. Napirei M, Karsunky H, Zevnik B, Stephan H, Mannherz HG, Moroy T. Features of systemic lupus erythematosus in Dnase1-deficient mice. *Nat Genet.* (2000) 25:177–81. doi: 10.1038/76032
89. Rodero MP, Tesser A, Bartok E, Rice GI, Della Mina E, Depp M, et al. Type I interferon-mediated autoinflammation due to DNase II deficiency. *Nat Commun.* (2017) 8:2176. doi: 10.1038/s41467-017-01932-3
90. Pullabhatla V, Roberts AL, Lewis MJ, Mauro D, Morris DL, Odhams CA, et al. *De novo* mutations implicate novel genes in systemic lupus erythematosus. *Hum Mol Genet.* (2018) 27:421–9. doi: 10.1093/hmg/ddx407

Conflict of Interest Statement: The authors declare that the research was conducted in the absence of any commercial or financial relationships that could be construed as a potential conflict of interest.

frontiers in Immunology

REVIEW
published: 16 November 2018
doi: 10.3389/fimmu.2018.02658

Novel Treatments in Lupus

*Milena Vukelic†, Yi Li† and Vasileios C. Kyttaris**

Division of Rheumatology, Beth Israel Deaconess Medical Center, Harvard Medical School, Boston, MA, United States

Purpose of Review: The standard treatment options for systemic lupus erythematosus (SLE) are focused on non-specific immunosuppression. Over the past few years, scientific studies and ongoing clinical trials have shifted the paradigm with rapid advances in developing biologics and small molecules. A number of monoclonal antibodies and small molecule inhibitors have been developed to target specific pathways involved in SLE. Many of these novel therapeutic agents are already being tested in clinical trials and they may 1 day reshape the landscape of SLE treatment. Herein we review potential future therapeutic options for SLE.

Keywords: lupus, biologics, small molecules, treatment, clinical trails

OPEN ACCESS

Edited by:
José Carlos Crispín, Instituto Nacional de Ciencias Médicas y Nutrición Salvador Zubirán (INCMNSZ), Mexico

Reviewed by:
Pier Luigi Meroni, Istituto Auxologico Italiano (IRCCS), Italy
Cheng-De Yang, Shanghai Jiao Tong University, China

****Correspondence:***
Vasileios C. Kyttaris
vkyttari@bidmc.harvard.edu

† These authors have contributed equally to this work

Specialty section:
This article was submitted to Autoimmune and Autoinflammatory Disorders, a section of the journal Frontiers in Immunology

Received: *03 September 2018*
Accepted: *29 October 2018*
Published: *16 November 2018*

Citation:
Vukelic M, Li Y and Kyttaris VC (2018) Novel Treatments in Lupus. Front. Immunol. 9:2658. doi: 10.3389/fimmu.2018.02658

INTRODUCTION

In the past few years, greater understanding of the pathogenesis of SLE has translated into the development of more targeted therapeutic agents in various stages of clinical trials. Current treatment regiments for SLE typically comprise some combination of glucocorticoids, antimalarials, immune suppressive drugs, and cytotoxic agents in severe cases. The first biologic agent approved for SLE, Belimumab, has been in clinical practice for more than 5 years with overall positive albeit modest results (1). Therefore, developing more effective treatment for lupus remains a priority in the field.

Recent studies have identified numerous immunological checkpoints that are dysregulated in SLE and contribute to the loss of self-tolerance. A pipeline of novel agents are being developed to specifically target intracellular signaling pathways, inflammatory cytokines, chemokines, cell surface costimulation molecules, and the proteasome (**Figure 1**). Herein we will review the potential novel treatment options that are currently being tested in clinical trials for SLE.

B Cell Inhibition

Systemic lupus erythematosus is a multisystem autoimmune disease characterized by the production of autoantibodies that primarily target a variety of nuclear antigens, deposit in tissues and activate complement. Plasma cells and their precursors, B cells, are fundamental to the development of these antibodies, and therefore are a prime therapeutic target for intervention in the disease.

B Lymphocyte Stimulator (BLyS)/A Proliferation-Inducing Ligand (APRIL) Belimumab was the first FDA approved fully humanized monoclonal anti-BLyS antibody for use in SLE more than 5 years ago. Administration of Belimumab was found to benefit SLE patients who had positive anti-double-stranded (ds) DNA and low complement (C3 or C4) levels. Moreover, the pivotal trials that lead to the approval of belimumab used a novel at the time composite outcome measure, the SLEDAI response index (SRI). Patients would be regarded SRI responders if they have (1) at least 4 points decrease in their SLEDAI scores over the period of the study, (2) No worsening of the physician global assessment (PGA), and (3). No new BILAG A or more than one BILAG B scores. The original SRI can be modified to require higher decrease in SLEDAI score e.g., by 5 or 6 points (SRI-5, SRI-6, respectively).

Compared to the placebo group's 44% SLEDAI response index (SRI)-4, the belimumab group had SRI-4 of 58%, indicating a statistically significant but yet modest effect. This modest effectiveness was later confirmed by an extensive post- marketing surveillance, as well as, its overall safety profile. Subcutaneously administered belimumab had similar efficacy at week 52 with SRI-4 response of 61.4% vs. placebo 48.4% ($p = 0.0006$) (2). It is worth mentioning that the effectiveness of belimumab remains unclear in severe renal and CNS disease as patients with these manifestations were excluded from the initial studies (1, 3). A study investigating the usefulness of belimumab in patients with lupus nephritis is currently ongoing (NCT01639339).

Tabalumab, a monoclonal antibody against BLyS that neutralizes membrane-bound and soluble BLyS, was assessed for its effectiveness in moderately active lupus in two large phase III clinical trials (ILLUMINATE-1 & 2). Although tabalumab treatment resulted in favorable changes in disease biomarkers (anti-dsDNA abs and complement levels), efficacy was marginal with SRI-5 of 38.4% in the tabalumab-treated vs. 27.7% in the placebo group ($p = 0.002$) in one trial. There was no statistical difference between the two groups in the second trial. Again, the treatment with tabalumab was found to be relatively safe as was the case with belimumab (4–6).

Blisibimod is a BLyS -neutralizing agent composed of a tetrameric BLyS binding domain fused to a human IgG1 Fc region. It binds both soluble and membrane-bound BLyS. In the recently completed phase III trial (CHABLISSC1) in patients with severe disease (SELENA-SLEDAI score $\geq$10), blisibimod showed a statistically significant steroid-sparing effect, reduction in SLE autoantibodies, B cell count, and proteinuria while increasing complement levels (7). SRI-6 as a primary end point was not met since response rate in the control subjects in this study was very high compared to prior SLE trials; 46.9% in the Blisibimod vs. 42.3% jn the control group. Higher steroid dosing in the placebo arm may have contributed to the relatively high response rates, confounding the primary efficacy outcome. Blisibimod was well-tolerated and the most common adverse events were upper respiratory or urinary tract infection and diarrhea (7).

Atacicept is a fully human recombinant fusion protein made of the extracellular portion of the TACI receptor and the Fc portion of human IgG. As atacicept blocks both BLyS and APRIL (8), it was predicted that atacicept may have a more potent effect on immunoglobulin production. Indeed, a significant high risk of severe infection and a decreased in immunoglobulin levels lead to a terminated phase II/III APRIL-SLE trial in nephritis (9). Similar effect on immunoglobulin levels was seen in the ADDRESS II trial (10) where effectiveness of atacicept to improve serologic markers and prevent lupus flares was superior to placebo only with 150 mg twice weekly dosing. The safety profile was acceptable with no reportedly increase in the overall frequency of serious adverse effects as compared to placebo. However, further assessment of the long-term safety of atacicept is warranted as this study only evaluated the safety and efficacy at 24-weeks (10). Given these results, the initial enthusiasm with this molecule has largely dissipated.

Overall, anti-BLyS but probably not anti-APRIL therapies, represent a moderately effective and safe approach in the management of patients with moderately active SLE with musculoskeletal and skin manifestations, especially if they remain corticosteroid dependent.

Anti-CD 20

Unlike BLyS inhibition with the capacity of altering B cell maturation, CD20 targeting therapy depletes mature B cells without affecting plasma cells. Rituximab (RTX) is the most widely used anti-CD20 antibody; due to its chimeric nature, it was found to cause allergic reactions in approximately 10% of patients. Therefore, in the past few years several fully humanized anti-CD20 antibodies have been developed, such as ocrelizumab, ofatumumab, and obinutuzumab. Small uncontrolled trials showed that rituximab, already known to be effective in rheumatoid arthritis (11), can also ameliorate lupus (12). The non-randomized "Rituxilup" trial ($n = 50$) used rituximab and methyl prednisolone followed by mycophenolate mofetil in newly diagnosed lupus nephritis. Ninety percent of patients achieving a partial or complete remission by 37 weeks of treatement. A randomized multicenter clinical trial conducted by Rovin et al., was recently terminated prematurely due to slow recruitment (CTN84054592). But other pivotal trials in lupus nephritis (LUNAR) (13) and non-renal SLE (EXPLORER) were largely negative (14). Currently, the European League Against Rheumatism (EULAR) recommends rituximab as a treatment of last resort in severe lupus (15).

More recently, a few case reports (16, 17) and a phase 2A open-label proof-of-concept suggested that the combination of RTX and anti-BLyS (belimumab, BLM) could be effective. 11/16 patients with refractory SLE achieved renal responses (defined as proteinuria decreased to $\leq$0.7 g/24 h, normal serum albumin, stable creatinine and a normal urinary sediment). Importantly, RTX + BLM reduced nuclear autoantibody titers, and prevented the spike of circulating BLyS that is common after B-cell depletion. Similar results were observed in another small case series of patients with refractory SLE, who entered long term remission and discontinued corticosteroids (18, 19).

Similarly, the humanized anti-CD20 ocrelizumab failed to show significant efficacy in two early terminated phase III trials (BELONG and BEGIN). Patients with class III and IV nephritis were enrolled in BELONG (20) that compared ocrelizumab to placebo. Patients also received mycophenolate mofetil or cyclophosphamide (euro-lupus nephritis treatment protocol). Non-renal SLE patients were enrolled in the BEGIN trial. Both trials were terminated after significant increases of severe infections were noted in the ocrelizumab group. It has to be noted that efficacy analysis showed a trend favoring ocrelizumab over placebo.

Ofatumumab was administered to 16 SLE patients who could not tolerate rituximab; 87% (14/16) of these patients tolerated the infusion. About 85% patient achieved B cell-depletion with associated improvements in serological markers of disease activity (ANA, anti-dsDNA and complement levels). Half of the patients with lupus nephritis achieved renal remission by 6 months. Overall safety profile seems acceptable with 5/16 patients developing grade III infections; no malignancies or deaths were reported during the 28 months follow up (21).

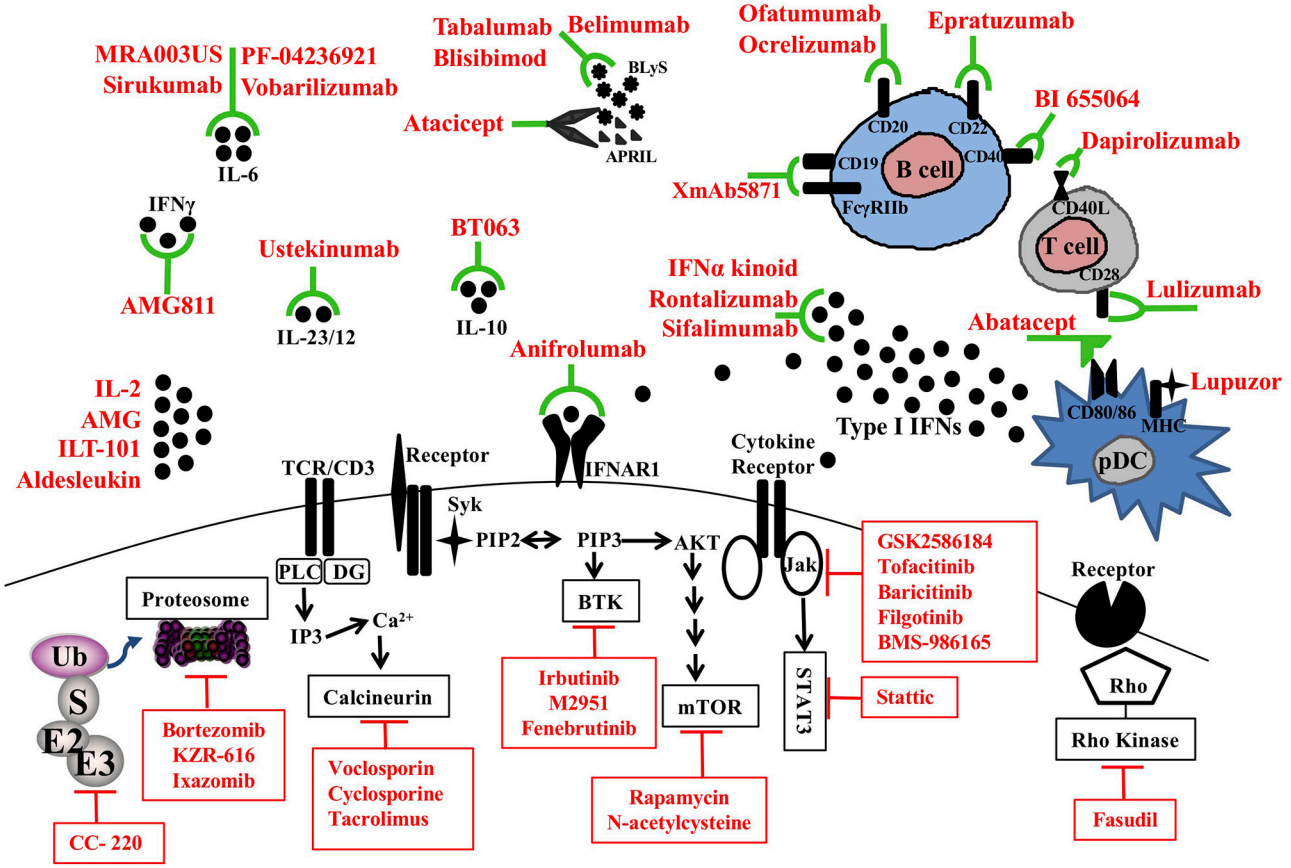

FIGURE 1 | Therapeutic targets and novel treatments in SLE. Target molecules (black) and corresponding therapeutic agents (red) in clinical trials are illustrated. pDC, plasmacytoid dendritic cell; MHC, major histocompatibility complex; CD, cluster of differentiation; APRIL, a proliferating-induced ligand; BLys, B-lymphocyte stimulator; IL, interleukin; TCR, T cell receptor; IFNAR1, Interferon alpha receptor 1; BTK, Bruton's tyrosine kinase; mTOR, mammalian target of rapamycin; Jak, Janus kinases; STAT, signal transducer and activator of transcription proteins; Ub, ubiquitin; E3, Ubiquitin protein ligases.

One SLE patient with autoimmune hemolytic anemia who failed rituximab, achieved clinical remission after ofatumumab (22). Four patients with nephritis achieved reduction of proteinuria and anti-dsDNA levels (23). There are no active formal clinical trials in SLE. A 52-week, phase II trial studying safety and efficacy of obinutuzumab, a different anti-CD20 antibody, in lupus neprhritis is currently active with estimated completion date in December 2019 (NCT02550652).

As per EULAR recommendations, anti-CD20 treatment can be tried in refractory SLE patients. Severe infections remain a concern as many of these patients are already receiving other immunosuppressive medications.

Anti-CD22

CD22 is a surface molecule that modulates B cell activation and migration. Epratuzumab is a humanized anti-CD22 antibody, initially showed positive results reaching its primary endpoint (BICLA response) in the EMBLEM phase II trials (24). However, the beneficial effect was not replicated in the larger and more stringently performed phase III EMBODY trial (25). The reason of failure was thought due to sub-optimal dosing, high placebo response rates, and inadequate optimization of standard of care. Interestingly, some promising response was observed in subgroups of patient with features of Sjogren's syndrome and positive anti-SSA antibodies. Further research is needed to explore this and other potential sub-groups that might respond (26).

Anti-CD19

CD19 is a surface receptor found exclusively on B cells. XmAb5871 is an antibody that co-engages CD19 and the inhibitory FcγRIIb receptor, resulting in B cell inhibition but not ablation (27). There is an ongoing randomized, double-blinded, placebo-controlled study of XmAb5871 to determine its ability to maintain SLE remission achieved by a brief course of steroid therapy (NCT02725515). This clinical trial has an interesting design: Moderately active SLE patients are taken off traditional therapies and are given high dose parenteral steroids. In theory most patients will become clinically inactive. Then the patients of both XmAb5871 and placebo group are observed for development of flare. The outcome measure would be time to relapse after the initial induction of remission. This

unconventional study design is likely to reduce the placebo response by eliminating the effect of background therapy.

Proteasome Inhibitors

The lack of expression of CD20 on plasma cells, especially long-lived plasma cells may be one of the reasons for the poor performance of anti-CD20 therapies in SLE (28). This can be addressed by targeting specifically the plasma cell ability to produce immune globulins by inhibiting the proteasome. This organelle handles misfolded proteins, produced at high levels during immune-globulin assembly, and has proven critical for plasma cell function.

Bortezomib is a proteasome inhibitor, that is efficacious in plasma cell cancers. In lupus prone MPL/lpr mice, administration of bortezomib was found effective in preventing and more importantly treating established disease (29). Similar effects were observed with two other proteasome inhibitors, carfilzomib (30), and delanzomib (31) when used in preclinical models of lupus nephritis (NZBW F1 and MRL/lpr mice). Following these successful studies, bortezomib was infused in 12 patients with refractory SLE. The patients had significant improvement in several clinical parameters such as dermatitis, proteinuria, arthritis, and serositis. Neuropathy developed in 2/12 patients as a major side effect. Currently, bortezomib is assessed in a phase II clinical trial in SLE patients (NCT02102594) with estimated completion date in December 2018.

Although proteasome inhibition is attractive, the main concern for adding these seemingly potent medications in the SLE therapeutic armamentarium remains the severe toxicity associated with their chronic use.

INTRACELLULAR SIGNALING

Bruton's Tyrosine Kinase (Btk)

Btk is a B-cell receptor (BCR) associated kinase that activates the NFkB pathway (32). Importantly though it also associates with the Fc receptor in monocytes (33) and can bridge BCR and TLR9 signaling (34). Mutations in the *Btk* gene result in agammaglobulinemia (35). Ibrutinib is already in use for B cell malignancies and has good safety profile (36). In mouse models of lupus nephritis treatment with Btk inhibitors PF-06250112 (37) and ibrutinib (38) resulted in less severe nephritis. This served as the base for the Btk inhibitor MSC2364447C (M2951) to be evaluated in a phase Ib trial in SLE patients with mild to moderate disease (NCT02537028). Fenebrutinib (GDC-0853), an orally available inhibitor of Btk, is evaluated in a phase II clinical study in patients with moderate to severe active SLE (NCT03407482). Participants will receive GDC-0853 twice daily for 48 weeks and will be followed for additional 8 weeks to evaluate the long-term safety and efficacy.

Cereblon Modulator (CC-220)

CC-220 binds to cereblon (CRBN), a substrate receptor of $CUL4^{CRBN}$ E3 ubiquitin ligase complex. As an immunomodulatory compound, CC-220 can lead a substrate specific ubiquitination of transcription factors Ikaros (IKZF1) and Aiolos (IKZF3) both essential for antibody production (38–40). A Pilot phase II randomized, placebo-controlled, double-blind study is underway to evaluate efficacy, safety, tolerability, pharmacokinetics of CC-220 in patients with SLE (NCT02185040). CC-220 showed some efficacy but there were important safety issues in a 12-week, phase II, dose-escalation study of 42 patients and 14% of patients stopped treatment because of adverse effects. Higher doses of CC-220 were associated with neutropenia, pneumonia, and dermatitis (41).

Calcineurin Inhibitors

Activated lupus T cells show an exaggerated calcium response, which leads to early and sustained activation of the phosphatase calcineurin and its substrate, the transcription factor nuclear factor of activated T cells (NFAT). NFAT upregulates a number of genes, including CD154 (also called CD40L) (42), a critical molecule for T:B cell interaction. Calcineurin inhibitors cyclosporine and tacrolimus, have been successfully used in preventing transplant rejection through blocking this important pathway. Moreover, calcineurin inhibitors may have an antiproteinuric effect, rendering them an important treatment alternative or adjuvant therapy for lupus nephritis. Compared to mycophenolate mofetil, tacrolimus was found to be non-inferior in induction of remission (62 vs. 59%). However, there was a trend for more flares in the tacrolimus group (43).

Voclosporin, a novel calcineurin inhibitor, was investigated in a phase II trial for lupus nephritis as a combination therapy with mycophenolate mofetil (AURA trial). Patients received mycophenolate alone or Voclosporin at 39.5 or 27.5 mg combined with mycophenolate. Remission rates at 6 months favored the combination therapy over mycophenolate alone (OR = 2.03). Unfortunately, the voclosporin-mycophenolate combination resulted in severe side effects including 12 deaths vs. 1 death in the mycophenolate group alone (44) despite the use of rather low corticosteroid doses. Double-blind, placebo-controlled AURORA (NCT03021499) phase 3 clinical trial has started with a plan to include 320 patients with nephritis. It will determine if a combination of voclosporin and a standard of care therapy with mycophenolate mofetil increases kidney function, compared with to standard of therapy alone.

Overall, calcineurin inhibitors alone or combined with mycophenolate represent acceptable alternatives for lupus nephritis treatment; the combination though may carry a significant risk for serious infections.

Mammalian Target of Rapamycin (mTOR) Signaling Inhibitor

mTOR is a highly conserved serine/threonine kinase and is well known to be essential for the regulation of cell metabolism, growth, and proliferation (45, 46). Activated mTOR in lupus T cells is associated with several abnormalities including expansion of both T_H17 and $CD3^+CD4^-CD8^-$ double negative T, as well as, contraction of Tregs (47, 48).

Administration of the mTOR inhibitor rapamycin, results in immediate inhibition of mTORC1 signaling and delayed inhibition of mTORC2 signaling. It has a marked effect on the immune system, partly by interrupting metabolic demands associated with lymphocyte proliferation and effector function.

In the context of SLE, rapamycin ameliorated nephritis and improved IL-2 production in MRL/lpr mice (49). In an open-label clinical trial, rapamycin improved the clinical and laboratory parameters in patients with recalcitrant SLE (50). A larger clinical trial in SLE (NCT00779194) is under way.

The N-acetylcysteine (NAC), a potent anti-oxidant and glutathione precursor, also inhibits mTOR. NAC administration in SLE patients resulted in improvement of disease activity (51). NAC also led to the expansion of $CD4^+CD25^+FoxP3^+$ Tregs and depletion of phospho-S6RPhi DN T cells (52). NAC is well tolerated with its major side-effect being nausea at high doses (over 4.8 g per day).

JAK/STAT Inhibitors

The Janus kinase (JAK)/signal transducer and activator of transcription (STAT) system fine-tunes immune cell activation (53), defining their differentiation. In SLE, there is mounting evidence of the critical involvement of this system in disease pathogenesis. In a recent study, it was shown that increased STAT5 signaling in lupus T cells is related to changes in circulating CD4 T cell subsets and correlated with more aggressive disease (54).

Following the success in treating RA with tofacitinib, the first oral JAK inhibitor (55), several JAK inhibitors are currently under investigation. As type I interferons, known to be upregulated in SLE, transduce their signal through JAK, the JAK1 inhibitor GSK2586184 was used in a small trial to block the expression of interferon-related genes in SLE. The trial failed to show a difference (56) without being powered to address the broader effect JAK inhibition may have on disease activity.

Tofacitinib was studied in phase Ib trial in patients with mild to moderate lupus, stratified based on the presence or absence of STAT4 risk alleles. Although data are not available to date, this study is one of the first to address the link between genetic susceptibility and response to treatment in SLE. Baricitinib, a more selective JAK 1/2 inhibitor was evaluated in a phase II trial in SLE patients that was completed with positive yet modest results (57). A third JAK1 inhibitor, Filgotinib, is currently being evaluated in patients with moderate to severe active cutaneous lupus (NCT03134222) and with membranous lupus nephropathy (NCT03285711).

BMS-986165 is broad inhibitor against a panel of 265 kinases and pseudokinases. BMS-986165 protected NZB/W lupus-prone mice from nephritis possibly through its effect on interferon signaling (58). BMS-986165 also suppresses IL-23/IL-17 and IL-12. An ongoing phase 2 randomized, double-blind, placebo-controlled trial is exploring the efficacy and safety in patients with SLE (59). Finally, our group identified STAT3 that associates with JAK and mediates IL-6 and IL-23 signaling, as a potential therapeutic target in SLE (60, 61). STAT3 influences SLE T cell cytokine production, cell migration and B cell activity in lupus prone mice (62). In a preclinical study, Stattic, a small molecular STAT3 blocker, alleviated nephritis in lupus prone MRL/lpr mice (58, 63).

The Jak-STAT pathway therefore represents a very promising therapeutic target in both non-renal and renal lupus. Moreover, the use of small molecular oral agents to inhibit this pathway as opposed to biologic inhibitors of cytokines, makes this approach even more appealing.

Rho Kinase (ROCK) Inhibitors

ROCKs are a family of serine-threonine kinases (59) that function as downstream effectors for the GTPase Rho. The main isoforms ROCK1 and ROCK2 regulate multiple biological functions, including proliferation, differentiation, and migration by cytoskeletal reorganization. The potential of this pathway as a treatment target in SLE, was first shown by the ROCK inhibitor Y27632 that blocked the ability of SLE T cells to migrate *in vitro* (64, 65). Subsequently, ROCK2 was found to be selectively activated in murine lupus T cells. In these lupus models, ROCK2 regulates IRF4 and increases IL-17 and IL-21 production (66).

A wide array of available ROCK inhibitors has been investigated in SLE including Fasudil and Y27632. Fasudil is non-isoform selective ROCK inhibitor that attenuates disease activity in MRL/lpr mice and NZBWF1 mice (64). Fasudil can also cause vasodilation and hence was evaluated for the treatment of systemic sclerosis patients with Raynaud's phenomenon. A single oral dose of 40 or 80 mg fasudil though, did not improve skin temperature recovery or increase digital blood flow (67).

Although, there are no current clinical trials investigating ROCK inhibitors in patient with SLE, they are evaluated in patients with angina pectoris, pulmonary hypertension (68), idiopathic pulmonary fibrosis (NCT02688647) and psoriasis vulgaris (NCT02317627).

CO-STIMULATION

T cell activation is a tightly controlled process that consists of several steps to allow proper T cell differentiation. Each step in this process has the potential to serve as therapeutic target for autoimmune diseases. Following antigenic binding to the T-cell receptor, the strength of the immune response depends on the expression and interaction of costimulatory surface molecules on antigen presenting cells with those on T cells (68, 69). Here we review the role of disrupting the two most important co-stimulatory pairs, CD28/B7 and CD40/CD154 as a therapeutic strategy in SLE.

CD28/B7

Inhibition of co-stimulatory pathway has already been utilized in in the treatment of rheumatoid arthritis with abatacept. This is a fusion protein made of CTLA4 (cytotoxic T-lymphocyte-associated protein 4) and an immunoglobulin chain (CTLA4-Ig). It binds CD80/86 with a higher affinity than CD28. This interaction leads to both inhibition of T cell proliferation and B cell antibody production (70, 71). Efficacy and safety of abatacept added to standard of care with mycophenolate mofetil and steroids was evaluated in a phase III double-blind placebo-controlled trial that randomized over 400 lupus patients with class III or IV nephritis. The study end point was complete renal remission and corticosteroid dose assessed at 52 weeks. The trial did not reach its primary endpoint with 35% of patients treated with abatacept achieving remission vs. 33% in the placebo group ($p = 0.73$). Abatacept treatment was

associated with improvement of immunologic markers (anti-ds DNA, C3, and C4 levels) as compared to placebo. In patients with nephrotic-range proteinuria, treatment with abatacept led to more rapid and greater reduction of proteinuria compared with placebo. Infection rates were similar as previously reported for RA patients. Thus, far, there have been several other trials of abatacept in active lupus nephritis but none achieved its primary endpoint (72, 73).

Targeting the CD28 instead of B7 has been challenging by the lack of inhibitory antibodies that would not crosslink CD28 and trigger a cytokine storm (74). One solution was to develop pegylated monovalent anti-CD28 antibodies such as lulizumab (75). Lulizumab was evaluated in phase II trial in non-renal lupus following acceptable safety profile in phase I trial. The trial was terminated early as it failed to meet protocol objectives (NCT02265744).

CD154/CD40

Another pair of co-stimulatory receptor-ligand system whose engagement has profound effects on B, dendritic and endothelial cells is the CD40-CD40 ligand (CD154). Following T cell activation, CD154 is expressed on the surface of the cell, allowing binding to B cells through CD40; that in turn leads to IgG class switching (76). Two drugs are currently explored as therapeutic agents in phase II trials for patients with moderately to severely active SLE. The first one, Dapirolizumab, a polyethylene glycol conjugated anti-CD40L Fab' fragment, was well tolerated in phase I study (77). At 12 weeks of treatment 46% of high disease activity patients showed reduction in disease activity measured by BILAG and 41% had improved SRI-4. The second one, BI 655064 is a humanized monoclonal anti-CD40 antibody. Its efficacy will be assessed in a double-blind, randomized, placebo-controlled trial for patients with active class III and IV lupus nephritis (NCT03385564). The study is actively enrolling and the primary endpoint is defined as complete renal response at 1 year.

CYTOKINES

SLE is characterized by skewed cytokine production that can directly cause local tissue damage and contribute to systemic symptomatology. Besides the interferons, other inflammatory and immunomodulatory cytokines have been investigated as therapeutic targets for SLE.

Interleukin-2 (IL-2)

There has been resurgent interest in interleukin-2 since the discovery of its homeostatic potential on CD4 T cells and its ability to redirect immune responses toward tolerance. IL-2 promotes the expansion and survival of regulatory T cells, and can be used in low doses to promote tolerance averting graft vs. host disease in bone marrow recipients (78–80). In SLE, low-dose IL-2 therapy is of particular interest, as these patients have low levels of IL-2, defective regulatory T cell function, and overactive T effector cells (81, 82). This imbalance can potentially be reversed with the addition of IL-2 (83). In preclinical studies, low dose IL-2 abrogated the development of nephritis in lupus-prone mice and mediated selective expansion of regulatory T cells in SLE patients (84, 85). This approach was tested in an open label phase I/II trial of subcutaneous low-dose IL-2 injection on alternate days for 3 cycles in 38 SLE patients. More than 80% of patients showed significant SRI-4 response by week 12, in addition to increased numbers of regulatory T cells, decreased Th17, follicular helper and double negative T cells (86, 87). This paved the way for larger placebo-controlled trials of low dose IL-2, using different IL-2 preparations and dosing schedules: AMG 592 (NCT03451422); LUPIL-2 trial with ILT-101 (NCT02955615); and Charact-IL-2 with Aldesleukin (NCT03312335).

Interleukin (IL)-12/23

Elevated IL-23 levels have been found in patients with lupus nephritis (83, 88, 89). Activation of IL-23/IL-17A axis induces expansion of highly pathogenic T_H17 cells, ultimately contributing to pathogenesis of lupus nephritis by enhancing immunoglobulin and complement deposition (90, 91). Sole targeting of IL-17 in murine lupus nephritis models either with genetic deletion or utilizing a blocking antibody against IL-17A had no impact on the disease (92, 93). However, upstream targeting of this axis with ustekinumab, a monoclonal anti-IL-12/23 antibody that is already approved and well tolerated in patients with a variety of autoimmune diseases, showed promising data. Ustekinumab was evaluated in placebo-controlled phase II trial that recruited 102 SLE patients with active disease despite ongoing standard of care therapy (steroid, antimalarial and/or immunosuppressive therapies) (94). The protocol allowed intravenous loading, followed by subcutaneous administration every 8 weeks. At week 24, ustekinumab arm showed a significant improvement of the SLEDAI-2K score compared to placebo (SRI-4: 60 vs. 31%, respectively, $p = 0.0046$), which was the predetermined primary endpoint. A number of other metrics also improved, including anti-dsDNA, C3 levels, musculoskeletal and mucocutaneous manifestations. Moreover, a significant lower risk of a new BILAG flare was found in the ustekinumab group ($p = 0.0078$) but there was no difference in BILAG or BICLA scores at week 24 among the groups. Safety and adverse events of ustekinumab were similar to safety profile reported for other indications. Overall, this is very promising therapeutic option with an ongoing phase III trial that will address ultimately its usefulness in SLE.

IL-10

IL-10 has been shown to be increased in the serum of SLE patients and levels do correlate with disease activity (95). Its exact role in the propagation of the disease is unclear as IL-10 has both pro and anti-inflammatory effects. The anti-IL-10 antibody, BT063, is currently undergoing a phase II trial (NCT02554019); the trial aims at recruiting 36 patients with SLE who are to receive 50 mg of BT063. Safety and efficacy will be compared to standard of care. The drug will be administered over 8 cycles of intravenous infusion in 12 weeks period. Although no data are available, the clinical development program for this molecule is active.

IL-6

IL-6 is a proinflammatory cytokine found to be elevated in patients with active SLE (96). Rationale for its therapeutic blockade comes from data that showed diverse biologic function, spanning from promoting terminal differentiation of B and T_H17 cells to locally driving tissue damage (97–99). Additionally, in animal models of SLE, disrupting IL-6 signaling either by utilizing an anti-IL-6 monoclonal antibody or anti-IL-6 receptor antibody led to improved survival, decreased levels of ds-DNA and proteinuria (100, 101). The opposite was found when mice were injected with recombinant human IL-6 (101, 102). Unfortunately, the clinical trials though have not been as encouraging.

PF-04236921, a monoclonal IL-6 antibody failed to meet its primary efficacy endpoint (SRI-4) a phase II trial that enrolled 183 patients assigned to receive subcutaneous 10 mg, 50 mg or 200 mg drug or placebo (103). In the 200 mg dose group, there were four deaths secondary to infections and thrombosis. A subgroup analysis showed that benefit can be seen in patients with high disease activity at baseline who received the 10 mg dose. They had significantly improved SRI-4 and BICLA response rates compared to placebo (49 vs. 25.1%, $p < 0.05$) and decreased incidence of severe lupus flares. Two other monoclonal antibodies failed to demonstrate efficacy in phase II trials, sirukumab (104), and vobarilizumab. Finally, the monoclonal antibody MRA003US is currently in a phase I trial (NCT00046774) and no results have been released to date.

The Interferons (IFN)

The hypothesis that IFNs have an important role in SLE pathogenesis is supported by plethora of findings both in humans and animals. Patients with active lupus have elevated levels of type I IFN. Moreover, patients with active and quiescent disease have evidence of continuous exposure to type I interferons based on multiple gene expression studies that show upregulated interferon responsive genes, collectively known as "IFN signature" (105–108). Given modulatory potential of IFNs to initiate or amplify immune responses leading to organ damage in lupus, this cytokine system became an excellent therapeutic target.

Sifalimumab, an anti-IFNα monoclonal antibody was evaluated in a phase II clinical trial in patients with moderate to severe SLE (109). Compared to placebo, patients receiving monthly IV infusions of sifalimumab (1,200, 600, and 200 mg groups) had statistically superior SRI-4 response index compared to placebo that received standard of care treatment at 52 weeks (sifalimumab: 59.8, 56.5, and 58.3 vs. 45.4% placebo, respectfully). At baseline, approximately 80% of patients had the IFN signature of gene expression at baseline, and tended to have better responses. The most common infectious complication was herpes zoster in patients receiving high dose (9.3 vs. 0.9% in the placebo group) that responded to treatment. There was one recurrence among patients who continued receiving sifalimumab. Overall, this was a positive study but given the modest effect size, there was no further development of this drug.

Rontalizumab is another humanized IgG1 anti-IFNα antibody that can neutralize all 12 subtypes of interferon-alpha. It was evaluated in the placebo control phase II trial, ROSE (110). At baseline, 76% of patients had high IFN regulated gene expression. At 24 weeks of treatment, the drug failed to meet the primary endpoint. Unexpectedly, treatment with rontalizumab showed consistent benefits with higher SRI-4 responses compared to controls in the subgroup of patients who had low interferon signature detected (72.7 vs. 41.7% placebo) and this group achieved meaningful rates of prednisone dose reduction to $\leq$10 mg daily. Rontalizumab was well tolerated and serious adverse events were 14.6 vs. 8.3% in the placebo group, all classified as unrelated to the study drug. Therefore, higher doses of rontalizumab would be well tolerated and possibly more effective but no additional trials are planned to answer this question. There are currently two phase I trials with other monoclonal antibodies against IFN-α: IAGS-009 completed phase I (NCT00960362) and JNJ-55920839 is in recruiting phase (NCT02609789).

Another strategy to inhibit the IFN-I pathway is to block its receptor, the interferon alpha receptor 1 (IFNAR1) that binds all type I IFNs including IFNα and IFNβ. Anifrolumab, a monoclonal antibody against IFNAR1, was granted fast- track status by the FDA and was successful in phase II open-label trial (108, 109). In this study, 75% of patients had high IFN signature at baseline. The primary endpoint consisting of composite SRI-4 combined with a measure of steroid sparing to <10 mg/day was achieved in both anifrolumab dose groups at higher rates than placebo (28.8% in the 1,000 mg IV monthly, 34.3% in 300 mg IV monthly vs. 17.6% in the placebo group). At 1 year, 56.4% of the patients taking a 300 mg dose met the SRI end-point, as compared to 31.7% receiving 1000 mg dose ($p = 0.595$) and 26.6% on placebo. Regarding the infections rate, patients receiving anifrolumab had dose-dependent increase in herpes zoster cases (placebo: 2.0%; 300 mg: 5.1%; 1,000 mg: 9.5%) and a greater number of influenza infections (placebo: 2.0%; 300 mg: 6.1%; 1,000 mg: 7.6%). However, most cases of influenza were unconfirmed. With this positive data, two phase III studies are currently underway via the TULIP (NCT02547922) program. TULIP-LN1 on the other hand is phase IIb study designed to assess efficacy and safety of two intravenous doses of anifrolumab vs. placebo while taking standard of care treatment with mycophenolate mofetil and corticosteroids in adults with active proliferative lupus nephritis. On August 31, 2018, it was reported that in one of the phase III trials (TULIP I), anifrolumab failed to meet its primary endpoint.

In conclusion, IFNAR blocking has been a promising therapeutic approach for SLE patients who fail to respond to available therapies. The recently released result though from the phase III trial dampen the enthusiasm for the usefulness of this approach.

Interferon-γ (IFNγ)

The pathogenic role of IFNγ has been better characterized in mice, as opposed to humans (111), where elevated levels and correlation with disease activity is found in both NZB/W and MRL/lpr mice. Administration of IFN-γ accelerates murine lupus while early treatment with anti-IFNγ antibody rescues mice from

TABLE 1 | New and emerging therapies in SLE.

Molecular target	Treatment	Status
B CELLS		
BAFF/APRIL	Belimumab	Approved for non-renal SLE Ongoing phase IV for efficacy, safety, and tolerability Ongoing phase III in combination with Rituximab
	Tabalumab	Phase III without significant effect (terminated)
	Blisibimod	Phase III did not meet SRI-6 primary end point
	Atacicept	APRIL-SLE study terminated due to increased infection rate ADDRESS II study has acceptable safety profile
CD20	Rituximab	Phase III failed (nephritis and non-nephritis)
	Ocrelizumab	Phase III trial completed
CD22	Epratuzumab	Phase III failed
CD19	XmAb5871	Phase II trial
Proteasome inhibitors	Bortezomib	Phase II trial
INTRACELLULAR SIGNALING		
Btk	M2951	Ongoing phase II
	Fenebrutinib	Ongoing phase II trial
mTOR	N-acetylcysteine	Small study showed decrease in SLEDAI, no further development
	Rapamycin	Open-label study showed an effect on BILAG. Larger study planned.
JAK/STAT	GSK2586184	Ineffective on interferon signature in phase II, safety data do not support further study
JAK 2	Baricitinib	Phase II positive data; Phase III trial ongoing
JAK3	Tofacitinib	Ongoing Phase I/II trial
ROCK	Fasudil	Effective in preclinical studies in patient with Raynaud's, phase III completed with uninterpretable data.
CO-STIMULATION		
CD40:CD154	Dapirolizumab	Ongoing phase II trial
	BI 655064	Ongoing phase II trial
CD28:B7	Abatacept	Ineffective in phase III in nephritis and general SLE
	Lulizumab	Phase II trial terminated—failed to meet protocol objectives
CYTOKINES		
	Sifalimumab	Limited effect in phase II and III. No further development
	Rontalizumab	Phase II without significant results
Interferon-α	Anifrolumab	Phase II positive data; 2 Phase III trials ongoing (one reported negative)
	IAGS-009	Completed phase I, no data released
	JNJ-55920839	In recruiting phase
	IFNα-k	Successful phase I; ongoing phase II trial
Interleukin-2	Aldesleukin	Ongoing open-label phase II trial
	AMG 592	Ongoing phase Ib and IIa trial
	ILT-101	Ongoing phase II trial
Interleukin 12/23	Ustekinumab	Met primary end-point in phase II trial; ongoing phase III trial
Interleukin-6	PF-04236921	Failed phase II trial; safety compromised
	Sirukumab	Failed phase II trial
	MRA003US	Ongoing phase II trial
	Vobarilizumab	Ongoing phase I trial
Interleukin-10	BT063	Ongoing phase II trial
OTHER		
	Lupuzor	Phase III trial failed to meet the primary end point

(Continued)

disease (112). Unfortunately two phase I studies of the anti-IFNγ antibody AMG811 in the treatment of mild to moderate systemic and cutaneous lupus (113) showed safety with favorable immunogenicity profile but did not show significant therapeutic effect despite decreasing IFNγ-related gene expression (114). The negative results from these small studies led to discontinuation of the development program for AMG811.

IFNα Kinoid (IFNα-K)

This is another interesting approach for neutralizing I IFN that received fast track status by the FDA. It is currently in phase IIb trial aiming at recruiting 185 patients (NCT02665364). Patients are assigned to receive IFNα-K immunotherapy or placebo in addition to standard treatment with immunosuppressives, antimalarials, and/or steroids. The drug is composed of inactivated IFN-α coupled to the keyhole limpet haemocyanin protein and when injected, leads to induction of polyclonal anti-IFNα responses with transient immunity against all 13 subtypes of interferon alpha. In preclinical stage, IFNα-K was able to slow disease progression in NZB/W mice (115). From an infectious standpoint, this would be an advantageous approach as cellular tolerance and host defense against viral infections would remain intact. The primary end point in the phase II is the BILAG-based Composite Lupus Assessment (BICLA) response at week 36.

Other

Lupuzor/P140 peptide or regiremod, is a 21-mer linear peptide derived from nuclear ribonucleoprotein U1-70K that needs to be phosphorylated at the Ser140 position in order to exert its immunomodulatory properties via binding to MHC class II. This allows recognition in the context of T cell receptor, both in lupus patients and mice and alters autoreactive T cell phenotype. In a phase IIb data, patients receiving Lupuzor 200 μg subcutaneously every 4 weeks achieved the SRI response at week 12 at higher rates than standard of care therapy that included stroids, antimalarials, azathioprine or methotrexate (53.1 vs. 36.2%). These positive results in IIb trial were more pronounced among patients with SLEDAI-2K ≥6 at baseline,

showing that 61.9% achieved SRI response at week 12 vs. 38.6% in the placebo group. Nevertheless, in the phase III clinical trial, Lupuzor failed to meet the primary endpoint ($p = 0.2631$ vs. placebo). The investigational treatment in this trial though holds promise for patients with anti-dsDNA autoantibodies as 7.6% of these patients in the Lupuzor group went into full remission, compared with none in the placebo treated group. The company launched 6 months open label extension study for all participants of phase III trial, allowing continuation of Lupuzor treatment in combination with standard therapy for additional 48 weeks. Finally, this study confirmed the already known Lupuzor's good safety profile with zero adverse effects reported.

CONCLUSIONS

To date, belimumab (anti-BLyS) is the only FDA approved biologic for treating SLE. Over the last decade and despite the setbacks including the recent failure of the highly promising anti-IFNαR therapy, our understanding of the mechanisms of SLE contributed to expansion of the drug pipeline for SLE (**Table 1**). Currently, drugs representing a variety of therapeutic strategies are moving to phase III trials. These include: cytokine infusions (low dose IL-2); antibodies against cytokines (ustekinumab); and finally, small molecule inhibitors against kinases (Jak inhibitors) and phosphatases (calcineurin inhibitors). It is highly likely that these targeted therapies in conjunction with biomarker development and more rigorous outcome measures will finally result in a fundamental change of the stagnant therapeutic paradigm in SLE.

AUTHOR CONTRIBUTIONS

All authors listed have made a substantial, direct and intellectual contribution to the work, and approved it for publication.

REFERENCES

1. Furie R, Petri M, Zamani O, Cervera R, Wallace DJ, Tegzova D, et al. A phase III, randomized, placebo-controlled study of belimumab, a monoclonal antibody that inhibits B lymphocyte stimulator, in patients with systemic lupus erythematosus. *Arthritis Rheum.* (2011) 63:3918–30. doi: 10.1002/art.30613
2. Stohl W, Schwarting A, Okada M, Scheinberg M, Doria A, Hammer AE, et al. Efficacy and safety of subcutaneous belimumab in systemic lupus erythematosus: a fifty-two-week randomized, double-blind, placebo-controlled study. *Arthritis Rheumatol.* (2017) 69:1016–27. doi: 10.1002/art.40049
3. Doria A, Stohl W, Schwarting A, Okada M, Scheinberg M, van Vollenhoven R, et al. Efficacy and safety of subcutaneous belimumab in anti-double-stranded DNA-positive, hypocomplementemic patients with systemic lupus erythematosus. *Arthritis Rheumatol.* (2018) 70:1256–64. doi: 10.1002/art.40511
4. Isenberg DA, Petri M, Kalunian K, Tanaka Y, Urowitz MB, Hoffman RW, et al. Efficacy and safety of subcutaneous tabalumab in patients with systemic lupus erythematosus: results from ILLUMINATE-1, a 52-week, phase III, multicentre, randomised, double-blind, placebo-controlled study. *Ann Rheum Dis.* (2016) 75:323–31. doi: 10.1136/annrheumdis-2015-207653
5. Isenberg D. Further thoughts about the ILLUMINATE studies of tabalumab in SLE. *Ann Rheum Dis.* (2016) 75:e11. doi: 10.1136/annrheumdis-2015-208709
6. Merrill JT, van Vollenhoven RF, Buyon JP, Furie RA, Stohl W, Morgan-Cox M, et al. Efficacy and safety of subcutaneous tabalumab, a monoclonal antibody to B-cell activating factor, in patients with systemic lupus erythematosus: results from ILLUMINATE-2, a 52-week, phase III, multicentre, randomised, double-blind, placebo-controlled study. *Ann Rheum Dis.* (2016) 75:332–40. doi: 10.1136/annrheumdis-2015-207654
7. Merrill JT, Shanahan WR, Scheinberg M, Kalunian KC, Wofsy D, Martin RS. Phase III trial results with blisibimod, a selective inhibitor of B-cell activating factor, in subjects with systemic lupus erythematosus (SLE): results from a randomised, double-blind, placebo-controlled trial. *Ann Rheum Dis.* (2018) 77:883–9. doi: 10.1136/annrheumdis-2018-213032
8. Dall'Era M, Chakravarty E, Wallace D, Genovese M, Weisman M, Kavanaugh A, et al. Reduced B lymphocyte and immunoglobulin levels after atacicept treatment in patients with systemic lupus erythematosus: results of a multicenter, phase Ib, double-blind, placebo-controlled, dose-escalating trial. *Arthritis Rheum.* (2007) 56:4142–50. doi: 10.1002/art.23047
9. Isenberg D, Gordon C, Licu D, Copt S, Rossi CP, Wofsy D. Efficacy and safety of atacicept for prevention of flares in patients with moderate-to-severe systemic lupus erythematosus (SLE): 52-week data (APRIL-SLE randomised trial). *Ann Rheum Dis.* (2015) 74:2006–15. doi: 10.1136/annrheumdis-2013-205067
10. Merrill JT, Wallace DJ, Wax S, Kao A, Fraser PA, Chang P, et al. Efficacy and safety of atacicept in patients with systemic lupus erythematosus: results of a twenty-four-week, multicenter, randomized, double-blind, placebo-controlled, parallel-arm, phase IIb study. *Arthritis Rheumatol.* (2018) 70:266–76. doi: 10.1002/art.40360
11. Edwards JC, Szczepanski L, Szechinski J, Filipowicz-Sosnowska A, Emery P, Close DR, et al. Efficacy of B-cell-targeted therapy with rituximab in patients with rheumatoid arthritis. *N Engl J Med.* (2004) 350:2572–81. doi: 10.1056/NEJMoa032534
12. Ramos-Casals M, Soto MJ, Cuadrado MJ, Khamashta MA. Rituximab in systemic lupus erythematosus: a systematic review of off-label use in 188 cases. *Lupus* (2009) 18:767–76. doi: 10.1177/0961203309106174
13. Rovin BH, Furie R, Latinis K, Looney RJ, Fervenza FC, Sanchez-Guerrero J, et al. Efficacy and safety of rituximab in patients with active proliferative lupus nephritis: the Lupus Nephritis Assessment with Rituximab study. *Arthritis Rheum.* (2012) 64:1215–26. doi: 10.1002/art.34359
14. Merrill JT, Neuwelt CM, Wallace DJ, Shanahan JC, Latinis KM, Oates JC, et al. Efficacy and safety of rituximab in moderately-to-severely active systemic lupus erythematosus: the randomized, double-blind, phase II/III systemic lupus erythematosus evaluation of rituximab trial. *Arthritis Rheum.* (2010) 62:222–33. doi: 10.1002/art.27233
15. Bertsias GK, Tektonidou M, Amoura Z, Aringer M, Bajema I, Berden JH, et al. Joint European League Against Rheumatism and European Renal Association-European Dialysis and Transplant Association (EULAR/ERA-EDTA) recommendations for the management of adult and paediatric lupus nephritis. *Ann Rheum Dis.* (2012) 71:1771–82. doi: 10.1136/annrheumdis-2012-201940
16. Simonetta F, Allali D, Roux-Lombard P, Chizzolini C. Successful treatment of refractory lupus nephritis by the sequential use of rituximab and belimumab. *Joint Bone Spine* (2017) 84:235–6. doi: 10.1016/j.jbspin.2016.01.008
17. Gonzalez-Echavarri C, Ugarte A, Ruiz-Irastorza G. Rituximab-refractory lupus nephritis successfully treated with belimumab. *Clin Exp Rheumatol.* (2016) 34:355–6.
18. Kraaij T, Kamerling SWA, de Rooij ENM, van Daele PLA, Bredewold OW, Bakker JA, et al. The NET-effect of combining rituximab with belimumab in severe systemic lupus erythematosus. *J Autoimmun.* (2018) 91:45–54. doi: 10.1016/j.jaut.2018.03.003

19. Gualtierotti R, Borghi MO, Gerosa M, Schioppo T, Larghi P, Geginat J, et al. Successful sequential therapy with rituximab and belimumab in patients with active systemic lupus erythematosus: a case series. *Clin Exp Rheumatol.* (2018) 36:643–7.
20. Mysler EF, Spindler AJ, Guzman R, Bijl M, Jayne D, Furie RA, et al. Efficacy and safety of ocrelizumab in active proliferative lupus nephritis: results from a randomized, double-blind, phase III study. *Arthritis Rheum.* (2013) 65:2368–79. doi: 10.1002/art.38037
21. Masoud S, McAdoo SP, Bedi R, Cairns TD, Lightstone L. Ofatumumab for B cell depletion in patients with systemic lupus erythematosus who are allergic to rituximab. *Rheumatology* (2018) doi: 10.1093/rheumatology/key042. [Epub ahead of print].
22. Karageorgas T, Zomas A, Kazakou P, Katsimbri P, Mantzourani M, Boumpas D. Successful treatment of life-threatening autoimmune haemolytic anaemia with ofatumumab in a patient with systemic lupus erythematosus. *Rheumatology* (2016) 55:2085–7. doi: 10.1093/rheumatology/kew267
23. Haarhaus ML, Svenungsson E, Gunnarsson I. Ofatumumab treatment in lupus nephritis patients. *Clin Kidney J.* (2016) 9:552–5. doi: 10.1093/ckj/sfw022
24. Wallace DJ, Gordon C, Strand V, Hobbs K, Petri M, Kalunian K, et al. Efficacy and safety of epratuzumab in patients with moderate/severe flaring systemic lupus erythematosus: results from two randomized, double-blind, placebo-controlled, multicentre studies (ALLEVIATE) and follow-up. *Rheumatology* (2013) 52:1313–22. doi: 10.1093/rheumatology/ket129
25. Clowse ME, Wallace DJ, Furie RA, Petri MA, Pike MC, Leszczynski P, et al. Efficacy and safety of epratuzumab in moderately to severely active systemic lupus erythematosus: results from two phase III randomized, double-blind, placebo-controlled trials. *Arthritis Rheumatol.* (2017) 69:362–75. doi: 10.1002/art.39856
26. Gottenberg JE, Dorner T, Bootsma H, Devauchelle-Pensec V, Bowman SJ, Mariette X, et al. Efficacy of epratuzumab, an anti-CD22 monoclonal IgG antibody, in systemic lupus erythematosus patients with associated sjogren's syndrome: post hoc analyses from the EMBODY trials. *Arthritis Rheumatol.* (2018) 70:763–73. doi: 10.1002/art.40425
27. Chu SY, Yeter K, Kotha R, Pong E, Miranda Y, Phung S, et al. Suppression of rheumatoid arthritis B cells by XmAb5871, an anti-CD19 antibody that coengages B cell antigen receptor complex and Fcgamma receptor IIb inhibitory receptor. *Arthritis Rheumatol.* (2014) 66:1153–64. doi: 10.1002/art.38334
28. Slifka MK, Ahmed R. Long-lived plasma cells: a mechanism for maintaining persistent antibody production. *Curr Opin Immunol.* (1998) 10:252–8. doi: 10.1016/S0952-7915(98)80162-3
29. Neubert K, Meister S, Moser K, Weisel F, Maseda D, Amann K, et al. The proteasome inhibitor bortezomib depletes plasma cells and protects mice with lupus-like disease from nephritis. *Nat Med.* (2008) 14:748–55. doi: 10.1038/nm1763
30. Ichikawa HT, Conley T, Muchamuel T, Jiang J, Lee S, Owen T, et al. Beneficial effect of novel proteasome inhibitors in murine lupus via dual inhibition of type I interferon and autoantibody-secreting cells. *Arthritis Rheum.* (2012) 64:493–503. doi: 10.1002/art.33333
31. Seavey MM, Lu LD, Stump KL, Wallace NH, Ruggeri BA. Novel, orally active, proteasome inhibitor, delanzomib (CEP-18770), ameliorates disease symptoms and glomerulonephritis in two preclinical mouse models of SLE. *Int Immunopharmacol.* (2012) 12:257–70. doi: 10.1016/j.intimp.2011.11.019
32. Kurosaki T. Regulation of BCR signaling. *Mol Immunol.* (2011) 48:1287–91. doi: 10.1016/j.molimm.2010.12.007
33. Jongstra-Bilen J, Puig Cano A, Hasija M, Xiao H, Smith CI, Cybulsky MI. Dual functions of Bruton's tyrosine kinase and Tec kinase during Fcgamma receptor-induced signaling and phagocytosis. *J Immunol.* (2008) 181:288–98. doi: 10.4049/jimmunol.181.1.288
34. Kenny EF, Quinn SR, Doyle SL, Vink PM, van Eenennaam H, O'Neill LA. Bruton's tyrosine kinase mediates the synergistic signalling between TLR9 and the B cell receptor by regulating calcium and calmodulin. *PLoS ONE* (2013) 8:e74103. doi: 10.1371/journal.pone.0074103
35. Thomas JD, Sideras P, Smith CI, Vorechovsky I, Chapman V, Paul WE. Colocalization of X-linked agammaglobulinemia and X-linked immunodeficiency genes. *Science* (1993) 261:355–8. doi: 10.1126/science.8332900
36. Burger JA, Tedeschi A, Barr PM, Robak T, Owen C, Ghia P, et al. Ibrutinib as initial therapy for patients with chronic lymphocytic leukemia. *N Engl J Med.* (2015) 373:2425–37. doi: 10.1056/NEJMoa1509388
37. Rankin AL, Seth N, Keegan S, Andreyeva T, Cook TA, Edmonds J, et al. Selective inhibition of BTK prevents murine lupus and antibody-mediated glomerulonephritis. *J Immunol.* (2013) 191:4540–50. doi: 10.4049/jimmunol.1301553
38. Hutcheson J, Vanarsa K, Bashmakov A, Grewal S, Sajitharan D, Chang BY, et al. Modulating proximal cell signaling by targeting Btk ameliorates humoral autoimmunity and end-organ disease in murine lupus. *Arthritis Res Ther.* (2012) 14:R243. doi: 10.1186/ar4086
39. Schafer PH, Ye Y, Wu L, Kosek J, Ringheim G, Yang Z, et al. Cereblon modulator iberdomide induces degradation of the transcription factors Ikaros and Aiolos: immunomodulation in healthy volunteers and relevance to systemic lupus erythematosus. *Ann Rheum Dis.* (2018) 77:1516–23. doi: 10.1136/annrheumdis-2017-212916
40. Lessard CJ, Adrianto I, Ice JA, Wiley GB, Kelly JA, Glenn SB, et al. Identification of IRF8, TMEM39A, and IKZF3-ZPBP2 as susceptibility loci for systemic lupus erythematosus in a large-scale multiracial replication study. *Am J Hum Genet.* (2012) 90:648–60. doi: 10.1016/j.ajhg.2012.02.023
41. Gaudy AYY, Korish S, Houg D, Weiswasser S, Choi S, Furie R, Werth V, Schafer P. *Cereblon Modulator CC-220 Decreases Naïve and Memory B cells and Plasmacytoid Dendritic Cells in Systemic Lupus Erythematosus (SLE) Patients: Exposure-Response Results From a Phase 2A Proof of Concept Study*. EULAR Abstract, Madrid (2017).
42. Crist SA, Sprague DL, Ratliff TL. Nuclear factor of activated T cells (NFAT) mediates CD154 expression in megakaryocytes. *Blood* (2008) 111:3553–61. doi: 10.1182/blood-2007-05-088161
43. Mok CC, Ying KY, Yim CW, Siu YP, Tong KH, To CH, et al. Tacrolimus versus mycophenolate mofetil for induction therapy of lupus nephritis: a randomised controlled trial and long-term follow-up. *Ann Rheum Dis.* (2016) 75:30–6. doi: 10.1136/annrheumdis-2014-206456
44. Dooley MA, PendergraftI, Ginzler EM, Olsen NJ, Tumlin J, Rovin BH, et al., editors. Speed of remission with the use of voclosporin, MMF and low dose steroids: results of a global lupus nephritis study [abstract]. *Arthritis Rheumatol.* (2016).
45. Sarbassov DD, Sabatini DM. Redox regulation of the nutrient-sensitive raptor-mTOR pathway and complex. *J Biol Chem.* (2005) 280:39505–9. doi: 10.1074/jbc.M506096200
46. Zoncu R, Bar-Peled L, Efeyan A, Wang S, Sancak Y, Sabatini DM. mTORC1 senses lysosomal amino acids through an inside-out mechanism that requires the vacuolar H(+)-ATPase. *Science* (2011) 334:678–83. doi: 10.1126/science.1207056
47. Fernandez DR, Telarico T, Bonilla E, Li Q, Banerjee S, Middleton FA, et al. Activation of mammalian target of rapamycin controls the loss of TCRzeta in lupus T cells through HRES-1/Rab4-regulated lysosomal degradation. *J Immunol.* (2009) 182:2063–73. doi: 10.4049/jimmunol.0803600
48. Kato H, Perl A. Mechanistic target of rapamycin complex 1 expands Th17 and IL-4+ CD4-CD8- double-negative T cells and contracts regulatory T cells in systemic lupus erythematosus. *J Immunol.* (2014) 192:4134–44. doi: 10.4049/jimmunol.1301859
49. Warner LM, Adams LM, Sehgal SN. Rapamycin prolongs survival and arrests pathophysiologic changes in murine systemic lupus erythematosus. *Arthritis Rheum.* (1994) 37:289–97. doi: 10.1002/art.1780370219
50. Fernandez D, Bonilla E, Mirza N, Niland B, Perl A. Rapamycin reduces disease activity and normalizes T cell activation-induced calcium fluxing in patients with systemic lupus erythematosus. *Arthritis Rheum.* (2006) 54:2983–8. doi: 10.1002/art.22085
51. Lai ZW, Hanczko R, Bonilla E, Caza TN, Clair B, Bartos A, et al. N-acetylcysteine reduces disease activity by blocking mammalian target of rapamycin in T cells from systemic lupus erythematosus patients: a randomized, double-blind, placebo-controlled trial. *Arthritis Rheum.* (2012) 64:2937–46. doi: 10.1002/art.34502
52. Perl A, Hanczko R, Lai ZW, Oaks Z, Kelly R, Borsuk R, et al. Comprehensive metabolome analyses reveal N-acetylcysteine-responsive accumulation of kynurenine in systemic lupus erythematosus: implications for activation of the mechanistic target of rapamycin. *Metabolomics* (2015) 11:1157–74. doi: 10.1007/s11306-015-0772-0

53. Schwartz DM, Bonelli M, Gadina M, O'Shea JJ. Type I/II cytokines, JAKs, and new strategies for treating autoimmune diseases. *Nat Rev Rheumatol.* (2016) 12:25–36. doi: 10.1038/nrrheum.2015.167
54. Goropevsek A, Gorenjak M, Gradisnik S, Dai K, Holc I, Hojs R, et al. STAT5 phosphorylation in CD4 T cells from patients with SLE is related to changes in their subsets and follow-up disease severity. *J Leukoc Biol.* (2017) 101:1405–18. doi: 10.1189/jlb.5A0416-194R
55. Fleischmann R, Kremer J, Cush J, Schulze-Koops H, Connell CA, Bradley JD, et al. Placebo-controlled trial of tofacitinib monotherapy in rheumatoid arthritis. *N Engl J Med*. (2012) 367:495–507. doi: 10.1056/NEJMoa1109071
56. Kahl L, Patel J, Layton M, Binks M, Hicks K, Leon G, et al. Safety, tolerability, efficacy and pharmacodynamics of the selective JAK1 inhibitor GSK2586184 in patients with systemic lupus erythematosus. *Lupus* (2016) 25:1420–30. doi: 10.1177/0961203316640910
57. Wallace DJ, Furie RA, Tanaka Y, Kalunian KC, Mosca M, Petri MA, et al. Baricitinib for systemic lupus erythematosus: a double-blind, randomised, placebo-controlled, phase 2 trial. *Lancet* (2018) 392:222–31. doi: 10.1016/S0140-6736(18)31363-1
58. Gillooly K, Yifan Y, Yang X, Zupa-Fernandez A, Cheng L, Strnad J, Cunningham M, editors. BMS-986165 is a highly potent and selective allosteric inhibitor of Tyk2, blocks IL-12, IL-23 and type I interferon signaling and provides for robust efficacy in preclinical models of systemic lupus erythematosus and inflammatory bowel disease [abstract]. *Arthritis Rheumatol.* (2016).
59. Isgro J, Gupta S, Jacek E, Pavri T, Duculan R, Kim M, et al. Enhanced rho-associated protein kinase activation in patients with systemic lupus erythematosus. *Arthritis Rheum.* (2013) 65:1592–602. doi: 10.1002/art.37934
60. Harada T, Kyttaris V, Li Y, Juang YT, Wang Y, Tsokos GC. Increased expression of STAT3 in SLE T cells contributes to enhanced chemokine-mediated cell migration. *Autoimmunity* (2007) 40:1–8. doi: 10.1080/08916930601095148
61. Li Y, Harada T, Juang YT, Kyttaris VC, Wang Y, Zidanic M, et al. Phosphorylated ERM is responsible for increased T cell polarization, adhesion, and migration in patients with systemic lupus erythematosus. *J Immunol*. (2007) 178:1938–47. doi: 10.4049/jimmunol.178.3.1938
62. Nakagawa O, Fujisawa K, Ishizaki T, Saito Y, Nakao K, Narumiya S. ROCK-I and ROCK-II, two isoforms of Rho-associated coiled-coil forming protein serine/threonine kinase in mice. *FEBS Lett.* (1996) 392:189–93. doi: 10.1016/0014-5793(96)00811-3
63. Edwards LJ, Mizui M, Kyttaris V. Signal transducer and activator of transcription (STAT) 3 inhibition delays the onset of lupus nephritis in MRL/lpr mice. *Clin Immunol.* (2015) 158:221–30. doi: 10.1016/j.clim.2015.04.004
64. Stirzaker RA, Biswas PS, Gupta S, Song L, Bhagat G, Pernis AB. Administration of fasudil, a ROCK inhibitor, attenuates disease in lupus-prone NZB/W F1 female mice. *Lupus* (2012) 21:656–61. doi: 10.1177/0961203312436862
65. Vicari RM, Chaitman B, Keefe D, Smith WB, Chrysant SG, Tonkon MJ, et al. Efficacy and safety of fasudil in patients with stable angina: a double-blind, placebo-controlled, phase 2 trial. *J Am Coll Cardiol.* (2005) 46:1803–11. doi: 10.1016/j.jacc.2005.07.047
66. Biswas PS, Gupta S, Chang E, Song L, Stirzaker RA, Liao JK, et al. Phosphorylation of IRF4 by ROCK2 regulates IL-17 and IL-21 production and the development of autoimmunity in mice. *J Clin Invest.* (2010) 120:3280–95. doi: 10.1172/JCI42856
67. Fava A, Wung PK, Wigley FM, Hummers LK, Daya NR, Ghazarian SR, et al. Efficacy of Rho kinase inhibitor fasudil in secondary Raynaud's phenomenon. *Arthritis Care Res.* (2012) 64:925–9. doi: 10.1002/acr.21622
68. Fukumoto Y, Yamada N, Matsubara H, Mizoguchi M, Uchino K, Yao A, et al. Double-blind, placebo-controlled clinical trial with a rho-kinase inhibitor in pulmonary arterial hypertension. *Circ J.* (2013) 77:2619–25. doi: 10.1253/circj.CJ-13-0443
69. Chen L, Flies DB. Molecular mechanisms of T cell co-stimulation and co-inhibition. *Nat Rev Immunol.* (2013) 13:227–42. doi: 10.1038/nri3405
70. Genovese MC, Pacheco-Tena C, Covarrubias A, Leon G, Mysler E, Keiserman M, et al. Longterm safety and efficacy of subcutaneous abatacept in patients with rheumatoid arthritis: 5-year results from a Phase IIIb trial. *J Rheumatol.* (2018) 45:1085–92. doi: 10.3899/jrheum.170344
71. Picchianti Diamanti A, Rosado MM, Scarsella M, Germano V, Giorda E, Cascioli S, et al. Abatacept (cytotoxic T lymphocyte antigen 4-immunoglobulin) improves B cell function and regulatory T cell inhibitory capacity in rheumatoid arthritis patients non-responding to anti-tumour necrosis factor-alpha agents. *Clin Exp Immunol.* (2014) 177:630–40. doi: 10.1111/cei.12367
72. Furie R, Nicholls K, Cheng TT, Houssiau F, Burgos-Vargas R, Chen SL, et al. Efficacy and safety of abatacept in lupus nephritis: a twelve-month, randomized, double-blind study. *Arthritis Rheumatol.* (2014) 66:379–89. doi: 10.1002/art.38260
73. Group AT. Treatment of lupus nephritis with abatacept: the Abatacept and Cyclophosphamide Combination Efficacy and Safety Study. *Arthritis Rheumatol.* (2014) 66:3096–104. doi: 10.1002/art.38790
74. Suntharalingam G, Perry MR, Ward S, Brett SJ, Castello-Cortes A, Brunner MD, et al. Cytokine storm in a phase 1 trial of the anti-CD28 monoclonal antibody TGN1412. *N Engl J Med*. (2006) 355:1018–28. doi: 10.1056/NEJMoa063842
75. Shi R, Honczarenko M, Zhang S, Fleener C, Mora J, Lee SK, et al. Pharmacokinetic, pharmacodynamic, and safety profile of a novel anti-CD28 domain antibody antagonist in healthy subjects. *J Clin Pharmacol.* (2017) 57:161–72. doi: 10.1002/jcph.791
76. Crow MK, Kirou KA. Regulation of CD40 ligand expression in systemic lupus erythematosus. *Curr Opin Rheumatol.* (2001) 13:361–9. doi: 10.1097/00002281-200109000-00004
77. Chamberlain C, Colman PJ, Ranger AM, Burkly LC, Johnston GI, Otoul C, et al. Repeated administration of dapirolizumab pegol in a randomised phase I study is well tolerated and accompanied by improvements in several composite measures of systemic lupus erythematosus disease activity and changes in whole blood transcriptomic profiles. *Ann Rheum Dis*. (2017) 76:1837–44. doi: 10.1136/annrheumdis-2017-211388
78. Boyman O, Sprent J. The role of interleukin-2 during homeostasis and activation of the immune system. *Nat Rev Immunol.* (2012) 12:180–90. doi: 10.1038/nri3156
79. Yu A, Zhu L, Altman NH, Malek TR. A low interleukin-2 receptor signaling threshold supports the development and homeostasis of T regulatory cells. *Immunity* (2009) 30:204–17. doi: 10.1016/j.immuni.2008.11.014
80. Mizui M, Tsokos GC. Low-Dose IL-2 in the treatment of lupus. *Curr Rheumatol Rep*. (2016) 18:68. doi: 10.1007/s11926-016-0617-5
81. Lieberman LA, Tsokos GC. The IL-2 defect in systemic lupus erythematosus disease has an expansive effect on host immunity. *J Biomed Biotechnol.* (2010) 2010:740619. doi: 10.1155/2010/740619
82. Comte D, Karampetsou MP, Tsokos GC. T cells as a therapeutic target in SLE. *Lupus* (2015) 24:351–63. doi: 10.1177/0961203314556139
83. Dai H, He F, Tsokos GC, Kyttaris VC. IL-23 Limits the production of IL-2 and promotes autoimmunity in lupus. *J Immunol.* (2017) 199:903–10. doi: 10.4049/jimmunol.1700418
84. Koreth J, Matsuoka K, Kim HT, McDonough SM, Bindra B, Alyea EP III, et al. Interleukin-2 and regulatory T cells in graft-versus-host disease. *N Engl J Med*. (2011) 365:2055–66. doi: 10.1056/NEJMoa1108188
85. Mizui M, Koga T, Lieberman LA, Beltran J, Yoshida N, Johnson MC, et al. IL-2 protects lupus-prone mice from multiple end-organ damage by limiting CD4-CD8- IL-17-producing T cells. *J Immunol*. (2014) 193:2168–77. doi: 10.4049/jimmunol.1400977
86. Crispin JC, Oukka M, Bayliss G, Cohen RA, Van Beek CA, Stillman IE, et al. Expanded double negative T cells in patients with systemic lupus erythematosus produce IL-17 and infiltrate the kidneys. *J Immunol*. (2008) 181:8761–6. doi: 10.4049/jimmunol.181.12.8761
87. He J, Zhang X, Wei Y, Sun X, Chen Y, Deng J, et al. Low-dose interleukin-2 treatment selectively modulates CD4(+) T cell subsets in patients with systemic lupus erythematosus. *Nat Med.* (2016) 22:991–3. doi: 10.1038/nm.4148
88. Zhang Z, Kyttaris VC, Tsokos GC. The role of IL-23/IL-17 axis in lupus nephritis. *J Immunol*. (2009) 183:3160–9. doi: 10.4049/jimmunol.0900385
89. Wong CK, Lit LC, Tam LS, Li EK, Wong PT, Lam CW. Hyperproduction of IL-23 and IL-17 in patients with systemic lupus erythematosus: implications for Th17-mediated inflammation in auto-immunity. *Clin Immunol.* (2008) 127:385–93. doi: 10.1016/j.clim.2008.01.019

90. Zickert A, Amoudruz P, Sundstrom Y, Ronnelid J, Malmstrom V, Gunnarsson I. IL-17 and IL-23 in lupus nephritis - association to histopathology and response to treatment. *BMC Immunol.* (2015) 16:7. doi: 10.1186/s12865-015-0070-7
91. Schmidt T, Paust HJ, Krebs CF, Turner JE, Kaffke A, Bennstein SB, et al. Function of the Th17/interleukin-17A immune response in murine lupus nephritis. *Arthritis Rheumatol.* (2015) 67:475–87. doi: 10.1002/art.38955
92. Kyttaris VC, Zhang Z, Kuchroo VK, Oukka M, Tsokos GC. Cutting edge: IL-23 receptor deficiency prevents the development of lupus nephritis in C57BL/6-lpr/lpr mice. *J Immunol.* (2010) 184:4605–9. doi: 10.4049/jimmunol.0903595
93. Kyttaris VC, Kampagianni O, Tsokos GC. Treatment with anti-interleukin 23 antibody ameliorates disease in lupus-prone mice. *Biomed Res Int.* (2013) 2013:861028. doi: 10.1155/2013/861028
94. van Vollenhoven R, Hahn BH, Tsokos GC, Wagner C, Lipsky P, Hsu B, et al., editors. Efficacy and safety of ustekinumab, an interleukin 12/23 inhibitor, in patients with active systemic lupus erythematosus: results of a phase 2, Randomized Placebo-Controlled Study [abstract]. *Arthritis Rheumatol.* (2017).
95. Godsell J, Rudloff I, Kandane-Rathnayake R, Hoi A, Nold MF, Morand EF, et al. Clinical associations of IL-10 and IL-37 in systemic lupus erythematosus. *Sci Rep.* (2016) 6:34604. doi: 10.1038/srep34604
96. Chun HY, Chung JW, Kim HA, Yun JM, Jeon JY, Ye YM, et al. Cytokine IL-6 and IL-10 as biomarkers in systemic lupus erythematosus. *J Clin Immunol.* (2007) 27:461–6. doi: 10.1007/s10875-007-9104-0
97. Ripley BJ, Goncalves B, Isenberg DA, Latchman DS, Rahman A. Raised levels of interleukin 6 in systemic lupus erythematosus correlate with anaemia. *Ann Rheum Dis.* (2005) 64:849–53. doi: 10.1136/ard.2004.022681
98. Maeda K, Mehta H, Drevets DA, Coggeshall KM. IL-6 increases B-cell IgG production in a feed-forward proinflammatory mechanism to skew hematopoiesis and elevate myeloid production. *Blood* (2010) 115:4699–706. doi: 10.1182/blood-2009-07-230631
99. Kimura A, Kishimoto T. IL-6: regulator of Treg/Th17 balance. *Eur J Immunol.* (2010) 40:1830–5. doi: 10.1002/eji.201040391
100. Ryffel B, Car BD, Gunn H, Roman D, Hiestand P, Mihatsch MJ. Interleukin-6 exacerbates glomerulonephritis in (NZB x NZW)F1 mice. *Am J Pathol.* (1994) 144:927–37.
101. Finck BK, Chan B, Wofsy D. Interleukin 6 promotes murine lupus in NZB/NZW F1 mice. *J Clin Invest.* (1994) 94:585–91. doi: 10.1172/JCI117373
102. Mihara M, Takagi N, Takeda Y, Ohsugi Y. IL-6 receptor blockage inhibits the onset of autoimmune kidney disease in NZB/W F1 mice. *Clin Exp Immunol.* (1998) 112:397–402. doi: 10.1046/j.1365-2249.1998.00612.x
103. Wallace DJ, Strand V, Merrill JT, Popa S, Spindler AJ, Eimon A, et al. Efficacy and safety of an interleukin 6 monoclonal antibody for the treatment of systemic lupus erythematosus: a phase II dose-ranging randomised controlled trial. *Ann Rheum Dis.* (2017) 76:534–42. doi: 10.1136/annrheumdis-2016-209668
104. Szepietowski JC, Nilganuwong S, Wozniacka A, Kuhn A, Nyberg F, van Vollenhoven RF, et al. Phase I, randomized, double-blind, placebo-controlled, multiple intravenous, dose-ascending study of sirukumab in cutaneous or systemic lupus erythematosus. *Arthritis Rheum.* (2013) 65:2661–71. doi: 10.1002/art.38091
105. Kirou KA, Lee C, George S, Louca K, Papagiannis IG, Peterson MG, et al. Coordinate overexpression of interferon-alpha-induced genes in systemic lupus erythematosus. *Arthritis Rheum.* (2004) 50:3958–67. doi: 10.1002/art.20798
106. Niewold TB, Hua J, Lehman TJ, Harley JB, Crow MK. High serum IFN-alpha activity is a heritable risk factor for systemic lupus erythematosus. *Genes Immun.* (2007) 8:492–502. doi: 10.1038/sj.gene.6364408
107. Coit P, Jeffries M, Altorok N, Dozmorov MG, Koelsch KA, Wren JD, et al. Genome-wide DNA methylation study suggests epigenetic accessibility and transcriptional poising of interferon-regulated genes in naive CD4+ T cells from lupus patients. *J Autoimmun.* (2013) 43:78–84. doi: 10.1016/j.jaut.2013.04.003
108. Baechler EC, Batliwalla FM, Karypis G, Gaffney PM, Ortmann WA, Espe KJ, et al. Interferon-inducible gene expression signature in peripheral blood cells of patients with severe lupus. *Proc Natl Acad Sci USA.* (2003) 100:2610–5. doi: 10.1073/pnas.0337679100
109. Khamashta M, Merrill JT, Werth VP, Furie R, Kalunian K, Illei GG, et al. Sifalimumab, an anti-interferon-alpha monoclonal antibody, in moderate to severe systemic lupus erythematosus: a randomised, double-blind, placebo-controlled study. *Ann Rheum Dis.* (2016) 75:1909–16. doi: 10.1136/annrheumdis-2015-208562
110. Kalunian KC, Merrill JT, Maciuca R, McBride JM, Townsend MJ, Wei X, et al. A Phase II study of the efficacy and safety of rontalizumab (rhuMAb interferon-alpha) in patients with systemic lupus erythematosus (ROSE). *Ann Rheum Dis.* (2016) 75:196–202. doi: 10.1136/annrheumdis-2014-206090
111. Welcher AA, Boedigheimer M, Kivitz AJ, Amoura Z, Buyon J, Rudinskaya A, et al. Blockade of interferon-gamma normalizes interferon-regulated gene expression and serum CXCL10 levels in patients with systemic lupus erythematosus. *Arthritis Rheumatol.* (2015) 67:2713–22. doi: 10.1002/art.39248
112. Balomenos D, Rumold R, Theofilopoulos AN. Interferon-gamma is required for lupus-like disease and lymphoaccumulation in MRL-lpr mice. *J Clin Invest.* (1998) 101:364–71. doi: 10.1172/JCI750
113. Werth VP, Fiorentino D, Cohen SB, Fivenson D, Hansen C, Zoog S, et al. A Phase I single-dose crossover study to evaluate the safety, tolerability, pharmacokinetics, pharmacodynamics, and clinical efficacy of AMG 811 (anti-IFN-gamma). In: *Subjects With Discoid Lupus Erythematosus*. Boston, MA: American College of Rheumatology Annual Meeting 2014 (2014).
114. Martin D, Amoura Z, Romero-Diaz J, Chong Y, Sanchez-Guerrero J, Chan T, et al. A multiple dose study of AMG 811 (anti-IFNgamma) in subjects with systemic lupus erythematosus and active nephritis [abstract]. *Ann Rheum Dis.* (2015) 74:337. doi: 10.1136/annrheumdis-2015-eular.2916
115. Ducreux J, Houssiau FA, Vandepapeliere P, Jorgensen C, Lazaro E, Spertini F, et al. Interferon alpha kinoid induces neutralizing anti-interferon alpha antibodies that decrease the expression of interferon-induced and B cell activation associated transcripts: analysis of extended follow-up data from the interferon alpha kinoid phase I/II study. *Rheumatology* (2016) 55:1901–5. doi: 10.1093/rheumatology/kew262

Conflict of Interest Statement: VK is a site PI for the EMD Serono sponsored phase II, study to evaluate the safety and efficacy of M2951 in subjects with SLE.

The remaining authors declare that the research was conducted in the absence of any commercial or financial relationships that could be construed as a potential conflict of interest.

frontiers in Immunology

ORIGINAL RESEARCH
published: 18 December 2018
doi: 10.3389/fimmu.2018.02967

Identification of LncRNA Linc00513 Containing Lupus-Associated Genetic Variants as a Novel Regulator of Interferon Signaling Pathway

Zhixin Xue[1†], Chaojie Cui[1†], Zhuojun Liao[1†], Shiwei Xia[1], Pingjing Zhang[1], Jialin Qin[1], Qiang Guo[1], Sheng Chen[1], Qiong Fu[1], Zhihua Yin[2], Zhizhong Ye[2], Yuanjia Tang[1] and Nan Shen[1,3,4,5]**

[1] Shanghai Institute of Rheumatology, Renji Hospital, School of Medicine, Shanghai Jiaotong University, Shanghai, China, [2] Shenzhen Futian Hospital for Rheumatic Diseases, Shenzhen, China, [3] Center for Autoimmune Genomics and Etiology, Cincinnati Children's Hospital Medical Center, Cincinnati, OH, United States, [4] Department of Pediatrics, University of Cincinnati College of Medicine, Cincinnati, OH, United States, [5] State Key Laboratory of Oncogenes and Related Genes, Shanghai Cancer Institute, Renji Hospital, School of Medicine, Shanghai Jiaotong University, Shanghai, China

Systemic lupus erythematosus (SLE) is a complex autoimmune disease characterized by augmented type I interferon signaling. High-throughput technologies have identified plenty of SLE susceptibility single-nucleotide polymorphisms (SNPs) yet the exact roles of most of them are still unknown. Functional studies are principally focused on SNPs in the coding regions, with limited attention paid to the SNPs in non-coding regions. Long non-coding RNAs (lncRNAs) are important players in shaping the immune response and show relationship to autoimmune diseases. In order to reveal the role of SNPs located near SLE related lncRNAs, we performed a transcriptome profiling of SLE patients and identified linc00513 as a significantly over expressed lncRNA containing functional SLE susceptibility loci in the promoter region. The risk-associated G allele of rs205764 and A allele of rs547311 enhanced linc00513 promoter activity and related to increased expression of linc00513 in SLE. We also identified linc00513 to be a novel positive regulator of type I interferon pathway by promoting the phosphorylation of STAT1 and STAT2. Elevated linc00513 expression positively correlated with IFN score in SLE patients. Linc00513 expression was higher in active disease patients than those inactive ones. In conclusion, our data identify two functional promoter variants of linc00513 that contribute to increased level of linc00513 and confer susceptibility on SLE. The study provides new insights into the genetics of SLE and extends the role of lncRNAs in the pathogenesis of SLE.

Keywords: single-nucleotide polymorphism, long non-coding RNA, systemic lupus erythematosus, interferon, CRISPR-dCas9

OPEN ACCESS

Edited by:
José Carlos Crispín, Instituto Nacional de Ciencias Médicas y Nutrición Salvador Zubirán (INCMNSZ), Mexico

Reviewed by:
Iris Karina Madera-Salcedo, Instituto Nacional de Ciencias Médicas y Nutrición Salvador Zubirán, Mexico
Carmelo Carmona-Rivera, National Institute of Arthritis and Musculoskeletal and Skin Diseases (NIAMS), United States

***Correspondence:**
Yuanjia Tang
tangyuanjia028@163.com
Nan Shen
nanshensibs@gmail.com

[†] These authors have contributed equally to this work

Specialty section:
This article was submitted to Autoimmune and Autoinflammatory Disorders, a section of the journal Frontiers in Immunology

Received: *16 September 2018*
Accepted: *03 December 2018*
Published: *18 December 2018*

Citation:
Xue Z, Cui C, Liao Z, Xia S, Zhang P, Qin J, Guo Q, Chen S, Fu Q, Yin Z, Ye Z, Tang Y and Shen N (2018) Identification of LncRNA Linc00513 Containing Lupus-Associated Genetic Variants as a Novel Regulator of Interferon Signaling Pathway. Front. Immunol. 9:2967. doi: 10.3389/fimmu.2018.02967

INTRODUCTION

Systemic lupus erythematosus (SLE) is a heterogenous autoimmune disease with complex immune phenotype and diverse clinical manifestations (1, 2). Genetic and environmental factors are considered the two most important pathogenic factors, however the exact etiology of SLE remains obscure (3–5). High-throughput technologies used in genome-wide association studies (GWASs) have identified plenty of important SLE susceptibility loci (6–8) yet the exact roles of these SNPs are still largely unknown. It is interesting to note that the vast majority of the identified SNPs are located in non-coding regions, and some of them have been proven to be functional. For instance, our previous study revealed a variant in miR-146a promoter could regulate miR-146a expression and contribute to SLE disease risk (9). However, most of the functional studies are focused on SNPs in the coding regions (10–13), with limited attention paid to the function of SNPs that located in the non-coding regions, markedly in the regions around disease related lncRNAs.

LncRNAs have been proved to be effective regulators of gene expression and important modulator in diverse biological processes (14–16). Deregulation of lncRNAs was demonstrated to have relevance to aberrant immune response and linked to autoimmune diseases such as multiple sclerosis (MS), rheumatoid arthritis (RA) and SLE (17–19). Although SLE is a highly heterogeneous disease, a large part of the patients have the common feature of high expression levels of interferon (IFN)-inducible genes, which is so called IFN signature (20–22). As recently revealed by hitherto the largest transcriptional profiling of SLE patients, about 80% of the SLE patients have the IFN signature (23). Type I IFN is the cytokine that functions in shaping various immune responses (24–26). Many potential mechanisms have been identified to be implicated in exacerbation of SLE disease by IFN (27–30). Hence type I IFN is thought to be one of the most important signaling pathways involved in SLE pathogenesis. Non-coding RNAs like microRNAs miR-146a and miR-155 have been reported to be effective regulators of type I IFN pathway (31, 32). It is conceivable that lncRNAs may probably also play a non-negligible role in regulating IFN pathway and contribute to SLE disease development.

In an effort to reveal the role of SNPs located near SLE related lncRNAs, we made an attempt to dissect the function of SLE susceptible variants by focusing on those near the candidate lncRNA selected based on high-throughput transcriptome analysis. We identified linc00513 from a group of distinctly over expressed lncRNAs as it contained SLE susceptible SNP in the promoter (6). We demonstrated that linc00513 was a novel positive regulator of IFN signaling pathway and was responsible for the amplified IFN signaling in SLE patients. Our data also provided evidence that SNPs rs205764 and rs547311 in the promoter region of linc00513, which modulate its expression, can affect disease susceptibility of SLE.

MATERIALS AND METHODS

Patients and Ethics Statement

139 SLE patients were recruited for the genotyping and mRNA expression studies. All patients that recruited met the 1997 American College of Rheumatology (ACR) criteria for SLE. The study was conducted in accordance with the principles expressed in the Declaration of Helsinki and was approved by the Research Ethics Board of Renji Hospital, School of Medicine, Shanghai Jiaotong University.

IFN Scores Calculation

The IFN scores were calculated from the expression data for three representative IFN-inducible genes according to a previously described algorithm (33). In this study we selected three typically type I IFN-inducible genes IFI44, Mx1, and OAS1 to calculate (20, 21, 34). The mean IFN score for the SLE patients was 19.37 $\pm$ 22.25, and the mean IFN score for the 21 sex- and age-matched healthy controls was 0 $\pm$ 2.82.

DNA Isolation and Genotyping

Genomic DNA was isolated from human whole blood samples using QIAamp DNA blood kit (Qiagen) and quantified using a NanoDrop spectrophotometer (NanoDrop Technologies). SNPs rs205764 and rs547311 were genotyped with specified TaqMan SNP genotyping probes (Applied Biosystems) following the manufacturer's recommendations for allelic discrimination in the QuantStudio™ 7 Flex Real-Time PCR System (Applied Biosystems).

RNA Sequencing

RNAs isolated from 22 SLE patients and 7 sex- and age-matched controls renal tissues were qualified by agarose electrophoresis and Agilent 2100 bioanalyzer system under a criteria of 260/280 within 1.8- 2.0, RIN >7, 28S/18S >1.5 and concentration >50 ng/μl. Strand-specific cDNA library was generated from 3μg of RNA using NEBNext Ultra Directional RNA Library Prep Kit for Illumina (NEB, New England Biolabs) after removal of rRNA by Ribo-Zero Gold rRNA Removal Kit (Illumina). Libraries were then sequenced on a Illumina HiSeq 4000 instrument with paired-end reads 150 bp per sample. Filtered and trimmed reads were mapped to human genome reference sequence (UCSC hg38), count the mapped reads to estimate transcriptome abundance. Differential expression analysis was performed using R software. The threshold to define up-regulation was fold change >2 and $p < 0.05$.

Antisense Oligonucleotides (ASOs) and Constructs

ASOs were designed from Sfold website according to a set of principles and synthesized by Sangon Biotech, Shanghai. Seeded hela cells were transfected with 200 nM ASO or negative control using Lipofectamine RNAimax (Invitrogen) according to the manufacturer's instructions for 24 h and then either treated with 1,000 units/ml type I IFN (PBL) according to the experimental needs. To compare the activity of linc00513 promoter containing

the two different alleles, linc00513 promoter–luciferase reporter vectors containing four different combinations of alleles were generated by cloning a 1.12 kb region upstream and approximate to the TSS of linc00513 (−684 to +439) into the pGL3-basic luciferase vector (Promega). To create dCas9/CRISPRi lncRNA expression regulation system, single-guide RNAs (sgRNAs) were designed on Optimized CRISPR Design Website (http://crispr.mit.edu), and cloned either into sgRNA vector that constructed from pEMT vector backbone by our laboratory or into SAM-sgRNA vector that kindly provided by Professor Feng Zhang from MIT. DCas9-Krab and dCas9-VP64 vector were kindly provided by Professor Lei S. Qi from Stanford University and Professor Feng Zhang from MIT, respectively. The sequences of the ASOs, sgRNAs and cloning primers of promoter used in this study were listed in the Supplementary Materials (**Table S1**, **Figure S1**).

Cell Culture, Stimulation, and Transfection

Hela and THP-1 cells were obtained from the Cell Bank, Shanghai Institutes for Biological Sciences, Chinese Academy of Sciences and grown in Dulbecco's modified Eagle's medium (Gibco) or RPMI 1640 (Gibco) containing 10% fetal bovine serum (Gibco). PBMCs were isolated freshly from human peripheral blood using Ficoll-Paque (GE Healthcare). Neutrophils were isolated from the buffy coat after lysis of red blood cells. PBMCs and neutrophils were cultured in RPMI 1640 (Gibco) supplemented with 10% FBS. All cells were maintained at 37°C with a 5% CO_2 atmosphere. Type I IFN (PBL) was added in the final concentration of 1,000 units/ml. Plasmids and ASOs were transfected into hela cells with Lipofectamine 2000 (Invitrogen) and Lipofectamine RNAiMAX (Invitrogen) according to the manufacturer's instructions, respectively. Plasmids, ASOs and transfection reagents were diluted with Opti-MEMI medium (Gibco) and incubation at room temperature for 20 min after gently mixed, and then the transfection mixture was added to the cell culture. Fresh media were exchanged 5 h after transfection.

RNA Extraction and Real-Time PCR

Total RNA was extracted using TRIzol (Ambion), and then cDNA was synthesized by reverse transcription using PrimeScript RT Reagent kit (Takara) followed by amplification and quantification by real-time PCR with SYBR Premix Ex Taq™ kit (Takara) in QuantStudio™ 7 Flex Real-Time PCR System (Applied Biosystems). The relative expression levels of target genes and lncRNA were calculated using the $2^{-\Delta CT}$ method normalized to GAPDH. The primers used in the experiments were shown in the Supplementary Materials (**Table S1**).

Reporter Gene Assay

One hundred nanogram of 1.12 kb–linc00513 promoter luciferase reporter vector or control pGL3-basic luciferase vector together with 10 ng of Renilla vector were transfected into each well of hela cells that seeded in 96-well plate. Twenty four hours after transfection, cell lysates were added to a 96-well black flat bottom microplate (Greiner Bio-one) and their luciferase activities were measured on a CENTRO XS3 LB 960 luminometer (Berthold) using Dual-Luciferase Reporter Assay System (Promega). The ratio of firefly to Renilla luciferase of each well was calculated and analyzed. All experiments were performed in triplicate or quadruplicate.

Rapid Amplification of cDNA Ends (RACE)

RACE was performed using SMARTer RACE 5′/3′ Kit (Clontech, Takara) according to manufacturer's instructions to identify the whole sequence of linc00513 transcripts. Briefly, total RNA was extracted freshly from hela cells and 3′- and 5′-RACE-ready cDNAs were synthesized using SMARTScribe Reverse Transcriptase. The amplified PCR products were purified by electrophoresis in 1% agarose gel followed by gel extraction. The purified PCR fragments were cloned into linearized pRACE vector and then sequenced. 3′- and 5′-RACE gene-specific primers (GSPs) were designed according to the reads sequence obtained from RNA-seq. The 3′- and 5′- GSPs and nest GSPs sequences were available in the Supplementary Materials (**Table S1**).

Fluorescence *in situ* Hybridization

Hela cells were seeded and grew on the surface of a poly-L-lysine prepared slide inside a 10-cm cell culture dish and then fixed with ethanol. Fixed cells were permeated with DEPC treated 0.1% tritonX-100 for 15 min and wished twice with PBS. Slides were successively treated with SSC, 75, 85, and 100% ethanol and then dried at room temperature. Cells on the slides were detected with 100 μl of the pre-heated hybridization buffer containing probe by incubating in the dark at 37°C in a humidified chamber over night. 5 ng/ml DAPI was used to counter stain the nuclei in the dark at 37°C for 30 min. Slides were washed and observed under a fluorescence microscope. Probe used in FISH experiment was 5′CY3 modified. Probe sequence was shown in the Supplementary Materials (**Table S1**).

Western Blotting

Hela cells were seeded at 4×10^5/well in a 6-well plate and transfected with ASO at the final concentration of 200 nM for 24 h. Then cells were stimulated with IFN (1,000 units/ml) for 15 min or 1 h and lysed with RIPA buffer (Pierce, Thermo Scientific) supplemented with protease inhibitor cocktail (Pierce, Thermo Scientific). The cell protein was loaded to SDS-PAGE gel electrophoresis and blotted with the appropriate antibodies. Band signals were visualized with a SuperSignal West Pico kit (Pierce, Thermo Scientific). The antibodies used were as follows: GAPDH rabbit mAb (HRP conjugate), STAT1 rabbit mAb, phospho-STAT1 rabbit mAb, STAT2 rabbit mAb, phospho-STAT2 rabbit mAb, IRF9 rabbit mAb, HRP-linked anti-rabbit IgG. All the antibodies were from Cell Signaling Technology. The primary antibodies were diluted by 1:1,000. The secondary antibody was diluted by 1:2,000.

Flow Imaging Cytometry

Hela cells transfected with NC or ASOs were stimulated with IFN (1,000 units/ml) for 30 min and then fixed and permeated with eBioscience transcription factor staining buffer set (Invitrogen) according to the manufacturer's protocol. Cells were resuspended in 100 μl of FACS buffer and incubated with antibody (diluted by

1:50) for at least 30 min at room temperature in dark. DAPI was used to stain cell nuclei for <3 min. Cells were then washed and resuspended in FACS buffer (volume between 20 and 200 μl) in an appropriate cell concentration of 1–2 × 10^7/ml. Cell samples were loaded and analyzed using Amnis ImageStream MarkII (Merck). Similarity between STAT1 and nuclei staining pattern were calculated. The antibody used in flow imaging cytometry experiment was STAT1 rabbit mAb (PE Conjugate; Cell Signaling Technology).

Data Analysis

Statistical tests were performed with GraphPad Prism software, version 5.01. Figure data are expressed as the arithmetic mean ± SEM. The nonparametric Mann–Whitney *U*-test was used to compare linc00513 expression between the genotype groups and gene expression between the patients and controls. The unpaired *t*-test was used to compare the expression of genes and the luciferase activity of the reporter genes. Spearman's test was used for correlation analysis. Two-tailed *p*-values < 0.05 were considered to be statistically significant. Linkage disequilibrium (LD) patterns were analyzed and displayed with HaploView (35).

RESULTS

Linc00513 Is an Over Expressed LncRNA in SLE Containing Disease Susceptibility Loci in the Promoter Region

To identify the aberrant LncRNA expression profile in SLE, we performed transcriptome analysis in 22 lupus patients and 7 controls renal tissues and found 56 significantly over expressed lncRNAs with fold change >2 and *p*-value < 0.05 (**Table S2**). Then we selected candidate lncRNA from the list using two approaches. The first approach took advantage of differentially expressed lncRNAs profiling in SLE. LncRNAs that aberrantly expressed as compared with controls were selected. In the second approach, we focused on the SNPs identified by previous reported GWAS to have association with lupus susceptibility that closely located to the candidate lncRNAs (**Figure 1A**). Linc00513 was then chosen for further analysis as it ranked the second over expression and meanwhile contained lupus susceptibility SNP rs547311(G>A) approximate to the transcriptional starting region (**Figure 1B**). According to the GWAS of SLE in a Chinese Han population genotyping 1,047 cases and 1,205 controls, the minor A allele (14.95%) of rs547311 confer risk on SLE, odds ratio [OR] = 1.46, *p* value = 3.88 × 10^{-4} (6). We also analyzed another SNP rs205764 (T>G) in close proximity to linc00513 transcriptional starting site in the HapMap database. The two SNPs had very high LD ($r^2 = 0.9$. **Figure 2A**), which implied the two SNPs in linc00513 promoter region, rs205764 along with rs547311 could play a role in the pathogenesis of SLE.

Rs205764 and Rs547311 Modulate Linc00513 Expression

According to GWASdb database (36, 37), up to 50 SNPs in 400 kb region around rs205764 and rs547311 have been reported to show human disease susceptibility, which indicates the gene region could be important to human diseases. In order to examine whether the two SNPs in the promoter region of linc00513 were functional, we cloned the promoter of linc00513 (1.12 kb, from −684 to +439) carrying different SNP alleles into the pGL3-basic dual fluorescent reporter gene vector, and determined that the minor alleles (G of rs205764 and A of rs547311) significantly enhanced the transcriptional activity of the linc00513 promoter (**Figure 2B**). We further tested whether different alleles were associated with linc00513 expression level in SLE patients. Because many confounding factors could disturb the result of expression quantitative trait loci (eQTL) effect, it is preferable to study gene expression in a single cell subset. We examined the eQTL effect in neutrophils because of their good availability and good representativeness of peripheral blood cells. Meanwhile, neutrophils were recently considered very important player in lupus pathogenesis (23, 38–40). We genotyped 139 SLE

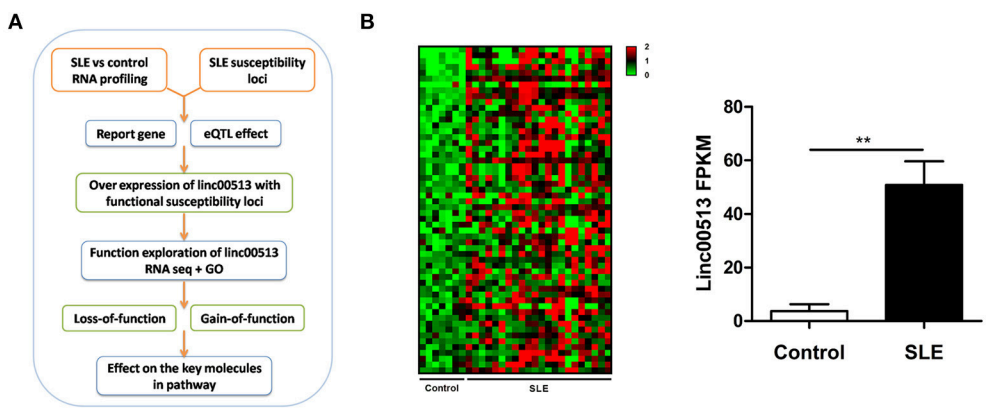

FIGURE 1 | Identification of linc00513 as a significantly over expressed lncRNA in SLE that contains lupus susceptibility SNP in the promoter region. **(A)** Schematic diagram of the whole experiment process. **(B)** 56 lncRNAs showed significant over expression in transcriptome profiling of renal tissues from 22 SLE and 7 controls. FPKM of linc00513 in SLE and control samples were compared using non-parametric Mann-Whitney *U*-test, **indicates $p < 0.01$. Linc00513 ranked the second over expression and meanwhile contained lupus susceptibility SNPs approximate to the transcriptional starting region mentioned by previous GWAS report.

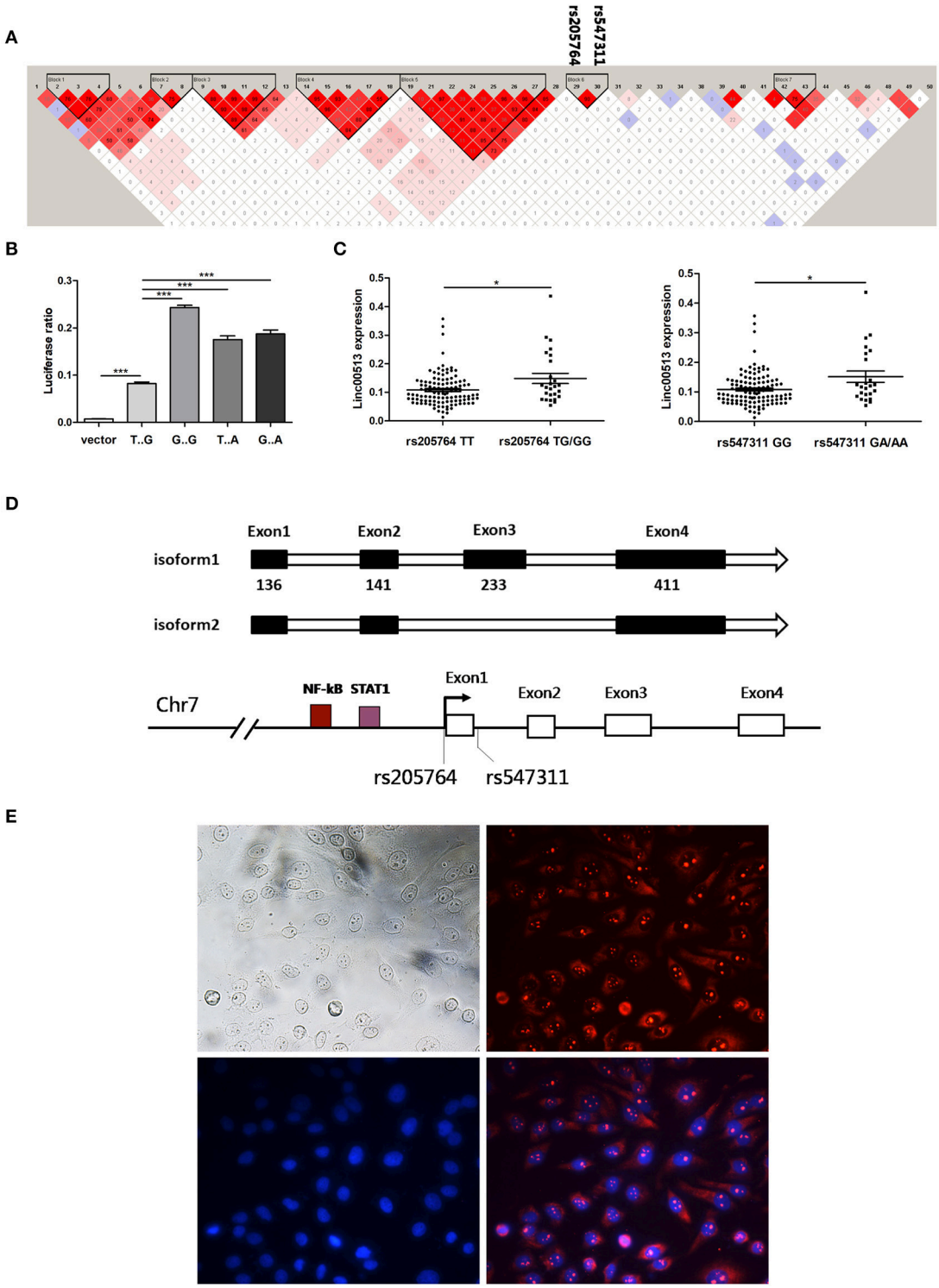

FIGURE 2 | Rs205764 and rs547311 could modulate the expression of linc00513 expression. **(A)** LD patterns of 50 human disease related SNPs in the gene region. Two haplotype blocks were constructed based on the strength of LD in each gene region. **(B)** Luciferase reporter gene assay of linc00513 promoter. 1.12 kb approximate to the TSS of linc00513 (−684 to +439) was cloned into the pGL3-basic luciferase vector. HeLa cells were transfected with linc00513 promoter or control pGL3-basic luciferase reporter vector and Renilla reporter vector. 24 h after transfection, cells were lysed and ratio of firefly to Renilla luciferase activity was analyzed. The data shown are means ± SEM and are representative of three independent experiments performed in triplicate or quadruplicate. *P*-values were

(Continued)

FIGURE 2 | analyzed with two-tailed unpaired *t*-test. ***indicates $p < 0.001$. Rs205764 G allele and rs547311 A allele improved linc00513 promoter activity. **(C)** Relative expression level of linc00513 was measured for the different genotypes of rs205764 and rs547311 in neutrophils from 139 SLE individuals (rs205764: TT, $n = 113$; TG, $n = 24$; GG, $n = 2$. rs547311: GG, $n = 115$; GA, $n = 22$; AA, $n = 2$.) *P*-values were analyzed with non-parametric Mann-Whitney *U*-test. *indicates $p < 0.05$. **(D)** Gene structural models of linc00513 as determined by 3′ and 5′ RACE. **(E)** Nuclear and plasma distribution of linc00513 in hela cells as showed by FISH. Upper left: white light; upper right: linc00513 (red); lower left: DAPI (blue); lower right: merge of linc00513 and DAPI.

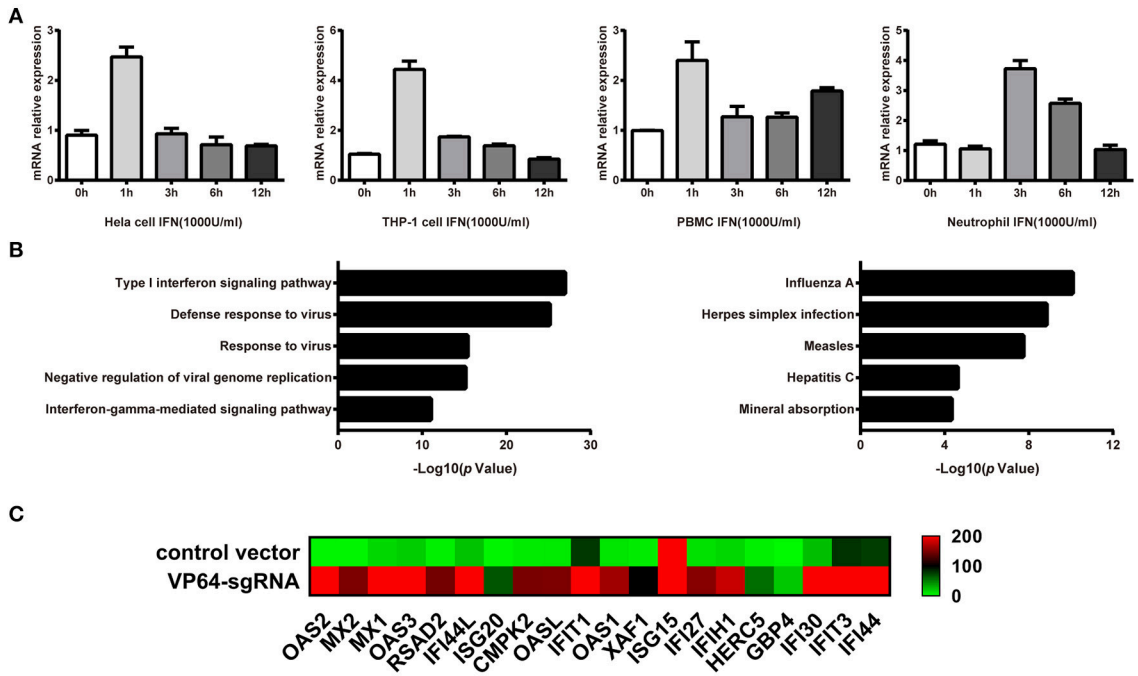

FIGURE 3 | Identification of genes that are regulated by IFN-stimulated lncRNA linc00513. **(A)** Induction of linc00513 by 1,000 U/ml type I IFN in four different cell types on indicated time points, 0, 1, 3, 6, 12h. **(B)** GO and Pathway analysis of linc00513-regulated genes from RNA-seq result in hela cells. **(C)** Expression change of ISGs in hela cells after up-regulation of linc00513 by CRISPR/dCas9-VP64 as compared with cells transfected with empty vectors.

patients and quantified linc00513 expression in their neutrophils. Patients with TG/GG of rs205764 or GA/AA of rs547311 showed higher expression level of linc00513. So rs205764 (T>G) and rs547311 (G>A) presented eQTL effects on linc00513 in SLE patients (**Figure 2C**).

Since we have demonstrated that linc00513 was distinctly high expressed in SLE and its promoter could be propelled by two SLE risk related SNPs, so linc00513 could probably be an important lncRNA in SLE. We identified the whole sequence of linc00513 transcript in hela cells using RACE technology, and determined a 921 nt 4-exons isoform of linc00513. An alternative isoform lacking the third exon was also found (**Figure 2D**, **Figures S2, S3**). On the basis of whole sequence identification, specific probe was designed for FISH experiment to explore its subcellular localization. As the result revealed, linc00513 showed punctate aggregation distribution in the nucleus with partially dispersed in the cytoplasm (**Figure 2E**).

Identification of Linc00513-Regulated Genes

Genomatix prediction revealed the possible binding sites of STAT1 and NF-kB in linc00513 promoter, which were crucial transcription factors downstream of IFN signaling pathway. This result suggested linc00513 might be an IFN-stimulated lncRNA. In order to verify this issue, we treated hela cells with 1,000 U/ml type I IFN and found linc00513 could be induced by IFN with strongest induction on 1 h (**Figure 3A**). We also showed the induction of linc00513 in response to type I IFN treatment is not restricted to specific cell types. In addition to hela cells, the induction were also observed in other human cell lines and primary blood cells, including THP-1 cells, peripheral blood mononuclear cells (PBMCs) and neutrophils (**Figure 3A**). We then intended to detect the exact role of linc00513 in SLE. We overviewed the landscape of genes that might be regulated by linc00513. As CRISPR/dCas9-VP64 vector system could be applied to up-regulate gene transcription *in situ* (41, 42), we constructed CRISPR/dCas9-VP64 vector system by designing a sgRNA targeting linc00513 promoter region to effectively promote linc00513 transcription. Then we performed RNA-seq transcriptome analysis in hela cells and revealed 615 genes significantly changed after up-regulating linc00513 (Fold change >2). Intriguingly, we could see genes regulated by linc00513 were mainly interferon-inducible genes, and GO enrichment and KEGG pathways analysis revealed significant involvement

of IFN signaling pathway in linc00513-regulated gene network (**Figures 3B,C**). These results strongly imply that linc00513 may play an important role in regulating the downstream pathway of IFN.

Linc00513 Promotes the Expression of Downstream Genes of IFN Pathway

To explore the effect of linc00513 on the IFN signaling pathway, we knocked down the expression of linc00513 in hela cells by two different means, ASOs transfection and CRISPR/dCas9-KRAB vector system. The knock down efficiency of ASOs and CRISPR/dCas9-KRAB vector system were about 75 and 60%, respectively. After knockdown of linc00513, IFN-stimulated gene (ISG) IFIT1 expression was significantly inhibited either with or without IFN stimulation. OAS1 expression also significantly decreased after IFN stimulation, though it didn't significantly decrease without IFN stimulation (**Figures 4A,B**). We also performed linc00513 up-regulation experiment using CRISPR/dCas9-VP64 vector system. Similarly, up-regulation of linc00513 significantly promoted IFIT1 and OAS1 expression (**Figure 4C**). Taken together, these data indicate that linc00513 is the positive regulator of the IFN signaling pathway.

Effects of Linc00513 on the Phosphorylation of Key Molecules in Type I IFN Signaling Pathway

Several lncRNAs that involved in immune pathways have been reported may act through altering the phosphorylation of important transcription factors (43, 44). We tested whether

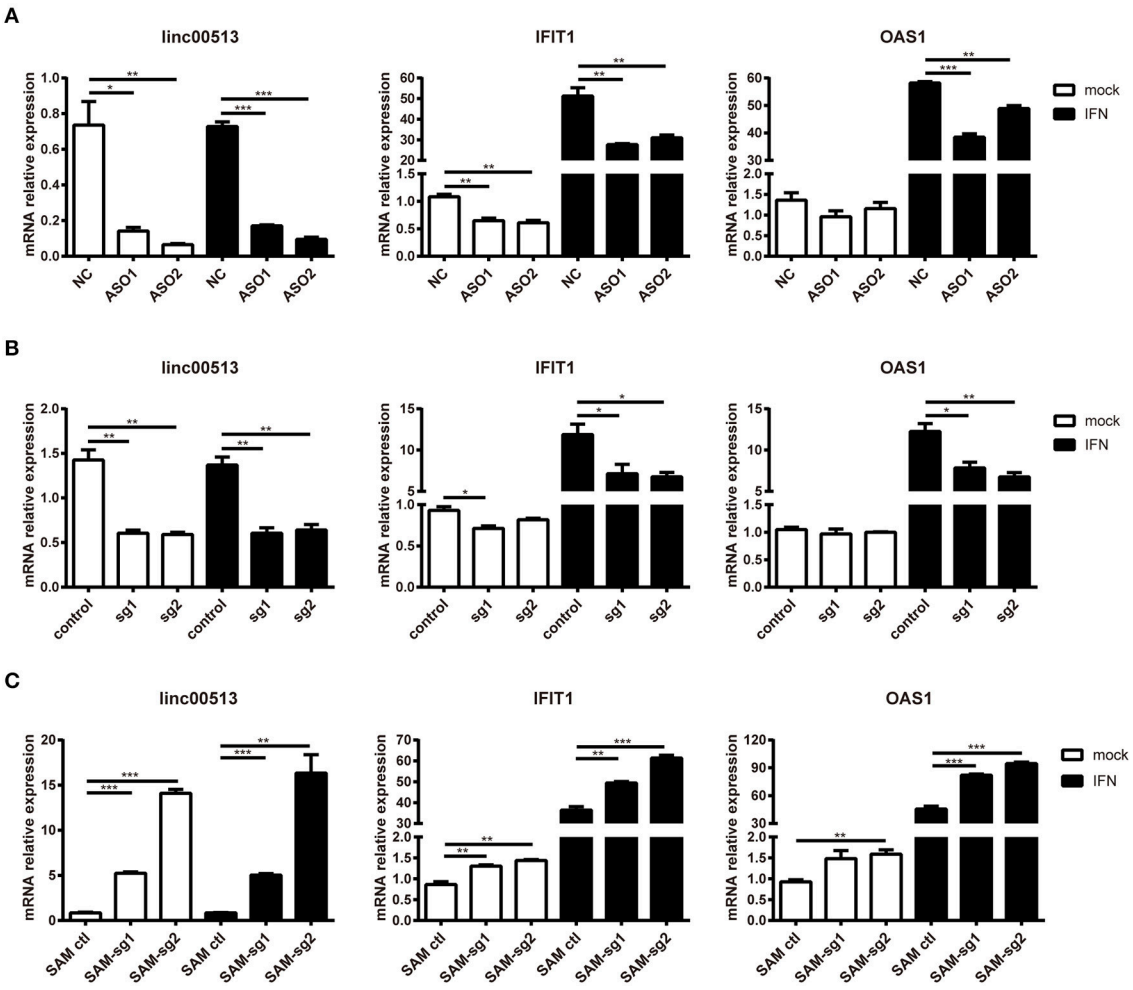

FIGURE 4 | Promotion of the downstream genes of IFN pathway by linc00513. **(A)** Hela cells were transfected with NC or specific ASOs (200 nM) for 24 h and then stimulated with type I IFN. **(B)** Hela cells were transfected with control vectors or specific sgRNA and dCas9-Krab vectors for 24 h and then stimulated with type I IFN. **(C)** Hela cells were transfected with control vectors or specific SAM-sgRNA and dCas9-VP64 vectors for 48 h and then stimulated with type I IFN. Type I IFN was used at the final concentration of 1,000 U/ml for 6 h. The relative expression of linc00513, IFIT1, and OAS1 were analyzed by qPCR. The data shown are means ± SEM and are representative of three independent experiments performed in triplicate. *P*-values were analyzed with two-tailed unpaired *t*-test. *indicates $p < 0.05$, **$p < 0.01$, ***$p < 0.001$.

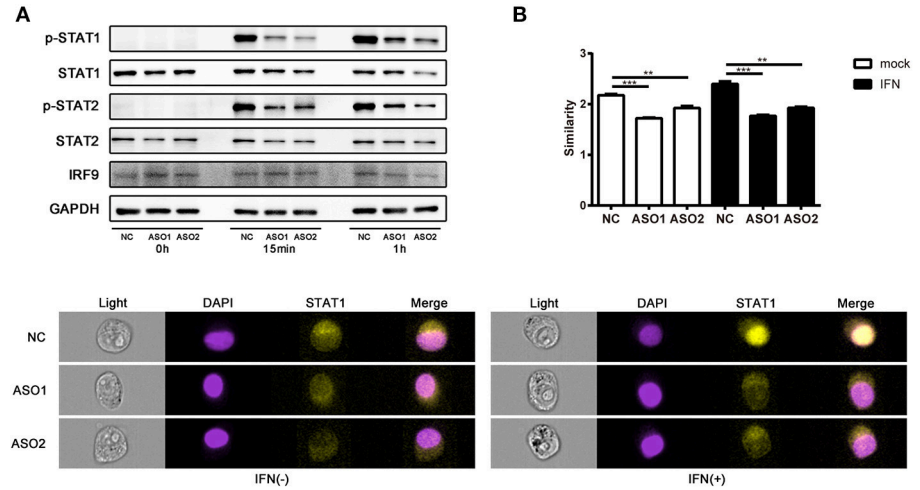

FIGURE 5 | Linc00513 affects the phosphorylation of STAT1 and STAT2 in type I IFN pathway. **(A)** Western blotting of hela cells transfected with NC or specific ASOs (200 nM) for 24 h and then stimulated with type I IFN (1,000 U/ml) for 15 min or 1 h. Blots are representative of three repeated experiments. Quantification of band intensities analysis was shown in **Figure S4**. **(B)** Flow imaging cytometry of hela cells transfected with NC or specific ASOs (200 nM) for 24 h and then stimulated with type I IFN (1,000 U/ml) for 30 min. Cells were stained with antibody to STAT1 and DAPI after fixation and permeabilization. Values of similarity represent the extent of STAT1 translocation to the nuclei. The data shown are means ± SEM and are representative of three repeated experiments. *P*-values were analyzed with two-tailed unpaired *t*-test. **indicates $p < 0.01$, ***$p < 0.001$. Cell images are representative of three repeated experiments.

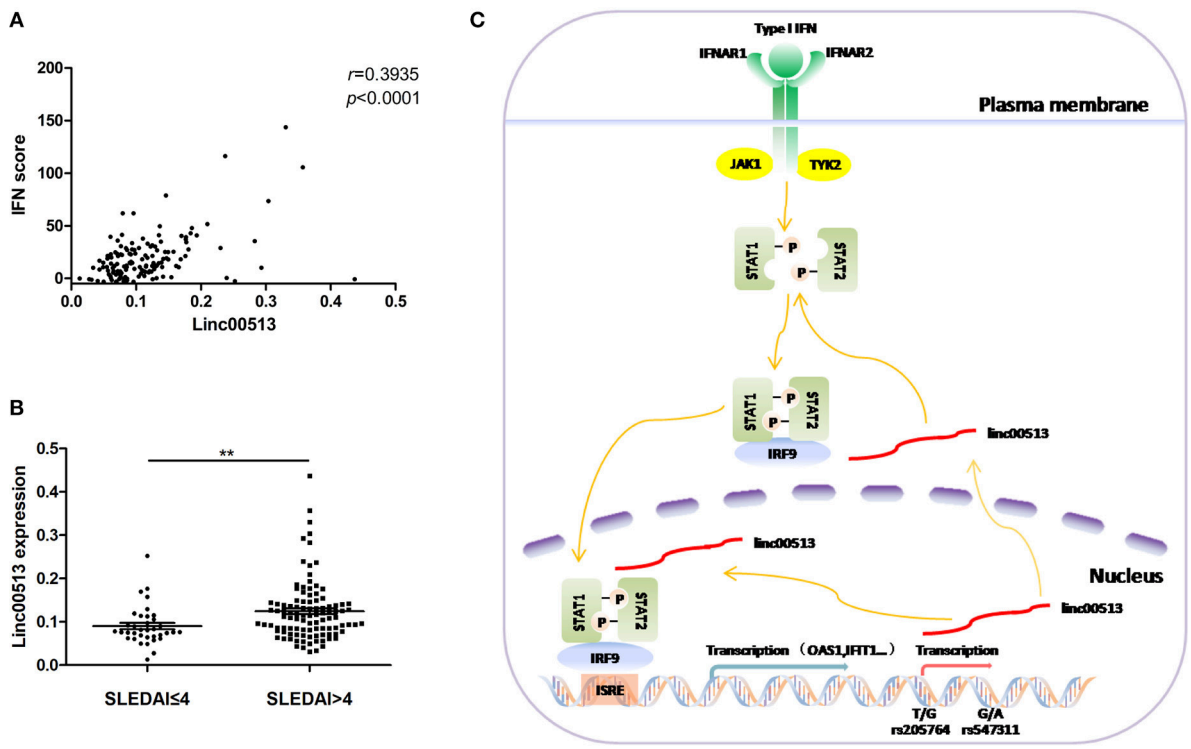

FIGURE 6 | Association between linc00513 and SLE Disease. **(A)** Positive correlation between the expression of linc00513 and IFN scores in SLE patients. *P*-value was determined by Spearman's correlation test. **(B)** The expression of linc00513 was higher in active SLE patients ($n = 36$) than those inactive ones ($n = 103$). *P*-value was determined by non-parametric Mann-Whitney *U*-test, **indicates $p < 0.01$. **(C)** Overview of the modulation of linc00513 by SLE-associated genetic variants and the regulation of type I IFN signaling pathway by linc00513.

linc00513 played a role in the IFN signaling pathway by modulating key pathway molecules phosphorylation. Western blotting was performed in hela cells tranfected with ASOs targeting linc00513. Knockdown of linc00513 significantly reduced the phosphorylation of STAT1 and STAT2. Intriguingly, to a certain extent, STAT1, STAT2, and IRF9 are also interferon-inducible genes, so it could be explicable that total STAT1, total STAT2, and IRF9 expression also slightly decreased after linc00513 down-regulation (**Figure 5A**). We then also performed western blotting in hela cells that over expressed linc00513 by CRISPR/dCas9-VP64 vector system transfection. Up-regulation of linc00513 could significantly increase the phosphorylation of STAT1 and STAT2 (**Figure S5**). Both results supported the role of linc00513 in type I IFN signaling pathway. In type I IFN pathway, the phosphorylation of STAT1 and STAT2 occurs downstream of IFNAR activation, leading to the assembly of the ISGF3 complex which is composed of STAT1-STAT2 dimers and IRF9 (45, 46). ISGF3 translocates into the nucleus and binds to IFN-stimulated response elements (ISRE) in the promoters of IFN-inducible genes to regulate their expression. We further verified the previous result by using flow imaging cytometry and determined the nuclear translocation of STAT1 was reduced after knockdown of linc00513 (**Figure 5B**). Therefore, we concluded that linc00513 promotes IFN pathway by modulating the phosphorylation of key transcription factors STAT1 and STAT2.

Association Between Elevated Linc00513 and SLE Disease

Our data have showed the expression of linc00513 was elevated in lupus patients and linc00513 was a positive regulator of IFN pathway. Then we explored whether there was a correlation between linc00513 expression and IFN score in lupus patients. We analyzed neutrophils from 139 SLE patients and found a significant positive correlation between linc00513 expression and IFN score ($r = 0.3935$, $p < 0.0001$; **Figure 6A**). Clinical information of the patients was listed in **Table 1**. In addition, we also analyzed the relationship between linc00513 expression levels and SLE disease activity in the same group of patients. Linc00513 expression was higher in active disease patients (SLEDAI-2K > 4) than those inactive ones (SLEDAI-2K ≤ 4; $p = 0.0017$; **Figure 6B**). Taken together, these data indicate that linc00513 is responsible for the amplified IFN signaling in SLE patients and can contribute to SLE disease activity.

TABLE 1 | Demographic, clinical, and laboratory features of the SLE patients.

Characteristics	$n = 139$
Females	130 (93.5%)
Age (years)	33.8 ± 13.2
ANA (+)	139 (100%)
Anti-dsDNA (+)	106 (76.3%)
Anti-Sm (+)	30 (21.6%)
SLEDAI-2K	10.2 ± 5.8

DISCUSSION

LncRNAs are emerging as indispensable regulators in various biological processes. Aberrations in the lncRNA-mediated immune responses regulation has been linked to autoimmune and autoinflammatory diseases (18, 47, 48). In lupus, over expression of lncRNA NEAT1 was reported to promote secretion of multiple pro-inflammatory cytokines and positively correlated with lupus disease activity (17). The expression of another lncRNA linc0949 was significantly decreased in lupus patients PBMCs and was associated with complement component C3 level and incidence of lupus nephritis (49). While certain lncRNAs have been reported to be involved in SLE pathogenesis, systemic profiling of differentially expressed lncRNAs in SLE is still limited. Our transcriptional profiling in renal tissues of SLE patients and controls revealed abnormally expressed lncRNAs in SLE and identified linc00513 as one of the most significantly over expressed lncRNAs with lupus susceptible SNP loci in the promoter region.

SLE is a complex autoimmune disease with obscure etiology. The type I IFN signaling pathway is recognized to play a pivotal role in SLE pathogenesis among the diverse immunological aberrations present in SLE patients. Several coding genes have been previously identified capable of balancing IFN signaling, like cyclin-dependent kinase 1 (CDK1), a cell cycle regulatory protein gene, could contribute to the over activation of IFN pathway in SLE (50). Our recent research characterized the role of a lncRNA as a positive regulator of the type I IFN signaling by modulating the phosphorylation of key transcription factors STAT1 and STAT2 in this pathway. Knockdown of linc00513 in hela cells reduced the expression of IFIT1 and OAS1, two representative IFN-inducible genes. Similarly, up-regulation of linc00513 promoted ISGs expression. The expression level of linc00513 positively correlated with the IFN score of lupus patients. Thus, we identified linc00513 as a novel robust regulator of type I IFN pathway, providing new evidence for the contribution of non-coding RNAs to the pathogenesis of lupus.

The role of genetic factors in autoimmune disease risk has long been established, however studies on functional exploration of SNPs are quite limited, especially for SNPs in lupus related lncRNA regions. By contrast, it's remarkable that functional studies of cancer related lncRNA SNPs are making continuous progresses. Several specialized databases have even been set up (51, 52). As for lupus, in 2006, six SNPs in the promoter region of Growth arrest-specific 5 (GAS5) had been identified to cause 11-fold down-regulation of the lncRNA expression and correlated with nephritis susceptibility in spontaneous lupus nephritis mouse model BXSB strain (53). Here in our study, we demonstrated rs205764 and rs547311 in the promoter of linc00513 could augment its transcription as determined by reporter gene assay and eQTL effect, thus making linc00513 a distinctly high expressed lncRNA in lupus patients and promoting disease development. To the best of our knowledge, this is the first report to reveal a functional genetic variant in a lncRNA promoter that

contributing to SLE disease in human. Our work spotlights the importance of exploring SNP variants in lncRNA regions, which have been more or less ignored in previous genetic studies.

In conclusion, our findings reveal the over expression of linc00513 plays a role in lupus pathogenesis by promoting IFN signaling pathway. SNP variants of the linc00513 promoter are functionally significant in regulating linc00513 expression and conferring susceptibility on SLE (**Figure 6C**). The study provides new insights into the genetics of SLE and suggests lncRNAs can be novel biomarkers of SLE pathogenesis.

AUTHOR CONTRIBUTIONS

All authors were involved in drafting the article or revising it critically for important intellectual content, and all authors approved the final version to be published. ZX, YT, and NS conceived and designed the experiments, ZX, CC, ZL and SX performed the experiments, ZX, CC, and ZL analyzed and interpreted the data, NS, YT, PZ, JQ, QG, SC, QF, ZhY, and ZzY contributed reagents, materials, analysis tools.

FUNDING

This work was supported by the National Key Research and Development Program of China (No. 2017YFC0909000), the National Natural Science Foundation of China (No. 81571576, 81871287, 31630021, and 81421001), the Doctoral Innovation Fund Projects from Shanghai Jiaotong University School of Medicine (grant BXJ201618), the Shanghai Pujiang Young Rheumatologists Training Program (grant SPROG201802), and the Shenzhen Futian Public Welfare Scientific Research Project (grant FTWS2017020).

ACKNOWLEDGMENTS

We thank Prof. Lei S. Qi (Stanford University) for providing dCas9-Krab system vectors and Prof. Wanlin Yang (The University of Hong Kong) for assistance with data analysis.

SUPPLEMENTARY MATERIAL

The Supplementary Material for this article can be found online at: https://www.frontiersin.org/articles/10.3389/fimmu.2018.02967/full#supplementary-material

REFERENCES

1. D'Cruz DP, Khamashta MA, Hughes GR. Systemic lupus erythematosus. *Lancet* (2007) 369:587–96. doi: 10.1016/S0140-6736(07)60279-7
2. Tsokos GC. Systemic lupus erythematosus. *N Engl J Med.* (2011) 365:2110–21. doi: 10.1056/NEJMra1100359
3. Wakeland EK, Liu K, Graham RR, Behrens TW. Delineating the genetic basis of systemic lupus erythematosus. *Immunity* (2001) 15:397–408. doi: 10.1016/S1074-7613(01)00201-1
4. Eroglu GE, Kohler PF. Familial systemic lupus erythematosus: the role of genetic and environmental factors. *Ann Rheum Dis.* (2002) 61:29–31. doi: 10.1136/ard.61.1.29
5. Barbhaiya M, Costenbader KH. Environmental exposures and the development of systemic lupus erythematosus. *Curr Opin Rheumatol.* (2016) 28:497–505. doi: 10.1097/BOR.0000000000000318
6. Han JW, Zheng HF, Cui Y, Sun LD, Ye DQ, Hu Z, et al. Genome-wide association study in a Chinese Han population identifies nine new susceptibility loci for systemic lupus erythematosus. *Nat Genet.* (2009) 41:1234–37. doi: 10.1038/ng.472
7. Lee HS, Kim T, Bang SY, Na YJ, Kim I, Kim K, et al. Ethnic specificity of lupus-associated loci identified in a genome-wide association study in Korean women. *Ann Rheum Dis.* (2014) 73:1240–45. doi: 10.1136/annrheumdis-2012-202675
8. Zhao J, Ma J, Deng Y, Kelly JA, Kim K, Bang SY, et al. A missense variant in NCF1 is associated with susceptibility to multiple autoimmune diseases. *Nat Genet.* (2017) 49:433–37. doi: 10.1038/ng.3782
9. Luo X, Yang W, Ye DQ, Cui H, Zhang Y, Hirankarn N, et al. A functional variant in microRNA-146a promoter modulates its expression and confers disease risk for systemic lupus erythematosus. *PLoS Genet.* (2011) 7:e1002128. doi: 10.1371/journal.pgen.1002128
10. Kozyrev SV, Abelson AK, Wojcik J, Zaghlool A, Linga RM, Sanchez E, et al. Functional variants in the B-cell gene BANK1 are associated with systemic lupus erythematosus. *Nat Genet.* (2008) 40:211–16. doi: 10.1038/ng.79
11. Theodorou E, Nezos A, Antypa E, Ioakeimidis D, Koutsilieris M, Tektonidou M, et al. B-cell activating factor and related genetic variants in lupus related atherosclerosis. *J Autoimmun.* (2018) 92:87–92. doi: 10.1016/j.jaut.2018.05.002
12. Zhang J, Liu X, Meng Y, Wu H, Wu Y, Yang B, et al. Autoimmune disease associated IFIH1 single nucleotide polymorphism related with IL-18 serum levels in Chinese systemic lupus erythematosus patients. *Sci Rep.* (2018) 8:9442. doi: 10.1038/s41598-018-27782-7
13. Wang R, Zeng YL, Qin HM, Lu YL, Huang HT, Lei M, et al. Association of interleukin 22 gene polymorphisms and serum IL-22 level with risk of systemic lupus erythematosus in a Chinese population. *Clin Exp Immunol.* (2018) 193:143–51. doi: 10.1111/cei.13133
14. Lee JT. Epigenetic regulation by long noncoding RNAs. *Science* (2012) 338:1435–39. doi: 10.1126/science.1231776
15. Beermann J, Piccoli MT, Viereck J, Thum T. Non-coding RNAs in development and disease: background, mechanisms, and therapeutic approaches. *Physiol Rev.* (2016) 96:1297–325. doi: 10.1152/physrev.00041.2015
16. Chen YG, Satpathy AT, Chang HY. Gene regulation in the immune system by long noncoding RNAs. *Nat Immunol.* (2017) 18:962–72. doi: 10.1038/ni.3771
17. Zhang F, Wu L, Qian J, Qu B, Xia S, La T, et al. Identification of the long noncoding RNA NEAT1 as a novel inflammatory regulator acting through MAPK pathway in human lupus. *J Autoimmun.* (2016) 75: 96–104. doi: 10.1016/j.jaut.2016.07.012
18. Tang Y, Zhou T, Yu X, Xue Z, Shen N. The role of long non-coding RNAs in rheumatic diseases. *Nat Rev Rheumatol.* (2017) 13:657–69. doi: 10.1038/nrrheum.2017.162
19. Pahlevan KM, Nikravesh A, Shirvani FZ, Sahraian MA, Behmanesh M. HOTAIR but not ANRIL long non-coding RNA contributes to the pathogenesis of multiple sclerosis. *Immunology* (2018) 153:479–87. doi: 10.1111/imm.12850
20. Baechler EC, Batliwalla FM, Karypis G, Gaffney PM, Ortmann WA, Espe KJ, et al. Interferon-inducible gene expression signature in peripheral blood cells of patients with severe lupus. *Proc Natl Acad Sci USA.* (2003) 100:2610–15. doi: 10.1073/pnas.0337679100
21. Bennett L, Palucka AK, Arce E, Cantrell V, Borvak J, Banchereau J, et al. Interferon and granulopoiesis signatures in systemic lupus erythematosus blood. *J Exp Med.* (2003) 197:711–23. doi: 10.1084/jem.20021553
22. Kirou KA, Lee C, George S, Louca K, Peterson MG, Crow MK. Activation of the interferon-alpha pathway identifies a subgroup of systemic lupus

erythematosus patients with distinct serologic features and active disease. *Arthritis Rheum.* (2005) 52:1491–503. doi: 10.1002/art.21031
23. Banchereau R, Hong S, Cantarel B, Baldwin N, Baisch J, Edens M, et al. Personalized immunomonitoring uncovers molecular networks that stratify lupus patients. *Cell* (2016) 165:551–65. doi: 10.1016/j.cell.2016.03.008
24. Le Bon A, Schiavoni G, D'Agostino G, Gresser I, Belardelli F, Tough DF. Type i interferons potently enhance humoral immunity and can promote isotype switching by stimulating dendritic cells *in vivo*. *Immunity* (2001) 14:461–70. doi: 10.1016/S1074-7613(01)00126-1
25. Ray JP, Marshall HD, Laidlaw BJ, Staron MM, Kaech SM, Craft J. Transcription factor STAT3 and type I interferons are corepressive insulators for differentiation of follicular helper and T helper 1 cells. *Immunity* (2014) 40:367–77. doi: 10.1016/j.immuni.2014.02.005
26. Wu D, Sanin DE, Everts B, Chen Q, Qiu J, Buck MD, et al. Type 1 interferons induce changes in core metabolism that are critical for immune function. *Immunity* (2016) 44:1325–36. doi: 10.1016/j.immuni.2016.06.006
27. Pascual V, Farkas L, Banchereau J. Systemic lupus erythematosus: all roads lead to type I interferons. *Curr Opin Immunol.* (2006) 18:676–82. doi: 10.1016/j.coi.2006.09.014
28. Ronnblom L, Eloranta ML, Alm GV. The type I interferon system in systemic lupus erythematosus. *Arthritis Rheum.* (2006) 54:408–20. doi: 10.1002/art.21571
29. Banchereau J, Pascual V. Type I interferon in systemic lupus erythematosus and other autoimmune diseases. *Immunity* (2006) 25:383–92. doi: 10.1016/j.immuni.2006.08.010
30. Thacker SG, Zhao W, Smith CK, Luo W, Wang H, Vivekanandan-Giri A, et al. Type I interferons modulate vascular function, repair, thrombosis, and plaque progression in murine models of lupus and atherosclerosis. *Arthritis Rheum.* (2012) 64:2975–85. doi: 10.1002/art.34504
31. Tang Y, Luo X, Cui H, Ni X, Yuan M, Guo Y, et al. MicroRNA-146A contributes to abnormal activation of the type I interferon pathway in human lupus by targeting the key signaling proteins. *Arthritis Rheum.* (2009) 60:1065–75. doi: 10.1002/art.24436
32. Zhou H, Huang X, Cui H, Luo X, Tang Y, Chen S, et al. miR-155 and its star-form partner miR-155* cooperatively regulate type I interferon production by human plasmacytoid dendritic cells. *Blood* (2010) 116:5885–94. doi: 10.1182/blood-2010-04-280156
33. Feng X, Wu H, Grossman JM, Hanvivadhanakul P, FitzGerald JD, Park GS, et al. Association of increased interferon-inducible gene expression with disease activity and lupus nephritis in patients with systemic lupus erythematosus. *Arthritis Rheum.* (2006) 54:2951–62. doi: 10.1002/art.22044
34. Yao Y, Higgs BW, Morehouse C, de Los RM, Trigona W, Brohawn P, et al. Development of potential pharmacodynamic and diagnostic markers for anti-IFN-alpha monoclonal antibody trials in systemic lupus erythematosus. *Hum Genomics Proteomics* (2009) 2009:374312. doi: 10.4061/2009/374312
35. Barrett JC, Fry B, Maller J, Daly MJ. Haploview: analysis and visualization of LD and haplotype maps. *Bioinformatics* (2005) 21:263–65. doi: 10.1093/bioinformatics/bth457
36. Li MJ, Liu Z, Wang P, Wong MP, Nelson MR, Kocher JP, et al. GWASdb v2: an update database for human genetic variants identified by genome-wide association studies. *Nucleic Acids Res.* (2016) 44:D869–76. doi: 10.1093/nar/gkv1317
37. Li MJ, Wang P, Liu X, Lim EL, Wang Z, Yeager M, et al. GWASdb: a database for human genetic variants identified by genome-wide association studies. *Nucleic Acids Res.* (2012) 40:D1047–54. doi: 10.1093/nar/gkr1182
38. Denny MF, Yalavarthi S, Zhao W, Thacker SG, Anderson M, Sandy AR, et al. A distinct subset of proinflammatory neutrophils isolated from patients with systemic lupus erythematosus induces vascular damage and synthesizes type I IFNs. *J Immunol.* (2010) 184:3284–97. doi: 10.4049/jimmunol.0902199
39. Leffler J, Martin M, Gullstrand B, Tyden H, Lood C, Truedsson L, et al. Neutrophil extracellular traps that are not degraded in systemic lupus erythematosus activate complement exacerbating the disease. *J Immunol.* (2012) 188:3522–31. doi: 10.4049/jimmunol.1102404
40. Lindau D, Mussard J, Rabsteyn A, Ribon M, Kotter I, Igney A, et al. TLR9 independent interferon alpha production by neutrophils on NETosis in response to circulating chromatin, a key lupus autoantigen. *Ann Rheum Dis.* (2014) 73:2199–207. doi: 10.1136/annrheumdis-2012-203041
41. Konermann S, Brigham MD, Trevino AE, Joung J, Abudayyeh OO, Barcena C, et al. Genome-scale transcriptional activation by an engineered CRISPR-Cas9 complex. *Nature* (2015) 517:583–88. doi: 10.1038/nature14136
42. Chen M, Wei L, Law CT, Tsang FH, Shen J, Cheng CL, et al. RNA N6-methyladenosine methyltransferase-like 3 promotes liver cancer progression through YTHDF2-dependent posttranscriptional silencing of SOCS2. *Hepatology* (2018) 67:2254–70. doi: 10.1002/hep.29683
43. Wang P, Xue Y, Han Y, Lin L, Wu C, Xu S, et al. The STAT3-binding long noncoding RNA lnc-DC controls human dendritic cell differentiation. *Science* (2014) 344:310–3. doi: 10.1126/science.1251456
44. Liu B, Sun L, Liu Q, Gong C, Yao Y, Lv X, et al. A cytoplasmic NF-kappaB interacting long noncoding RNA blocks IkappaB phosphorylation and suppresses breast cancer metastasis. *Cancer Cell* (2015) 27:370–81. doi: 10.1016/j.ccell.2015.02.004
45. Platanias LC. Mechanisms of type-I- and type-II-interferon-mediated signalling. *Nat Rev Immunol.* (2005) 5:375–86. doi: 10.1038/nri1604
46. Chen K, Liu J, Cao X. Regulation of type I interferon signaling in immunity and inflammation: a comprehensive review. *J Autoimmun.* (2017) 83:1–11. doi: 10.1016/j.jaut.2017.03.008
47. Tsoi LC, Iyer MK, Stuart PE, Swindell WR, Gudjonsson JE, Tejasvi T, et al. Analysis of long non-coding RNAs highlights tissue-specific expression patterns and epigenetic profiles in normal and psoriatic skin. *Genome Biol.* (2015) 16:24. doi: 10.1186/s13059-014-0570-4
48. Wu GC, Pan HF, Leng RX, Wang DG, Li XP, Li XM, et al. Emerging role of long noncoding RNAs in autoimmune diseases. *Autoimmun Rev.* (2015) 14:798–805. doi: 10.1016/j.autrev.2015.05.004
49. Wu Y, Zhang F, Ma J, Zhang X, Wu L, Qu B, et al. Association of large intergenic noncoding RNA expression with disease activity and organ damage in systemic lupus erythematosus. *Arthritis Res Ther.* (2015) 17:131. doi: 10.1186/s13075-015-0632-3
50. Wu L, Qin Y, Xia S, Dai M, Han X, Wu Y, et al. Identification of cyclin-dependent kinase 1 as a novel regulator of type I interferon signaling in systemic lupus erythematosus. *Arthritis Rheumatol.* (2016) 68:1222–32. doi: 10.1002/art.39543
51. Gong J, Liu W, Zhang J, Miao X, Guo AY. lncRNASNP: a database of SNPs in lncRNAs and their potential functions in human and mouse. *Nucleic Acids Res.* (2015) 43:D181–86. doi: 10.1093/nar/gku1000
52. Miao YR, Liu W, Zhang Q, Guo AY. lncRNASNP2: an updated database of functional SNPs and mutations in human and mouse lncRNAs. *Nucleic Acids Res.* (2018) 46:D276–80. doi: 10.1093/nar/gkx1004
53. Haywood ME, Rose SJ, Horswell S, Lees MJ, Fu G, Walport MJ, et al. Overlapping BXSB congenic intervals, in combination with microarray gene expression, reveal novel lupus candidate genes. *Genes Immun.* (2006) 7:250–63. doi: 10.1038/sj.gene.6364294

Conflict of Interest Statement: The authors declare that the research was conducted in the absence of any commercial or financial relationships that could be construed as a potential conflict of interest.

frontiers in Immunology

ORIGINAL RESEARCH
published: 25 January 2019
doi: 10.3389/fimmu.2019.00044

The *TYK2*-P1104A Autoimmune Protective Variant Limits Coordinate Signals Required to Generate Specialized T Cell Subsets

Jacquelyn A. Gorman[1†], Christian Hundhausen[2†], Mackenzie Kinsman[2], Tanvi Arkatkar[1], Eric J. Allenspach[1,3], Courtnee Clough[1], Samuel E. West[1], Kerri Thomas[1,4], Ahmet Eken[1], Socheath Khim[1], Malika Hale[1,4], Mohamed Oukka[1,3,4], Shaun W. Jackson[1,3], Karen Cerosaletti[2], Jane H. Buckner[2] and David J. Rawlings[1,3,4]**

[1] Center for Immunity and Immunotherapies, Seattle Children's Research Institute, Seattle, WA, United States, [2] Translational Research Program, Benaroya Research Institute, Seattle, WA, United States, [3] Department of Pediatrics, University of Washington, Seattle, WA, United States, [4] Department of Immunology, University of Washington, Seattle, WA, United States

OPEN ACCESS

Edited by:
Laurence Morel,
University of Florida, United States

Reviewed by:
Dwight Kono,
The Scripps Research Institute, United States
Takaomi Sanda,
National University of Singapore, Singapore

***Correspondence:**
Jane H. Buckner
jbuckner@benaroyaresearch.org
David J. Rawlings
drawling@uw.edu

[†]These authors have contributed equally to this work

Specialty section:
This article was submitted to Autoimmune and Autoinflammatory Disorders, a section of the journal Frontiers in Immunology

Received: 05 November 2018
Accepted: 09 January 2019
Published: 25 January 2019

Citation:
Gorman JA, Hundhausen C, Kinsman M, Arkatkar T, Allenspach EJ, Clough C, West SE, Thomas K, Eken A, Khim S, Hale M, Oukka M, Jackson SW, Cerosaletti K, Buckner JH and Rawlings DJ (2019) The TYK2-P1104A Autoimmune Protective Variant Limits Coordinate Signals Required to Generate Specialized T Cell Subsets. Front. Immunol. 10:44. doi: 10.3389/fimmu.2019.00044

TYK2 is a JAK family member that functions downstream of multiple cytokine receptors. Genome wide association studies have linked a SNP (rs34536443) within *TYK2* encoding a Proline to Alanine substitution at amino acid 1104, to protection from multiple autoimmune diseases including systemic lupus erythematosus (SLE) and multiple sclerosis (MS). The protective role of this SNP in autoimmune pathogenesis, however, remains incompletely understood. Here we found that T follicular helper (Tfh) cells, switched memory B cells, and IFNAR signaling were decreased in healthy individuals that expressed the protective variant $TYK2^{A1104}$ ($TYK2^{P}$). To study this variant *in vivo*, we developed a knock-in murine model of this allele. Murine $Tyk2^{P}$ expressing T cells homozygous for the protective allele, but not cells heterozygous for this change, manifest decreased IL-12 receptor signaling, important for Tfh lineage commitment. Further, homozygous $Tyk2^{P}$ T cells exhibited diminished *in vitro* Th1 skewing. Surprisingly, despite these signaling changes, *in vivo* formation of Tfh and GC B cells was unaffected in two models of T cell dependent immune responses and in two alternative SLE models. TYK2 is also activated downstream of IL-23 receptor engagement. Here, we found that $Tyk2^{P}$ expressing T cells had reduced IL-23 dependent signaling as well as a diminished ability to skew toward Th17 *in vitro*. Consistent with these findings, homozygous, but not heterozygous, $Tyk2^{P}$ mice were fully protected in a murine model of MS. Homozygous $Tyk2^{P}$ mice had fewer infiltrating $CD4^{+}$ T cells within the CNS. Most strikingly, homozygous mice had a decreased proportion of $IL\text{-}17^{+}/IFN\gamma^{+}$, double positive, pathogenic $CD4^{+}$ T cells in both the draining lymph nodes (LN) and CNS. Thus, in an autoimmune model, such as EAE, impacted by both altered Th1 and Th17 signaling, the $Tyk2^{P}$ allele can effectively shield animals from disease. Taken together, our findings suggest that $TYK2^{P}$ diminishes IL-12, IL-23, and IFN I signaling and that its protective effect is most likely manifest in the setting of autoimmune triggers that concurrently dysregulate at least two of these important signaling cascades.

Keywords: TYK2, autoimmunity, lupus, Tfh, IL-12, IL-23, IFNAR, germinal center

INTRODUCTION

Systemic lupus erythematosus (SLE) comprises a group of heterogenous disorders classified under a broad clinical phenotype of systemic autoimmunity (1, 2). Loss of tolerance and sustained autoantibodies are key factors in the SLE pathogenesis (1). T cells play a critical role in SLE pathogenesis and previous work has identified alterations in $CD4^+$ T cell subsets in patients with lupus (1). This reflects differentiation of naïve $CD4^+$ T cells into alternative specialized T helper (Th) subtypes, including Th1, Th2, Th17, and T follicular helper (Tfh) cells. Differentiation is dependent on the cytokine milieu that the T cell encounters, and appropriate signaling through multiple cytokine pathways is required for lineage commitment. In SLE, heightened percentages of Tfh-like cells are present in both germinal centers and peripheral blood and correlate with serum autoantibody titers (3, 4). Tfh cells are key components of the adaptive immune response, providing the T cell help necessary for the development and maintenance of germinal center (GC) B cells and a robust antibody response (3, 5–7). Commitment to the Tfh lineage is driven by expression of transcription factor Bcl-6 expression (8). A number of cytokine signals have been implicated in the regulation of Bcl-6 expression, including IL-6, IL-21, IL-12, IL-2, IL-23, TGF-β, and IFN-γ through the Janus Kinase (JAK)-STAT pathways (9–13). Not surprisingly, dysregulation of these cytokine programs can contribute to disease through preferential expansion or depletion of particular Th lineages (3, 14).

Consistent with the altered T cell subsets observed in SLE, IL-12, and IL-23 levels have been found to be increased in SLE patients (3, 15, 16). Further, a positive correlation between levels of IL-12 and SLEDAI were seen in these lupus patients and active lupus nephritis had even higher levels of IL-12 compared to inactive SLE patients (15, 16). Type I interferons (IFN I) are also frequently upregulated in SLE subjects. IFN I impacts T cell subset commitment by promoting Bcl-6 expression, independent of STAT3 signaling and IL-21 production (17). However, IFN I has also been shown to be a corepressor of Tfh in the absence of STAT3 while augmenting interferon stimulated genes (ISGs) and Th1-like commitment (18). Given the complexity of T cell subset generation and the genetic heterogeneity of human autoimmunity, further work is needed to define the interplay of signals that control Tfh development and survival, and the role of T cell subsets in the pathogenesis of SLE and other autoimmune disorders.

TYK2 (non-receptor tyrosine-protein kinase), a member of the Janus Kinase (JAK) family, has been identified as a mediator in signaling cascades for IL-12, IL-23, IFN I, IL-6, IL-10, and IL-13 (19). The first human subject described with *TYK2* deficiency presented with hyper-IgE syndrome (HIES) (20). However, studies of additional *TYK2*-deficient subjects revealed specific alterations in cytokine signaling cascades without evidence for HIES (21, 22). Specifically, *TYK2*-deficient human T cells exhibited impaired responses to IL-12, IL-23, IFN-α, and IL-10 and these subjects presented with mycobacterial and viral infections (21). Consistent with these human data, *Tyk2*-deficient mice exhibit defective IL-12, IL-23, IFN I signaling and decreased Th1 *in vitro* skewing (23, 24). Further, TYK2 regulates early responses of IL-10 through Jak1-STAT3-SOCS3 signaling cascade (25). $Tyk2^{-/-}$ mice are also more susceptible to vesicular stomatitis virus (VSV), and murine cytomegalovirus (MCMV) but, intriguingly, are protected from experimental autoimmune encephalomyelitis (EAE) (19, 23, 26, 27).

Genome wide association studies (GWAS) have identified a single nucleotide polymorphism (SNP; rs34536443) in the *TYK2* gene associated with several autoimmune diseases (28–33). This SNP results in a proline to alanine substitution at amino acid 1,104 in the kinase domain of the protein (P1104A; A1104 referred to hereafter as $TYK2^P$) (31). Strikingly, the $TYK2^P$ variant has been associated with protection from multiple autoimmune diseases including: SLE, type 1 diabetes (T1D), multiple sclerosis (MS), rheumatoid arthritis, psoriasis, Crohn's disease, inflammatory bowel disease, and ulcerative colitis (28–34). Early studies suggested that $TYK2^P$ was a hypomorphic allele (35, 36). However, these studies reported conflicting results using alternative cell lineages suggesting that the signaling activity of the variant might depend on context and cell type (35, 36). More recent work has shown that $TYK2^P$ leads to hypomorphic signaling including reduced IFN I responses in all cell types and reduced IL-12/IL-23 signaling in human and murine T cells (33). The precise role(s) for $TYK2^P$ in altering autoimmune pathogenesis, however, remains poorly elucidated.

In the current study, we utilized cells from healthy human subjects with the variant and knock-in mice to assess the impact of $TYK2^P$ on T cell subsets and cytokine signaling and on normal and autoimmune responses *in vivo*. First, we demonstrate that healthy individuals with the protective variant exhibit decreased IFN I signaling and have a decreased frequency of circulating Tfh cells and switched memory B cells. We established a knock-in murine model of this allele and show that homozygous $Tyk2^P$ T cells exhibit decreased IL-12 receptor signaling and diminished *in vitro* Th1 skewing. Surprisingly, *in vivo* formation of Tfh and GC B cells was unaffected by $Tyk2^P$ expression in alternative murine models of T cell dependent immune responses. Further, expression of the protective variant did not protect against murine lupus in alternative murine SLE models. Additionally, we found that $Tyk2^P$ expressing T cells had reduced IL-23 dependent signaling and diminished ability to skew toward Th17 *in vitro*. Unlike lupus murine models, homozygous $Tyk2^P$ mice were fully protected from EAE, and infiltrating $CD4^+$ T cells within the CNS. Moreover, homozygous variant mice had a markedly decreased population of pathogenic $IL\text{-}17^+/IFN\gamma^+$ $CD4^+$ T cells in both the draining lymph nodes (LN) and CNS. Thus, our data suggest that $TYK2^P$ reduces IFN I, IL-12, and IL-23 signaling in T cells, and that only when autoimmune disease synchronously dysregulates multiple cytokine signaling programs will the protective phenotype be observed.

MATERIALS AND METHODS

Human Samples and Genotyping

Cryopreserved PBMCs were obtained from adult participants in the Benaroya Research Institute (BRI) Immune Mediated Diseases Registry and Repository. Subjects were selected based on

TYK2 genotype and the absence of autoimmune disease or any family history of autoimmunity. Study groups were designated as follows: subjects homozygous for the non-protective (NP) allele "C" at rs34536443: "NP/NP"; subjects homozygous for the protective (P) allele "G" at rs34536443: "P/P", and heterozygous subjects: "NP/P". *TYK2* SNP rs2304256 was held constant "C/A" as far as possible (all NP/NP and NP/P subjects). The "P/P" group was homozygous "A/A" at rs2304256 in all cases. Subjects were age matched (mean age: NP/NP group, 37.7 ± 12.6 years; NP/P group, 37.7 ± 14.3 years; P/P group, 45.3 ± 18.1 years) and sex matched as far as possible (NP/NP group, 21 males and 20 females; NP/P group, 15 males and 17 females; P/P group 3 male and 1 female). All experiments were performed in a blinded manner with respect to *TYK2* genotype. Genomic DNA was genotyped for the *TYK2* SNPs rs34536443 (C/G) (P1104A) and rs2304256 (C/A) (V362F) using a Taqman SNP genotyping assay (Applied Biosciences) or were genotyped using the Illumina ImmunoChip by the University of Virginia Center for Public Health Genomics. The Taqman genotyping assay was validated using HapMap DNAs of known genotype, and controls of each genotype were included in every genotyping experiment. Results were checked for adherence to Hardy-Weinberg equilibrium. The research protocols were approved by the Institutional Review Board at BRI (#07109-148).

Mice

A construct designed to generate a P1124A mutation in exon 21 of *Tyk2* by homologous recombination in C57BL/6J mice was generated and injected by Biocytogen as previously described (37). After successful recombination, two FRT sequences with a neomycin-resistance selection cassette were inserted into intron 21. To create lineage-specific deletion, *loxP* sites were also present in intron 19 and 21. C57BL/6J embryonic stem (ES) cells had the introduction of the construct and clones were obtained by limited dilution. G418 selection was used to select clones. Clones that contained successful integration of the knock-in template into the locus were confirmed by Southern blot and PCR analysis of genomic DNA. Successfully targeted clones were injected into BALB/c blastocysts and were subsequently transferred into pseudopregnant females. One clone gave rise to a line with germline transmission of the allele. The mutation was confirmed by sequencing of Exon 21 (**Supplementary Figure 1**), and PCR was used to genotype all litters (using the following primers: 5′-CCACTCCTAACCTTGTAGAGCAC-3′ and 5′-AACGCAAATCTCTACAACAGTGG-3′). Mice were crossed with B6.Cg-Tg(ACTFLPe)9205Dym/J (Jackson Laboratory) mice to delete the neomycin-resistance selection cassette. In Th1 skewing assays, *Tyk2* knockout mice were created by Dr. Mathias Müller and were kindly provided by Dr. George Yap (23). *Tyk2* knockout mice were also generated by crossing *TYK2^{P}* mice with B6.C-Tg(CMV-cre)1Cgn/J (Jackson Laboratory) strain to make a global knockout of *Tyk2*. Deletion was confirmed by sequencing *loxP* sites (**Supplementary Figure 1**), and PCR was used to genotype all litters (using the following primers: 5′-CCACTCCTAACCTTGTAGAGCAC-3′ and 5′-CCTCCCTGTGTGTGATGTGG-3′). WAS–/– mice are on a C57BL/6J background (38). All strains were maintained in a specific-pathogen-free facility, and studies were performed in accordance with procedures approved by the Institutional Animal Care and Use Committees of Seattle Children's Research Institute.

In vitro Stimulation and Th Skewing Assays

For IL-12 signaling, thawed PBMCs were washed and resuspended in complete medium (RPMI, 10% human serum, 1% PenStrep) at 4 × 10^6 cells/ml. Cells were activated with anti-CD3/CD28 Dynabeads (ThermoFisher) at a bead to cell ratio of 1:10 for 72 h. Following removal of the magnetic beads, cells were rested in *X-vivo* 15 medium (Lonza) for 2 h, washed with PBS and stimulated with 2.5 ng/ml of recombinant human IL-12 (BD Pharmingen) for 30 min. For IFN-α signaling, thawed PBMCs were washed and rested in *X-vivo* 15 medium for 45 min. Cells were washed and stimulated with 2,000 IU/ml of recombinant IFN-α (PBL) for 12 min.

Mouse spleens went through RBC lysis and made into single cell suspensions. $CD4^+$ T cells were positively isolated (Miltenyi Biotec) and placed into wells that were coated with anti-CD3/CD28 (5 μg/ml; 145-2c11/37.51; BioXcell and UCSF Monoclonal Antibody Core). Murine cells were cultured in complete media containing RMPI-1640 supplemented with 10% FBS, 1% non-essential amino acids, 1% sodium pyruvate, 1% GlutaMAX, and 0.1% β-ME. For IL-12 stimulation, cells were activated for 72 h and let rest for 24 h. Cells were then stimulated with IL-12 for 20 min and subsequently analyzed for intracellular pSTAT3. For Th1 skewing assays, cell cultures were supplemented with the following Th0 and Th1 cytokines respectively; anti-IFN-γ (30 μg/ml; BioXcell) and anti-IL-4 (20 μg/ml; BioXcell); IL-2 (50 ng/ml; Peprotech), IL-12 (20 ng/ml; R&D systems), and anti-IL-4 (20 μg/ml; BioXcell). At 48 h, cells were split into two wells and fresh media was added to each condition with the respective cytokines described above. Cells were harvested on day 5 and examined for intracellular IFN-γ. For IL-23/pSTAT3 stimulation, total splenocytes were cultured in media containing anti-CD3 (2.5 μg/ml; BioXcell), IL-6 (30 ng/ml), TGF-β (3 ng/ml; R&D systems), and anti-IFN-γ (10 μg/ml). At 72 h, anti-IFN-γ and IL-23 (10 ng/ml; R&D systems) were added to the cultures. Cells were harvested on day 6 and stimulated with IL-23 for 15 min at 37°C. $CD4^+$ T cells were than analyzed for intracellular pSTAT3. For Th17 skewing assays, total splenocytes were cultured with the same supplements as described for IL-23/pSTAT3 stimulation above. At 72 h, anti-IFN-γ and IL-23 were added to the cultures on day 3, 7, and 10. On day 12, cells were stimulated with PMA (50 ng/ml; EMD Millipore), Ionomycin (1 μg/ml; Sigma-Aldrich), and Monensin (20 ng/ml; eBioscience) to be analyzed for intracellular IL-17.

In vitro Tfh Generation

Splenic $CD4^+$ T cells were isolated as described above. All cells were stimulated with anti-CD3/CD28 coated beads (Thermo Fisher), with IL-2 (Peprotech) and supplemented with the following for Th0 and Tfh, respectively: anti-IFN-γ (30 μg/ml; BioXcell) and anti-IL-4 (20 μg/ml; BioXcell); IL-12 alone (20 ng/ml). Beads were removed after 48 h of stimulation and fresh

media was added to each condition with the respective cytokines described above. Cells were harvested six days after initial stimulation to assess for Tfh surface markers.

In vitro GC Stimulation

Splenic B cells were purified from mice with CD43$^+$ depletion (Miltenyi Biotec). Cells were cultured in complete media (RMPI-1640 supplemented with 10% FBS, 1% penicillin-streptomycin, 1% sodium pyruvate, 1% Hepes, 1% GlutaMAX, and 0.1% β-ME) for 48 h at 37°C. B cells were stimulated with or without the following reagents; R848 (5 ng/ml); anti-mouse IgM F(ab')$_2$ fragment (1 μg/ml; Jackson ImmunoResearch, Inc.); anti-mouse CD40 (1 μg/ml; SouthernBiotech); IL-12 (20 ng/ml). Supernatant was collected and evaluated with an IL-6 ELISA (eBioscience).

In vivo Immunizations

VLPs were made with bacteriophage Qβ capsid protein that contain single-stranded RNA which were kindly provided by Dr. Baidong Hou (39). Mice were injected with 2 μg of VLPs i.p. Twelve days post-immunization, spleens and serum were harvested from the mice. Cells were stained with surface markers for Tfh and GC B cells. Serum was analyzed for VLP-specific antibodies as previously described (40).

Mice were immunized by i.p. with 200 μl of PBS containing 20% sheep red blood cells (SRBCs). Spleens and serum were harvested on day 5 to assess surface markers and total IgG1 by ELISA.

Bone Marrow Transplantation

BM was harvested from the femora and tibiae of *Was*$^{-/-}$.*Tyk2*^{P}, *Was*$^{-/-}$.*Tyk2*^{NP}, *Was*$^{-/-}$.*Tyk2*$^{NP/P}$ and *Was*$^{-/-}$.*IL12R*$^{-/-}$ mice. Single cell suspensions were depleted for CD138$^+$ cells (Miltenyi Biotec). CD138-depleted *Was*$^{-/-}$.*Tyk2*^{P}, *Was*$^{-/-}$.*Tyk2*^{NP}, *Was*$^{-/-}$.*Tyk2*$^{NP/P}$ and *Was*$^{-/-}$.*IL12Rβ2*$^{-/-}$ donor BM was mixed with respective *Tyk2*^{P}.*μMT*, *Tyk2*^{NP}.*μMT*, *Tyk2*$^{NP/P}$.*μMT*, and *IL12Rβ2*$^{-/-}$ *μMT* at a 20:80 ratio, and 6 × 10^6 total BM cells were injected retro-orbitally into lethally irradiated mice (450cGy x 2 doses) to generate WAS chimeras in which all hematopoietic lineages express the variant *Tyk2*^{P}allele. Resulting BM chimeras were bled at 12 weeks and 24 weeks post-transplant date by retro-orbital puncture and sacrificed at 24–26 weeks post-transplant. Serum dsDNA antibodies were assessed as previously described (37).

Experimental Autoimmune Encephalomyelitis (EAE)

EAE was induced with s.c. immunization of the flanks with an emulsified mixture containing CFA, MOG$_{35-55}$ peptide (100 μg), and Mycobacterium tuberculosis extract H37Ra (4 μg/ml; Difco). Each animal also received i.p. immunization of pertussis toxin (200 ng) on days 0 and 2. Mice were assessed daily for clinical symptoms of EAE and scored according to the following criteria: 0-no signs of disease; 1-limp tail; 2-hind limb weakness; 3-hind limb paralysis; 4-hind limb, and forelimb paralysis.

Flow Cytometry

PBMCs were thawed, washed with PBS and rested in *X-vivo* 15 medium (Lonza) at 37°C and 5% CO_2 for 45 min. Cells were washed with PBS and 1 × 10^6 cells were stained in FACS buffer (PBS/0.5% BSA/0.1 NaN_3) with a cocktail of fluorophore-conjugated antibodies at RT for 20 min. For human IL-12/pSTAT signaling, cells were fixed and permeabilized using Fix buffer I (BD Biosciences) and Perm buffer III (BD Biosciences), respectively, according to the manufacturer's instructions. Cells were washed and stained simultaneously for surface markers and intracellular pSTAT3 and pSTAT4 at RT for 45 min. For human IFN-α, cells were washed and stained simultaneously for surface markers and intracellular pSTAT1 at RT for 45 min. IFNAR surface levels were determined in unfixed, non-permeabilized cells. The following antibodies were used for the detection of proteins in human samples: CD3-AF700 (UCHT1), CXCR3-PE (G025H7), CCR6-PerCP/Cy5.5 (G034E3), PD1-BV605 (EH12.2H7), CD3-PerCp/Cy5.5 (UCHT1), CD19-AF700 (HIB19), IgM-FITC (MHM-88), CD38-PE-Cy5 (Hit5), CD24-BV510 (ML5), CD10-PE-Cy7 (HI10a), CD8-PerCP/Cy5.5 (RPA-T8), CD45RA-PE-Cy7 (HI100), CD56-BV421 (HCD56), from BioLegend; CD8-PE-Cy7 (SFCI21Thy2D3) from Beckman Coulter; CD4-BV510 (SK3), CD45RA-PE-Cy5 (HI100), CXCR5-BV421 (RF8B2), CD27-BV605 (L128), IL-12Rb1- APC (2.4E6), pSTAT3-PE (4/P-STAT3), pSTAT4-PerCP/Cy5.5 (38/p-Stat4), pSTAT1-AF488 (4a) from BD Biosciences; IFNAR-APC (85228) from R&D Systems. The following antibodies were used for the detection in mouse samples: pSTAT3-Alexa647 (4/P-STAT3), CXCR5-Biotin (2G8), Streptavidin-PE-Cy7, CD19-PE-Cy7 (1D3), FAS-PE (Jo2) from BD Biosciences; CD4-Pacific Blue (RM4-5), IFNg-APC (XMG1.2), B220-PerCP-Cy5.5 (RA3-6B2), IL-17A-PE (TC11-18H10.1), IL-17A-PerCP-Cy5.5 (TC11-18H10.1) were from BioLegend; CD3-APC-eFLuor780 (17A2), GL7-Alexa 647 (GL-7), PE-IFNg (XMG1.2), PE-Cy5 (GK1.5), CD3e-Fitc (eBio500A2), CD3e-PerCP-Cy5.5 (145-2c11) were from eBioscience; CD4-APC (GK.1) were from Southern Biotech; PD1 Fitc (J43) were from Life Technologies; PNA-FITC (FI-1071) were from Vector Labs. Live/Dead Near-IR Dead Cell Stain Kit (Invitrogen) was used to assess viability by flow cytometry. Alexa Fluor 647-labeld Q-VLP was kindly provided by Dr. Baidong Hou (39, 41). FlowJo (version 10) was used for data analysis.

Statistical Analysis

All statistical analysis was performed using GraphPad Prism (version 7). All statistical tests and *P*-values are specified in the figure legends.

RESULTS

Healthy Subjects With the *TYK2*^{P} Variant Exhibit a Decrease in Both Tfh Cells and Switched Memory B Cells

To evaluate the effect of *TYK2*^{P} on lymphocyte populations, we examined peripheral blood mononuclear cells (PBMC) in healthy individuals with no family history of autoimmunity.

Specifically, we assessed adaptive immune cells which require TYK2-dependent pathways for development and activation (27). Thawed PBMCs were stained with fluorophore-conjugated antibodies for a panel of T and B cell subset markers and analyzed by flow cytometry. We observed no effect of *TYK2^{P}* on the frequency of CD4^{+} naïve (RA^{+}) and memory (RA^{-}) T cells or of total CD3^{-}CD19^{+} or memory CD3^{-}CD19^{+}CD27^{+}CD10^{-} B cells. In contrast, we found that individuals expressing the *TYK2^{P}* allele have decreased circulating CD4^{+}CD45RA^{-}PD1^{+}CXCR5^{+} Tfh cells (**Figures 1A,B**). Consistent with the role for Tfh cells in promoting B cell GC responses, we also observed a reduced frequency of CD3^{-}CD19^{+}CD27^{+}CD10-IgM^{-} switched memory B cells (**Figures 1C,D**) in individuals with the protective allele. Thus, individuals expressing *TYK2^{P}* exhibited low frequencies of Tfh cells, essential for germinal center formation, and switched memory B cells, products of germinal centers, suggesting that TYK2 plays a role in cytokine pathways important for regulation of germinal centers and immune activation.

In vitro IL-12 Driven Tfh Generation and B Cell IL-6 Production Is Decreased Using Murine *Tyk2^{P}* Cells

To gain better understanding of the function of TYK2^{P} in cytokine signaling and autoimmune disease, we generated a knock-in mouse strain containing the identical amino-acid substitution in the murine TYK2 protein (*Tyk2-P1124A*), hereafter referred to as *Tyk2^{P}* mice or as *Tyk2$^{NP/P}$* and *Tyk2$^{P/P}$* for heterozygous and homozygous animals, respectively (further detailed explanation of genotypes, please see **Supplementary Table 1**). To generate founder mice, we used homologous recombination on the non-autoimmune prone C57BL/6 genetic background (**Supplementary Figures 1A–C**). Gene targeting produced the variant coding change (encoding the substitution P1124A) in exon 21 of *Tyk2* (**Supplementary Figure 1B**). Based upon our targeting strategy, we also crossed *Tyk2^{P}* mice with a murine line ubiquitously expressing CRE to create *Tyk2* knockout (*Tyk2$^{-/-}$*) animals of an identical genetic background for use in some studies (**Supplementary Figures 1A,C**).

The TYK2-dependent IL-12 cytokine pathway is important for Tfh generation by promoting phosphorylation of STAT3 (pSTAT3) (12). To test pSTAT3 levels in murine cells, we isolated CD4^{+} T cells from littermate control (*Tyk2$^{NP/NP}$*), heterozygous (*Tyk2$^{NP/P}$*) or homozygous (*Tyk2$^{P/P}$*) and assessed for IL-12-induced pSTAT3. We found that homozygous *Tyk2$^{P/P}$* cells exhibited diminished pSTAT3 (**Figure 2A**). Further, *Tyk2$^{P/P}$* CD4^{+} T cells were also unable to skew toward a Th1 phenotype *in vitro*, a process also dependent on IL-12 signaling (**Figure 2B**). Similar to previously published findings, *Tyk2$^{-/-}$* CD4^{+} T cells exhibited a similar decrease in the capacity to skew toward a Th1 phenotype (24, 42). These data mirrored our findings using *Tyk2$^{P/P}$* CD4^{+} T cells implying that the protective allele encoded for a TYK2 protein with reduced functional activity. Despite the decreased Tfh cells in the circulation in human subjects heterozygous for the protective variant, we could not discern significant differences in IL-12-induced pSTAT3 or pSTAT4 using primary human CD4^{+} T cells from a cohort of heterozygous healthy subjects (**Supplementary Figures 2A–H).**

To explore the role of TYK2^{P} in IL-12-induced Tfh cell generation, we used an *in vitro* assay to examine this question. *Tyk2$^{P/P}$* CD4^{+} T cells were not able to generate Tfh-like cells as efficiently as *Tyk2$^{NP/NP}$* cells in response to IL-12 alone (**Figure 2C**). Based on the diminished switched memory population in healthy donors with the protective variant (**Figure 1D**), we assessed the role of IL-12 signaling in modulating the activation of *Tyk2^{P}* murine B cells. Previous work has implicated IL-12 in promoting B cell activation and antibody production (43, 44). We used an *in vitro* "GC-like" stimulation with and without the addition of IL-12 and monitored the production of IL-6. IL-6 is produced by activated B cells and promotes GC B and Tfh cell development (45), and B cell intrinsic IL-6 production is required for autoimmune GC B cell responses (46). Under all conditions, *Tyk2$^{P/P}$* B cells exhibited a trend for diminished IL-6 production compared to control *Tyk2$^{NP/NP}$* or heterozygous *(Tyk2$^{NP/P}$)* B cells (**Figure 2D)** but these differences did not reach statistical significance. In summary, diminished *in vitro* Tfh-like and Th1 generated T cells from *Tyk2$^{P/P}$* mice were most likely secondary to diminished IL-12 signaling.

Tyk2^{P} Does Not Impact Tfh and GC B Cell Formation Following T-Dependent Immunization

Next, based on its impact on Tfh cells *in vitro* and in human subjects, we examined the effect of *Tyk2^{P}* on generation of Tfh and GC B cells *in vivo*. We first assessed T cell-dependent immunization using TLR7-loaded virus-like particles (VLP) in control (*Tyk2$^{NP/NP}$*) mice, mice heterozygous *(Tyk2$^{NP/P}$)*, or homozygous (*Tyk2$^{P/P}$*) for the protective variant. At the peak of the immune response, there was no difference in the proportion or number of Tfh cells or GC B cells generated by these strains (**Figures 3A–C**). Additionally, we saw no differences in VLP-specific GC B cells or in high-affinity anti-VLP IgG2c antibodies (**Figures 3D,E**). We expanded upon this result by using a second immunization strategy designed to promote a more sustained GC response triggered via delivery of sheep red blood cells (SRBCs) and also included cohorts of *Tyk2$^{-/-}$* animals. Again, all strains exhibited equivalent production of GC B cells, Tfh cells, and antibodies (**Supplemental Figures 3A–D**). Taken together, *Tyk2^{P}* appears to have little or no impact on T-dependent GC and antibody formation in response to immunization strategies that rely on the formation and function of Th1/Th2 cells.

Tyk2^{P} Does Not Affect Tfh and GC B Cell Formation in Murine Lupus Models

TYK2^{P} has been associated with protection from multiple autoimmune diseases including SLE (32). Therefore, we next

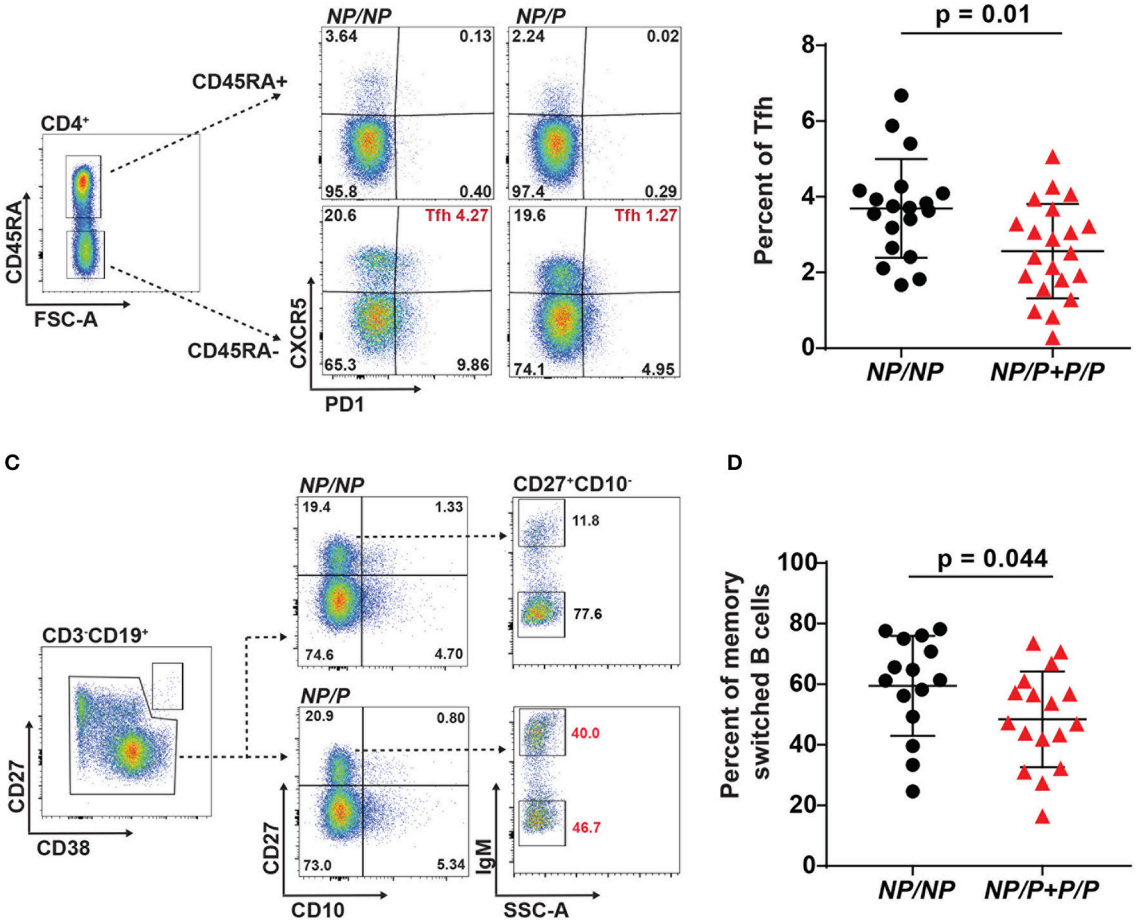

FIGURE 1 | Healthy subjects expressing the *TyK2* protective variant exhibit decreased proportion of circulating Tfh and switched memory B cells. **(A)** Gating strategy for T follicular helper (Tfh) cells, defined as $CD4^+CD45RA^-CXCR5^+PD1^+$ T cells. Shown are representative dot plots of the Tfh cell frequency in subjects with $TYK2^{NP/NP}$ (*NP/NP*), $TYK2^{NP/P}$ (*NP/P*), or $TYK2^{P/P}$ (*P/P*) (non-protective (*NP*) vs. protective (*P*) alleles of rs34536443; encoding for Alanine-1104 vs. Proline-1104). **(B)** Quantification of Tfh cell frequency. **(C)** Gating strategy for switched memory B cells, defined as plasmablast (PB) negative $CD3^-CD19^+CD27^+CD10^-IgM^-$ B cells. Shown are representative dot plots of the switched memory B cell frequency in subjects. **(D)** Quantification of switched memory B cell frequency (Each symbol represents an individual donor) **(B,D)**; small horizontal lines indicate the mean (± s.d.). Data from a combined total of $n = 19$ $Tyk2^{NP/NP}$ donors, $n = 19$ $TYK2^{NP/P}$ donors, and $n = 2$ $TYK2^{P/P}$ donors **(A,B)**; $n = 15$ $TYK2^{NP/NP}$ donors, $n = 13$ $TYK2^{NP/P}$ donors, and $n = 4$ $TYK2^{P/P}$ donors **(C,D)**. Statistical analysis indicated from a Mann-Whitney U **(B,D)**.

directly assessed the role of the protective variant in disease development using alternative murine lupus models utilizing $Tyk2^P$ mice. As an initial test, we used the BM12 T cell adoptive transfer model of lupus. The BM12 strain was derived from C57BL/6 mice and contains a three-amino-acid change in the major histocompatibility complex class II molecule H2-AB1^b (47). An autoimmune GC response is generated when BM12 $CD4^+$ T cells are adoptively transferred into C57BL/6 recipients leading to production of autoantibodies directed against dsDNA within ∼3 weeks following the cell transfer (48, 49). Therefore, to assess the impact of $Tyk2^P$ in this setting, we transferred BM12 $CD4^+$ T cells into control ($Tyk2^{NP/NP}$), heterozygous ($Tyk2^{NP/P}$), or homozygous ($Tyk2^{P/P}$) recipient mice. Following $CD4^+$ T cell transfer, there was no difference in the proportion of Tfh and GC B cells in any strain (data not shown). We also observed no differences in autoantibody levels at disease peak (**Figures 4A–C**).

To further examine the role of $Tyk2^P$ in murine lupus, we utilized the Wiskott-Aldrich Deficient ($WASp^{-/-}$) B cell bone marrow (BM) chimera lupus model (38, 46, 50–53). In chimeras with B cell intrinsic loss of $WASp^{-/-}$, mice display spontaneous GCs, autoantibodies, renal histopathology, and early mortality (38). In order to assess the impact of various $Tyk2^P$ alleles in all relevant cell lineages in the development of lupus in this model, we first intercrossed $\mu MT^{-/-}$ mice with our knock-in strain to establish $\mu MT^{-/-}$ mice co-expressing $Tyk2^{NP/NP}$,

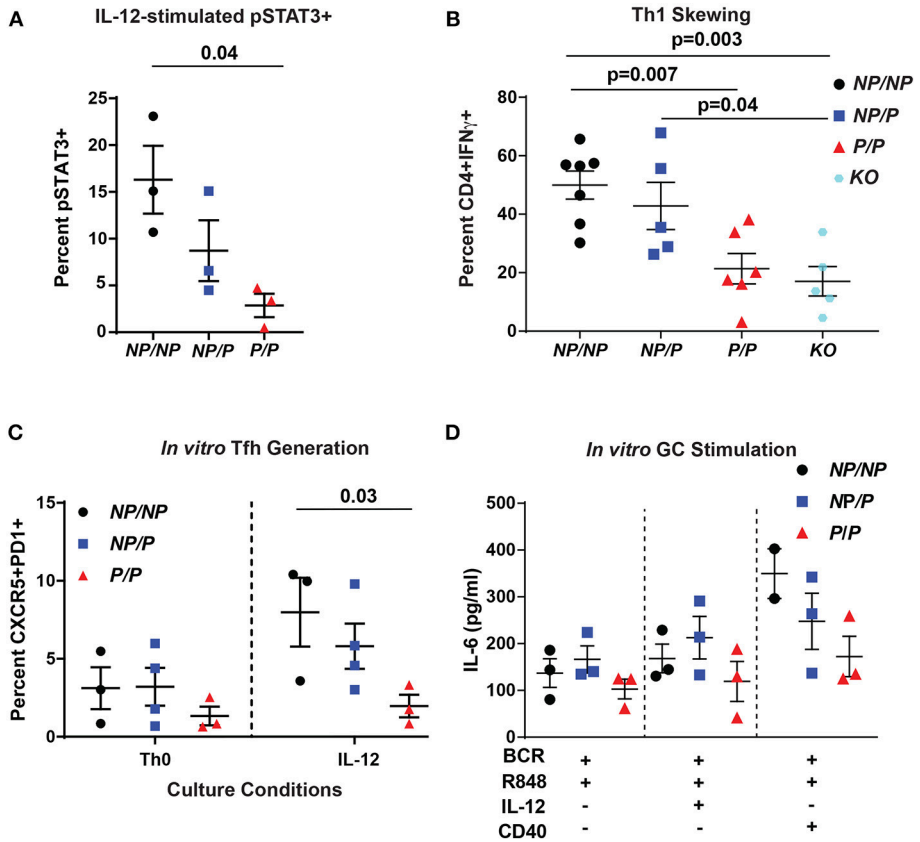

FIGURE 2 | Murine *Tyk2*^{P} lymphocytes exhibit decreased IL-12 signaling and reduced *in vitro* generation Tfh cells and IL-6 production in response to GC programming. **(A–C)** Splenic CD4^{+} T cells were isolated from *Tyk2*$^{NP/NP}$ (*NP/NP*), *Tyk2*$^{NP/P}$ (*NP/P*), *Tyk2*$^{P/P}$ (*P/P*), or *Tyk2*$^{-/-}$ (*KO*) mice. **(A)** CD4^{+} T cells were stimulated with 2 ng/mL of IL-12 for 20 min and assessed for phosphorylation of STAT3 (pSTAT3) using flow cytometry. **(B)** Frequency of IFN-γ^{+} CD4^{+} T cells following *in vitro* Th1 skewing culture conditions with IL-12, IL-2, and anti-IL-4 for five days and analyzed by flow cytometry. **(C)** Frequency of Tfh-like T cells (CD4^{+} CXCR5^{+}PD1^{+}) following culture with the indicated cytokines for six days. **(D)** Splenic B cells were isolated from *Tyk2*$^{NP/NP}$ (*NP/NP*), *Tyk2*$^{NP/P}$ (*NP/P*), or *Tyk2*$^{P/P}$ (*P/P*) mice. IL-6 production from B cells stimulated with the indicated cytokines for 48 h. Small horizontal lines indicate the mean (± s.e.m.). Statistical analysis were performed using Friedman Test with Dunn's multiple comparison **(A)**, one-way ANOVA with Tukey's multiple comparisons test **(B,D)**, and two-way ANOVA with Tukey's multiple comparisons test **(C)**. Data are derived from three **(A,C,D)** or seven independent experiments **(B)**. Each symbol represents an individual biological replicate (individual mouse); *Tyk2*$^{NP/NP}$ $n = 3$, *Tyk2*$^{NP/P}$ $n = 3$, or *Tyk2*$^{P/P}$ $n = 3$ **(A,D)**; *Tyk2*$^{NP/NP}$ $n = 7$, *Tyk2*$^{NP/P}$ $n = 5$,*Tyk2*$^{P/P}$ $n = 6$ or *Tyk2*^{KO} $n = 5$ **(B)**; *Tyk2*$^{NP/NP}$ $n = 3$, *Tyk2*$^{NP/P}$ $n = 4$, or *Tyk2*$^{P/P}$ $n = 3$ **(C)**.

Tyk2$^{NP/P}$, or *Tyk2*$^{P/P}$, respectively. As shown schematically in **Figure 4D,** cohorts of animals for each of these $\mu MT^{-/-}$ strains were lethally irradiated and reconstituted by BM transplantation using a mixture of 80% $\mu MT^{-/-}$ BM (expressing *Tyk2*$^{NP/NP}$, *Tyk2*$^{NP/P}$, or *Tyk2*$^{P/P}$, respectively) and 20% *WAS*$^{-/-}$ BM (co-expressing *Tyk2*$^{NP/NP}$, *Tyk2*$^{NP/P}$, or *Tyk2*$^{P/P}$, respectively; **Figure 4D**). As an additional control to assess the impact of IL-12 receptor signaling in disease development, we utilized $\mu MT^{-/-}$ recipient strains and donor BM cells both deficient for IL-12Rβ2 (**Figure 4D**). Strikingly, all recipients of *WAS*$^{-/-}$ BM developed high-titer class-switched IgG2c anti-dsDNA and anti-smRNP antibodies within 4 months post-transplant. We also observed no differences in relative levels of autoantibody production, GC B cells, or Tfh cells between recipients with alternative *Tyk2*^{P} alleles (**Figures 4D–H**). Moreover, despite the anticipated role for IL-12 in modulating T and B cell activation, IL-12Rβ2 deficiency exerted no appreciable impact on disease within this model with recipients developing autoantibodies, GC B cells, and Tfh cells as efficiently as *WAS*$^{-/-}$ chimeras (**Figures 4D–H**). Taken together, these findings suggest that *Tyk2*^{P} does not play a major role in development of autoimmune GC responses or in modulating autoantibody production in murine SLE.

Type I Interferon Signaling Is Reduced in T Cells From *TYK2*^{P} Healthy Subjects

Another pathway with a requirement for TYK2 is type I interferon (IFN I) signaling (18). This pathway may also impact Tfh generation. To test the role of TYK2^{P} in type I interferon receptor (IFNAR) signaling, we stimulated PBMCs from healthy control subjects and subjects heterozygous for the protective variant using IFN-α and examined phosphorylated STAT1 (pSTAT1) levels following activation. Naïve *TYK2*$^{NP/P}$ CD4^{+} and CD8^{+} T cells exhibited a decrease in IFN-α induced

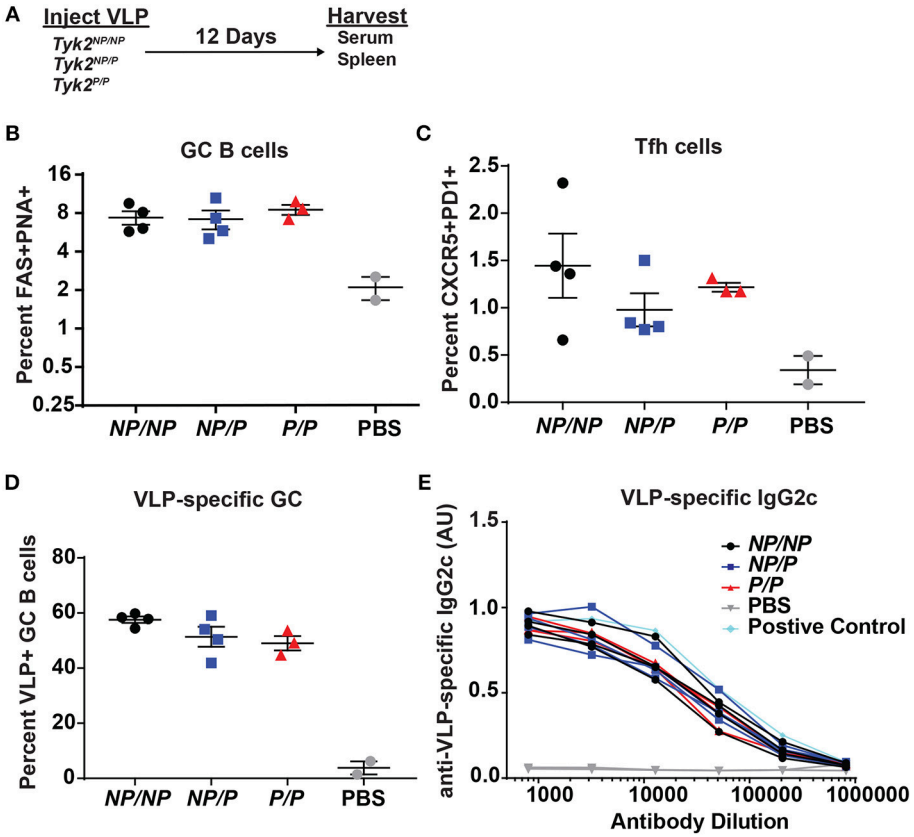

FIGURE 3 | Tfh and GC B cell formation *in vivo* in response to immunization with virus-like particles is not impacted by *Tyk2*^{P} expression. **(A)** Experimental schematic for VLP immunization. *Tyk2*$^{NP/NP}$ (*NP/NP*), *Tyk2*$^{NP/P}$ (*NP/P*), or *Tyk2*$^{P/P}$ (*P/P*) mice were immunized i.p. with 2 μg of TLR7-loaded virus-like particles (VLP) or with PBS as control. Splenocytes were analyzed for frequency of: **(B)** germinal center (GC) B cells (B220^{+}FAS^{+}PNA^{+}); **(C)** Tfh cells (CD4^{+}CXCR5^{+}PD1^{+}); and **(D)** VLP+ GC B cells at day 12 post-immunization. **(E)** Sera was collected at day 12 post-immunization and assessed by ELISA for VLP-specific IgG2c antibodies. Small horizontal lines indicate the mean (± s.e.m.). ELISA results are displayed as absorbance at 450 nm normalized to results using a blank well and presented in arbitrary units (AU) **(E)**. Representative data are shown from one of two independent experiments **(B–E)**. Statistical analysis was performed using one-way ANOVA with Tukey's multiple comparisons test **(B–D)**. Each symbol represents an individual biological replicate; *Tyk2*$^{NP/NP}$ $n = 4$, *Tyk2*$^{NP/P}$ $n = 4$, *Tyk2*$^{P/P}$ $n = 3$, PBS $n = 2$, or Positive Control $n = 1$ **(B–E)**.

pSTAT1 levels compared to cells from control *TYK2*$^{NP/NP}$ subjects (**Figures 5A–D**), a difference that was not due to altered IFNAR surface expression. These findings were consistent with a previous report showing diminished pSTAT1 and pSTAT3 levels following IFN-α stimulation in subjects with the protective allele (33). Thus, IFNAR signaling is reduced by the expression of TYK2^{P}.

TYK2^{P} Is Involved in IL-23 Signaling, Th17 Skewing, and Tfh-17 Formation

Circulating human Tfh cells are comprised of three distinct developmental subsets that can be discriminated based on relative surface expression levels of CXCR3, CCR6, and CCR7 (14). Therefore, we next investigated whether a specific Tfh lineage was preferentially impacted by expression of *TYK2*^{P}. Though not statistically different, we discovered that individuals expressing the protective variant exhibited a trend for a decrease in the relative proportion Tfh-17 cells ($p = 0.123$) but exhibited no changes in the proportion of Tfh-1 or Tfh-2 cells (**Figures 6A–C**). Consistent with this data, TYK2 is activated downstream of the IL-23 receptor engagement (19). To further study the role of TYK2^{P} in Th17 commitment and in Tfh-17 cells, we investigated IL-23 signaling in the murine CD4^{+} T cells derived from control (*Tyk2*$^{NP/NP}$), heterozygous (*Tyk2*$^{NP/P}$) or homozygous (*Tyk2*$^{P/P}$) mice and from *Tyk2*$^{-/-}$ animals. Both *Tyk2*$^{P/P}$ and *Tyk2*$^{-/-}$ T cells exhibited decreased IL-23 dependent pSTAT3 and heterozygous *Tyk2*$^{NP/P}$ T cells exhibited a trend consistent with an intermediate phenotype (**Figure 6D**). Further, both *Tyk2*$^{P/P}$ and *Tyk2*$^{-/-}$ T cells displayed a diminished Th17 skewing *in vitro* (**Figure 6E**). In summary, TYK2^{P} plays a role in IL-23 signaling mostly likely contributing to the observed decrease in Tfh-17 cells in subjects expressing the protective variant.

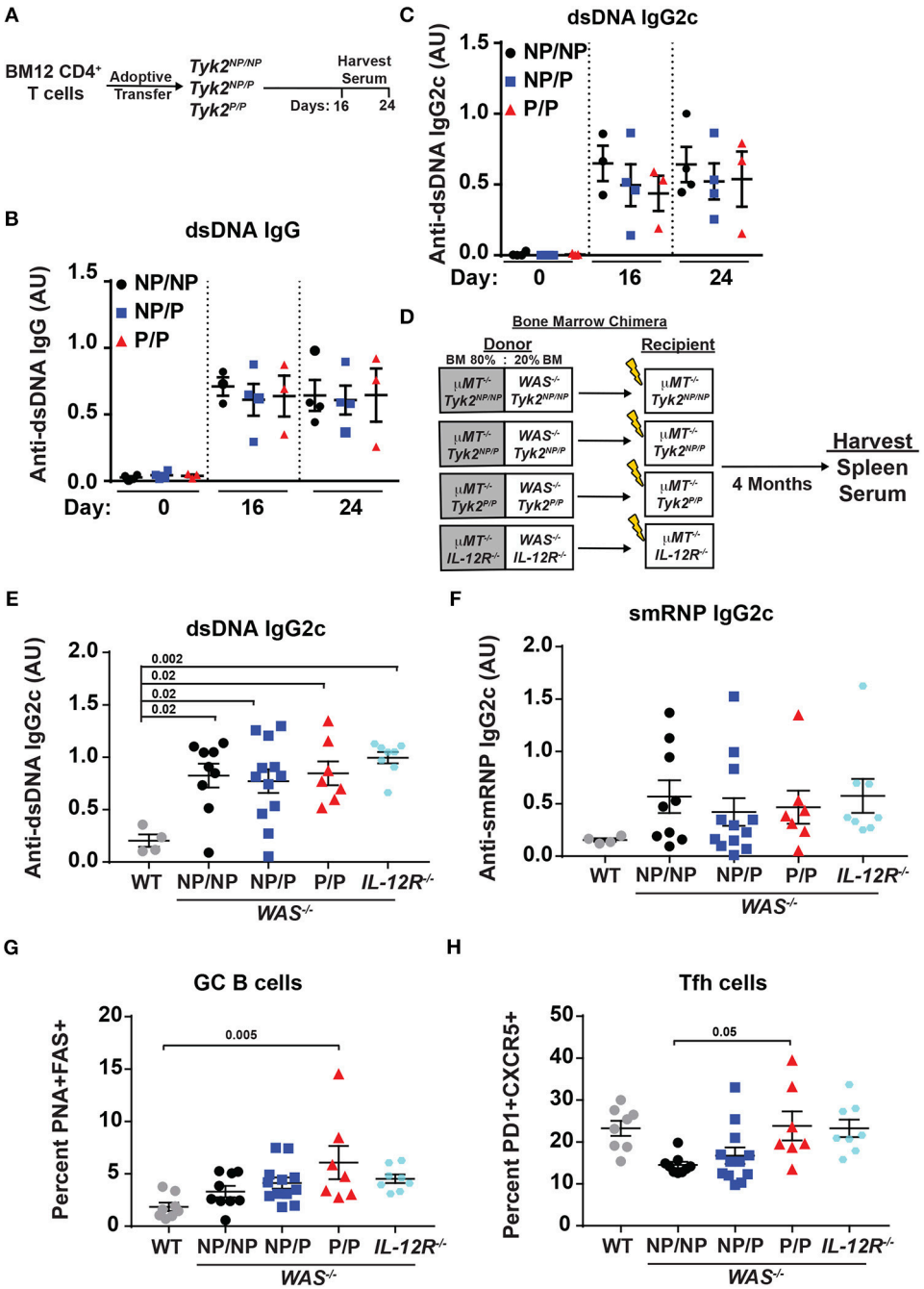

FIGURE 4 | *Tyk2*^{P} and *IL* − *12R*$^{-/-}$ mice are not protected in murine models of lupus. **(A)** Experimental schematic for BM12 CD4^{+} T cell adoptive transfer model. 5.0 × 10^{6} BM12 CD4^{+} T cells were adoptively transferred into *Tyk2*$^{NP/NP}$, *Tyk2*$^{NP/P}$, or *Tyk2*$^{P/P}$ recipient mice and autoantibodies and splenic cell populations (not shown) were assessed at indicated times. Serum ELISA analysis for: **(B)** anti-dsDNA IgG and **(C)** anti-dsDNA IgG2c autoantibodies. **(D)** Schematic for establishment of B cell-specific bone marrow (BM) chimeras using an 80%:20% mixture of bone marrow from $\mu MT^{-/-}$ mice and WT or Wiskott-Aldrich knock-out (*WAS*$^{-/-}$) donor cells with the indicated *Tyk2* or *IL-12R* alleles (*WAS*$^{-/-}$*Tyk2*$^{NP/NP}$, *WAS*$^{-/-}$*Tyk2*$^{NP/P}$, *WAS*$^{-/-}$*Tyk2*$^{P/P}$, *WAS*$^{-/-}$*IL-12R*$^{-/-}$), respectively. Yellow lightning bolt represents irradiation of recipient mice. See methods for additional details of experimental design. **(E,F)** ELISA analysis of serum at 16 week post-transplantation for: **(E)** anti-dsDNA IgG2c and **(F)** anti-smRNP IgG2c autoantibodies in indicated recipient mice. **(G,H)** Splenocytes were isolated at 16 week and analyzed by flow cytometry for frequency of: **(G)** GC and **(H)** Tfh cells as described in **Figure 2**. Small horizontal lines indicate the mean (± s.e.m.). ELISA results are displayed as absorbance at 450 nm normalized to results of a blank well and presented in arbitrary units (AU). **(B,C,E,F)** Statistical analysis was performed using one-way ANOVA with Tukey's multiple comparisons test. Data are representative of two independent experiments **(B,C)** or data combined from two independent experiments **(E–H)**. Each symbol represents an individual biological replicate;*Tyk2*$^{NP/NP}$ $n = 3$, *Tyk2*$^{NP/P}$ $n = 4$,*Tyk2*$^{P/P}$ $n = 3$ or PBS $n = 2$ **(A-C)**; WT $n = 4$,*Tyk2*$^{NP/NP}$ $n = 9$, *Tyk2*$^{NP/P}$ $n = 12$,*Tyk2*$^{P/P}$ $n = 7$ or *IL-12R*$^{-/-}$ $n = 8$ **(E,F)**; WT $n = 8$,*Tyk2*$^{NP/NP}$ $n = 9$, *Tyk2*$^{NP/P}$ $n = 12$,*Tyk2*$^{P/P}$ $n = 7$ or *IL-12R*$^{-/-}$ $n = 8$ **(G,H)**.

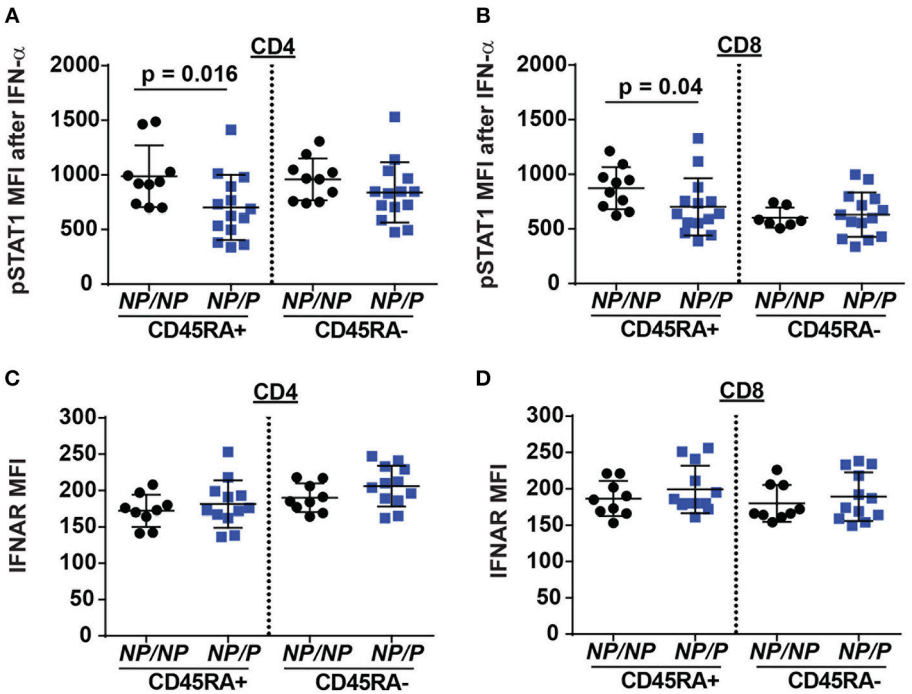

FIGURE 5 | Decreased IFN-α/pSTAT1 signaling in naive T cells from healthy subjects expressing the TYK2 protective variant. PBMC from healthy subjects with *TYK2*$^{NP/NP}$ (*NP/NP*) or heterozygote for the protective allele *TYK2*$^{NP/P}$ (*NP/P*), were thawed and stimulated with 2,000 IU/ml recombinant IFN-α for 12 min and assessed using flow-cytometry for phosphorylation of STAT1 (pSTAT1) or IFN I receptor (IFNAR) surface expression. Quantification of pSTAT1 MFI following IFN-α stimulation in: **(A)** naive (RA+) and memory (RA-) CD4$^+$ and **(B)** CD8$^+$ T cells. Quantification of IFNAR mean fluorescence intensity (MFI) in: **(C)** naive (RA+) and memory (RA-) CD4$^+$ and **(D)** CD8$^+$ T cells. Each symbol represents an individual donor **(A–D)**; small horizontal lines indicate the mean (± s.d.). Data from a combined total of $n = 10$ *TYK2*$^{NP/NP}$ donors or $n = 14$ *TYK2*$^{NP/P}$ donors **(A–D)**. Statistical analysis performed using Mann-Whitney U testing **(A–D)**.

Tyk2^P Mice Are Protected From EAE and Exhibit Reduced Numbers of IFN-γ$^+$/IL-17$^+$ Pathogenic CD4$^+$ T Cells

TYK2^P has also been associated with protection in MS (31). We used a murine model of MS, experimental autoimmune encephalomyelitis (EAE), to test the role of *Tyk2*^{P} in modulating disease. As shown schematically in **Figure 7A**, control (*Tyk2*$^{NP/NP}$), heterozygous *Tyk2*$^{NP/P}$ and homozygous *Tyk2*$^{P/P}$ mice were immunized with MOG peptide in complete Freund's adjuvant (CFA) and also treated with pertussis toxin to increase permeability of the blood brain barrier. While both control and heterozygous *Tyk2*$^{NP/P}$ animals developed disease manifestations beginning at ∼10 days post-immunization, mice expressing *Tyk2*$^{P/P}$ were completely protected from EAE (**Figure 7A**, lower panel). Both Th1 and Th17 cells have been shown to be important for EAE disease development (54). Notably, the proportion of draining LN T cells expressing IL-17$^+$ was similar in *Tyk2*$^{NP/NP}$, *Tyk2*$^{NP/P}$ and *Tyk2*$^{P/P}$ animals and there was only a trend toward a reduced proportion of IFN-γ$^+$ cells in *Tyk2*$^{P/P}$ animals (**Figures 7B–E**). In contrast, the proportion of double-positive IFN-γ$^+$/IL-17$^+$ pathogenic CD4$^+$ T cells was specifically decreased in *Tyk2*$^{P/P}$ mice (**Figure 7E**). The number of CD4$^+$ T infiltrating the central nervous system (CNS) was markedly reduced in *Tyk2*$^{P/P}$ mice and included reduction in both IFN-γ$^+$ or IFN-γ$^+$/IL-17$^+$ double positive T cells (**Figures 7F–I**). Altogether, these data demonstrate that *Tyk2*^{P} protects from EAE by decreasing pathogenic CD4$^+$ T cells which depend on both IL-12 and IL-17 signaling to promote disease development.

DISCUSSION

While *TYK2*^{P} has been shown to be a hypomorphic allele, its protective role in autoimmunity still remains largely unexplored. Here we show that *TYK2*^{P} limits signaling in response to IL-12, IL-23, and IFN I cytokines. Despite these cytokine defects, *Tyk2*^{P} mice were not protected in two independent lupus models and exhibited no difference in the response toward two different T dependent immunization models. Yet healthy individuals expressing *TYK2*^{P} displayed diminished Tfh and switched memory B cells, and homozygous *Tyk2*^{P} mice were fully protected in a murine model of MS. Our findings highlight the complexity of the cytokine milieu that regulate immune responses in both man and mouse, and the likely requirement for concurrent alterations in multiple cytokine signals in order for this variant to manifest a disease protective phenotype.

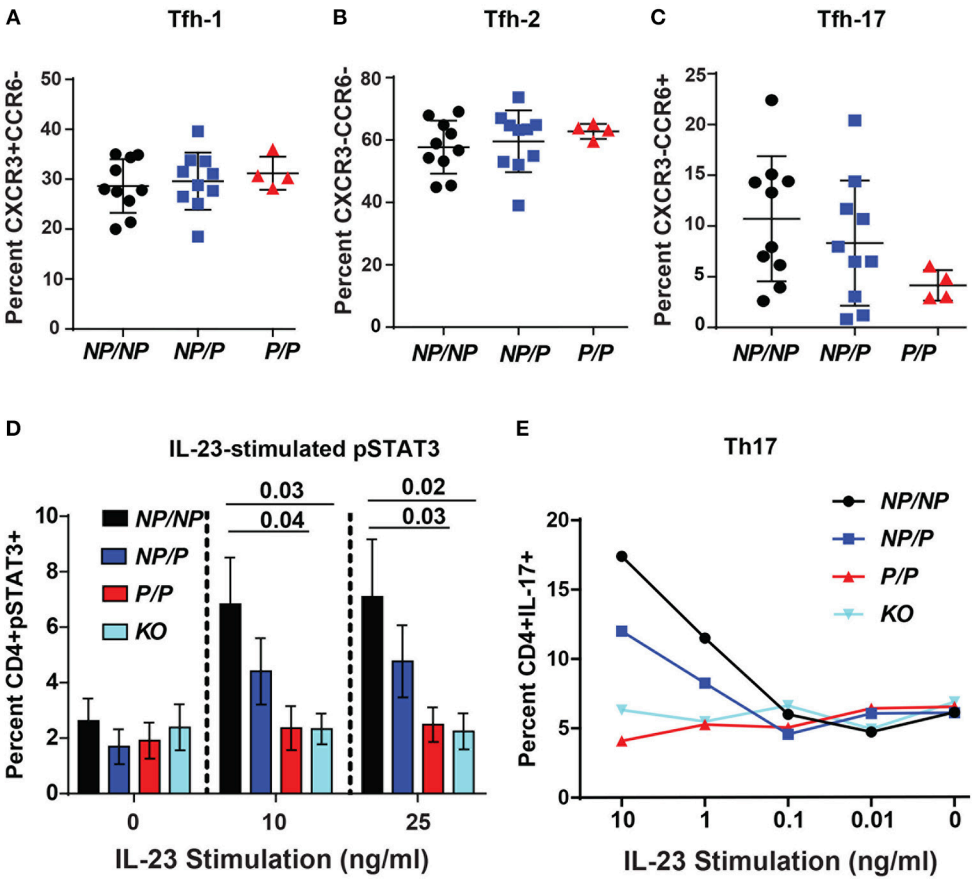

FIGURE 6 | Healthy subjects expressing the TYK2 protective variant exhibit decreased circulating Tfh-17 cells and *Tyk2*^{P} mice exhibit reduced IL-23 signaling and Th17 skewing. **(A–C)**, Quantification of Tfh subsets in healthy subjects with *TYK2*$^{NP/NP}$ (*NP/NP*), *TYK2*$^{NP/P}$ (*NP/P*), or *TYK2*$^{P/P}$ (*P/P*) alleles, respectively. Results of flow cytometry studies assessing the frequency of: **(A)**, CXCR3^{+}CCR6^{-} Tfh-1; **(B)** CXCR3^{-}CCR6^{-} Tfh-2; and **(C)** CXCR3^{-}CCR6^{+} Tfh-17 T cells within the CD4^{+}CXCR5^{+} cell population. Each symbol represents an individual donor. **(D,E)** Splenic CD4^{+} T cells were isolated from *Tyk2*$^{NP/NP}$ (*NP/NP*), *Tyk2*$^{NP/P}$ (*NP/P*), *Tyk2*$^{P/P}$ (*P/P*) or *Tyk2*$^{-/-}$ (*KO*) mice. **(D)** CD4^{+} T cells were stimulated with using the indicated amounts of IL-23 for 15 min and assessed using flow cytometry for phosphorylation of STAT3 (pSTAT3). **(E)** CD4^{+} T cells were cultured in Th-17 skewing conditions with indicated amounts of IL-23 and assessed for the frequency of IL-17^{+} CD4 (Th-17) T cells. **(A–C)** small horizontal lines indicate the mean (± s.d.) and **(D)** mean (± s.e.m.). Data from a combined total of $n = 10$ *TYK2*$^{NP/NP}$ donors, $n = 10$ *TYK2*$^{NP/P}$ donors, and $n = 4$ *TYK2*$^{P/P}$ donors **(A–C)**. Data are representative of three independent experiments **(D)** and one experiment **(E)**. Statistical analysis were performed using Kruskal-Wallis **(A–C)** and two-way ANOVA with Tukey's multiple comparisons test **(D)**.

Functional Role of *TYK2*^{P} in Cytokine Signaling

In our murine model, we found a deficiency in IL-12 induced pSTAT3 in homozygous *Tyk2*^{P} expressing CD4^{+} T cells. This was complimentary to a recent study that developed a similar mouse model of *Tyk2*^{P1104A} and showed decreased IL-12 induced pSTAT4 (33). Similar to the murine data, Dendrou et al. found diminished IL-12 induced pSTAT4 in human CD4^{+} T cells expressing *TYK2*$^{P/P}$ compared to *TYK2*$^{NP/NP}$ T cells (33). In contrast, we did not identify differences in pSTAT3 or pSTAT4 following IL-12 stimulation in homozygous non-protective vs. heterozygous protective individuals. Our findings are consistent with a recent data set comparing *TYK2*$^{NP/NP}$ to *TYK2*$^{NP/P}$ participants (55). Differences between our studies likely reflect the large number of homozygous *TYK2*^{P} individuals (7 vs. 2) studied by Dendrou et al. and/or differences in stimulation conditions. Further, we found that IL-23 signaling and IL-17^{+} cells were decreased in murine homozygous *Tyk2*^{P} CD4^{+} Th17 populations consistent with previous mouse and human data (33). Lastly, we demonstrate that TYK2^{P} also limits type I interferon signaling in humans, and in the *Tyk2*^{P} murine model (data not shown) as observed in human *TYK2*^{P} T cells (33). Of note, while *Tyk2*$^{NP/NP}$ and *Tyk2*$^{NP/P}$ T and B cells did not exhibit statistically significant differences in IL-12 mediated signals (**Figures 2A–D**), in each assay, *Tyk2*$^{NP/P}$ cells showed a slight decrease in pSTAT3 and Th skewing (and in IL-12 triggered B cell IL-6 production) compared to *Tyk2*$^{NP/NP}$ cells suggesting a potential dose-dependent effect on *in vitro* IL-12 signaling. The findings mimicked the impact of heterozygous dosage of the protective variant in human cells in various settings. Taken together, our observations support the conclusion that TYK2^{P} exerts an allele-dose dependent

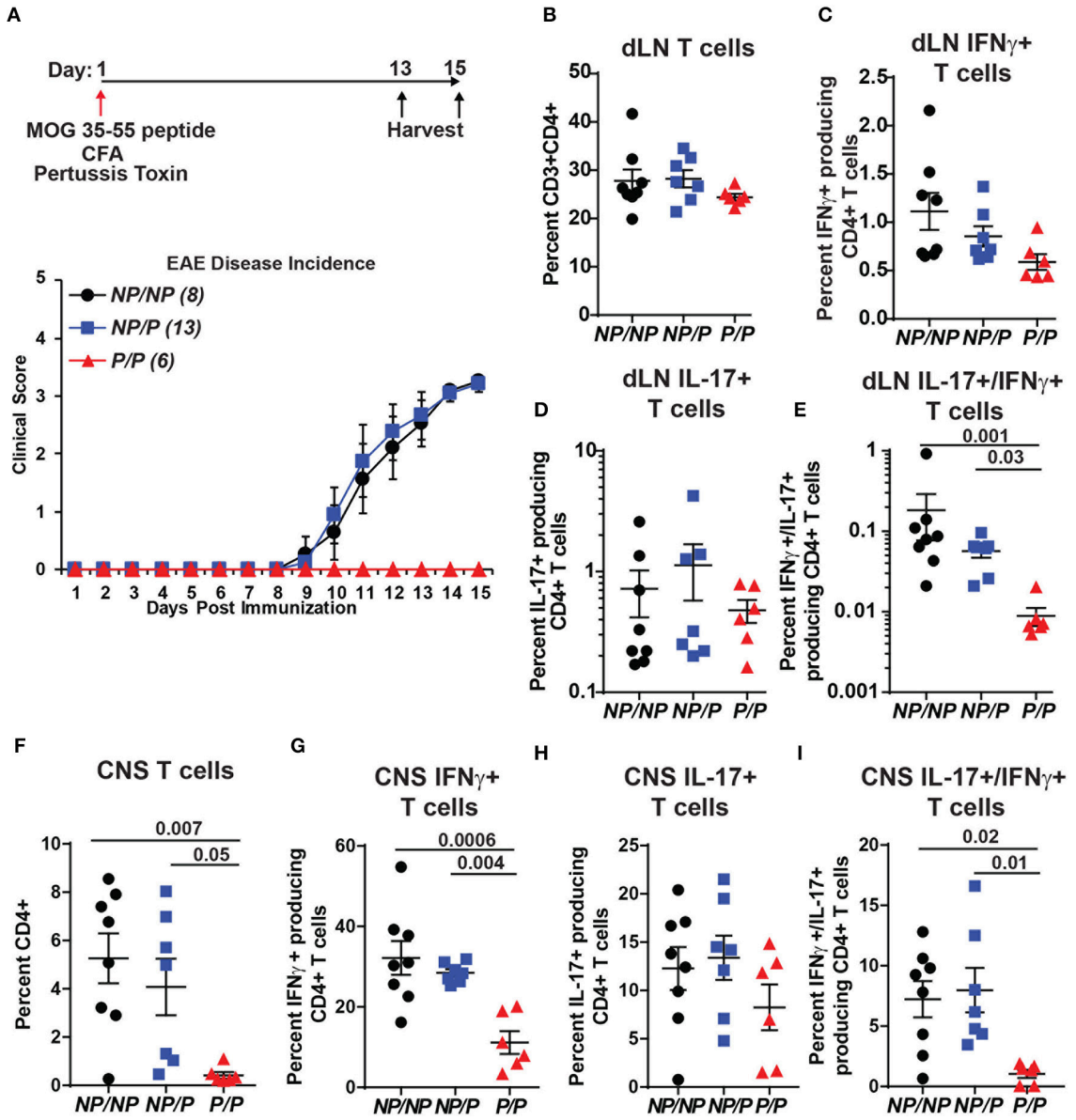

FIGURE 7 | *Tyk2*^{P} variant mice are protected in a murine model of multiple sclerosis. **(A)** (*Upper*) Schematic of experimental design for induction of EAE by immunization with MOG peptide. *Tyk2*$^{NP/NP}$(n = 8), *Tyk2*$^{NP/P}$(n = 13), and *Tyk2*$^{P/P}$(n = 6) mice were immunized (red arrow) and evaluated clinically for 15 days. (*Lower*) EAE clinical score was determined as per methods (1=Tail limp, 2=1 hind leg paralyzed, 3=2 hind legs paralyzed, 4=front leg paralyzed). **(B–G)** Tissues were collected at Day 13 or Day 15 post-immunization and T lymphocyte populations were evaluated using flow cytometry. **(B–D)** Frequency of T cells within the draining lymph nodes (dLN) showing: **(B)** total T cells; **(C)** IFN-γ^+ T cells **(D)** IL-17$^+$ T cells, and **(E)** IL-17$^+$/IFN-γ^+ double positive T cells **(F–I)**. Frequency of T cells within the central nervous system (CNS) showing: **(F)** total T cells; **(G)** IFN-γ^+ T cells; **(H)**, IL-17$^+$ T cells; and **(I)** IL-17$^+$/IFN-γ^+ T cells. **(B–I)**; Each symbol represents an individual animal; small horizontal lines indicate the mean (± s.e.m.). Flow cytometry data shown are from 2 independent experiments including: *Tyk2*$^{NP/NP}$ (n = 7) *Tyk2*$^{NP/P}$ (n = 7) and *Tyk2*$^{P/P}$ (n = 6) animals. **(C–I)** Data shown are combined from cells collected on day 13 or 15. Statistical analysis was performed using a two-way ANOVA with Tukey's multiple comparisons test.

limiting effect on *in vitro* responses to IL-12, IL-23, and IFN I signaling.

Individuals that are *TYK2*-deficient manifest impaired cytokine responses to IL-12, IL-23, IFN-α, and IL-10 (21). Moreover, these patients exhibit an increased risk for mycobacterial and viral infections (21). Consistent with this phenotype, *TYK2*^{P} individuals also exhibit signaling defects in IL-12, IL-23, and IFN-α. However, based upon the clinical data within our biorepository, the small number of homozygous protective variant-expressing subjects have not displayed increased infections similar to the *TYK2*-deficient patients (21) and other studies to date also have not reported an increase

in infectious risk for such individuals; suggesting that larger populations studies are likely required to address this question (33). Differences between complete *TYK2* deficiency versus a hypomorphic allele may reflect retention of a protein scaffold function. This idea may also be consistent with observations that individuals or mice heterozygous for the protective allele exhibit subtle alterations in lymphocyte subsets and signaling activity, implying a possible dominant negative effect of the protective allele. Studies have also linked loss of TYK2 expression to altered stability of STAT proteins in murine cells and TYK2 associated receptor surface expression on human cells (20, 21, 23, 33). Similar findings have not been previously reported or observed in our *Tyk2*^{P} murine model (data not shown). TYK2^{P} expression was shown not to affect IFNAR surface expression (**Figures 5C,D**) and IL-12R (33). More work is needed to fully elucidate the TYK2 interactome in various cell lineages and its impact(s) in modulation of cytokine signaling.

Dysregulation of the IL-12, IL-23, or IFN signaling pathways may also contribute to SLE disease (3, 15, 16). However, signaling molecules within these pathways seem to compensate for each other. Hence, there is the need for multiple aberrant pathways to lead to complex autoimmune diseases such as SLE. There is evidence that these pathways are on a fine axis. When one is dysregulated, it throws off the balance of the other pathways leading to further abnormal signaling, irregular activation and ultimately autoimmune disease. One example of this is deficiency in STAT3 which causes a decrease in Tfh and GC B cells, leading Th cells to take on the Th1-like phenotype. However, in STAT3 deficient cells the normal populations are rescued when IFNAR is blocked (18). Together these cytokine pathways are dependent on one another *in vivo* and must be studied collectively to get a complete picture of how such signals contribute to disease.

TYK2^{P} and T Helper Subsets

IL-12 and IL-23 represent critical cytokines for generation of Th1 and Th17 cells, respectively. Herein we show that IL-12 and IL-23 signaling and their respective Th subsets are diminished in an *in vitro* setting when TYK2^{P} is expressed. Importantly, these cytokines are also involved in Tfh cell generation. We show for the first time that Tfh cells, specifically the Tfh-17 cell subset which has superior ability to provide B cell help (56), are reduced in healthy human subjects with the *TYK2*^{P} allele. Further, we show that naïve murine *Tyk2*^{P} CD4^{+} T cells exhibit a defect in *in vitro* Tfh generation. Consistent with these findings, individuals lacking *IL-12Rβ1* exhibit diminished circulating memory Tfh and memory B cells (57). IL-23 also signals through STAT3 and can to contribute to Tfh generation (13). Our combined observations support a model wherein combined reduction in IL-12 and IL-23 signals leads to a reduced number of Tfh-17 cells in healthy *TYK2*^{P} donors. Thus, TYK2^{P} is a critical regulator for Tfh populations by reducing IL-12 and IL-23 signaling cascades.

Herein we also found healthy individuals expressing TYK2^{P} to have diminished switched memory B cells. This is consistent with *IL-12Rβ1* deficient subjects who exhibited both reduced switched and unswitched memory B cells (57). This reduction is most likely due to defective GC responses from diminished IL-12 signaling in T cells. IL-12 is an efficient inducer of IL-21 production from Tfh cells, a cytokine critical for the activation of human GC B cells (14, 58). Additionally, *IL-12Rβ1*-, *TYK2*-, or *STAT3*-deficient CD4^{+} T cells display reduced IL-12 induced IL-21 production *in vitro* (12). However, *Tyk2*^{P} mice did not display any differences in GC responses post-immunization. Further investigation is needed to assess GC formation and its link to memory B cells in *Tyk2*^{P} mice.

TYK2^{P} in Autoimmune Disease

TYK2^{P} has been associated with protection from MS (31) and *Tyk2*$^{-/-}$ mice are fully protected from EAE (26). In our study, we found that homozygous *Tyk2*$^{P/P}$ mice are completely protected from EAE. Infiltrating T cells within the CNS were markedly reduced in *Tyk2*$^{P/P}$ mice and protection correlated most strongly with a reduction in double-positive IFN-γ^{+}/IL-17^{+} CD4^{+} T cells within both the draining lymph nodes and the CNS. Of note, consistent with the partial *in vitro* phenotype in response to cytokine stimulation, heterozygous *Tyk2*$^{NP/P}$ mice exhibited a trend toward reduced single IFN-γ^{+} and double-positive IFN-γ^{+}/IL-17^{+} CD4^{+} T cells in the draining lymph nodes. However, heterozygous animals were not protected from EAE *in vivo*. Our combined findings are consistent with and expand upon previous data from Dendrou et al. (33). Both the IL-12 and IL-23 signaling programs contribute to EAE disease (59). Protection for EAE in *Tyk2*$^{P/P}$ mice aligns with the reduced IL-12 and IL-23 signaling and reduced Th1 and Th17 *in vitro* skewing described above. MS patients also exhibit populations of Tfh-1 and Tfh-17 cells and the relative proportions of these effectors varies among MS cohorts, with IL-23 signaling playing a more dominant role in some subjects(3, 60). More work is required to determine whether protection from MS in *TYK2*^{P} carriers might be predicted based upon the proportion of Tfh-17 cells and/or dual-positive IFN-γ^{+}/IL-17^{+} CD4^{+} effector T cells.

In contrast to the EAE data, we show that *Tyk2*^{P} does not shield mice from autoantibody production and disease progression in two separate lupus models even though GWAS has linked this variant to protection from SLE (28–30, 33). SLE is a heterogeneous disorder that reflects both variable genetic and environmental contributions. The lack of protection observed in our studies may reflect the specific disease models studied. We observed no impact of *Tyk2*^{P} in the BM12 adoptive transfer lupus model where autoantibody production is driven by self-reactive T cell triggered autoimmune GC responses that are characterized by expanded Tfh populations. Despite our findings of altered Tfh and memory B cell populations in healthy *TYK2*^{P} subjects, we did not observe alterations in Tfh or autoantibody generation in this model. We also showed no impact of *Tyk2*^{P} in the *WAS* B cell chimera lupus model. This latter model leads to spontaneous autoimmune GC responses driven by altered B cell receptor (BCR) and TLR7 signaling. Autoimmune GC production is also dependent upon B cell intrinsic antigen presenting cell (APC) activity, IFNγ1-R1 signaling, and IL-6 production (46, 51). Surprisingly, in the current study, we also show that the *WAS* chimera model is not impacted by global *Il12rb2* deficiency and our previous work has shown that B cell-intrinsic IFNAR is also dispensable for lupus development in this model (51). Thus,

two key programs modulated by *Tyk2*^{P} play a limited role in this model. As noted above, TYK2^{P} can function to limit IFN I signaling. IFN I signaling is increased in a subset of SLE subjects and IFN I blockade has provided partial benefit in some patients (61–63). Thus, the potential protective impact of *Tyk2*^{P} may be most relevant in lupus models that are driven or accelerated by an altered IFN I program. Future studies using co-modeling with other relevant SLE GWAS risk alleles, including the common *IFIH*1 risk variant (37), may provide insight into the impact of TYK2^{P} in SLE disease pathogenesis.

TYK2^{A1104} allele is a rare variant at ∼2.7% overall allelic frequency (64). Thus, the association with protection in multiple autoimmune disorders is predominantly within heterozygous individuals. As noted above, while we observed alterations in key lymphocyte populations in healthy subjects with the protective allele, we observed only trends toward reduced signaling activity using heterozygous *Tyk2*$^{NP/P}$ murine and human cells in our *in vitro* studies. Disease protection *in vivo*, when present, was only evident in *Tyk2*$^{P/P}$ animals. The requirement for homozygous TYK2^{P} expression to manifest differences in our assays suggests that protection likely involves a more complex process than simply altering a single cytokine program. Instead, the variant appears to provide protection by modestly altering multiple pathways, thereby subtly diminishing immune responses that lead to autoimmunity. This complex role for TYK2^{P} in protection from autoimmune pathogenesis highlights the value of our combinatorial studies using both murine models and healthy human subjects to assess its impact on human disease. Whether protection primarily reflects diminished Tfh cell populations or another cell type remains to be fully defined the ability of TYK2 to impact a subset of key cytokine pathways highlights its potential utility as a therapeutic target. Consistent with this concept, recent findings using an oral TYK2 inhibitor have demonstrated beneficial effects in treatment of adult subjects with psoriasis (65). Taken together, our findings suggest that targeting TYK2 kinase activity may provide a relatively broad therapeutic window for protection from autoimmune disease while limiting the potential risk for immunosuppression.

DATA AVAILABILITY STATEMENT

The data that support the findings of this study are available for the corresponding author upon request.

AUTHOR CONTRIBUTIONS

JG designed and performed experiments, analyzed data, and wrote the manuscript. CH designed and performed experiments, analyzed data, and edited manuscript. MK, TA, EA, CC, SW, KT, AE, SK, MH, and MO developed required models/strains or reagents and/or performed experiments and/or edited manuscript. SWJ designed and interpreted WASp mouse studies. KC genotyped human subjects, interpreted data, and edited manuscript. JHB and DJR conceived and supervised the study, interpreted data, and edited the manuscript.

FUNDING

This work was supported by grants from the NIH: DP3-DK097672 (to JHB), DP3-DK111802 (to DJR), T32-AR007108 (to JG), K08AI112993 (to SWJ), and R01AI133885 (to MO). Additional support was provided by the Children's Guild Association Endowed Chair in Pediatric Immunology and the Benaroya Family Gift Fund (to DR); National Multiple Sclerosis Society (NMSS) RG-5044-A-2 (to MO); American College of Rheumatology (ACR) Rheumatology Research Foundation (RRF) Career Development K Supplement (to SWJ); and by a Lupus Research Alliance, Novel Research Grant (to SWJ). The content is solely the responsibility of the authors and does not necessarily represent the official views of the National Institutes of Health.

ACKNOWLEDGMENTS

The authors would like to thank Karen Sommer for laboratory management. Dr. Nathan Camp, Jared Delahaye, and Megan Maerz for assistance in experiments. Dr. Mridu Acharya and Dr. Anne Hocking intellectual guidance and editing of the manuscript. Dr. Baidong Hou for reagents for VLP experiments. Dr. Mathias Muller and Dr. George Yap for the original *Tyk2*$^{-/-}$ mice.

SUPPLEMENTARY MATERIAL

The Supplementary Material for this article can be found online at: https://www.frontiersin.org/articles/10.3389/fimmu.2019.00044/full#supplementary-material

REFERENCES

1. Tsokos GC, Lo MS, Reis PC, Sullivan KE. New insights into the immunopathogenesis of systemic lupus erythematosus. *Nat Rev Rheumatol.* (2016) 12:716–30. doi: 10.1038/nrrheum.2016.186
2. Kaul A, Gordon C, Crow MK, Touma Z, Urowitz MB, van Vollenhoven R, et al. Systemic lupus erythematosus. *Nat Rev Dis Primers* (2016) 2:16039. doi: 10.1038/nrdp.2016.39
3. Qiu H, Wu H, Chan V, Lau C-S, Lu Q. Transcriptional and epigenetic regulation of follicular T-helper cells and their role in autoimmunity. *Autoimmunity* (2017) 50:71–81. doi: 10.1080/08916934.2017.1284821
4. Choi JY, Ho JHE, Pasoto SG, Bunin V, Kim ST, Carrasco S, et al. Circulating follicular helper–like T cells in systemic lupus erythematosus: association with disease activity. *Arthritis Rheumatol.* (2015) 67:988–99. doi: 10.1002/art.39020
5. Victora GD, Nussenzweig MC. Germinal Centers. *Ann Rev Immunol.* (2012) 30:429–57. doi: 10.1146/annurev-immunol-020711-075032
6. Chtanova T, Tangye SG, Newton R, Frank N, Hodge MR, Rolph MS, et al. T follicular helper cells express a distinctive transcriptional profile, reflecting their role as non-th1/Th2 effector cells that provide help for B cells. *J Immunol.* (2004) 173:68–78. doi: 10.4049/jimmunol.173.1.68
7. Kim CH, Lim HW, Kim JR, Rott L, Hillsamer P, Butcher EC. Unique gene expression program of human germinal center T helper cells. *Blood* (2004) 104:1952–60. doi: 10.1182/blood-2004-03-1206

8. Yu D, Rao S, Tsai LM, Lee SK, He Y, Sutcliffe EL, et al. The transcriptional repressor bcl-6 directs t follicular helper cell lineage commitment. *Immunity* (2009) 31:457–68. doi: 10.1016/j.immuni.2009.07.002
9. Nurieva RI, Chung Y, Hwang D, Yang XO, Kang HS, Ma L, et al. Generation of T follicular helper cells is mediated by interleukin-21 but independent of T helper 1, 2, or 17 cell lineages. *Immunity* (2008) 29:138–49. doi: 10.1016/j.immuni.2008.05.009
10. Choi YS, Eto D, Yang JA, Lao C, Crotty S. Cutting edge: STAT1 is required for IL-6–mediated Bcl6 induction for early follicular helper cell differentiation. *J Immunol.* (2013) 190:1203032–53. doi: 10.4049/jimmunol.1203032
11. Eto D, Lao C, DiToro D, Barnett B, Escobar TC, Kageyama R, et al. IL-21 and IL-6 are critical for different aspects of B cell immunity and redundantly induce optimal follicular helper CD4 T cell (Tfh) differentiation. *PLoS ONE* (2011) 6:e17739. doi: 10.1371/journal.pone.0017739
12. Ma CS, Avery DT, Chan A, Batten M, Bustamante J, Boisson-Dupuis S, et al. Functional STAT3 deficiency compromises the generation of human T follicular helper cells. *Blood* (2012) 119:3997–4008. doi: 10.1182/blood-2011-11-392985
13. Schmitt N, Liu Y, Bentebibel S-E, Munagala I, Bourdery L, Venuprasad K, et al. The cytokine TGF-β co-opts signaling via STAT3-STAT4 to promote the differentiation of human T_{FH} cells. *Nat Immunol.* (2014) 15:856–65. doi: 10.1038/ni.2947
14. Kim SJ, Lee K, Diamond B. Follicular helper T cells in systemic lupus erythematosus. *Front Immunol.* (2018) 9:289. doi: 10.3389/fimmu.2018.01793
15. Wong CK, Lit LCW, Tam LS, Li EKM, Wong PTY, Lam CWK. Hyperproduction of IL-23 and IL-17 in patients with systemic lupus erythematosus: implications for Th17-mediated inflammation in auto-immunity. *Clin Immunol.* (2008) 127:385–93. doi: 10.1016/j.clim.2008.01.019
16. Koenig KF, Groeschl I, Pesickova SS, Tesar V, Eisenberger U, Trendelenburg M. Serum cytokine profile in patients with active lupus nephritis. *Cytokine* (2012) 60:410–6. doi: 10.1016/j.cyto.2012.07.004
17. Nakayamada S, Poholek AC, Lu KT, Takahashi H, Kato M, Iwata S, et al. Type I IFN induces binding of STAT1 to Bcl6: divergent roles of STAT family transcription factors in the T follicular helper cell genetic program. *J Immunol.* (2014) 192:1300675–2166. doi: 10.4049/jimmunol.1300675
18. Ray JP, Marshall HD, Laidlaw BJ, Staron MM, Kaech SM, Craft J. Transcription factor STAT3 and type I interferons are corepressive insulators for differentiation of follicular helper and T helper 1 cells. *Immunity* (2014) 40:367–77. doi: 10.1016/j.immuni.2014.02.005
19. Strobl B, Stoiber D, Sexl V, Mueller M. Tyrosine kinase 2 (TYK2) in cytokine signalling and host immunity. *Front Biosci.* (2011) 16:3214–32. doi: 10.2741/3908
20. Minegishi Y, Saito M, Morio T, Watanabe K, Agematsu K, Tsuchiya S, et al. Human tyrosine kinase 2 deficiency reveals its requisite roles in multiple cytokine signals involved in innate and acquired immunity. *Immunity* (2006) 25:745–55. doi: 10.1016/j.immuni.2006.09.009
21. Kreins AY, Ciancanelli MJ, Okada S, Kong X-F, Ramírez-Alejo N, Kilic SS, et al. Human TYK2 deficiency: mycobacterial and viral infections without hyper-IgE syndrome. *J Exp Med.* (2015) 212:1641–62. doi: 10.1084/jem.20140280
22. Casanova J-L, Holland SM, Notarangelo LD. Inborn errors of human JAKs and STATs. *Immunity* (2012) 36:515–28. doi: 10.1016/j.immuni.2012.03.016
23. Karaghiosoff M, Neubauer H, Lassnig C, Kovarik P, Schindler H, Pircher H, et al. Partial impairment of cytokine responses in Tyk2-deficient mice. *Immunity* (2000) 13:549–60. doi: 10.1016/S1074-7613(00)00054-6
24. Shimoda K, Kato K, Aoki K, Matsuda T, Miyamoto A, Shibamori M, et al. Tyk2 plays a restricted role in IFNα signaling, although it is required for IL-12-mediated T cell function. *Immunity* (2000) 13:561–71. doi: 10.1016/S1074-7613(00)00055-8
25. Wilbers RHP, van Raaij DR, Westerhof LB, Bakker J, Smant G, Schots A. Re-evaluation of IL-10 signaling reveals novel insights on the contribution of the intracellular domain of the IL-10R2 chain. *PLoS ONE* (2017) 12:e0186317. doi: 10.1371/journal.pone.0186317
26. Oyamada A, Ikebe H, Itsumi M, Saiwai H, Okada S, Shimoda K, et al. Tyrosine kinase 2 plays critical roles in the pathogenic CD4 T cell responses for the development of experimental autoimmune encephalomyelitis. *J Immunol.* (2009) 183:7539–46. doi: 10.4049/jimmunol.0902740
27. Strobl B, Bubic I, Bruns U, Steinborn R, Lajko R, Kolbe T, et al. Novel functions of tyrosine kinase 2 in the antiviral defense against murine cytomegalovirus. *J Immunol.* (2005) 175:4000–8. doi: 10.4049/jimmunol.175.6.4000
28. Hellquist A, Järvinen TM, Koskenmies S, Zucchelli M, Orsmark-Pietras C, Berglind L, et al. Evidence for genetic association and interaction between the TYK2 and IRF5 genes in systemic lupus erythematosus. *J Rheumatol.* (2009) 36: 1631–8. doi: 10.3899/jrheum.081160
29. Sigurdsson S, Nordmark G, Göring HHH, Lindroos K, Wiman A-C, Sturfelt G, et al. Polymorphisms in the tyrosine kinase 2 and interferon regulatory factor 5 genes are associated with systemic lupus erythematosus. *Am J Human Genet.* (2005) 76:528–37. doi: 10.1086/428480
30. Graham DSC, Morris DL, Bhangale TR, Criswell LA, Syvänen A-C, Rönnblom L, et al. Association of NCF2, IKZF1, IRF8, IFIH1, and TYK2 with systemic lupus erythematosus. *PLOS Genet.* (2011) 7:e1002341. doi: 10.1371/journal.pgen.1002341
31. Ban M, Goris A, Lorentzen ÅR, Baker A, Mihalova T, Ingram G, et al. Replication analysis identifies TYK2 as a multiple sclerosis susceptibility factor. *Eur J Human Genet* (2009) 17:1309–13. doi: 10.1038/ejhg.2009.41
32. Diogo D, Bastarache L, Liao KP, Graham RR, Fulton RS, Greenberg JD, et al. TYK2 protein-coding variants protect against rheumatoid arthritis and autoimmunity, with no evidence of major pleiotropic effects on non-autoimmune complex traits. *PLoS ONE* (2015) 10:e0122271. doi: 10.1371/journal.pone.0122271
33. Dendrou CA, Cortes A, Shipman L, Evans HG, Attfield KE, Jostins L, et al. Resolving TYK2 locus genotype-to-phenotype differences in autoimmunity. *Sci Transl Med.* (2016) 8:363ra149. doi: 10.1126/scitranslmed.aag1974
34. Type 1 Diabetes Genetics Consortium, Onengut-Gumuscu S, Chen W-M, Burren O, Cooper NJ, Quinlan AR, et al. Fine mapping of type 1 diabetes susceptibility loci and evidence for colocalization of causal variants with lymphoid gene enhancers. *Nat Genet.* (2015) 47:381–6. doi: 10.1038/ng.3245
35. Li Z, Gakovic M, Ragimbeau J, Eloranta M-L, Rönnblom L, Michel F, et al. Two rare disease-associated Tyk2 variants are catalytically impaired but signaling competent. *J Immunol.* (2013) 190:2344. doi: 10.4049/jimmunol.1203118
36. Couturier N, Bucciarelli F, Nurtdinov RN, Debouverie M, Lebrun-Frenay C, Defer G, et al. Tyrosine kinase 2 variant influences T lymphocyte polarization and multiple sclerosis susceptibility. *Brain* (2011) 134:693–703. doi: 10.1093/brain/awr010
37. Gorman JA, Hundhausen C, Errett JS, Stone AE, Allenspach EJ, Ge Y, et al. The A946T variant of the RNA sensor IFIH1 mediates an interferon program that limits viral infection but increases the risk for autoimmunity. *Nat Immunol.* (2017) 18:744–52. doi: 10.1038/ni.3766
38. Becker-Herman S, Meyer-Bahlburg A, Schwartz MA, Jackson SW, Hudkins KL, Liu C, et al. WASp-deficient B cells play a critical, cell-intrinsic role in triggering autoimmunity. *J Exp Med.* (2011) 208:2033–42. doi: 10.1084/jem.20110200
39. Hou B, Saudan P, Ott G, Wheeler ML, Ji M, Kuzmich L, et al. Selective utilization of toll-like receptor and MyD88 signaling in B cells for enhancement of the antiviral germinal center response. *Immunity* (2011) 34:375–84. doi: 10.1016/j.immuni.2011.01.011
40. Raso F, Sagadiev S, Du S, Gage E, Arkatkar T, Metzler G, et al. αv Integrins regulate germinal center B cell responses through noncanonical autophagy. *J Clini Invest.* (2018) 128:4163–78. doi: 10.1172/JCI99597
41. Jegerlehner A, Maurer P, Bessa J, Hinton HJ, Kopf M, Bachmann MF. TLR9 signaling in B cells determines class switch recombination to IgG2a. *J Immunol.* (2007) 178:2415–20. doi: 10.4049/jimmunol.178.4.2415
42. Schleicher U, Mattner J, Blos M, Schindler H, Röllinghoff M, Karaghiosoff M, et al. Control of Leishmania major in the absence of Tyk2 kinase. *Eur J Immunol.* (2004) 34:519–29. doi: 10.1002/eji.200324465
43. Kim SJ, Caton M, Wang C, Khalil M, Zhou Z-J, Hardin J, et al. Increased IL-12 inhibits B cells' differentiation to germinal center cells and promotes differentiation to short-lived plasmablasts. *J Exp Med.* (2008) 205:2437–48. doi: 10.1084/jem.20070731
44. McGaha TL, Karlsson MCI, Ravetch JV. FcgammaRIIB deficiency leads to autoimmunity and a defective response to apoptosis in Mrl-MpJ mice. *J Immunol.* (2008) 180:5670–9. doi: 10.4049/jimmunol.180.8.5670

45. Nurieva RI, Chung Y, Martinez GJ, Yang XO, Tanaka S, Matskevitch TD, et al. Bcl6 mediates the development of T follicular helper cells. *Science* (2009) 325:1001–5. doi: 10.1126/science.1176676
46. Arkatkar T, Du SW, Jacobs HM, Dam EM, Hou B, Buckner JH, et al. B cell–derived IL-6 initiates spontaneous germinal center formation during systemic autoimmunity. *J Exp Med.* (2017) 214:3207–17. doi: 10.1084/jem.20170580
47. Perry D, Sang A, Yin Y, Research YZB. Murine models of systemic lupus erythematosus. *J Biomed Biotechnol.* (2011) 2011:271694. doi: 10.1155/2011/271694
48. Klarquist J, Janssen EM. The bm12 inducible model of systemic lupus erythematosus (SLE) in C57BL/6 mice. *J Vis Exp.* (2015) e53319. doi: 10.3791/53319
49. Ma Z, Chen F, Madaio MP, Cohen PL, Eisenberg RA. Modulation of autoimmunity by TLR9 in the chronic graft-vs-host model of systemic lupus erythematosus. *J Immunol.* (2006) 177:7444–50. doi: 10.4049/jimmunol.177.10.7444
50. Jackson SW, Scharping NE, Kolhatkar NS, Khim S, Schwartz MA, Li Q-Z, et al. Opposing impact of B cell–intrinsic TLR7 and TLR9 signals on autoantibody repertoire and systemic inflammation. *J Immunol.* (2014) 192:1400098–4532. doi: 10.4049/jimmunol.1400098
51. Jackson SW, Jacobs HM, Arkatkar T, Dam EM, Scharping NE, Kolhatkar NS, et al. B cell IFN-γ receptor signaling promotes autoimmune germinal centers via cell-intrinsic induction of BCL-6. *J Exp Med.* (2016) 213:733–50. doi: 10.1084/jem.20151724
52. Kolhatkar NS, Brahmandam A, Thouvenel CD, Becker-Herman S, Jacobs HM, Schwartz MA, et al. Altered BCR and TLR signals promote enhanced positive selection of autoreactive transitional B cells in Wiskott-Aldrich syndrome. *J Exp Med.* (2015) 212:1663–77. doi: 10.1084/jem.20150585
53. Kolhatkar NS, Scharping NE, Sullivan JM, Jacobs HM, Schwartz MA, Khim S, et al. B-cell intrinsic TLR7 signals promote depletion of the marginal zone in a murine model of Wiskott–Aldrich syndrome. *Eur J Immunol.* (2015) 45:2773–9. doi: 10.1002/eji.201545644
54. Rostami A, Ciric B. Role of Th17 cells in the pathogenesis of CNS inflammatory demyelination. *J Neurol Sci.* (2013) 333:76–87. doi: 10.1016/j.jns.2013.03.002
55. Enerbäck C, Sandin C, Lambert S, Zawistowski M, Stuart PE, Verma D, et al. The psoriasis-protective TYK2 I684S variant impairs IL-12 stimulated pSTAT4 response in skin-homing CD4+ and CD8+ memory T-cells. *Sci Rep.* (2018) 8:7043. doi: 10.1038/s41598-018-25282-2
56. Ueno H, Banchereau J, Vinuesa CG. Pathophysiology of T follicular helper cells in humans and mice. *Nat Immunol.* (2015) 16:142–52. doi: 10.1038/ni.3054
57. Schmitt N, Bustamante J, Bourdery L, Bentebibel S-E, Boisson-Dupuis S, Hamlin F, et al. IL-12 receptor β1 deficiency alters *in vivo* T follicular helper cell response in humans. *Blood* (2013) 121:3375–85. doi: 10.1182/blood-2012-08-448902
58. Ma CS, Suryani S, Avery DT, Chan A, Nanan R, Nanan BS, et al. Early commitment of naïve human CD4+ T cells to the T follicular helper (TFH) cell lineage is induced by IL-12. *Immunol Cell Biol.* (2009) 87:590–600. doi: 10.1038/icb.2009.64
59. Dardalhon V, Korn T, Kuchroo VK, Anderson AC. Role of Th1 and Th17 cells in organ-specific autoimmunity. *J Autoimmun.* (2008) 31:252–6. doi: 10.1016/j.jaut.2008.04.017
60. Christensen JR, Börnsen L, Ratzer R, Piehl F, Khademi M, Olsson T, et al. Systemic inflammation in progressive multiple sclerosis involves follicular T-helper, Th17- and activated B-cells and correlates with progression. *PLoS ONE* (2013) 8: e57820. doi: 10.1371/journal.pone.0057820
61. Lauwerys BR, Hachulla E, Spertini F, Lazaro E, Jorgensen C, Mariette X, et al. Down-regulation of interferon signature in systemic lupus erythematosus patients by active immunization with interferon α-kinoid. *Arthritis Rheumat.* (2013) 65:447–56. doi: 10.1002/art.37785
62. Muskardin TLW, Niewold TB. Type I interferon in rheumatic diseases. *Nat Rev Rheumatol.* (2018) 14:214–28. doi: 10.1038/nrrheum.2018.31
63. Tarbell KV, Egen JG. Breaking self-tolerance during autoimmunity and cancer immunity: myeloid cells and type I IFN response regulation. *J Leukocyte Biol.* (2018) 103:1117–1129. doi: 10.1002/JLB.3MIR1017-400R
64. Lek M, Karczewski KJ, Minikel EV, Samocha KE, Banks E, Fennell T, et al. Analysis of protein-coding genetic variation in 60,706 humans. *Nature* (2016) 536:285–291. doi: 10.1038/nature19057
65. Papp K, Gordon K, Thaçi D, Morita A, Gooderham M, Foley P, et al. Phase 2 Trial of Selective Tyrosine Kinase 2 Inhibition in Psoriasis. *N Engl J Med.* (2018) 379:1313–1321. doi: 10.1056/nejmoa1806382

Conflict of Interest Statement: The authors declare that the research was conducted in the absence of any commercial or financial relationships that could be construed as a potential conflict of interest.

frontiers in Immunology

ORIGINAL RESEARCH
published: 26 February 2019
doi: 10.3389/fimmu.2019.00258

Exploring Impact of Rare Variation in Systemic Lupus Erythematosus by a Genome Wide Imputation Approach

Manuel Martínez-Bueno[1]* *and Marta E. Alarcón-Riquelme*[2]

[1] Department of Medical Genomics, GENYO, Center for Genomics and Oncological Research Pfizer, University of Granada, Granada, Spain, [2] Unit of Chronic Inflammation, Institute for Environmental Medicine, Karolinska Institute, Stockholm, Sweden

The importance of low frequency and rare variation in complex disease genetics is difficult to estimate in patient populations. Genome-wide association studies are therefore, underpowered to detect rare variation. We have used a combined approach of genome-wide-based imputation with a highly stringent sequence kernel association (SKAT) test and a case-control burden test. We identified 98 candidate genes containing rare variation that in aggregate show association with SLE many of which have recognized immunological function, but also function and expression related to relevant tissues such as the joints, skin, blood or central nervous system. In addition we also find that there is a significant enrichment of genes annotated for disease-causing mutations in the OMIM database, suggesting that in complex diseases such as SLE, such mutations may be involved in subtle or combined phenotypes or could accelerate specific organ abnormalities found in the disease. We here provide an important resource of candidate genes for SLE.

Keywords: SLE, systemic lupus erythematosus, imputated rare variation, GWAS—genome-wide association study, sequence kernel association test, aggregated case-control enrichment

OPEN ACCESS

Edited by:
Laurence Morel,
University of Florida, United States

Reviewed by:
Jason Weinstein,
Rutgers Biomedical and Health Sciences, United States
Celine Berthier,
University of Michigan, United States
Wentian Li,
Feinstein Institute for Medical Research, United States

***Correspondence:**
Manuel Martínez-Bueno
manuel.martinez@genyo.es

Specialty section:
This article was submitted to Autoimmune and Autoinflammatory Disorders, a section of the journal Frontiers in Immunology

Received: *27 July 2018*
Accepted: *29 January 2019*
Published: *26 February 2019*

Citation:
Martínez-Bueno M and Alarcón-Riquelme ME (2019) Exploring Impact of Rare Variation in Systemic Lupus Erythematosus by a Genome Wide Imputation Approach. Front. Immunol. 10:258. doi: 10.3389/fimmu.2019.00258

INTRODUCTION

Genome-wide association studies have been designed primarily to capture common variation and so far some 10,000 common genetic variants have been robustly associated with a wide range of complex diseases (1). Therefore, this methodology is underpowered to detect the effects of rare variants. There has been much debate as to the role of rare genetic variation on complex traits (2–4) and how rare variant studies complement GWASs (5). It is now accepted that rare variants located in different genes could in fact play a more important role in disease susceptibility than common variants (4). The challenge arises in measuring and statistically analyzing rare variation. It would be very unexpected to find rare variants that could have substantial effect sizes and therefore high penetrance contributing to complex traits, being more likely to have mutations with modest effects. For small effect sizes association testing may require composite tests of overall "mutational load," pooling rare variants for analysis by addressing the question: do rare variants increase or decrease disease risk? (6). In-depth whole-genome sequencing is the most comprehensive approach for measuring rare and common variation in both coding and non-coding regions. However, nowadays, its application is limited by the costs and various computational challenges, especially for large-scale cohorts. Whole-exome sequencing is a cost-effective alternative, however one of its obvious drawback is the absence of variants in non-coding regions, which may be especially relevant in the context of complex disease genetics. Genotype imputation is likely to remain a valuable tool.

At this point an interesting cost and a computationally effective alternative would be to combine genotype imputation with targeted sequencing in a gene-centered strategy. For dense genotyping arrays, imputation is able to predict nearly all missing common variation with high accuracy, but as the variant minor allele frequency (MAF) decreases, so does the accuracy of imputation, depending mainly on the size of the reference panel and the ancestry of the imputed samples, with the best efficiencies in European cohorts, mainly due to the sufficiently large size of the European reference panels (7–13).

We have previously tested the overall effect of imputed rare variation on particular genes in systemic autoimmunity (14). Recently, we have implemented and successfully applied a method based on genotype imputation of rare variation, on a set of genes detected by exome sequencing as possible candidates for association to systemic lupus erythematosus (SLE) by mutation in members of Icelandic SLE-multicase families (15).

In the present work the method has been brought to the genome level to scan for association of protein coding genes with SLE by rare variation in the European ancestry population. We executed stringent imputation in a densely genotyped set for analyzing association with SLE in a sample from the European population selecting the protein coding genes of the genome and then applying tests to detect those that significantly associated with the disease by rare-variation. This procedure provided a set of 98 genes as good candidates for association with SLE by mutation. Many of these genes showed immunological related functions or effects on other organs or tissues affected by the pathology, such as joints, skin, central nervous system or blood and some were involved in human energy metabolism and more specifically as part of the respiratory chain. Such a diversity of functions is to be expected because of the phenotypic heterogeneity of a complex disease as SLE.

MATERIALS AND METHODS

Genome-Wide Association Analysis

We used GWAS data from 5,478 individuals of European ancestry including 4254 SLE patients and 1,224 controls genotyped using the Illumina HumanOmni1_Quad_v1-0_B chip. In order to increase the number of controls, additional data from European subjects were obtained from the dbGaP database (http://www.ncbi.nlm.nih.gov/gap) including the DCEG Imputation Reference Dataset (phs000396.v1.p1) with 1,175 individuals representing general population, and controls subjects from two case-control studies: 1,047 from the High Density SNP Association Analysis of Melanoma (phs000187.v1.p1) and 903 from GENIE UK-ROI Diabetic Nephropathy GWAS (phs000389.v1.p1). Note that only control from both case-control studies were included in our analysis. In total, the initial dataset consisted of 4,254 SLE patients and 4,349 controls.

In order to obtain a quality-controlled working dataset satisfying current state-of-the-art criteria for association studies, data filtering was conducted using PLINK v1.07 1 (16) applying the following criteria: minimum total call rate per sample of 90%, minimum call rate per marker of 98%, minor allele frequency (MAF) threshold of 1%, Hardy-Weinberg Equilibrium (HWE) p-value for cases and controls at a minimum of 0.0001, and in addition at 0.01 only for controls, and finally a cutoff p-value of 0.00001 for differential missingness in, the software REAP was used (17) applying a kinship coefficient threshold <0.055. To correct for stratification, principal component analysis (PCA) was performed with smartpca, EIGENSOFT 4.0 beta package 2 (18). To confirm the European ancestry we ran a PCA with the set of independent markers ($r^2 < 0.1$) that maximized differences in allelic frequencies between the four main 1000 Genomes subpopulations (EUR, AFR, AMR, and ASN). No samples were detected as "non-European" (**Supplemental Figure 1**). Next, the PCA was performed with the set of $r^2 < 0.1$, that maximized differences in the allelic frequencies in 1000 Genomes EUR subpopulations (CEU, GBR, IBS, TSI, and FIN) and two additional subpopulations from our sample dataset, Greek and Turkish (GRK and TUR) representing the south-eastern European ancestry. The resulting PCs perfectly classified the individuals from reference populations by their geographical origin (**Supplemental Figure 2**). This last set of PCs was used for correcting for genetic stratification in the case-control association analysis (**Supplemental Figure 3**). This resulted in a $\lambda_{GC} = 1.05$ using the first 10 principal components. The final data set used for association analysis consisted of 4,212 cases and 4,065 controls.

Imputation

Release 19 (GRCh37.p13) was used as reference (https://www.encodeproject.org/files/gencode.v19.annotation/). Of 19,430 sequences annotated as "protein coding" in the gencode.v19.annotation.gtf file, 15,763 included in the final QC-filtered genotyping data set became our imputation working gene list. Each protein-coding gene region was extended 500,000 additional base pairs upstream and downstream, respectively, as it is known that large buffers may improve accuracy for low-frequency variants during imputation. Markers within each extended region were extracted from the GWAS data for imputation with IMPUTE2 (19) using the 1000 Genomes Project as reference panel. Specifically, we used 1000 Genomes Phase 3, b37 (October 2014), as these haplotypes have lower genotype discordance and improved imputation performance into downstream GWAS samples, especially for low frequency variants (20, 21). Genome-Wide Association Analysis of Imputed Rare Variants in complex diseases has been previously used as a gene-centered approach (7). In this paper imputation into a GWAS scaffold using the WTCCC European analysis cohort explicitly showed substantial gains in power to detect rare variant association within the gene where the extent of the increase in power depends crucially on the number of individuals in the reference panel. Therefore, power gains obtained from 500 to 4,000 samples in the reference panel were not as great as from 120 to 500 samples. Based on this, and for the objective of our study we considered as adequate the 2,504 samples present in the 1000 Genomes phase 3 reference panel (2014 release, http://mathgen.stats.ox.ac.uk/impute/1000GP_Phase3/) of which 503 are of European descent. Prior to imputation, each GWAS gene extended region was phased with SHAPEIT using the 1000 Genomes EUR subpopulation as reference (http://www.shapeit.

fr/). A restrictive QC-filter was applied on the imputed genotypes (SNP genotyping rate ≥ 99%, sample genotyping rate ≥ 95%) without restriction of allele frequencies, in order to include both rare and low frequency variants. To ensure a highly reliable imputation, a conservative IMPUTE info_value threshold of ≥ 0.75 for each marker were applied as imputation quality score.

Functional Annotation of Genetic Variants

Annotation of analyzed genetic variants in their different functional categories was carried out using ANNOVAR (22).

Gene Case-Control Association Analysis by Rare Variation

While there is no universally accepted definition of "rare variant," and a minor allele frequency (MAF) of 1% is the conventional definition of polymorphism, then a MAF < 1% would be understood as "rare variation." We tested whether any of the N genes in the human genome had statistical evidence of association with SLE in the general European population due to the combined effect of all rare variation within each gene (MAF < 1%). Each gene was analyzed using two procedures: the sequence kernel association (SKAT) test (20, 21) and a case-control burden test by adjusting a logistic regression model with a "transformed" "genetic variable" equals to the sum of minor frequency alleles for all markers below the (<1%) in the tested gene in each *i* individual (7). To note that in such case-control burden test, a result statistically significant indicates that the overall effect of rare variation on the gene goes in the same direction being either of risk (aggregate odd ratio > 1) or alternatively protective (aggregate odd ratio < 1). This feature of case-control burden analysis helps to interpret the effect of rare variation on the phenotype. In addition, running two association procedures, SKAT ⋂ case-control burden test would reduce the rate of false positives. Thus, we will consider as true positives those genes with significant association test for both procedures, SKAT and case-control burden test. However, in association tests that simultaneously include several markers, one effect of linkage disequilibrium (LD) between these markers could be collinearity. We have addressed the LD issue running the tests with a set of independent markers by applying a very restrictive LD threshold of $r^2 < 0.1$. It could be argued that association signals would be lost by applying such a strict threshold of r^2 but even so, if the signal remains it supports it as "true positive" (15). **Supplemental Figure 4** summarizes the study workflow.

Correcting for Stratification in Rare Variant Association Analysis

We verified that the set of Principal Components computed with common variation was able to correct stratification for rare variant association analysis in our sample (15). To be as stringent as possible, the 10 first principal components (PC's) and genomic control (GC) were used to correct for stratification in both tests. For case-control burden 10 PC's corrected tests, the genomic inflation factor (λ_{GC}) was equal to 1.11 and for SKAT 10 PC's corrected tests it was equal to 1.24. These λ_{GC} values were used for correction of the resulting inflation on each type of association test (GC correction = Statistic $_{10PC'c\_corrected}$/ λ_{GC}). When no PC's correction was used, the λ_{GC} for case-control burden tests was equal to 1.44 and 2.97 for SKAT. Thus, the 10 PC's correction reduced the inflation by 33% in the case-control burden tests, and in 174% in the SKAT tests.

Correcting for Multiple Testing in Gene Case-Control Association Analysis of Rare Variation

Regarding the question of correcting for multiple testing in gene association by rare variants, a genomic association threshold of 10^6 is accepted (equivalent to Bonferroni correction for 19,000–20,000 protein encoding genes in the genome). It is also accepted that Bonferroni, although mathematically right would be very penalizing for biological data, therefore we opted for techniques based on permutation processes. Our multi-test correction procedure brings together the genotypes of all rare variants in all tested genes as columns into a single table. For each gene a number of markers equal to that of the gene was randomly extracted from this table and its association test calculated. By repeating the procedure for N times an empirical corrected *P*-value was calculated for each tested gene. It can be argued that when randomization is done, LD relations are abrogated affecting the empirical *P*-values computation in random tests, but this problem did not affect our multi-testing correction procedure since we use a working set of independent markers ($r^2 < 0.1$) (15).

Enrichment in OMIM Annotations in the "Result-List" of Genes Associated to SLE by Rare Variation

Taking into account that pleiotropic effects on human complex traits was widespread (23), it would be expected that in a list of genes significantly enriched in rare variation there would also be an enrichment of diseases caused by mutations. To test this, we used three data sets. First, we downloaded the OMIM database (http://www.omim.org/downloads/; updated: March 23, 2015), and employed it to build a 'gene-disease' table with its 20,707 records ("gene-disease" pairs); second, the list of all GWAS imputed protein-coding genes in our final dataset; and thirdly, the list of *N* genes resulting as candidates to be SLE-associated from our rare variants association analysis. Then if our "result-list" of *N* associated genes provided annotations for *X* OMIM diseases, the procedure for testing enrichment in OMIM annotations was to randomly select a set of *N* genes from the list of GWAS imputed protein-coding genes, and count how many of them appeared on the OMIM "gene-disease" table. This procedure was repeated 1,000 times. The average number of OMIM disease and its standard deviation was calculated and then a Z-score test was performed providing the statistical significance of this enrichment.

RESULTS

Imputation

A total of 13,956 genes passed the QC filter of the imputation process, summing a set of 5,305,811 markers, 2,595,206 variants

with MAF > 1% (48.93%), and 2,709,605 variants (mutations) with MAF < 1% (51.07%). A set of 1,549,436 independent markers was obtained by applying a threshold of $r^2 < 0.1$. As expected, rare variation was much less affected by the linkage disequilibrium than common variation, which resulted in 87,853 variants with MAF > 1% (5.56%) and 1,491,583 variants with MAF <1% (94.44%) (**Figure 1**).

A working set of 1,306,324 independent ($r^2 < 0.1$) rare variants (MAF < 0.1) was used to test genes for case-control association to the SLE phenotype (185,219 were non-polymorphic). The reliability of these tests depends on the accuracy of the imputation. When analyzing reliability of imputation in rare variants 3 intervals are usually differentiated: "singletons," "very rare" variation and "rare" variation (4, 24). It is known that as the variant MAF decreases, so does the accuracy of imputation, improving with the size of the reference panel, and singletons, meaning that the minor allele is observed only in one chromosome, are not reliably imputed under any conditions. In our data set, 189,893 (14.5%) variants were singletons (in the 8,277 individuals sample this means a MAF = 0.006%) and if an additional threshold of MAF < 0.1% to distinguish rare variant from a category of "very" rare variant was applied, then 676,621 (51.8%) variants were classified as very rare-variants, while 439,810 (33.7%) had MAF between 0.1 and 1%. These results suggested that imputed genotype data used in the association analysis could be unreliable because of the predominance of markers belonging to the categories of very rare variants and singletons over the most reliable imputation category of rare variation, 0.1 < MAF ≤ 1%. However, in tests based on the combined effect of variants, the main factor is not the number of markers aggregated but more importantly the count of alleles of minor frequency in the sample of analyzed individuals. Thus, in our 8,277 individuals dataset the 3 categories of rare variation sum up 29,128,106 minor alleles. Singletons represented 14.5% of rare variation but only 0.65% of minor alleles. The 51.8% of the markers included in the very rare variation category add up to 4,671,537 minor frequency alleles, that is, 16.04%; while the remaining markers, sum up to 24,266,676 of minor frequency alleles, which represented the 83.33%, resulting in a 5 times greater ratio of "0.1%<MAF ≤ 1%" variation compared to the sum of the other two categories (**Table 1**, **Figure 2**). Therefore, despite its lower proportion, the expected effect of rare variation on the aggregate test would be greater than that of the "very rare" variation and singletons providing a higher reliability to the analysis.

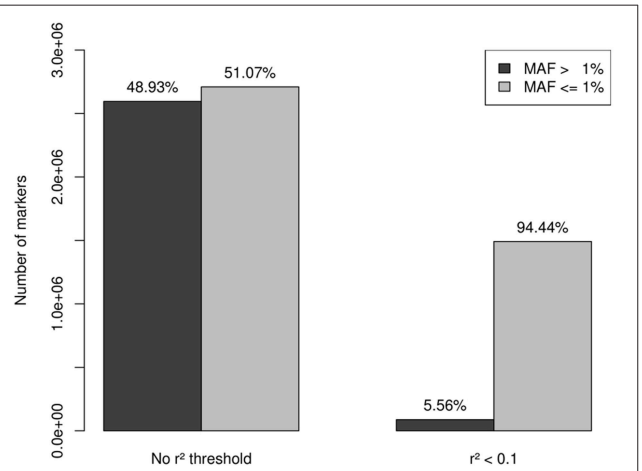

FIGURE 1 | After QC filtering, imputation provided a set of 5,305,811 markers: 2,595,206 with MAF > 1% (48.93%) and 2,709,605 with MAF < 1% (51.07%). A set of 1,549,436 independent markers was obtained by applying a threshold of $r^2 < 0.1$. Rare variation was less affected by the linkage disequilibrium than common variation, which resulted in 87,853 variants with MAF > 1% (5.56%) and 1,491,583 variants with MAF < 1% (94.44%). This last set of 1,491,583 independent rare-variants constituted our working set.

TABLE 1 | Number of independent rare variants vs. sum of minor alleles.

	Number of variants	Number of minor alleles
Singletons	189,893 (14.5%)	189,893 (0.64%)
MAF<0.01%	676,621 (51.8%)	4,671,537 (16.04%)
0.01% > MAF ≤ 1%	439,810 (33.7%)	24,266,676 (83.33%)
	1,306,324 (100%)	29,128,106 (100%)

Rare variation was classified into 3 categories by their minor allele frequencies (MAFs): (1) singletons that in the 8,277 individuals sample means a MAF = 0.006%, (2) "very rare-variants," 0.006% <MAF< 0.1%, (3) and rare variation in a "strict sense," 0.1% < MAF≤ 1%.

Note that the proportions of the different functional categories in the rare variation (MAF < 1% with and without r^2 filtering was similar (**Table 2**, **Figure 3**), being the intronic the most abundant category, 85% of the total, while the exonic rare variants represented only 2%, of which more than 98% were synonymous (**Figure 4**).

Rare-Variant Association Gene-Centered Analysis, and OMIM Annotation Enrichment

Under these conditions a set of 281 genes showed SKAT test with Genomic Control and multi-testing corrected $P < 0.05$ (**Supplemental Table 1**). Noted that 441 genes also presented Genomic Control and multi-testing corrected significant tests for enrichment in rare variation (**Supplemental Table 2**). When the OMIM annotation enrichment analysis were executed, the list of SKAT associated genes was significantly enriched with 119 OMIM diseases (**Supplemental Table 3**) instead of the 81 expected at random, which gave a value of $P = 3E\text{-}03$. Of these 281 genes, 139 were enriched in mutations in cases vs. controls and the remaining 142 were depleted. Note that the list of 139 genes enriched in mutations had 80 OMIM diseases annotations when expected was just 40, which gave a *P*-value of 6E-05. Remark that the 140 depleted genes showed no significant enrichment in OMIM diseases annotations (39 vs. 41 expected, $P = 0.59$).

As best candidates for SLE association by rare variation, we selected the set of 98 genes which simultaneously showed Genomic Control and multi-testing corrected $P < 0.05$ in both SKAT test and case-control burden test, with the purpose of reducing the proportion of possible spurious associations. These

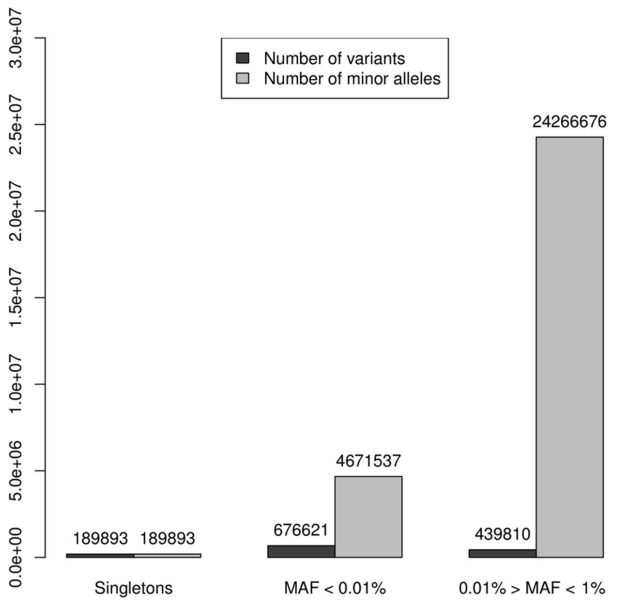

FIGURE 2 | Numbers of variants were represented by dark columns: in the set of 1,306,324 independent ($r^2 < 0.1$) polymorphic rare variants (MAF < 0.1), 189,893 (14.5%) were singletons (in the 8,277 individuals sample this means a MAF = 0.006%), 676,621 (51.8%) were classified as "very rare-variants" (0.006% <MAF < 0.1%), and 439,810 (33.7%) considered as a rare variation in a "strict sense" (0.1% < MAF ≤ 1%); these numbers of variants were represented by dark columns. Lighter columns represented the sums of alleles of minor frequency in each of the 3 categories of rare variation, these 3 categories sum up 29,128,106 minor alleles: the 189,893 singletons represented only 0.65% of minor alleles; the 676,621 the markers, which were very rare variation, add up to 4,671,537 minor frequency alleles, it was the 16.04%; while the remaining markers, sum up to 24,266,676 of minor frequency alleles representing the 83.33%.

TABLE 2 | Functional annotation of rare variation with and without r^2 filtering.

	No r^2 threshold	$r^2 < 0.1$
Intronic	2,305,643 (85.09%)	1,253,088 (84.011%)
Intergenic	175,180 (6.465%)	101,187 (6.784%)
UTR3	46,322 (1.71%)	27,637 (1.853%)
Exonic	46,133 (1.70%)	30,053 (2.015%)
Downstream	26,690 (0.985%)	16,688 (1.119%)
Upstream	23,791 (0.878%)	15,095 (1.012%)
UTR5	9,872 (0.364%)	6,215 (0.417%)
Splicing	231 (0.009%)	171 (0.012%)
ncRNA intronic	68,381 (2.524%)	36,967 (2.478%)
ncRNA exonic	6,066 (0.224%)	3,600 (0.241%)

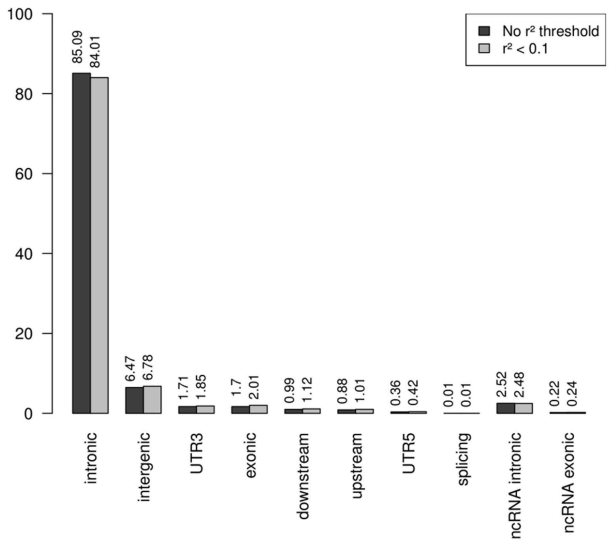

FIGURE 3 | Functional annotation of rare variation. Note that the percentages of the different functional categories in rare variation with and without r^2 filtering was similar, being the intronic the most abundant category, 85% of the total.

are shown in **Table 3**. Some of these are discussed as excellent candidates for the identification of individuals with particular clinical phenotypes that may be directly targeted for sequencing. ANNOVAR annotation of the independent mutations mapped on these 98 genes are shown in **Supplemental Table 5**.

DISCUSSION

We have described a strategy to identify the association of rare variation with a complex disease based on densely genotyped data and stringent imputation. Our study provides a first list of genes potentially involved in SLE through rare mutations that may have an impact on the clinical presentation of the disease.

Although it could seem difficult to justify the role of non-coding rare gene variation as causal, there are numerous examples that support it. Efforts to identify risk alleles usually are focused on exploring coding mutation by exome sequencing, noting Pullabhatla et al. (25), as a recent example in SLE, but analogous works for non-coding variants are scant. As examples supporting the causative role of rare non-coding gene variation in these complex phenotypes, it has been recently reported that non-noding mutation affected plasma lipid traits in a founder population (26), or in a more generalized perspective, it has been demonstrated that rare variants contribute to large gene expression changes across tissues and provide an integrative method for interpretation of rare variants effects (27).

It is important to point out that a significant test for aggregated case-control burden test would indicate that in the set of individuals forming the sample, the overall effect of the rare variation on the gene goes in the same direction being either of risk or protective. This feature of case-control burden analysis helps to interpret the effect of rare variation on the phenotype, which is measured by the overall OR values, OR > 1 or OR <1, risk or protection, respectively. Mutations associated with diseases were usually considered to be detrimental to health, increasing the risk of disease. However, there are a growing number of reported mutations shown to be protective, lowering the risk of certain diseases and conditions (28–31). In this context we can explain why the gene STAT4 associated to SLE by common variation (32–45) and our 20th SKAT best-hit, failed the burden test (**Supplemental Tables 1**, **4**). There were two sets of rare variation mapping on the gene with opposite join effects and therefore reducing the power of the overall burden

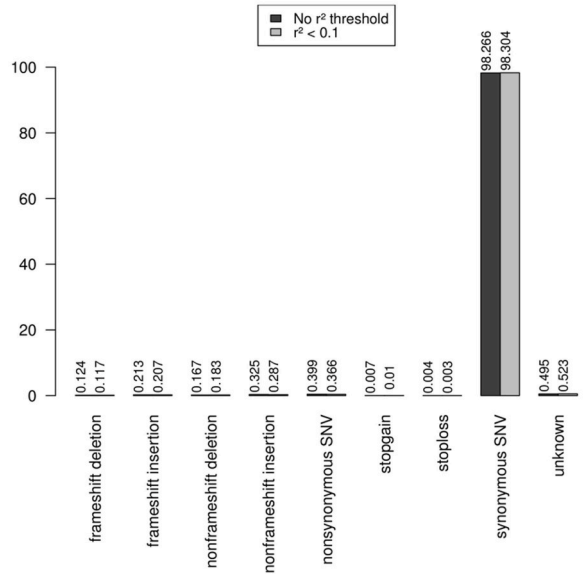

FIGURE 4 | Functional annotation of exonic rare variation. The exonic rare variants represented only 2%, and more than 98% of these exonic mutations were synonymous.

test. The same rationale could be applied to the other SLE associated genes by common variation also detected as targets by rare variation with SKAT but not by burden test in our study (**Supplemental Tables 1**, **4**): GTF2IRD1 (39, 42), DAB2 (41), NOTCH4 (37), CLEC16A (32, 42, 44), TNFSF4 (32, 40–46), and C2 (36). The same can be argued for DOCK8 ($OR_{burden.test}$ =2.33, $P_{SKAT.corr}$ = 0.03 and $P_{burden.test.corr}$ = 0.204) the cause of Hyper-IgE recurrent infection syndrome (HIES) autosomal recessive by homozygous or compound heterozygous mutation (OMIM #243700). Note that it has been reported a case of DOCK8 deficiency caused by a truncating mutation, associated with SLE (47).

Focusing on the best-hits which meet the criteria of simultaneous significant association in both rare variation tests, SKAT and burden test, we found some genes described as associated with SLE by common variation such as TMEM55B (46), SPATA8 (36), PRDM1 (32, 40, 42, 44, 48), and HLA-DRB1 (36, 40, 42, 43, 45) (**Table 3**). Note IRF7 also associated to SLE through common variants (32, 38, 44) had association values through rare variation close to statistical significance ($P_{SKAT.corr}$ = 0.082 and $P_{burden.test.corr}$ = 0.036) (**Supplemental Table 4**).

In this kind of studies it is usual to obtain lists of genes with a difficult functional justification. However, in this case we can relate many of the best hits in **Table 3** directly to immunological functions or with effects on other organs or tissues affected by SLE, such as skin, central nervous system or blood. For example our list contained C4A, $P_{SKAT.corr}$ = 0.014 and $P_{burden.test.corr}$ = 0.0034, $OR_{burden.test}$ = 0.43 and $CI_{95\%.burden.test}$ = (0.23, 0.79), which was early related to SLE through mutation [OMIM: 152700; (49)]. The zinc finger E-box binding homeobox 1 gene, ZEB1, $P_{SKAT.corr}$ < 1.00E-03 and $P_{burden.test.corr}$ < 1.00E-03, OR_{enrich} = 2.03 and CI $_{95\%.enrich}$ = (1.35, 3.05), acts as a transcriptional repressor inhibiting interleukin-2 (IL-2) gene expression. Note that IL-2 plays a critical role in immune tolerance, and insufficient IL-2 production upon stimulation has been recognized in SLE pathogenesis, particularly it has been described a new epigenetic pathway in the control of IL-2 production in SLE whereby low levels of miR-200a-3p accumulate the binding of the ZEB1-CtBP2 complex to the IL-2 promoter and suppresses IL-2 production (50). The role of CCR3 [$P_{SKAT.corr}$ = 0.00838 and $P_{burden.test.corr}$ < 1.00E-03, $OR_{burden.test}$ = 3.74 and CI $_{95\%.burden.test}$ = (1.74, 8.02)] in inflammation is widely known (OMIM *601268).

The protein encoded by CYP26B1, $P_{SKAT.corr}$ = 0.01 and $P_{burden.test.corr}$ < 1.00E-03, $OR_{burden.test}$ = 1.7 and CI $_{95\%.burden.test}$ = (1.31, 2.21), functions as a critical regulator of all-trans retinoic acid levels by the specific inactivation of all-trans retinoic acid to hydroxylated forms. Mast cells (MCs) are known to be regulators of inflammation. It has been reported that the ATP-P2X7 pathway induces MCs activation and consequently exacerbates inflammation. P2X7 expression on MCs was reduced by fibroblasts in the skin. Cyp26b1 was highly expressed in skin fibroblasts. Cyp26b1 inhibition resulted in upregulation of P2X7 on MCs and the presence of excessive amounts of retinoic acid correlated with the increased expression of P2X7 on skin MCs and consequent P2X7- and MC-dependent dermatitis (so-called retinoid dermatitis) (51).

The protein encoded by TIGD7 belongs to the "tigger subfamily of the pogo superfamily of DNA-mediated transposons" in humans, $P_{SKAT.corr}$ = 0.0139 and $P_{burden.test.corr}$ = 0.00179, $OR_{burden.test}$ = 3.04 and $CI_{95\%.burden.test}$ = (1.58, 5.86). The exact function of this gene is not known, but it is very similar to CENPB considered a major centromere auto-antigen recognized by sera from patients with anti-cetromere-antibodies (ACA), which occur in some autoimmune diseases, frequently in limited systemic scleroderma and occasionally in its diffuse form (52, 53).

AQP8, $P_{SKAT.corr}$ = 0.0115 and $P_{burden.test.corr}$ = 0.0063, $OR_{burden.test}$ = 2.5 and CI $_{95\%.burden.test}$ = (1.42, 4.41). It has been reported that efficient induction of B cell activation and differentiation requires H_2O_2 fluxes across the plasma membrane for signal amplification. NADPH-oxidase 2 is the main source of H_2O_2 and AQP8 is the transport facilitator across the plasma membrane. AQP8 silencing inducible B lymphoma cells responded poorly to TLR and BCR stimulation. Conversely a silencing-resistant AQP8 rescued responsiveness (54). In addition AQP8 was the major antibody target on human salivary glands in patients with primary Sjögren's syndrome (55).

It was known that SAMSN1 (=HACS1), $P_{SKAT.corr}$ = 0.012 and $P_{burden.test.corr}$ = 0.0091, $OR_{burden.test}$ = 1.74 and $CI_{95\%.burden.test}$ = (1.21, 2.5), is up-regulated by B cell activation signals and it participates in B cell activation and differentiation (56).

MICB, $P_{SKAT.corr}$ = 0.0297 and $P_{burden.test.corr}$ = 0.0062, $OR_{burden.test}$ = 0.62 and CI $_{95\%.burden.test}$ = (0.45, 0.84), acts as a stress-induced self-antigen that is recognized by gamma delta

TABLE 3 | Best gene candidates for SLE association through rare variation in European ancestry population.

Gene	Description	NMUT	nMAF.aff	nMAF.ctr	OR	$CI_{.95lo}$	CI_{95up}	$P_{burden.test.corr}$	$PSKAT_{corr}$
ZEB1	Zinc finger E-box binding homeobox 1	74	1077	886	2.03	1.35	3.05	<1.00E-03	<1.00E-03
PRKAG3	Protein kinase, AMP-activated, gamma 3 non-catalytic subunit	4	53	95	0.55	0.39	0.78	<1.00E-03	<1.00E-03
COQ10B	Coenzyme Q10 homolog B (S. cerevisiae)	3	11	38	0.25	0.13	0.5	<1.00E-03	<1.00E-03
MAD2L2	MAD2 mitotic arrest deficient-like 2 (yeast)	19	417	517	0.59	0.45	0.77	<1.00E-03	3.60E-03
TMEM69	Transmembrane protein 69	5	18	42	0.32	0.19	0.54	<1.00E-03	4.40E-03
KRTAP9-2	Keratin associated protein 9-2	3	4	14	0.16	0.05	0.5	<1.00E-03	6.20E-03
SERINC4	Serine incorporator 4	4	27	4	5.98	2.23	16.03	<1.00E-03	6.40E-03
CCR3	Chemokine (C-C motif) receptor 3	33	750	431	3.74	1.74	8.02	<1.00E-03	8.40E-03
CYP26B1	Cytochrome P450, family 26, subfamily B, polypeptide 1	20	170	93	1.7	1.31	2.21	<1.00E-03	1.01E-02
TMEM106B	Transmembrane protein 106B	24	103	244	0.56	0.38	0.82	<1.00E-03	1.77E-02
POU3F3	POU class 3 homeobox 3	2	66	33	3.47	1.46	8.22	<1.00E-03	2.41E-02
TIGD7	Tigger transposable element derived 7	14	109	55	3.04	1.58	5.86	1.80E-03	1.39E-02
KLF1	Kruppel-like factor 1 (erythroid)	3	90	48	3.01	1.46	6.2	1.80E-03	2.29E-02
PSMB8	Proteasome (prosome, macropain) subunit, beta type, 8 (large multifunctional peptidase 7)	30	439	490	0.64	0.48	0.84	1.80E-03	2.46E-02
MAPK15	Mitogen-activated protein kinase 15	6	55	78	0.57	0.4	0.82	1.80E-03	2.67E-02
AMACR	Alpha-methylacyl-CoA racemase	20	347	261	1.64	1.17	2.29	1.80E-03	2.77E-02
UBE3A	Ubiquitin protein ligase E3A	73	1164	1340	0.53	0.35	0.82	1.80E-03	3.93E-02
TRIM16L	Tripartite motif containing 16-like	13	179	227	0.52	0.34	0.78	3.40E-03	<1.00E-03
CTSK	Cathepsin K	3	23	41	0.26	0.1	0.68	3.40E-03	6.20E-03
HYPK	Huntingtin interacting protein K	3	33	6	13.76	2.45	77.3	3.40E-03	8.30E-03
C4A	Complement component 4A (Rodgers blood group)	2	17	33	0.43	0.23	0.79	3.40E-03	1.40E-02
WNT10A	Wingless-type MMTV integration site family, member 10A	16	153	215	0.52	0.34	0.81	3.40E-03	1.57E-02
OR5B12	Olfactory receptor, family 5, subfamily B, member 12	3	98	141	0.44	0.26	0.75	3.40E-03	1.78E-02
TAGLN3	Transgelin 3	27	225	275	0.58	0.4	0.84	3.40E-03	2.62E-02
PALM	Paralemmin	65	653	740	0.52	0.34	0.79	3.40E-03	2.84E-02
SPACA1	Sperm acrosome associated 1	25	405	279	2.02	1.3	3.12	4.80E-03	6.10E-03
POPDC2	Popeye domain containing 2	36	444	309	2.47	1.39	4.4	4.80E-03	6.30E-03
ALG11	Asparagine-linked glycosylation 11, alpha-1,2-mannosyltransferase homolog (yeast)	10	60	91	0.59	0.42	0.83	4.80E-03	7.90E-03
SF3B4	Splicing factor 3b, subunit 4, 49kDa	3	58	88	0.39	0.2	0.78	4.80E-03	1.78E-02
DUSP7	Dual specificity phosphatase 7	4	32	12	8.12	2.03	32.54	4.80E-03	3.11E-02
MRGPRX4	MAS-related GPR, member X4	9	74	108	0.62	0.46	0.85	6.30E-03	7.50E-03
AQP8	Aquaporin 8	9	141	83	2.5	1.42	4.41	6.30E-03	1.15E-02
PI3	Peptidase inhibitor 3, skin-derived	2	20	4	3.85	1.29	11.5	6.30E-03	1.58E-02
FRS3	Fibroblast growth factor receptor substrate 3	28	384	447	0.66	0.49	0.87	6.30E-03	2.78E-02
MICB	MHC class I polypeptide-related sequence B	47	1110	1166	0.62	0.45	0.84	6.30E-03	2.97E-02
GPBP1L1	GC-rich promoter binding protein 1-like 1	10	172	193	0.57	0.38	0.86	7.70E-03	<1.00E-03
DOLK	Dolichol kinase	1	15	3	5.66	1.59	20.2	7.70E-03	9.90E-03
CSTA	Cystatin A (stefin A)	23	266	200	2.26	1.28	3.97	7.70E-03	1.59E-02
KLHL31	Kelch-like 31 (Drosophila)	39	465	518	0.51	0.32	0.81	7.70E-03	1.61E-02
GPR26	G protein-coupled receptor 26	58	934	734	332	1.25	2.94	7.70E-03	1.65E-02
PRDM1	PR domain containing 1, with ZNF domain	26	278	332	0.62	0.44	0.86	7.70E-03	2.45E-02
COX17	COX17 cytochrome c oxidase assembly homolog (S. cerevisiae)	32	398	280	2.13	1.31	3.46	7.70E-03	3.26E-02

(Continued)

TABLE 3 | Continued

Gene	Description	NMUT	nMAF.aff	nMAF.ctr	OR	$CI._{95lo}$	CI_{95up}	$P_{burden.test.corr}$	$PSKAT_{corr}$
SAMSN1	SAM domain, SH3 domain and nuclear localization signals 1	129	1977	1622	1.74	1.21	2.5	9.10E-03	1.20E-02
ST8SIA2	ST8 alpha-N-acetyl-neuraminide alpha-2,8-sialyltransferase 2	153	1583	1653	0.51	0.32	0.81	9.10E-03	1.75E-02
MAS1L	MAS1 oncogene-like	12	141	171	0.52	0.32	0.83	9.10E-03	3.38E-02
TBCB	Tubulin folding cofactor B	21	236	174	1.66	1.14	2.42	1.05E-02	<1.00E-03
FGR	Gardner-Rasheed feline sarcoma viral (v-fgr) oncogene homolog	6	154	93	1.97	1.17	3.3	1.05E-02	2.67E-02
WNK4	WNK lysine deficient protein kinase 4	5	161	116	2.06	1.25	3.41	1.05E-02	4.41E-02
MGAT5	Mannosyl (alpha-1,6-)-glycoprotein beta-1,6-N-acetyl-glucosaminyltransferase	426	3961	3984	0.51	0.33	0.79	1.18E-02	2.64E-02
FEZF1	FEZ family zinc finger 1	3	49	74	0.37	0.18	0.79	1.18E-02	4.02E-02
ZNF461	Zinc finger protein 461	6	55	80	0.37	0.18	0.77	1.32E-02	2.34E-02
RAB25	RAB25, member RAS oncogene family	8	82	110	0.45	0.25	0.81	1.32E-02	3.94E-02
APLNR	Apelin receptor	5	65	44	2.67	1.21	5.87	1.45E-02	1.07E-02
DUS1L	Dihydrouridine synthase 1-like (S. cerevisiae)	15	58	89	0.38	0.19	0.75	1.45E-02	2.60E-02
ASAH2	N-acylsphingosine amidohydrolase (non-lysosomal ceramidase) 2	16	256	177	2.34	1.3	4.24	1.45E-02	2.76E-02
MRPS18B	Mitochondrial ribosomal protein S18B	23	554	584	0.61	0.42	0.88	1.58E-02	1.76E-02
IL18RAP	Interleukin 18 receptor accessory protein	22	278	213	1.62	1.12	2.34	1.58E-02	2.77E-02
BNIP2	BCL2/adenovirus E1B 19kDa interacting protein 2	21	196	246	0.59	0.4	0.87	1.58E-02	2.93E-02
HAX1	HCLS1 associated protein X-1	2	47	17	2.04	1.16	3.61	1.58E-02	3.08E-02
ITFG3	Integrin alpha FG-GAP repeat containing 3	72	993	1076	0.5	0.3	0.8	1.58E-02	3.63E-02
ZNF99	Zinc finger protein 99	8	18	32	0.24	0.08	0.74	1.71E-02	1.51E-02
ZIK1	zinc finger protein interacting with K protein 1 homolog (mouse)	15	173	116	1.9	1.18	3.06	1.71E-02	2.43E-02
PDZK1	PDZ domain containing 1	12	324	376	0.67	0.48	0.92	1.84E-02	2.43E-02
KRCC1	Lysine-rich coiled-coil 1	28	272	203	1.64	1.12	2.41	1.84E-02	4.45E-02
MAP1LC3C	Microtubule-associated protein 1 light chain 3 gamma	10	161	206	0.58	0.38	0.89	1.97E-02	2.24E-02
LRP4	Low density lipoprotein receptor-related protein 4	1	12	2	5.28	1.16	23.99	1.97E-02	2.59E-02
OR52K2	Olfactory receptor, family 52, subfamily K, member 2	14	158	196	0.57	0.36	0.88	1.97E-02	4.29E-02
GML	Glycosylphosphatidylinositol anchored molecule like protein	66	427	496	0.45	0.25	0.8	2.10E-02	1.30E-02
ARL4A	ADP-ribosylation factor-like 4A	19	163	97	1.96	1.17	3.28	2.10E-02	3.85E-02
ANKRD39	Ankyrin repeat domain 39	3	36	55	0.58	0.38	0.9	2.22E-02	1.95E-02
HLA-DRB1	Major histocompatibility complex, class II, DR beta 1	6	52	71	0.4	0.19	0.83	2.22E-02	2.51E-02
PNO1	Partner of NOB1 homolog (S. cerevisiae)	8	79	44	2.49	1.17	5.31	2.22E-02	3.94E-02
LCE2D	Late cornified envelope 2D	3	45	49	0.38	0.17	0.86	2.22E-02	4.75E-02
ANAPC11	Anaphase promoting complex subunit 11	1	18	33	0.52	0.29	0.94	2.35E-02	4.86E-02
OR7A17	Olfactory receptor, family 7, subfamily A, member 17	7	109	73	2.15	1.16	4.01	2.47E-02	3.93E-02
PTGDS	Prostaglandin D2 synthase 21kDa (brain)	17	166	124	1.76	1.09	2.86	2.60E-02	1.01E-02
CCR1	Chemokine (C-C motif) receptor 1	8	149	89	1.81	1.09	3	2.72E-02	7.30E-03
CCDC12	Coiled-coil domain containing 12	29	380	272	1.98	1.13	3.47	2.97E-02	1.95E-02
REEP4	Receptor accessory protein 4	10	115	83	2.03	1.13	3.65	3.09E-02	3.22E-02
ZNF513	Zinc finger protein 513	3	18	29	0.51	0.28	0.94	3.09E-02	3.56E-02
SPATA8	Spermatogenesis associated 8	19	145	100	1.87	1.1	3.16	3.22E-02	3.60E-03

(Continued)

TABLE 3 | Continued

Gene	Description	NMUT	nMAF.aff	nMAF.ctr	OR	$CI._{95lo}$	CI_{95up}	$P_{burden.test.corr}$	$PSKAT_{corr}$
TAF15	TAF15 RNA polymerase II, TATA box binding protein (TBP)-associated factor, 68kDa	49	439	346	1.89	1.12	3.19	3.22E-02	3.13E-02
POLR2I	Polymerase (RNA) II (DNA directed) polypeptide I, 14.5kDa	11	142	96	1.7	1.07	2.71	3.22E-02	3.84E-02
KCTD5	Potassium channel tetramerisation domain containing 5	24	217	250	0.54	0.33	0.89	3.34E-02	1.59E-02
NKX2-5	NK2 homeobox 5	11	109	74	2.06	1.11	3.79	3.46E-02	3.23E-02
SCARA3	Scavenger receptor class A, member 3	69	593	469	1.68	1.09	2.59	3.46E-02	4.51E-02
EFNA4	Ephrin-A4	7	37	51	0.39	0.16	0.93	3.70E-02	2.52E-02
NRM	Nurim (nuclear envelope membrane protein)	11	229	233	0.65	0.44	0.95	3.82E-02	2.26E-02
TMEM55B	Transmembrane protein 55B	8	72	45	1.57	1.06	2.31	3.94E-02	9.30E-03
MPL	Myeloproliferative leukemia virus oncogene	15	83	44	2.48	1.16	5.31	4.06E-02	1.93E-02
PTGS2	Prostaglandin-endoperoxide synthase 2 (prostaglandin G/H synthase and cyclooxygenase)	6	79	109	0.29	0.1	0.86	4.18E-02	3.61E-02
NT5DC1	5'-nucleotidase domain containing 1	87	736	558	2.43	1.09	5.41	4.18E-02	4.54E-02
MAFG	v-maf musculoaponeurotic fibrosarcoma oncogene homolog G (avian)	7	68	90	0.69	0.5	0.97	4.54E-02	1.11E-02
C5orf28	Chromosome 5 open reading frame 28	10	72	90	0.52	0.28	0.99	4.54E-02	3.22E-02
C8orf58	Chromosome 8 open reading frame 58	19	347	413	0.6	0.38	0.95	4.66E-02	3.85E-02
SNX5	Sorting nexin 5	63	490	374	1.99	1.08	3.64	4.77E-02	2.51E-02
PTER	Phosphotriesterase related	98	846	716	2.11	1.06	4.2	4.89E-02	5.50E-03
ZNF708	Zinc finger protein 708	8	68	88	0.54	0.31	0.96	4.89E-02	1.69E-02

We selected the set of 98 genes which simultaneously showed Genomic Control and multi-testing corrected P-values < 0.05 in both SKAT test and Case-Control burden test (Case-Control burden test helps to interpret the effect that the rare variation on each associated gene had on the phenotype, which is measured by the overall OR value and its 95% confidence interval).

NMUT, number of mutations on tested gene; nMAF.aff, sum of minor frequency alleles in nMUT mutations in cases (4,212 cases); nMAF.ctr, sum of minor frequency alleles in nMUT mutations in controls (4,065 controls); OR, case-control burden test Odds Ratio; $CI._{95lo}$, case-control burden test 95% Confidence Interval minor value; $CI._{95up}$: case-control burden test 95% Confidence Interval major value; $P_{burden.test.corr}$, case-control burden test corrected P-value; and $P_{SKAT.corr}$, SKAT corrected P-value.

T cells. MICB might play a role in both SLE and cutaneous LE (CLE) in european population (57). In addition MICB has been associated with susceptibility to SLE in Han Chinese Population (58, 59).

CTSK, $P_{SKAT.corr} = 0.0062$ and $P_{burden.test.corr} = 0.0034$, $OR_{burden.test} = 0.28$ and $CI_{95\%.burden.test} = (0.1, 0.68)$, is highly expressed by rheumatoid synovial fibroblasts (RSF) that are activated by toll-like receptor signaling pathways in rheumatoid arthritis and is known to play a key role in the degradation of type Iand type II collagen. Thus, cathepsin K is implicated in the degradation of bone and cartilage in RA (60). In addition it has been suggested that CTSK is involved in development of psoriasis-like skin lesions through TLR-dependent Th17 activation (61).

Autoinflammation, lipodystrophy, and dermatosis syndrome (ALDD) can be caused by homozygous mutations in the PSMB8 gene (OMIM: # 256040), $P_{SKAT.corr} = 0.0246$ and $P_{burden.test.corr} = 0.00179$, $OR_{burden.test} = 0.64$ and $CI_{95\%.burden.test} = (0.48, 0.84)$. This autosomal recessive systemic autoinflammatory disorder is characterized by early childhood onset of annular erythematous plaques on the face and extremities with subsequent development of partial lipodystrophy and laboratory evidence of immune dysregulation. More variable features include recurrent fever, severe joint contractures, muscle weakness and atrophy, hepatosplenomegaly, basal ganglia calcifications, and microcytic anemia (62–64). This disorder encompasses Nakajo-Nishimura syndrome (NKJO); joint In contractures, muscular atrophy, microcytic anemia, and panniculitis-induced lipodystrophy (JMP syndrome); and chronic atypical neutrophilic dermatosis with lipodystrophy and elevated temperature syndrome (CANDLE). Furthermore, mutations in PSMB8 and other proteasome unit genes were shown to lead to an increased type I interferon signature (65), a characteristic of SLE.

The roles of TRIM16L, $P_{SKAT.corr} = 0.0033$ and $P_{burden.test.corr} < 1.00E\text{-}03$, $OR_{burden.test} = 0.52$ and $CI_{95\%.burden.test} = (0.34, 0.78)$, in immune response are unknown, however it has been reported that in fish models TRIM16L exerted negative regulation of the interferon immune response against DNA virus infection (66). The early events that facilitate viral persistence in chronic viral infections have been linked to the activity of the immunoregulatory cytokine IL-10. It has been reported that IL-10 induced the expression of MGAT5, a glycosyltransferase that enhances N-glycan branching on surface glyco- proteins, $P_{SKAT.corr} = 0.0264$ and $P_{burden.test.corr} = 0.0118$, $OR_{burden.test} = 0.51$ and $CI_{95\%.burden.test} = (0.33, 0.79)$. Increased N-glycan branching on CD8+ T cells promoted the formation of a galectin 3-mediated membrane lattice, which restricted

the interaction of key glycoproteins, ultimately increasing the antigenic threshold required for T cell activation allowing the establishment of chronic infection (67).

The serine incorporator 4, SERINC4, P SKAT.corr = 0.0064 and $P_{burden.test.corr}$ < 1.00E-03, $OR_{burden.test}$ = 5.98 and $CI_{95\%.burden.test}$ = (2.23, 16.03), incorporates amino acid serine into membranes and facilitates the synthesis of two serine-derived lipids, phosphatidylserine and sphingolipids (68).

Gene KLF1, $P_{SKAT.corr}$ = 0.00179 and $P_{burden.test.corr}$ = 0.0229, $OR_{burden.test}$ = 3.01 and $CI_{95\%.burden.test}$ = (1.46, 6.20), encodes a hematopoietic-specific transcription factor that induces high-level expression of adult beta-globin and other erythroid genes. Heterozygous loss-of-function mutations in this gene result in the dominant In(Lu) blood phenotype (69). Compound heterozygosity for KLF1 mutations is associated with microcytic hypochromic anemia and increased fetal hemoglobin (70). Mutations in KLF1 cause dyserythropoietic anemia congenital type IV (OMIM: 613673).

TMEM106B [$P_{SKAT.corr}$ < 1.00E-03 and $P_{burden.test.corr}$ = 0.0177, $OR_{burden.test}$ = 0.56 and $CI_{95\%.burden.test}$ = (0.38, 0.82)] was associated with frontotemporal dementia (71, 72). In addition TMEM106B has been associated with inflammation, neuronal loss, and cognitive deficits, even in the absence of known brain disease, and their impact is highly selective for the frontal cerebral cortex of older individuals (73).

Mutations affecting the gene ALG11 [$P_{SKAT.corr}$ = 0.0079 and $P_{burden.test.corr}$ = 0.0048, $OR_{burden.test}$ = 0.56 and $CI_{95\%.burden.test}$ = (0.42, 0.83)] cause congenital disorder of glycosylation 1P (CDG1P) [OMIM: 613661], a multisystem disorder caused by a defect in glycoprotein biosynthesis and characterized by under-glycosylated serum glycoproteins. Congenital disorders of glycosylation result in a wide variety of clinical features, such as defects in the nervous system development, psychomotor retardation, dysmorphic features, hypotonia, coagulation disorders, and immunodeficiency (74, 75).

MAD2L2, $P_{SKAT.corr}$ < 0.001 and $P_{burden.test.corr}$ = 0.0036, $OR_{burden.test}$ = 0.59 and $CI_{95\%.burden.test}$ = (0.45, 0.77), controls DNA repair at telomeres and DNA breaks by inhibiting 5' end resection (76). Note that a role for MAPK15 (=ERK8), $P_{SKAT.corr}$ = 0.0018 and $P_{enrich.corr}$ = 0.0267, OR_{enrich} = 0.57 and $CI_{95\%.enrich}$ = (0.40,0.77), in the response to, or repair of, DNA single strand breaks has been proposed (77), and it is annotated as "positive regulation of telomerase activity," biological process (GO:0051973). MRGPRX4 (= MrgX4) [$P_{SKAT.corr}$ = 0.0063 and $P_{burden.test.corr}$ = 0.00748, $OR_{burden.test}$ = 0.62 and $CI_{95\%.burden.test}$ = (0.46, 0.85)] is a Mas-related G-protein coupled receptor X (MrgXs). It was described as an oncogene in human colorectal cancers (78), however, it has recently been linked to immunological functions. AG-30/5C is an angiogenic host defense peptide (HDP) that activates various functions of fibroblasts and endothelial cells, including cytokine/chemokine production and wound healing. It has been shown that AG-30/5C enhanced the production of cytokines/chemokines and facilitated keratinocyte migration and proliferation mainly via MrgX3 and MrgX4 receptors constitutively expressed in keratinocytes and up-regulated upon stimulation with TLR ligands. AG-30/5C-induced activation of keratinocytes was controlled by MAPK and NF-κB pathways (79).

In addition other genes associated to human energy metabolism and more specifically in the mitochondrion, as part of the respiratory chain, the best hit associated to SLE by rare variation was COQ10B, $P_{SKAT.corr}$ <0.001 and $P_{burden.test.corr}$ <0.001, $OR_{burden.test}$ = 0.25 and $CI_{95\%.burden.test}$ = (0.13, 0.50). It encodes coenzyme Q, an essential component of the electron transport chain. The copper metallochaperone COX17, $P_{SKAT.corr}$ = 0.0077 and $P_{burden.test.corr}$ = 0.0326, $OR_{burden.test}$ = 2.13 and $CI_{95\%.burden.test}$ = (1.31, 3.46), is essential for the assembly and activation of the cytochrome c oxidase complex (80), the terminal component of the mitochondrial respiratory chain that catalyzes the electron transfer from reduced cytochrome c to oxygen. Null mutations in COX17 elicit a loss of cytochrome oxidase due to the failure of the mutants to complete assembly of the complex [OMIM: *604813]. It has been reported that SLE T-cells have persistently hyperpolarized mitochondria associated with increased mitochondrial mass, high levels of reactive oxygen species (ROS) and low levels of ATP. These hyperpolarized mitochondria resist the depolarization required for activation-induced apoptosis and predispose T cells for necrosis, thus stimulating inflammation in SLE (81, 82). Necrotic cell lysates activate dendriticcells and might account for increased interferon a production and inflammation in lupus patients (83). Additionally, the mitochondrial ATP deficits also reduce the macrophage energy that is needed to clear apoptotic bodies (84). The mitochondrial transmembrane potential is result of the respiratory electron transport chain that drives the flow of electrons from NADH to molecular oxygen by its last enzyme the cytochrome c oxidadase. Note that it has been reported that COX17 is essential for activation of cytochrome C oxidase (80) linking the COX17 function with the SLE phenotype.

CONCLUSIONS

Here we present a set of 98 genes as good candidates for association with SLE by mutation affecting a diversity of functions in different organs and tissues. Considering that complex phenotypes involves the intervention of multiple genes associated by common variation, the same scheme could be expected for genes associated by rare variation. Thus, each gene or set of genes would influence in a small group of affected carriers explaining the clinical heterogeneity or complexity of this pathology. However, it is necessary to remark that these results are preliminary and would need to be confirmed by sequencing in the best candidate carriers in our sample data set.

AUTHOR CONTRIBUTIONS

MM-B contributed to the conception and design of the study, organized the database, performed the statistical analysis, wrote

the first draft of the manuscript, and participated in the manuscript revision. MA-R provided the raw genotype data sets, contributed to the conception and design of the study, interpretation of results, manuscript revision and wrote the final draft of the manuscript.

SUPPLEMENTARY MATERIAL

The Supplementary Material for this article can be found online at: https://www.frontiersin.org/articles/10.3389/fimmu.2019.00258/full#supplementary-material

REFERENCES

1. MacArthur J, Bowler E, Cerezo M, Gil L, Hall P, Hastings E, et al. The new NHGRI-EBI Catalog of published genome-wide association studies (GWAS Catalog). *Nucleic Acids Res.* (2017) 45:D896–901. doi: 10.1093/nar/gkw1133
2. Dickson SP, Wang K, Krantz I, Hakonarson H, Goldstein DB. Rare variants create synthetic genome-wide associations. *PLoS Biol.* (2010) 8:e1000294. doi: 10.1371/journal.pbio.1000294
3. Frazer KA, Murray SS, Schork NJ, Topol EJ. Human genetic variation and its contribution to complex traits. *Nat Rev Genet.* (2009) 10:241–51. doi: 10.1038/nrg2554
4. Saint Pierre A, Génin E. How important are rare variants in common disease? *Brief Funct Genomics* (2014) 13:353–61. doi: 10.1093/bfgp/elu025
5. Sazonovs A, Barrett JC. (2018). Rare-variant studies to complement genome-wide association studies. *Annu Rev Genomics Hum Genet*. (2018) 19:97–112. doi: 10.1146/annurev-genom-083117-021641
6. Manolio TA, Collins FS, Cox NJ, Goldstein DB, Hindorff LA, Hunter DJ, et al. Finding the missing heritability of complex diseases. *Nature* (2009) 461:747–53. doi: 10.1038/nature08494
7. Mägi R, Asimit JL, Day-Williams AG, Zeggini E, Morris AP. Genome-wide association analysis of imputed rare variants: application to seven common complex diseases. *Genet Epidemiol*. (2012) 36:785–96. doi: 10.1002/gepi.21675
8. Asimit JL, Zeggini E. Imputation of rare variants in next-generation association studies. *Hum Hered*. (2012) 74:196–204. doi: 10.1159/000345602
9. Zheng HF, Rong JJ, Liu M, Han F, Zhang XW, Richards JB, et al. Performance of genotype imputation for low frequency and rare variants from the 1000 genomes. *PLoS ONE* (2015) 10:e0116487. doi: 10.1371/journal.pone.0116487
10. Huang J, Howie B, McCarthy S, Memari Y, Walter K, Min JL, et al. Improved imputation of low-frequency and rare variants using the UK10K haplotype reference panel. *Nat Commun*. (2015) 6:8111. doi: 10.1038/ncomms9111
11. Mitt M, Kals M, Pärn K, Gabriel SB, Lander ES, Palotie A, et al. Improved imputation accuracy of rare and low-frequency variants using population-specific high-coverage WGS-based imputation reference panel. *Eur J Hum Genet.* (2017) 25:869–76. doi: 10.1038/ejhg.2017.51
12. Iglesias AI, van der Lee SJ, Bonnemaijer PWM, Höhn R, Nag A, Gharahkhani P, et al. Haplotype reference consortium panel: practical implications of imputations with large reference panels. *Hum Mutat*. (2017) 38:1025–32. doi: 10.1002/humu.23247
13. McCarthy S, Das S, Kretzschmar W, Delaneau O, Wood AR, Teumer A, et al. Haplotype reference consortium. A reference panel of 64,976 haplotypes for genotype imputation. *Nat Genet*. (2016) 48:1279–83. doi: 10.1038/ng.3643
14. Günther C, Kind B, Reijns MA, Berndt N, Martinez-Bueno M, Wolf C, et al. Defective removal of ribonucleotides from DNA promotes systemic autoimmunity. *J Clin Invest*. (2015) 125:413–24. doi: 10.1172/JCI78001
15. Delgado-Vega AM, Martínez-Bueno M, Oparina NY, López Herráez D, Kristjansdottir H, Steinsson K, et al. Whole exome sequencing of patients from multicase families with systemic lupus Erythematosus identifies multiple rare variants. *Sci Rep*. (2018) 8:8775. doi: 10.1038/s41598-018-26274-y
16. Purcell S, Neale B, Todd-Brown K, Thomas L, Ferreira MAR, Bender D, et al. PLINK: a toolset for whole-genome association and population-based linkage analysis. *Am J Human Genet.* (2007) 81:559–75. doi: 10.1086/519795
17. Thornton T, Tang H, Hoffman TJ, Ochs-Balcom HM, Baan BJ, Risch N. Estimating kinship in admixed populations. *Am J Human Genet*. (2012) 91:122–38. doi: 10.1016/j.ajhg.2012.05.024
18. Price AL, Patterson NJ, Plenge RM, Weinblatt ME, Shadick NA, Reich D. Principal components analysis corrects for stratification in genome-wide association studies. *Nat Genet.* (2006) 38:904–9. doi: 10.1038/ng1847
19. Howie BN, Donnelly P, Marchini J. A flexible and accurate genotype imputation method for the next generation of genome-wide association studies. *PLoS Genet.* (2009) 5:e1000529. doi: 10.1371/journal.pgen.1000529
20. Timbers TA, Garland SJ, Mohan S, Flibotte S, Edgley M, Muncaster Q, et al. Accelerating gene discovery by phenotyping whole-genome sequenced multi-mutation strains and using the Sequence Kernel Association Test (SKAT). *PLoS Genet*. (2016) 12:e1006235. doi: 10.1371/journal.pgen.1006235
21. Ward LD, Kellis M. HaploReg: a resource for exploring chromatin states, conservation, and regulatory motif alterations within sets of genetically linked variants. *Nucleic Acids Res*. (2012) 40:D930–4. doi: 10.1093/nar/gkr917
22. Wang K, Li M, Hakonarson H. ANNOVAR: functional annotation of genetic variants from next-generation sequencing data. *Nucleic Acids Res.* (2010) 38:e164. doi: 10.1093/nar/gkq603
23. Solovieff N, Cotsapas C, Lee PH, Purcell SM, Smoller JW. Pleiotropy in complex traits: challenges and strategies. *Nat Rev Genet.* (2013) 14:483–95. doi: 10.1038/nrg3461
24. Bodmer W, Bonilla C. Common and rare variants in multifactorial susceptibility to common diseases. *Nat Genet.* (2008) 40:695–701. doi: 10.1038/ng.f.136
25. Pullabhatla V, Roberts AL, Lewis MJ, Mauro D, Morris DL, Odhams CA, et al. *De novo* mutations implicate novel genes in systemic lupus erythematosus. *Hum Mol Genet*. (2018) 27:421–9. doi: 10.1093/hmg/ddx407
26. Igartua C, Mozaffari SV, Nicolae DL, Ober C. Rare non-coding variants are associated with plasma lipid traits in a founder population. *Sci Rep.* (2017) 7:16415. doi: 10.1038/s41598-017-16550-8
27. Li X, Kim Y, Tsang EK, Davis JR, Damani FN, Chiang C, et al. The impact of rare variation on gene expression across tissues. *Nature* (2017) 550:239–43. doi: 10.1038/nature24267
28. Butler JM, Hall N, Narendran N, Yang YC, Paraoan L. Identification of candidate protective variants for common diseases and evaluation of their protective potential. *BMC Genomics* (2017) 18:575. doi: 10.1186/s12864–017-3964–3
29. Steinthorsdottir V, Thorleifsson G, Sulem P, Helgason H, Grarup N, Sigurdsson A, et al. Identification of low-frequency and rare sequence variants associated with elevated or reduced risk of type 2 diabetes. *Nat Genet.* (2014) 46:294–8. doi: 10.1038/ng.2882
30. Cohen J, Pertsemlidis A, Kotowski IK, Graham R, Garcia CK, Hobbs HH. Low LDL cholesterol in individuals of African descent resulting from frequent nonsense mutations in PCSK9. *Nat Genet.* (2005) 37:161–5. doi: 10.1038/ng1509
31. Costford SR, Kavaslar N, Ahituv N, Chaudhry SN, Schackwitz WS, Dent R, et al. Gain-of-function R225W mutation in human AMPKgamma(3) causing increased glycogen and decreased triglyceride in skeletal muscle. *PLoS ONE* (2007) 2:e903. doi: 10.1371/journal.pone.0000903
32. Bentham J, Morris DL, Graham DSC, Pinder CL, Tombleson P, Behrens TW, et al. Genetic association analyses implicate aberrant regulation of innate and adaptive immunity genes in the pathogenesis of systemic lupus erythematosus. *Nat Genet.* (2015) 47:1457–64. doi: 10.1038/ng.3434
33. Lee YH, Bae SC, Choi SJ, Ji JD, Song GG. Genome-wide pathway analysis of genome-wide association studies on systemic lupus erythematosus and rheumatoid arthritis. *Mol Biol Rep.* (2012) 39:10627–35. doi: 10.1007/s11033-012-1952-x
34. Graham RR, Cotsapas C, Davies L, Hackett R, Lessard CJ, Leon JM, et al. Genetic variants near TNFAIP3 on 6q23 are associated with systemic lupus erythematosus. *Nat Genet*. (2008) 40:1059–61. doi: 10.1038/ng.200
35. Demirci FY, Wang X, Kelly JA, Morris DL, Barmada MM, Feingold E, et al. Identification of a new susceptibility locus for systemic lupus erythematosus on chromosome 12 in individuals of European ancestry. *Arthritis Rheumatol*. (2016) 68:174–83. doi: 10.1002/art.39403

36. Armstrong DL, Zidovetzki R, Alarcón-Riquelme ME, Tsao BP, Criswell LA, Kimberly RP, et al. GWAS identifies novel SLE susceptibility genes and explains the association of the HLA region. *Genes Immun*. (2014) 15:347–54. doi: 10.1038/gene.2014.23
37. Hom G, Graham RR, Modrek B, Taylor KE, Ortmann W, Garnier S, et al. Association of systemic lupus erythematosus with C8orf13-BLK and ITGAM-ITGAX. *N Engl J Med*. (2008) 358:900–9. doi: 10.1056/NEJMoa0707865.
38. Martin JE, Assassi S, Diaz-Gallo LM, Broen JC, Simeon CP, Castellvi I, et al. A systemic sclerosis and systemic lupus erythematosus pan-meta-GWAS reveals new shared susceptibility loci. *Hum Mol Genet*. (2013) 22:4021–9. doi: 10.1093/hmg/ddt248
39. Chung SA, Taylor KE, Graham RR, Nititham J, Lee AT, Ortmann WA, et al. Differential genetic associations for systemic lupus erythematosus based on anti-dsDNA autoantibody production. *PLoS Genet*. (2011) 7:e1001323. doi: 10.1371/journal.pgen.1001323
40. Han JW, Zheng HF, Cui Y, Sun LD, Ye DQ, Hu Z, et al. Genome-wide association study in a Chinese Han population identifies nine new susceptibility loci for systemic lupus erythematosus. *Nat Genet*. (2009) 41:1234–7. doi: 10.1038/ng.472
41. Lessard CJ, Sajuthi S, Zhao J, Kim K, Ice JA, Li H, et al. Identification of a systemic lupus erythematosus risk locus spanning ATG16L2, FCHSD2, and P2RY2 in Koreans. *Arthritis Rheumatol*. (2016) 68:1197–209. doi: 10.1002/art.39548
42. Yang W, Tang H, Zhang Y, Tang X, Zhang J, Sun L, et al. Meta-analysis followed by replication identifies loci in or near CDKN1B, TET3, CD80, DRAM1, and ARID5B as associated with systemic lupus erythematosus in Asians. *Am J Hum Genet*. (2013) 92:41–51. doi: 10.1016/j.ajhg.2012.11.018
43. Gateva V, Sandling JK, Hom G, Taylor KE, Chung SA, Sun X, et al. A large-scale replication study identifies TNIP1, PRDM1, JAZF1, UHRF1BP1 and IL10 as risk loci for systemic lupus erythematosus. *Nat Genet*. (2009) 41:1228–33. doi: 10.1038/ng.468
44. Morris DL, Sheng Y, Zhang Y, Wang YF, Zhu Z, Tombleson P, et al. Genome-wide association meta-analysis in Chinese and European individuals identifies ten new loci associated with systemic lupus erythematosus. *Nat Genet*. (2016) 48:940–6. doi: 10.1038/ng.3603
45. Alarcón-Riquelme ME, Ziegler JT, Molineros J, Howard TD, Moreno-Estrada A, Sánchez-Rodríguez E, et al. Genome-wide association study in an amerindian ancestry population reveals novel systemic lupus erythematosus risk loci and the role of european admixture. *Arthritis Rheumatol*. (2016) 68:932–43. doi: 10.1002/art.39504
46. International Consortium for Systemic Lupus Erythematosus Genetics (SLEGEN), Harley JB, Alarcón-Riquelme ME, Criswell LA, Jacob CO, Kimberly RP, et al. Genome-wide association scan in women with systemic lupus erythematosus identifies susceptibility variants in ITGAM, PXK, KIAA1542 and other loci. *Nat Genet*. (2008) 40:204–10. doi: 10.1038/ng.81
47. Jouhadi Z, Khadir K, Ailal F, Bouayad K, Nadifi S, Engelhardt KR, et al. Ten-year follow-up of a DOCK8-deficient child with features of systemic lupus erythematosus. *Pediatrics* (2014) 134:e1458–63. doi: 10.1542/peds.2013-1383
48. Márquez A, Vidal-Bralo L, Rodríguez-Rodríguez L, González-Gay MA, Balsa A, González-Álvaro I, et al. A combined large-scale meta-analysis identifies COG6 as a novel shared risk locus for rheumatoid arthritis and systemic lupus erythematosus. *Ann Rheum Dis*. (2017) 76:286–94. doi: 10.1136/annrheumdis-2016-209436
49. Rupert KL, Moulds JM, Yang Y, Arnett FC, Warren RW, Reveille JD, et al. The molecular basis of complete complement C4A and C4B deficiencies in a systemic lupus erythematosus patient with homozygous C4A and C4B mutant genes. *J Immunol*. (2002) 169:1570–8. doi: 10.4049/jimmunol.169.3.1570
50. Katsuyama E, Yan M, Watanabe KS, Matsushima S, Yamamura Y, Hiramatsu S, et al. Downregulation of miR-200a-3p, targeting CtBP2 complex, is involved in the hypoproduction of IL-2 in systemic lupus erythematosus-derived T cells. *J Immunol*. (2017) 198:4268–76. doi: 10.4049/jimmunol.1601705
51. Kurashima Y, Amiya T, Fujisawa K, Shibata N, Suzuki Y, Kogure Y, et al. The enzyme Cyp26b1 mediates inhibition of mast cell activation by fibroblasts to maintain skin-barrier homeostasis. *Immunity* (2014) 40:530–41. doi: 10.1016/j.immuni.2014.01.014
52. Hudson M, Mahler M, Pope J, You D, Tatibouet S, Steele R, et al. Clinical correlates of CENP-A and CENP-B antibodies in a large cohort of patients with systemic sclerosis. *J Rheumatol*. (2012) 39:787–94. doi: 10.3899/rheum.111133
53. Mahler M, Mierau R, Genth E, Blüthner M. Development of a CENP-A/CENP-B-specific immune response in a patient with systemic sclerosis. *Arthritis Rheum*. (2002) 46:1866–72. doi: 10.1002/art.10330
54. Bertolotti M, Farinelli G, Galli M, Aiuti A, Sitia R. AQP8 transports NOX2-generated H2O2 across the plasma membrane to promote signaling in B cells. *J Leukoc Biol*. (2016) 100:1071–9. doi: 10.1189/jlb.2AB0116-045R
55. Tzartos JS, Stergiou C, Daoussis D, Zisimopoulou P, Andonopoulos AP, Zolota V, et al. Antibodies to aquaporins are frequent in patients with primary Sjögren's syndrome. *Rheumatology* (2017) 56:2114–22. doi: 10.1093/rheumatology/kex328
56. Zhu YX, Benn S, Li ZH, Wei E, Masih-Khan E, Trieu Y, et al. The SH3-SAM adaptor HACS1 is up-regulated in B cell activation signaling cascades. *J Exp Med*. (2004) 200:737–47. doi: 10.1084/jem.20031816
57. Kunz M, König IR, Schillert A, Kruppa J, Ziegler A, Grallert H, et al. Genome-wide association study identifies new susceptibility loci for cutaneous lupus erythematosus. *Exp Dermatol*. (2015) 24:510–5. doi: 10.1111/exd.12708
58. Zhang Y-M, Zhou X-J, Cheng FJ, Qi Y-Y, Hou P, Zhao M-H, et al. Polymorphism rs(3828903) within MICB is associated with susceptibility to systemic lupus erythematosus in a northern han chinese population. *J Immunol Res*. (2016) 2016:1343760. doi: 10.1155/2016/1343760
59. Yu P, Zhu Q, Chen C, Fu X, Li Y, Liu L, et al. Association between major histocompatibility complex class i chain-related gene polymorphisms and susceptibility of systemic lupus erythematosus. *Am J Med Sci*. (2017) 354:430–5. doi: 10.1016/j.amjms.2017.06.003
60. Hirabara S, Kojima T, Takahashi N, Hanabayashi M, Ishiguro N. Hyaluronan inhibits TLR-4 dependent cathepsin K and matrix metalloproteinase 1 expression in human fibroblasts. *Biochem Biophys Res Commun*. (2013) 430:519–22. doi: 10.1016/j.bbrc.2012.12.003
61. Hirai T, Kanda T, Sato K, Takaishi M, Nakajima K, Yamamoto M, et al. Cathepsin K is involved in development of psoriasis-like skin lesions through TLR-dependent Th17 activation. *J Immunol*. (2013) 190:4805–11. doi: 10.4049/jimmunol.1200901
62. Agarwal AK, Xing C, DeMartino GN, Mizrachi D, Hernandez MD, Sousa AB, et al. PSMB8 encoding the β5i proteasome subunit is mutated in joint contractures, muscle atrophy, microcytic anemia, and panniculitis-induced lipodystrophy syndrome. *Am J Hum Genet*. (2010) 87:866–72. doi: 10.1016/j.ajhg.2010.10.031
63. Kitamura A, Maekawa Y, Uehara H, Izumi K, Kawachi I, Nishizawa M, et al. A mutation in the immunoproteasome subunit PSMB8 causes autoinflammation and lipodystrophy in humans. *J Clin Invest*. (2011) 121:4150–60. doi: 10.1172/JCI58414
64. Arima K, Kinoshita A, Mishima H, Kanazawa N, Kaneko T, Mizushima T, et al. Proteasome assembly defect due to a proteasome subunit beta type 8 (PSMB8) mutation causes the autoinflammatory disorder, Nakajo-Nishimura syndrome. *Proc Natl Acad Sci USA*. (2011) 108:14914–9. doi: 10.1073/pnas.1106015108
65. Kariuki SN, Ghodke-Puranik Y, Dorschner JM, Chrabot BS, Kelly JA, Tsao BP, et al. Genetic analysis of the pathogenic molecular sub-phenotype interferon-alpha identifies multiple novel loci involved in systemic lupus erythematosus. *Genes Immun*. (2015) 16:15–23. doi: 10.1038/gene.2014.57
66. Yu Y, Huang X, Zhang J, Liu J, Hu Y, Yang Y, et al. Fish TRIM16L exerts negative regulation on antiviral immune response against grouper iridoviruses. *Fish Shellfish Immunol*. (2016) 59:256–67. doi: 10.1016/j.fsi.2016.10.044
67. Smith LK, Boukhaled GM, Condotta SA, Mazouz S, Guthmiller JJ, Vijay R, et al. Interleukin-10 directly inhibits CD8+ T cell function by enhancing N-glycan branching to decrease antigen Sensitivity. *Immunity* (2018) 48:299–312.e5. doi: 10.1142/10755
68. Inuzuka M, Hayakawa M, Ingi T. Serinc, an activity-regulated protein family, incorporates serine into membrane lipid synthesis. *J Biol Chem*. (2005) 280:35776–83. doi: 10.1074/jbc.M505712200
69. Kawai M, Obara K, Onodera T, Enomoto T, Ogasawara K, Tsuneyama H, et al. Mutations of the KLF1 gene detected in Japanese with the In(Lu) phenotype. *Transfusion* (2017) 57:1072–7. doi: 10.1111/trf.13990

70. Huang J, Zhang X, Liu D, Wei X, Shang X, Xiong F, et al. Compound heterozygosity for KLF1 mutations is associated with microcytic hypochromic anemia and increased fetal hemoglobin. *Eur J Hum Genet.* (2015) 23:1341–8. doi: 10.1038/ejhg.2014.291
71. Premi E, Grassi M, van Swieten J, Galimberti D, Graff C, Masellis M, et al. Cognitive reserve and TMEM106B genotype modulate brain damage in presymptomatic frontotemporal dementia: a GENFI study. *Brain* (2017) 140:1784–91. doi: 10.1093/brain/awx103
72. Gallagher MD, Posavi M, Huang P, Unger TL, Berlyand Y, Gruenewald AL, et al. A dementia-associated risk variant near TMEM106B alters chromatin architecture and gene expression. *Am J Hum Genet*. (2017) 101:643–63. doi: 10.1016/j.ajhg.2017.09.004
73. Rhinn H, Abeliovich A. Differential aging analysis in human cerebral cortex identifies variants in TMEM106B and GRN that regulate aging phenotypes. *Cell Syst*. (2017) 4:404–15.e5. doi: 10.1016/j.cels.2017.02.009
74. Thiel C, Rind N, Popovici D, Hoffmann GF, Hanson K, Conway RL, et al. Improved diagnostics lead to identification of three new patients with congenital disorder of glycosylation-Ip. *Hum Mutat*. (2012) 33:485–7. doi: 10.1002/humu.22019
75. Rind N, Schmeiser V, Thiel C, Absmanner B, Lübbehusen J, Hocks J, et al. A severe human metabolic disease caused by deficiency of the endoplasmatic mannosyltransferase hALG11 leads to congenital disorder of glycosylation-Ip. *Hum Mol Genet*. (2010) 19:1413–24. doi: 10.1093/hmg/ddq016
76. Boersma V, Moatti N, Segura-Bayona S, Peuscher MH, van der Torre J, Wevers BA, et al. MAD2L2 controls DNA repair at telomeres and DNA breaks by inhibiting 5' end resection. *Nature* (2015) 521:537–40. doi: 10.1038/nature14216
77. Klevernic IV, Martin NM, Cohen P. Regulation of the activity and expression of ERK8 by DNA damage. *FEBS Lett.* (2009) 583:680–4. doi: 10.1016/j.febslet.2009.01.011
78. Gylfe AE, Kondelin J, Turunen M, Ristolainen H, Katainen R, Pitkänen E, et al. Identification of candidate oncogenes in human colorectal cancers with microsatellite instability. *Gastroenterology* (2013) 145:540–3.e22. doi: 10.1053/j.gastro.2013.05.015
79. Kiatsurayanon C, Niyonsaba F, Chieosilapatham P, Okumura K, Ikeda S, Ogawa H. Angiogenic peptide (AG)-30/5C activates human keratinocytes to produce cytokines/chemokines and to migrate and proliferate via MrgX receptors. *J Dermatol Sci*. (2016) 83:190–9. doi: 10.1016/j.jdermsci.2016.05.006
80. Takahashi Y, Kako K, Kashiwabara S, Takehara A, Inada Y, Arai H, et al. Mammalian copper chaperone Cox17p has an essential role in activation of cytochrome C oxidase and embryonic development. *Mol Cell Biol.* (2002) 22:7614–21. doi: 10.1128/MCB.22.21.7614-7621.2002
81. McGrath H Jr. Ultraviolet-A1 irradiation therapy for systemic lupus erythematosus. *Lupus* (2017) 26:1239–51. doi: 10.1177/0961203317707064
82. Gergely P Jr, Grossman C, Niland B, Puskas F, Neupane H, Allam F, et al. Mitochondrial hyperpolarization and ATP depletion in patients with systemic lupus erythematosus. *Arthritis Rheum*. (2002) 46:175–90. doi: 10.1002/1529-0131(200201)46:1<175::AID-ART10015>3.0.CO;2-H
83. Fernandez D, Perl A. Metabolic control of T cell activation and death in SLE. *Autoimmun Rev*. (2009) 8:184–9. doi: 10.1016/j.autrev.2008.07.041
84. Perl A, Gergely P Jr, Nagy G, Koncz A, Banki K. Mitochondrial hyperpolarization: a checkpoint of T-cell life, death and autoimmunity. *Trends Immunol.* (2004) 25:360–7. doi: 10.1016/j.it.2004.05.001

Conflict of Interest Statement: The authors declare that the research was conducted in the absence of any commercial or financial relationships that could be construed as a potential conflict of interest.

frontiers in Immunology

ORIGINAL RESEARCH
published: 02 April 2019
doi: 10.3389/fimmu.2019.00578

Lysosomal pH Is Regulated in a Sex Dependent Manner in Immune Cells Expressing *CXorf21*

Valerie M. Harris[1,2,3,4], *Isaac T. W. Harley*[5,6], *Biji T. Kurien*[1,3,4], *Kristi A. Koelsch*[1,3,4] *and Robert Hal Scofield*[1,2,3,4,7]*

[1] *Arthritis and Clinical Immunology Program, Oklahoma Medical Research Foundation, Oklahoma City, OK, United States,* [2] *Department of Pathology, College of Medicine, University of Oklahoma Health Sciences Center, Oklahoma City, OK, United States,* [3] *Department of Medicine, College of Medicine, University of Oklahoma Health Sciences Center, Oklahoma City, OK, United States,* [4] *Research Service, Oklahoma City Department of Veterans Affairs Health Care Center, Oklahoma City, OK, United States,* [5] *Division of Rheumatology, University of Colorado School of Medicine, Aurora, CO, United States,* [6] *Department of Immunology & Microbiology, University of Colorado School of Medicine, Aurora, CO, United States,* [7] *Medical Service, Oklahoma City Department of Veterans Affairs Health Care Center, Oklahoma City, OK, United States*

OPEN ACCESS

Edited by:
José Carlos Crispín, Instituto Nacional de Ciencias Médicas y Nutrición Salvador Zubirán (INCMNSZ), Mexico

Reviewed by:
Vasileios Kyttaris, Beth Israel Deaconess Medical Center and Harvard Medical School, United States
Abbe N. de Vallejo, University of Pittsburgh, United States

****Correspondence:***
Robert Hal Scofield
hal-scofield@omrf.ouhsc.edu

Specialty section:
This article was submitted to Autoimmune and Autoinflammatory Disorders, a section of the journal Frontiers in Immunology

Received: *07 November 2018*
Accepted: *04 March 2019*
Published: *02 April 2019*

Citation:
Harris VM, Harley ITW, Kurien BT, Koelsch KA and Scofield RH (2019) Lysosomal pH Is Regulated in a Sex Dependent Manner in Immune Cells Expressing CXorf21. Front. Immunol. 10:578. doi: 10.3389/fimmu.2019.00578

Background: *CXorf21* and *SLC15a4* both contain risk alleles for systemic lupus erythematosus (SLE) and Sjögren's syndrome (pSS). The former escapes X inactivation. Our group predicts specific endolysosomal-dependent immune responses are driven by the protein products of these genes, which form a complex at the endolysosomal surface. Our previous studies have shown that knocking out *CXorf21* increases lysosomal pH in female monocytes, and the present study assesses whether the lysosomal pH in 46,XX women, who overexpress CXorf21 in monocytes, B cells, and dendritic cells (DCs), differs from 46,XY men.

Methods: To determine endolysosome compartment pH we used both LysoSensor™ Yellow/Blue DND-160 and pHrodo® Red AM Intracellular pH Indicator in primary monocyte, B cells, DCs, NK cells, and T cells from healthy men and women volunteers.

Results: Compared to male samples, female monocytes, B cells, and DCs had lower endolysosomal pH (female/male pH value: monocytes 4.9/5.6 $p < 0.0001$; DCs 4.9/5.7 $p = 0.044$; B cells 5.0/5.6 $p < 0.05$). Interestingly, T cells and NK cells, which both express low levels of CXorf21, showed no differential pH levels between men and women.

Conclusion: We have previously shown that subjects with two or more X-chromosomes have increased CXorf21 expression in specific primary immune cells. Moreover, knockdown of CXorf21 increases lysosomal pH in female monocytes. The present data show that female monocytes, DC, B cells, where CXorf21 is robustly expressed, have lower lysosomal pH compared to the same immune cell populations from males. The lower pH levels observed in specific female immune cells provide a function to these SLE/SS-associated genes and a mechanism for the reported inflated endolysosomal-dependent immune response observed in women compared to men (i.e., TLR7/type I Interferon activity).

Keywords: systemic lupus erythematosus, Sjögren's syndrome, lysosome, pH, X chromosome, sex bias

INTRODUCTION

Systemic lupus erythematosus (SLE) and Sjögren's syndrome (SS) are chronic autoimmune diseases that are highly related in both clinical and serological manifestations. In terms of the latter, autoantibodies binding the Ro/La (or SSA/SSB) ribonucleoprotein particle are found in about half of patients with SLE and up to 80% of those with SS (1). Like most autoimmune diseases, both SLE and SS much more commonly affect women than men with ratios of about 10 to 1 for SLE, and up to 15 to 1 women to men in SS (2). While either disease can have its onset throughout the entire lifespan, the peak age of onset for SLE is about 30, while that for SS is in older adulthood.

The diseases are also related in regards to pathophysiology. For instance, most risk genes identified in genome wide association studies are shared between SLE and SS (3–6). Pertinent to the work presented herein, another aspect of shared pathophysiology involves interferon. There is increased expression of interferon-regulated genes in peripheral blood mononuclear cells from patients with either disease (7–10). Evidence from both human disease (11–13) and murine models (14–17) suggests that signaling through lysosomal, nucleic acid-binding toll-like receptors (TLR) 7 and 9 is in part responsible for the pathogenicity, including increased interferon activity in these diseases.

Signaling through stimulation of intracellular TLRs is exquisitely sensitive to lysosomal pH. The soluble carrier protein 15a4 (*SLC15a4*) and *CXorf21* genes have been identified as containing risk alleles for both SLE and SS (3, 6, 18). The protein products of these genes are binding partners on the lysosomal membrane (19). The SLC15a4 protein participates in movement of hydrogen ion and oligopeptides in and out of the lysosome. Thus, SLC15a4 regulates antigen processing in the lysosome along with TLR7/9–mediated cytokine secretion, NF-κB signaling and antibody production (20, 21). The regulatory role of SLC15a4 is at least in part mediated by control of lysosomal pH (21). A loss of function *Slc15a4* mutation ameliorates murine lupus and impairs interferon production mediated through TLR7 stimulation (20). An allele within *CXorf21* was recently identified as a lupus risk gene (18). Our data demonstrate the CXorf21 protein is expressed in only monocytes, B lymphocytes and dendritic cells. In addition, CXorf21 routinely escapes X inactivation (22) with both mRNA and protein levels higher in female cells compared to male cells (Harris et al., unpublished). CXorf21 knockdown using small guide RNA resulted in an abrogation of interferon production after exposure of female cells to TLR7 agonist. In addition, we found an increased lysosomal pH in female cells with CXorf21 knockdown (Harris et al., unpublished).

While there have been many theories concerning the increased risk for autoimmune disease in women, based on studies of X chromosome aneuploidies in subjects with SLE or SS, we propose that the female risk of SLE and SS is a result of a dose effect for the X chromosome. Our previous data show that Klinefelter men (47,XXY) are enriched 30-fold among men with either SLE or SS (23, 24). Also, SLE or SS affected women have an increased prevalence of 47,XXX compared to healthy control women or women with either rheumatoid arthritis or primary biliary cirrhosis (25). Because *CXorf21* escapes X inactivation; and, therefore, female cells have approximately twice the amount of CXorf21 protein, this gene is a candidate to mediate the X chromosome dose effect found for both SLE and SS, but not other studied, female-biased autoimmune diseases where no X dose effect was found.

We undertook the present study to further characterize the cellular function of CXorf21. In particular, the complex of SLC15a4 and CXorf21 affects lysosomal pH, and CXorf21 expression is greater in female cells compared to male cells. Thus, we sought to determine whether there is a difference in lysosomal pH between male and female immune cells, in which *CXorf21* is known to be expressed.

METHODS

Patients/Donors

Whole blood was donated by volunteer healthy controls. Healthy female and male controls were recruited pair-wise to control for day-to-day variability. EBV-transformed B cells or lymphoblastoid cell lines (LCLs) derived from healthy controls or SLE patients with and without chromosomal aneuploidies were obtained from the Lupus Family Registry and Repository (26). Eight male and 8 female buffy coats were obtained from the Oklahoma Blood Institute (OBI) (Oklahoma City, OK). All donors were Caucasian with ages ranging between 28 and 45 years old. Healthy subjects had no known chronic medical illness and tested negative for OBI blood safety screening panel. Buffy coats were stored at room temperature until cell isolation. All subjects gave written informed consent in accordance with the Declaration of Helsinki. The protocol was approved by the University of Oklahoma Health Sciences Center Institutional Review Board.

Isolation of Cells

STEMCELL EasySep™ monocyte, dendritic cells, B cell, natural killer cells (NK cells), and T cells were used to isolate monocytes, dendritic cells, B cells, NK cells, and T cells, respectively, from PBMCs of healthy controls. Briefly, PBMCs were first purified from buffy coats using density gradient centrifugation using Lymphoprep (STEMCELL Technologies, Cambridge, MA) according to the manufacturer's protocol. Cells were resuspended in EasySep™ buffer, the EasySep™ Magnet was used to sequentially isolate $CD14^+$ (using the EasySep™ Human CD14 enrichment kit), $CD19^+$ (using the EasySep Human CD19 positive selection kit II), CD3-CD56+ (EasySep™ Human NK Cell Isolation Kit) and CD3+ (EasySep™ Human T Cell Isolation Kit). Cell population purity was confirmed by Moxi-Flow cytometry with the protocol as described (27).

Western Blot Analysis

SDS-PAGE was carried out according to Laemmli et al., except for using pre-cast 4–20% gradient gels (Bio-Rad). Gel proteins were transferred to nitrocellulose membranes using Trans-Blot Turbo transfer system and Trans-Blot Turbo transfer pack

(Bio-Rad). Proteins were probed with anti-CXorf21 and anti-actin antibodies (Novus Biotechnologies) and detected with alkaline phosphatase/nitro blue tetrazolium/5-bromo-5-chloro-3-indolyl phosphate system. Protein bands were quantified using densitometry (ImageJ).

Lysosomal pH Determination

To detect differences in intracellular pH in live human male and female primary monocytes, dendritic cells, B cells, NK cells, and T cells, the LysoSensor™ Yellow/Blue DND-160 (Thermofisher) and pHrodo® Red AM Intracellular pH Indicator (Thermofisher) was used according to the manufacturer's suggested protocol. Briefly, primary cells were treated with LysoSensor reagents as ratiometric means for measuring lysosomal pH via fluorescence. The ratio of fluorescence allows for the adjustment for possible variability between particle uptake. To quantitate pH, primary cells plated on a 96-well plate were loaded with 5 μM pHrodo® Red AM intracellular pH indicators for 30 min. Cells were then washed with a series of Live Cell Imaging Media™ and standard buffers containing 10 μM nigericin and 10 μM valinomycin were added for 5 min in order to clamp intracellular pH values 4.5, 5.5, 6.5, and 7.5. We determined the mean cellular fluorescence in triplicate samples using a spectrophotometer (Synergy H1, Biotek). A standard curve for male or female samples showed a linear relationship between the intracellular pH and the relative fluorescence units.

Statistics

Statistical analyses were carried out using *T*-test, one-way ANOVA with multiple comparisons, or Fisher's Exact test using GraphPad Prism 7.

RESULTS

Primary Female Human Monocytes Have a More Acidic Lysosomal pH Compared to Male Cells

CXorf21 mRNA and protein are expressed at higher levels in primary monocytes, CD19+ B cells, and Lymphoblastoid cell lines (LCLs) from female healthy subjects compared to male controls (**Figure 1**: Harris et al., unpublished). Based on the function of the CXorf21 protein and its interaction with SLC15A4, which is known to regulate lysosomal pH, we hypothesized that, with greater expression of the CXorf21 protein, lysosomal pH would be lower in female male monocytes. In order to assess a difference in lysosomal pH between male and female monocytes, we performed *ex vivo* lysosomal pH measurements. Following a 30-min incubation period of the cells with pH calibration buffers, a standard curve for both male and female (**Figure 2A**) primary monocytes to determine pH based on male and female (**Figure 2B**) relative fluorescence was generated. We found that unstimulated female monocytes have a significantly more acidic lysosomal pH (4.9) compared to male monocytes (5.6) (**Figure 2C**) ($p = 0.0001$ by Fisher's exact test).

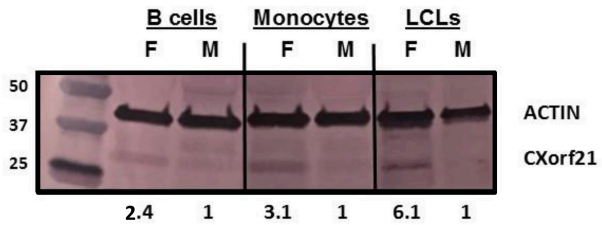

FIGURE 1 | CXorf21 is differentially expressed in primary immune cells of healthy controls and SLE-affected patients. Total protein extract was harvested from healthy male and female primary B cells (lane 1 and 2), primary monocytes (lanes 3 and 4), and lymphoblastoid cell lines (LCLs) (lane 5 and 6) and subjected to SDS-PAGE. Western blotting using human anti-CXorf21 antibody (34 kD) identifying bands at the appropriate molecular weight. Human anti-actin (42 kD) is shown as a loading control. Densitometry via Image J was used to quantitative optical density of protein bands.

Other Cell Types in Which CXorf21 Is Expressed Higher in Female Cells

This trend for lower pH in the lysosomes of female cells held true for both dendritic cells, where female DCs lysosomal pH was 4.9 and male DCs were 5.7 (*p-value* 0.044; **Figure 3**), as well as B lymphocytes, where female lysosomal pH was 5.0 and male lysosomal pH was 5.6 ($p = 0.0447$ by Fisher's exact test; **Figure 4**). These data suggest that female monocytes, DCs, and B cells, immune cells with increased CXorf21 and TLR7 expression, have a more favorable lysosomal processing environment compared to male cells, and may drive the robust TLRs/lysosomal-dependent immune response observed women compared to men (28).

Lysosomal pH in Cells That do Not Express CXorf21

In order to assess the role of female overexpression of *CXorf21* in lysosomal pH, we studied immune cells in which the expression of *CXorf21* is absent. To that end, we isolated primary T cell and NK cells, two immune cells with minimal CXorf21 and TLR7 levels. We found, while their lysosomal pH was optimal for lysosomal signaling, there was no significant difference in pH between the sexes (**Figures 4D,E**).

DISCUSSION

There are ∼80 autoimmune disease, the great majority of which affect women more than men. Both SLE and SS have a ratio of about 10 affected women for every one affected man (2). The sex bias in SLE is present among patients with childhood onset (29). In SLE and SS, more women are affected than men in older adulthood at ages where women are post-menopausal (30). Despite much investigation, a compelling explanation for this sex bias has not been forthcoming. Skewing of X chromosome inactivation, acquired X chromosome monosomy, sex hormone levels have all been studied and found to not explain the sex bias (30–34). SS is much less well studied than SLE; however, again no explanation of the marked predilection for women has been made.

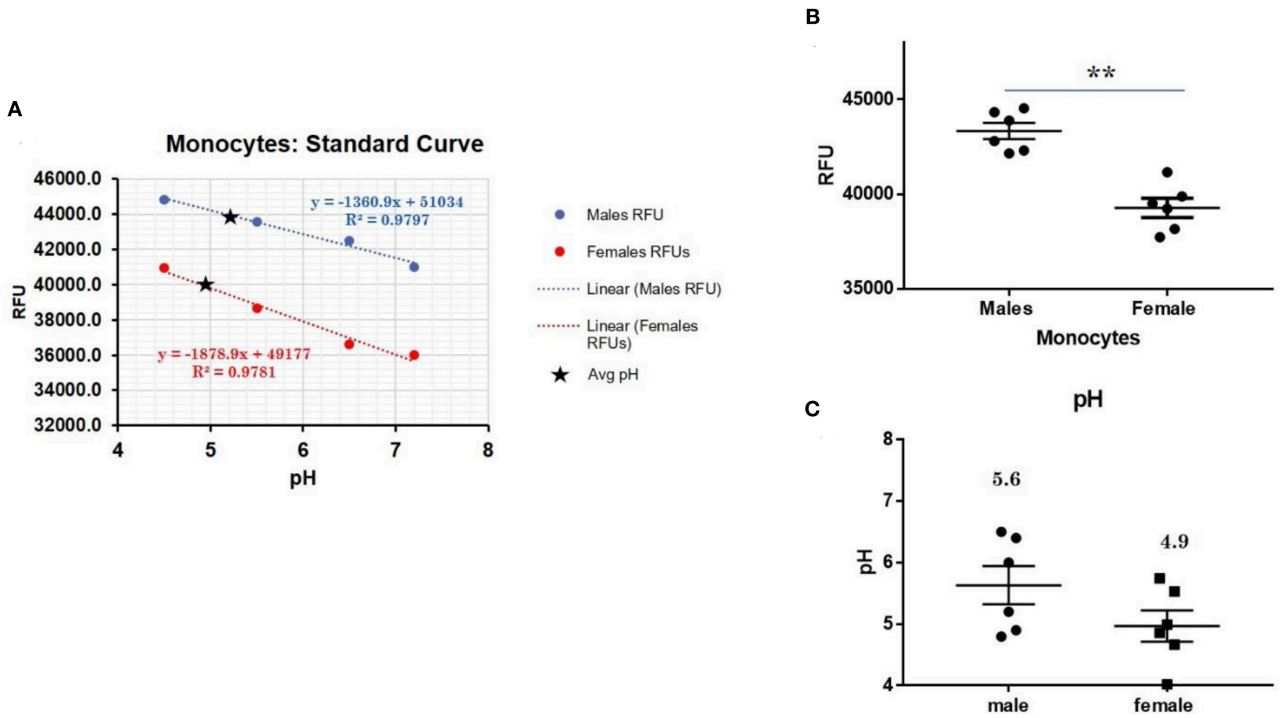

FIGURE 2 | Differences in lysosomal pH in female and male monocytes. **(A)** Male ($n = 6$) and female monocytes ($n = 6$) standard curve using pHrodo™ Red AM with Intracellular pH Calibration Buffer Kit for the translation of fluorescence ratios into pH. An average of six data points was plotted in the graph and a linear trend line was fitted to get a pH standard curve. **(B)** Male monocytes female monocytes were stained with pHrodo™ Red AM solution and relative fluorescence units (RFUs) were measured with multi-well plate reader (Details in Materials and Methods). **(C)** pH determined using pHrodo indication kit according to manufactures protocol. Student's *t*-test was used to determine statistical difference in RFUs that was converted into pH values via each standard curve. $^{**}p = 0.0001$; Error bar represent SEM.

Based on data concerning X chromosome aneuploidies, we have proposed that the increased female risk of SLE and SS is the result of the X chromosome complement. Men with Klinefelter's syndrome (47,XXY) are enriched 15-fold in these diseases (23, 24). In addition, 47,XXX women are also found in excess among those with either SLE or SS, but not rheumatoid arthritis or primary biliary cirrhosis (25). Very rare abnormalities of the X chromosome among patients with SLE or SS, including partial triplications, as well as rare patients with Turner's syndrome and SLE may localize the effect to the X chromosome distal p arm (35, 36).

Of course, in cells with two or more X chromosomes all but one X is inactivated in order to equalize gene dose compared to male cells. However, X inactivation is not an all or none phenomenon with a significant fraction (up to 20%) of X-linked human genes escaping X inactivation (22, 37). Thus, a key factor in the idea that an X chromosome gene dose effect mediates the sex bias of SLE and SS is the escape of X inactivation such that female cells have bi-allelic mRNA expression and potentially more functional protein of a given X-linked gene.

Two genes that escape X inactivation in immune cells, contain SLE-risk alleles, and have critical roles in production of interferon are *CXorf21* and *TLR7* (38). Thus, on this basis, these genes are candidates to mediate the X chromosome gene dose effect for the sex bias of SLE and SS. CXorf21 is a binding partner of another SLE-risk gene—*Slc15a4*. As noted above SLC15A4 is involved in transport of oligopeptides and hydrogen ions out of the lysosome, and knockout of *Slc15a4* results in abrogation of TLR7 signaling as well as amelioration of murine lupus (17, 18, 20, 21). We have shown that CXorf21 protein is expressed exclusively in monocytes, B cells, and dendritic cells, and the protein levels are two–three-fold higher in female cells compared to male cells. In addition knockdown of CXorf21 with CRISPR-Cas resulted in abrogation of interferon, TNF-α and IL6 secretion after TLR7 activation in female cells. Furthermore, lysosomal pH increased, suggesting an environment less conducive to lysosomal signaling (Harris et al., unpublished).

Because lysosomal pH was affected by decreased expression of CXorf21 and because female cells express more CXorf21 than do male cells, we hypothesized that female cells expressing CXorf21 would have a more acidic pH than male cells. Therefore, we studied lysosomal pH in B cells, monocytes and dendritic cells from healthy human subjects. In fact, the present results demonstrate that female cells had a more acidic lysosomal pH than did these cells from male subjects. T lymphocytes and NK cells, which do not express CXorf21 at appreciable levels, did not have a pH difference between male and female derived cells. Thus, we conclude that a possible functional role of CXorf21 is regulation of lysosomal pH,

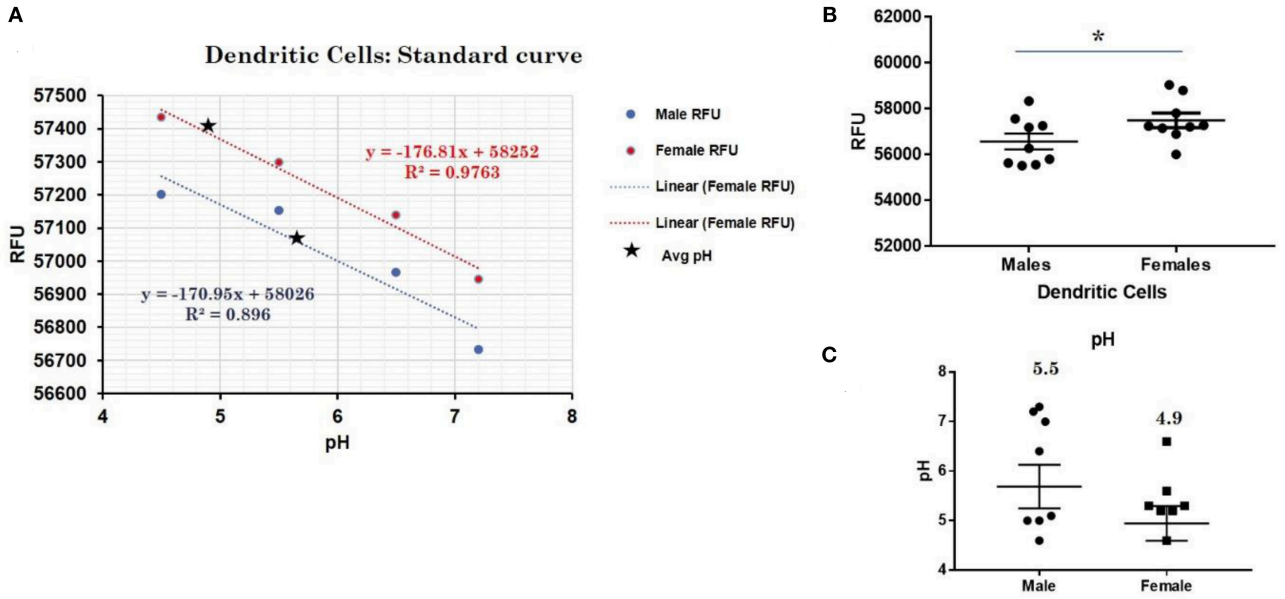

FIGURE 3 | Differences in lysosomal pH in female and male dendritic cells. **(A)** Male ($n = 6$) and female dendritic cells ($n = 6$) standard curve using pHrodo^{TM} Red AM with Intracellular pH Calibration Buffer Kit for the translation of fluorescence ratios into pH. An average of six data points was plotted in the graph and a linear trend line was fitted to get a pH standard curve. **(B)** Male DCs or female DCs were stained with pHrodo^{TM} Red AM solution and relative fluorescence units (RFUs) were measured with multi-well plate reader (Details in Material and Methods). **(C)** pH determined using pHrodo indication kit according to manufactures protocol. Student's *t*-test was used to determine statistical difference in RFUs that was converted into pH values via each standard curve. *p-value 0.044; Error bar represent SEM.

and that differing levels of expression between the sexes lead to distinct lysosomal pH. To our knowledge this is the first report of a lysosomal pH difference between male and female immune cells.

We have ventured to predict a mechanism of action for the uncharacterized protein CXorf21 as a short-chain dehydrogenase reductase. We put forth two plausible functions: (1) as a reductase CXorf21 utilizes NADPH to generate hydrogen ions for lysosome proton pump consumption (i.e., v-ATPase pump); or, (2) as a dehydrogenase generates NAPDH for lysosome superoxide production by the lysosomal-resident NOX2 complex. Both scenarios could result in changes in lysosomal pH.

What might be the functional consequences of this pH difference? Simply, altered (auto)antigen processing and presentation or modulation of endolysosomal resident TLR7 activity. As noted above, a recent report demonstrates that the X-linked *TLR7* gene is bi-allelically expressed in immune cells (that is, escapes X inactivation), and has increased protein levels in female cells compared to male cells (38). In addition to an increase in lysosomal pH and abrogation of TLR7 signaling, our data using *CXorf21* CRISPR-Cas knockdown show that there is a loss of TLR7 agonist-induced increased TLR7 expression (both mRNA and protein). Thus, CXorf21 is critically involved in TLR7 signaling, including a feedforward expression loop for TLR7. Thus, we propose increased expression of CXorf21, either because of the presence of two X chromosomes and the escape of X inactivation, or because the SLE-risk allele increases expression (18), leads to increased TLR7 signaling and increased interferon production.

The present study is limited, especially in regard to studying lysosomal pH and its regulation in regards to the pathogenesis and treatment of SLE. Endosomal TLR signaling, which leads to type 1 interferon production, is clearly important in SLE pathogenesis, both in humans and animal models (39). Furthermore, this signaling is exquisitely sensitive to changes in endolysosomal pH. *CXorf21, Slc15a4, TLR7*, and *NCF1* (encodes the p47phox NOX2 subunit) all contain SLE risk alleles (4–6). Published data discussed above demonstrate that SLC15A4 regulates endolysosomal pH, and data herein show that the protein product of *CXorf21* also regulates this pH. NOX2 is activated by phosphorylation of its p47phox subunit by TLR7 signaling (40, 41). Meanwhile, TLR7 and NOX2 signaling are both regulated by endolysosomal pH, and activated NOX2 regulates endolysosomal pH (42, 43). Both *CXorf21* and *TLR7* escape X inactivation (22). Thus, determining how these genes, all of which are involved in endososomal TLR signaling and type 1 interferon production, impact the pathogenesis and sex bias of SLE will need a great deal more investigation. The treatment of SLE may also be impacted by the interaction of these genes, their SLE-associated alleles and their protein products. Hydroxychloroquine, an important mainstay of SLE therapy (44–49), has a variety of effects (50–54), including altering endolysosomal pH, antigen presentation, TLR signaling and cytokine production. Obviously, these mechanisms of action intersect with the TLR7 signaling pathway and the genes

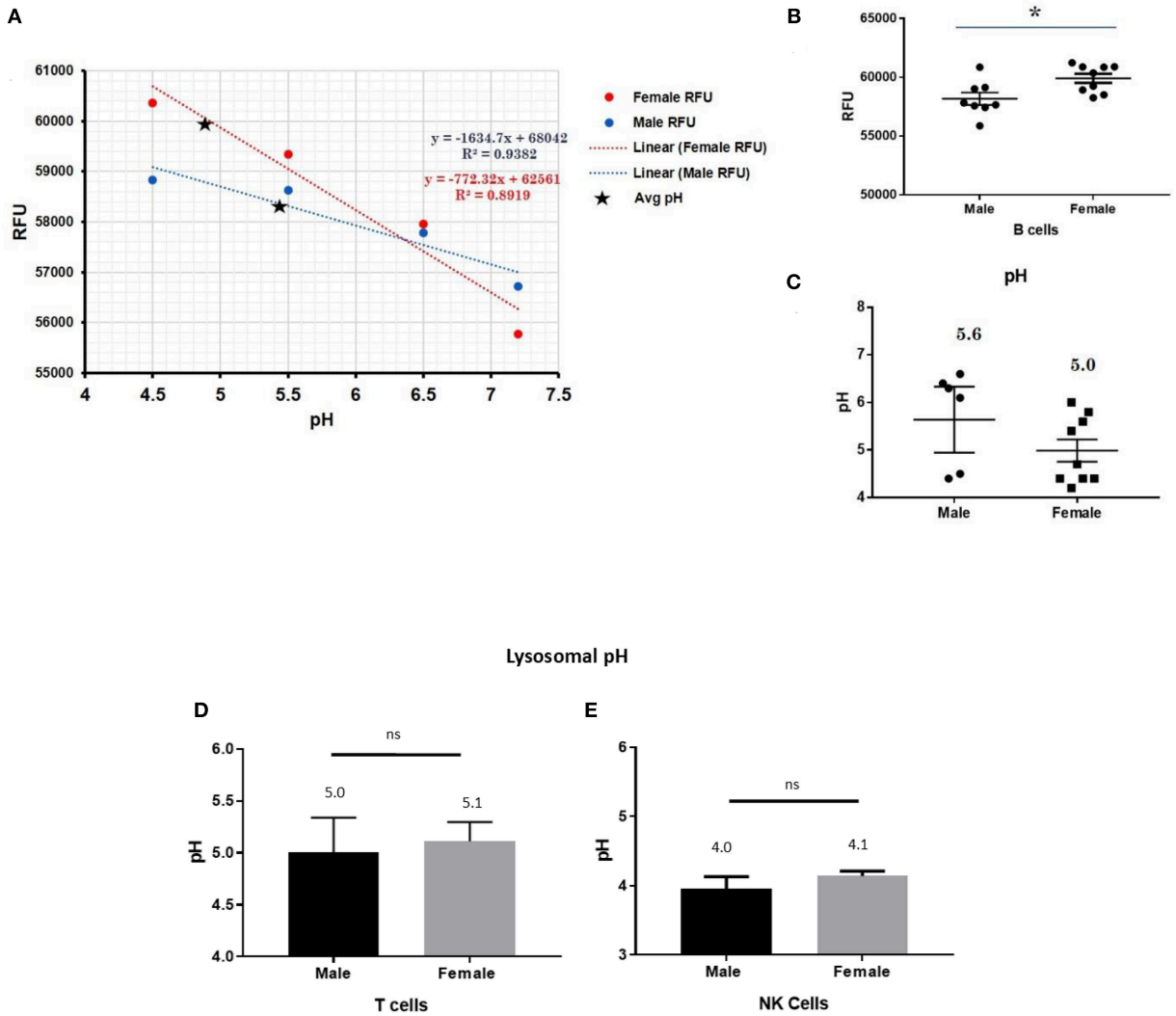

FIGURE 4 | Differences in lysosomal pH in female and male CD19+ B cells, pan-T cells, and NK cells. **(A)** Male and female B cells ($n = 6$) standard curve using pHrodo^{TM} Red AM with Intracellular pH Calibration Buffer Kit for the translation of fluorescence ratios into pH. An average of six data points was plotted in the graph and a linear trend line was fitted to get a pH standard curve. **(B)** Male B cells or female B cells were stained with pHrodo^{TM} Red AM solution and relative fluorescence units (RFUs) were measured with multi-well plate reader (Details in Material and Methods). **(C)** pH determined using pHrodo indication kit according to manufactures protocol. Male and Female **(D)** pan-T cells and **(E)** NK cell pH was determined as described above (standard curves and RFUs data not shown) Student's *t*-test was used to determine statistical difference in RFUs and pH that was converted into pH values via each standard curve; $^{*}p < 0.05$; ns=not significant; Error bar represent SEM.

discussed above. We have not addressed how the SLE-associated alleles in these four genes might influence the efficacy of hydroxychloroquine, which will likely require study of healthy controls as well as SLE patients with various combinations of these alleles.

These data demonstrate the function of SLC15A4 and CXorf21, which form a complex that regulates lysosomal pH, and in turn regulates TLR7 signaling. Furthermore, based on the differential expression of *CXorf21* between the sexes, we have shown that lysosomal pH, a key factor in signaling in this cellular compartment, is different between men and women. This difference and the resulting functional immune differences may contribute to the X chromosome gene dose that underlies the sex bias of SLE and SS.

DATA AVAILABILITY

All datasets generated for this study are included in the manuscript and/or the supplementary files.

AUTHOR CONTRIBUTIONS

VH designed the experiments, carried out the experiments, wrote the first draft, edited the paper, and approved the

final version. RS designed the experiments, wrote the manuscript, and approved the final version. IH designed the experiments, edited the paper, and approved the final version. BK carried out experiments, edited the paper, and approved the final version. KK designed the experiments, edited the paper, and approved the final version.

FUNDING

This work was supported in part by grants from the Lupus Research Institute (370617), the US Department of Veterans Affairs (5I01BX001451), and the US National Institutes of Health (AR053734, AR053483, AI082714, GM104938), and NIAMS Training grant 5T32AR007534-32.

REFERENCES

1. Harley JB, Scofield RH, Reichlin M. Anti-Ro in Sjogren's syndrome and systemic lupus erythematosus. *Rheum Dis Clin North Am*. (1992) 18:337–58.
2. Libert C, Dejager L, Pinheiro I. The X chromosome in immune functions: when a chromosome makes the difference. *Nat Rev Immunol*. (2010) 10:594–604. doi: 10.1038/nri2815
3. Lessard CJ, Li H, Adrianto I, Ice JA, Rasmussen A, Grundahl KM, et al. Variants at multiple loci implicated in both innate and adaptive immune responses are associated with Sjogren's syndrome. *Nat Genet*. (2013) 45:1284–92. doi: 10.1038/ng.2792
4. International Consortium for Systemic Lupus Erythematosus G, Harley JB, Alarcon-Riquelme ME, Criswell LA, Jacob CO, Kimberly RP, et al. Genome-wide association scan in women with systemic lupus erythematosus identifies susceptibility variants in ITGAM, PXK, KIAA1542 and other loci. *Nat Genet*. (2008) 40:204–10. doi: 10.1038/ng.81
5. Hom G, Graham RR, Modrek B, Taylor KE, Ortmann W, Garnier S, et al. Association of systemic lupus erythematosus with C8orf13-BLK and ITGAM-ITGAX. *N Engl J Med*. (2008) 358:900–9. doi: 10.1056/NEJMoa0707865
6. Morris DL, Sheng Y, Zhang Y, Wang YF, Zhu Z, Tombleson P, et al. Genome-wide association meta-analysis in Chinese and European individuals identifies ten new loci associated with systemic lupus erythematosus. *Nat Genet*. (2016) 48:940–6. doi: 10.1038/ng.3603
7. Emamian ES, Leon JM, Lessard CJ, Grandits M, Baechler EC, Gaffney PM, et al. Peripheral blood gene expression profiling in Sjogren's syndrome. *Genes Immun*. (2009) 10:285–96. doi: 10.1038/gene.2009.20
8. Bennett L, Palucka AK, Arce E, Cantrell V, Borvak J, Banchereau J, et al. Interferon and granulopoiesis signatures in systemic lupus erythematosus blood. *J Exp Med*. (2003) 197:711–23. doi: 10.1084/jem.20021553
9. Banchereau J, Pascual V. Type I interferon in systemic lupus erythematosus and other autoimmune diseases. *Immunity*. (2006) 25:383–92. doi: 10.1016/j.immuni.2006.08.010
10. Bae SC, Lee YH. Meta-analysis of gene expression profiles of peripheral blood cells in systemic lupus erythematosus. *Cell Mol Biol*. (2018) 64:40–9. doi: 10.14715/cmb/2018.64.10.7
11. Sakata K, Nakayamada S, Miyazaki Y, Kubo S, Ishii A, Nakano K, et al. Up-regulation of TLR7-mediated IFN-alpha production by plasmacytoid dendritic cells in patients with systemic lupus erythematosus. *Front Immunol*. (2018) 9:1957. doi: 10.3389/fimmu.2018.01957
12. Clancy RM, Markham AJ, Buyon JP. Endosomal Toll-like receptors in clinically overt and silent autoimmunity. *Immunol Rev*. (2016) 269:76–84. doi: 10.1111/imr.12383
13. Chauhan SK, Singh VV, Rai R, Rai M, Rai G. Distinct autoantibody profiles in systemic lupus erythematosus patients are selectively associated with TLR7 and TLR9 upregulation. *J Clin Immunol*. (2013) 33:954–64. doi: 10.1007/s10875-013-9887-0
14. Desnues B, Macedo AB, Ordonez-Rueda D, Roussel-Queval A, Malissen B, Bruhns P, et al. The transcriptional repressor Gfi1 prevents lupus autoimmunity by restraining TLR7 signaling. *Sci Immunol*. (2016) 46:2801–11. doi: 10.1002/eji.201646573
15. Wu YY, Kumar R, Iida R, Bagavant H, Alarcon-Riquelme ME. BANK1 regulates IgG production in a lupus model by controlling TLR7-dependent STAT1 activation. *PLoS ONE*. (2016) 11:e0156302. doi: 10.1371/journal.pone.0156302
16. Takagi H, Arimura K, Uto T, Fukaya T, Nakamura T, Choijookhuu N, et al. Plasmacytoid dendritic cells orchestrate TLR7-mediated innate and adaptive immunity for the initiation of autoimmune inflammation. *Sci Rep*. (2016) 6:24477. doi: 10.1038/srep24477
17. Clark AG, Buckley ES, Foster MH. Altered toll-like receptor responsiveness underlies a dominant heritable defect in B cell tolerance in autoimmune. *N Zeal Black Mice*. (2018) 48:492–7. doi: 10.1002/eji.201747287
18. Bentham J, Morris DL, Graham DSC, Pinder CL, Tombleson P, Behrens TW, et al. Genetic association analyses implicate aberrant regulation of innate and adaptive immunity genes in the pathogenesis of systemic lupus erythematosus. *Nat Genet*. (2015) 47:1457–64. doi: 10.1038/ng.3434
19. Huttlin EL, Ting L, Bruckner RJ, Gebreab F, Gygi MP, Szpyt J, et al. The bioplex network: a systematic exploration of the human interactome. *Cell*. (2015) 162:425–40. doi: 10.1016/j.cell.2015.06.043
20. Kobayashi T, Shimabukuro-Demoto S, Yoshida-Sugitani R, Furuyama-Tanaka K, Karyu H, Sugiura Y, et al. The histidine transporter SLC15A4 coordinates mTOR-dependent inflammatory responses and pathogenic antibody production. *Immunity*. (2014) 41:375–88. doi: 10.1016/j.immuni.2014.08.011
21. Lee J, Tattoli I, Wojtal KA, Vavricka SR, Philpott DJ, Girardin SE. pH-dependent internalization of muramyl peptides from early endosomes enables Nod1 and Nod2 signaling. *J Biol Chem*. (2009) 284:23818–29. doi: 10.1074/jbc.M109.033670
22. Tukiainen T, Villani AC, Yen A, Rivas MA, Marshall JL, Satija R, et al. Landscape of X chromosome inactivation across human tissues. *Nature*. (2017) 550:244–8. doi: 10.1038/nature24265
23. Scofield RH, Bruner GR, Namjou B, Kimberly RP, Ramsey-Goldman R, Petri M, et al. Klinefelter's syndrome (47,XXY) in male systemic lupus erythematosus patients: support for the notion of a gene-dose effect from the X chromosome. *Arthritis Rheum*. (2008) 58:2511–7. doi: 10.1002/art.23701
24. Harris VM, Sharma R, Cavett J, Kurien BT, Liu K, Koelsch KA, et al. Klinefelter's syndrome (47,XXY) is in excess among men with Sjogren's syndrome. *Clin Immunol*. (2016) 168:25–9. doi: 10.1016/j.clim.2016.04.002
25. Liu K, Kurien BT, Zimmerman SL, Kaufman KM, Taft DH, Kottyan LC, et al. X chromosome dose and sex bias in autoimmune diseases: increased prevalence of 47,XXX in systemic lupus erythematosus and Sjogren's syndrome. *Arthritis Rheumatol*. (2016) 68:1290–300. doi: 10.1002/art.39560
26. Rasmussen A, Sevier S, Kelly JA, Glenn SB, Aberle T, Cooney CM, et al. The lupus family registry and repository. *Rheumatology*. (2011) 50:47–59. doi: 10.1093/rheumatology/keq302
27. Park RJ, Wang T, Koundakjian D, Hultquist JF, Lamothe-Molina P, Monel B, et al. A genome-wide CRISPR screen identifies a restricted set of HIV host dependency factors. *Nat Genet*. (2017) 49:193–203. doi: 10.1038/ng.3741
28. Klein SL, Flanagan KL. Sex differences in immune responses. *Nat Rev Immunol*. (2016) 16:626–38. doi: 10.1038/nri.2016.90
29. Borchers AT, Naguwa SM, Shoenfeld Y, Gershwin ME. The geoepidemiology of systemic lupus erythematosus. *Autoimmun Rev*. (2010) 9:A277–87. doi: 10.1016/j.autrev.2009.12.008
30. Lalani S, Pope J, de Leon F, Peschken C, Members of Ca NFoL. Clinical features and prognosis of late-onset systemic lupus erythematosus: results from the 1000 faces of lupus study. *J Rheumatol*. (2010) 37:38–44. doi: 10.3899/jrheum.080957
31. Mackworth-Young CG, Parke AL, Morley KD, Fotherby K, Hughes GR. Sex hormones in male patients with systemic lupus erythematosus: a comparison with other disease groups. *Eur J Rheumatol Inflamm*. (1983) 6:228–32.
32. Chang DM, Chang CC, Kuo SY, Chu SJ, Chang ML. Hormonal profiles and immunological studies of male lupus in Taiwan. *Clin Rheumatol*. (1999) 18:158–62. doi: 10.1007/s100670050075

33. Invernizzi P, Miozzo M, Oertelt-Prigione S, Meroni PL, Persani L, Selmi C, et al. X monosomy in female systemic lupus erythematosus. *Ann N Y Acad Sci*. (2007) 1110:84–91. doi: 10.1196/annals.1423.010
34. Huang Q, Parfitt A, Grennan DM, Manolios N. X-chromosome inactivation in monozygotic twins with systemic lupus erythematosus. *Autoimmunity*. (1997) 26:85–93. doi: 10.3109/08916939709003851
35. Sharma R, Harris VM, Cavett J, Kurien BT, Liu K, Koelsch KA, et al. Rare X chromosome abnormalities in systemic lupus erythematosus and Sjogren's syndrome. *Arthritis Rheumatol*. (2017) 69:2187–92. doi: 10.1002/art.40207
36. Cooney CM, Bruner GR, Aberle T, Namjou-Khales B, Myers LK, Feo L, et al. 46,X,del(X)(q13) Turner's syndrome women with systemic lupus erythematosus in a pedigree multiplex for SLE. *Genes Immun*. (2009) 10:478–81. doi: 10.1038/gene.2009.37
37. Carrel L, Willard HF. X-inactivation profile reveals extensive variability in X-linked gene expression in females. *Nature*. (2005) 434:400–4. doi: 10.1038/nature03479
38. Souyris M. TLR7 escapes X chromosome inactivation in immune cells. *Eur J Immunol*. (2018) 3:19. doi: 10.1126/sciimmunol.aap8855
39. Tsokos GC, Lo MS, Costa Reis P, Sullivan KE. New insights into the immunopathogenesis of systemic lupus erythematosus. *Nat Rev Rheumatol*. (2016) 12:716–30. doi: 10.1038/nrrheum.2016.186
40. To EE, Vlahos R, Luong R, Halls ML, Reading PC, King PT, et al. Endosomal NOX2 oxidase exacerbates virus pathogenicity and is a target for antiviral therapy. *Nat Commun*. (2017) 8:69. doi: 10.1038/s41467-017-00057-x
41. Drummond GR, Selemidis S, Griendling KK, Sobey CG. Combating oxidative stress in vascular disease: NADPH oxidases as therapeutic targets. *Nat Rev Drug Discov*. (2011) 10:453–71. doi: 10.1038/nrd3403
42. Jancic C, Savina A, Wasmeier C, Tolmachova T, El-Benna J, Dang PM, et al. Rab27a regulates phagosomal pH and NADPH oxidase recruitment to dendritic cell phagosomes. *Nat Cell Biol*. (2007) 9:367–78. doi: 10.1038/ncb1552
43. Savina A, Jancic C, Hugues S, Guermonprez P, Vargas P, Moura IC, et al. NOX2 controls phagosomal pH to regulate antigen processing during crosspresentation by dendritic cells. *Cell*. (2006) 126:205–18. doi: 10.1016/j.cell.2006.05.035
44. Canadian Hydroxychloroquine Study G. A randomized study of the effect of withdrawing hydroxychloroquine sulfate in systemic lupus erythematosus. *N Engl J Med*. (1991) 324:150–4. doi: 10.1056/NEJM199101173240303
45. Levy RA, Vilela VS, Cataldo MJ, Ramos RC, Duarte JL, Tura BR, et al. Hydroxychloroquine (HCQ) in lupus pregnancy: double-blind and placebo-controlled study. *Lupus*. (2001) 10:401–4. doi: 10.1191/096120301678646137
46. Meinao IM, Sato EI, Andrade LE, Ferraz MB, Atra E. Controlled trial with chloroquine diphosphate in systemic lupus erythematosus. *Lupus*. (1996) 5:237–41. doi: 10.1177/096120339600500313
47. Molad Y, Gorshtein A, Wysenbeek AJ, Guedj D, Majadla R, Weinberger A, et al. Protective effect of hydroxychloroquine in systemic lupus erythematosus. Prospective long-term study of an Israeli cohort. *Lupus*. (2002) 11:356–61. doi: 10.1191/0961203302lu203ra
48. Fessler BJ, Alarcon GS, McGwin G Jr, Roseman J, Bastian HM, Friedman AW, et al. Systemic lupus erythematosus in three ethnic groups: XVI. Association of hydroxychloroquine use with reduced risk of damage accrual. *Arthritis Rheum*. (2005) 52:1473–80. doi: 10.1002/art.21039
49. Akhavan PS, Su J, Lou W, Gladman DD, Urowitz MB, Fortin PR. The early protective effect of hydroxychloroquine on the risk of cumulative damage in patients with systemic lupus erythematosus. *J Rheumatol*. (2013) 40:831–41. doi: 10.3899/jrheum.120572
50. Costedoat-Chalumeau N, Dunogue B, Morel N, Le Guern V, Guettrot-Imbert G. Hydroxychloroquine: a multifaceted treatment in lupus. *Presse Med*. (2014) 43(6 Pt 2):e167-80. doi: 10.1016/j.lpm.2014.03.007
51. van den Borne BE, Dijkmans BA, de Rooij HH, le Cessie S, Verweij CL. Chloroquine and hydroxychloroquine equally affect tumor necrosis factor-alpha, interleukin 6, and interferon-gamma production by peripheral blood mononuclear cells. *J Rheumatol*. (1997) 24:55–60.
52. Sacre K, Criswell LA, McCune JM. Hydroxychloroquine is associated with impaired interferon-alpha and tumor necrosis factor-alpha production by plasmacytoid dendritic cells in systemic lupus erythematosus. *Arthritis Res Ther*. (2012) 14:R155. doi: 10.1186/ar3895
53. Bondeson J, Sundler R. Antimalarial drugs inhibit phospholipase A2 activation and induction of interleukin 1beta and tumor necrosis factor alpha in macrophages: implications for their mode of action in rheumatoid arthritis. *Gen Pharmacol*. (1998) 30:357–66. doi: 10.1016/S0306-3623(97)00269-3
54. Sperber K, Quraishi H, Kalb TH, Panja A, Stecher V, Mayer L. Selective regulation of cytokine secretion by hydroxychloroquine: inhibition of interleukin 1 alpha (IL-1-alpha) and IL-6 in human monocytes and T cells. *J Rheumatol*. (1993) 20:803–8.

Conflict of Interest Statement: The authors declare that the research was conducted in the absence of any commercial or financial relationships that could be construed as a potential conflict of interest.

frontiers in Immunology

ORIGINAL RESEARCH
published: 02 April 2019
doi: 10.3389/fimmu.2019.00637

A Variant of the Histone-Binding Protein sNASP Contributes to Mouse Lupus

Jiyu Ju[1], Jia Xu[2], Yaoqiang Zhu[1], Xiaoyan Fu[1], Laurence Morel[3] and Zhiwei Xu[1,4]**

[1] Department of Immunology, Weifang Medical University, Weifang, China, [2] Department of Pathology, Beth Israel Deaconess Medical Center, Harvard Medical School, Boston, MA, United States, [3] Immunology and Laboratory Medicine, Department of Pathology, College of Medicine, University of Florida, Gainesville, FL, United States, [4] Department of Anatomy and Cell Biology, College of Medicine, University of Florida, Gainesville, FL, United States

The *Sle2c1rec1c* (*rec1c*) sublocus is derived from the mouse lupus susceptibility 2 (*Sle2*) locus identified in the NZM2410 model. Our current study dissected the functional characters and the genetic basis of the *rec1c* locus relative to lupus when co-expressed with the Fas^{lpr} mutation, an established inducer of autoimmunity. The rec1c.lpr mice exhibited mild expansion of lymph nodes and had a normal T cell cellularity, but developed significantly kidney and lung inflammation, indicating that the *rec1c* amplifies *lpr*-induced autoimmune pathogenesis. A variant of somatic nuclear autoantigenic sperm protein (sNASP) was identified from the *rec1c* interval as a substitution of two consecutive amino acid residues in the histone-binding domain, resulting in an increased binding affinity to histone H4 and H3.1/H4 tetramer. To determine the role of the *sNASP rec1c* allele in mouse lupus, a novel strain was generated by introducing the *rec1c* mutations into the B6 genome. In this transgenic model, the *sNASP* allele synergized with the *lpr* mutation leading to moderate autoimmune phenotypes and aggravating inflammatory pathology alterations in kidney and lung that were similar to those observed in the rec1c.lpr mice. These results establish that the *sNASP* allele is a pathogenic genetic element in the *rec1c* sublocus, which not only promotes autoimmunity, but also exacerbates the inflammation reaction of end organs in mouse lupus pathogenesis. It also shows the complexity of the *Sle2c* locus, initially mapped as the major locus associated with B1a cell expansion. In addition to *Cdkn2c*, which regulates this expansion, we have now identified in the same locus a protective allele of *Csf3r*, a variant of Skint6 associated with T cell activation, and now a variant of *sNASP* that amplifies autoimmunity and tissue damage.

Keywords: mouse, lupus, lupus nephritis, genetics, NASP, histone-binding protein

OPEN ACCESS

Edited by:
Michele Marie Kosiewicz, University of Louisville, United States

Reviewed by:
Stefania Gallucci, Temple University, United States
Shaun William Jackson, Seattle Children's Research Institute, United States

***Correspondence:**
Laurence Morel
morel@ufl.edu
Zhiwei Xu
xuzhiwei51888@gmail.com

Specialty section:
This article was submitted to Autoimmune and Autoinflammatory Disorders, a section of the journal Frontiers in Immunology

Received: *08 November 2018*
Accepted: *08 March 2019*
Published: *02 April 2019*

Citation:
Ju J, Xu J, Zhu Y, Fu X, Morel L and Xu Z (2019) A Variant of the Histone-Binding Protein sNASP Contributes to Mouse Lupus. Front. Immunol. 10:637. doi: 10.3389/fimmu.2019.00637

INTRODUCTION

Mouse models of systemic lupus erythematosus (SLE) have greatly contributed to the understanding of SLE pathogenesis, including by the identification of genetic pathways whose alterations lead to increased disease susceptibility or resistance (1). Although great efforts have been invested in the genetic analysis of spontaneous lupus mouse models, only a few lupus susceptibility genes have been identified with a putative causative etiology (2, 3). Although polymorphisms in these genes so far do not seem to be directly involved in human lupus, they fit into pathways that

have been associated with lupus or other rheumatic diseases (2). The murine lupus susceptibility locus *Sle2* was identified on chromosome 4 as one of the three major loci associated with nephritis in the NZM2410 model (4). *Sle2* expression on a non-autoimmune background in the B6.Sle2 congenic strain revealed that it regulates B cell hyperactivity (5) and B1a cell expansion (6), but is not sufficient for clinical disease. However, the co-expression of *Sle2* with the *lpr* mutation in the Fas gene in the B6.Sle2.lpr mice resulted in more severe lupus nephritis and marked lymphadenopathy compared with B6.lpr mice (7).

The dissection of *Sle2* revealed a complex genetic architecture, with three independent loci, *Sle2a*, *Sle2b*, and *Sle2c*, contributing to B1a cell expansion, with the NZB-derived *Sle2c* being the strongest contributor (8). We identified a hypomorph allele of *Cdkn2c* as responsible for the *Sle2c* B1a cell expansion (9, 10). *Sle2c* contains a suppressive *Sle2c2* sublocus (11) that we have mapped to a missense mutation in the *Csf3r* gene encoding for the GCSF receptor and regulates the development of $CD8a^{+}$ dendritic cells (11–13). In addition, we mapped the pathological phenotype synergizing with *lpr* to the centromeric portion of *Sle2c*, the *Sle2c1* sublocus (7). Subsequently, we generated a series of shorter *Sle2c1* intervals and investigated their epistatic interaction with *lpr* (14). Two non-overlapping subloci with non-redundant phenotypes were identified: The centromeric portion of *Sle2c1*, *Sle2c1rec1a*, which contains *Cdkn2c*, exerts a strong contribution to lupus autoimmunity without clinical phenotypes. A more telomeric sublocus named *Sle2c1rec1d* (*rec1d*) was associated with more severity of renal inflammation and lymphadenopathy, and higher frequency of dermatitis in the B6.Sle2c1rec1d.lpr (rec1d.lpr) mice than that in the B6.Sle2c1rec1a.lpr (rec1a.lpr) mice (14). It is reasonable to assume that the *Sle2c1rec1c* (*rec1c*) sublocus can contribute to mouse lupus by synergizing with the overlapping region of the *rec1a and rec1d* subloci, because the rec1d.lpr mice developed more severe autoimmune disease than rec1a.lpr mice (14).

Recently, we produced a novel recombinant *rec1d1* from the *rec1d* sublocus (**Figure 1**) that narrowed down the location of the gene responsible for the severe autoimmune disease with striking lymphadenopathy in the rec1d1.lpr mice (15). The only gene in the *rec1d1* interval that presented a non-synonymous mutation was *Skint6,* and this mutation resulted in a truncated secretory peptide (15). The *Skint6* protein is mainly expressed in mouse skin, and we obtained evidence that non-hematopoietic cells expressing the *rec1d1 Skint6* allele promoted T cell proliferation *in vivo*, suggesting that the *Skint6* variant is the most likely causal gene in the *rec1d1* sublocus.

The focus of this study was to analyze the phenotypes associated with the expression of *rec1c*, which is telomeric of *rec1d1* (14, 15). When combined with *lpr*, *rec1c* showed a modest effect on autoimmune phenotypes, and greatly aggravated kidney and lung pathology. Exon sequencing of all the coding genes

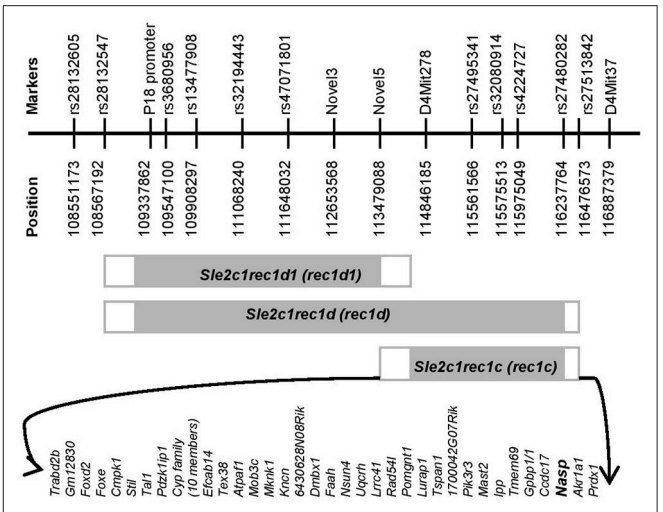

FIGURE 1 | Physical map of the *rec1c* interval. The gray rectangles indicate the *Sle2c1* NZB-derived genomic fragments on the B6 genomic background located on mouse chromosome 4. The white rectangles highlight the areas of recombination between the B6 and NZB genomes. Fine mapping of the ends of each recombinant interval was performed by using markers that are polymorphic between the NZB and B6 genomes and are shown with names and positions at the top. The protein-encoding genes in the *rec1c* interval and its recombination area are displayed at the bottom. All mouse genome informatics used in this project were calculated from the NCBI m37 assembly.

present in the *rec1c* sublocus identified two non-synonymous mutations in the *rec1c* allele of the *sNASP* gene. The sNASP is the somatic isoform of the NASP protein, a histone-binding protein that controls H3.1 folding and regulates the pool of soluble H3-H4 histones available for DNA synthesis (16). NASP controls the progression through the cell cycle (17, 18) and regulates chromatin folding (19, 20). More recently, it has been shown that NASP regulates chromatin accessibility by maintaining a pool of H3K9me1 methylated histones (21), an epigenetic mark associated with active transcription sites (22). We show here that the *rec1c* allele of sNASP has a greater binding affinity for H4 histone or H3.1/H4 tetramers *in vitro*. Further, B6.lpr mice in which the mutated *sNASP* has been knocked-in displayed phenotypes similar to that of the rec1c.lpr mice, but also showed some extra autoimmune alterations. These results identify a gain of function allele of *sNASP* with the ability of increasing autoimmunity and aggravating inflammatory damage in end organs during lupus development. This discovery adds a new member to the list of pathogenic genes in murine lupus models and provides insights into new mechanisms of autoimmune diseases. It also identifies for the first time a natural variant of a histone-binding gene as a lupus susceptibility gene, potentially by regulating chromatin accessibility.

MATERIALS AND METHODS

Mice

B6.lpr mice were purchased from Jackson Laboratory (Bar Harbor, ME, USA). The B6.Sle2c1rec1c.lpr strain was previously described (7). All available polymorphic genetic markers were

Abbreviations: NASP, nuclear autoantigenic sperm protein; sNASP, somatic nuclear autoantigenic sperm protein; SLE, systemic lupus erythematosus; SNPs, single nucleotide polymorphisms; ES, embryonic stem cell; KI, knockin; IPTG, Isopropyl β-D-1-thiogalactopyranoside; APS, aminopropylsilane; GN, glomerulonephritis; BLI, biolayer interferometer.

used to refine the *rec1c* interval and define its ends. The B6.ΔsNASP mouse with the mutated bases of the *rec1c sNASP* allele introduced into the B6 genome was created by Cyagen Biosciences Inc. with the targeting strategy presented in **Figure 6A**. The mutated bases of the *rec1c sNASP* allele are in exon 12 of Nasp-001 ENSMUST00000030456. To construct the targeting vector, two homology arms were generated by PCR using BAC clone RP24-384F21 and RP24-72F14 from the C57BL/6J library as template. The CTGTACTCCATGAGC sequence in exon 12 of the *NASP* gene, corresponding to exon 10 of the *sNASP* isoform, was mutated to CT**A**TA**T**TCCATGAGC in the 5′ homology arm. In the targeting vector, a Neo cassette was flanked by Frt sites and DTA was used for negative selection. The constructed targeting vector was electroporated into C57BL/6 mouse embryonic stem (ES) cells, and then selected positive ES clones were microinjected into blastocysts. Chimeric mice were screened by genotyping and then bred with an Flp-deleter mouse to generate F1 mouse with constitutive knockin (KI) *rec1c sNASP* allele through Flp-mediated recombination. Finally, F1 mice were intercrossed to obtain a homozygous transgenic B6.ΔsNASP model. Following the previously described protocol (6), the *lpr* mutation was bred into the B6.ΔsNASP mouse to generate a B6.ΔsNASP.lpr strain. Both male and female mice were used in this study, without difference between genders. The protocols for mice used in this research were approved by the Institute Animal Care and Use Committees of the University of Florida, USA and Weifang Medical University, China.

DNA Sequencing and RT-PCR

Genomic DNA of the lupus-prone strains MRL/MpJ-*Fas*^{lpr}/J, NZM2410/J, BXSB/MpJ, NZB/B1NJ, and NZW/Lac/J was purchased from Jackson Laboratory. The Agilent SureSelect XT Mouse All Exon Capture Kit (Agilent Technologies, Inc., Santa Clara, CA, USA) used in this project has 50 Mb capture, covering the complete mouse exome and spanning over 221,784 exons and 24,306 genes. Mouse whole exome sequencing was performed by the Beijing Genomics Institute (Shenzhen, China), including DNA fragmentation, adapter ligation, hybridization with capture library, next-generation Illumina sequencing with an average 30x coverage, and bioinformatics analysis according to mouse genome assembly NCBIm37 (strain C57BL/6J). We selected the homozygous SNPs corresponding to non-synonymous mutations, frameshifts, deletions, insertions, stop loss or gain in coding regions. Total RNA was purified from tissues using the Qiagen RNeasy kit (Qiagen, Valencia, CA, USA) and converted into cDNA by reverse transcription using the SuperScript III First-Strand Synthesis System (Thermo Fisher Scientific, Waltham, MA). The Sanger method was used to sequence cDNA or specific exons. RT-PCR was utilized to semi-quantitatively detect sNASP mRNA expression (Forward primer: 5′ ACAAGCCCATCTTAAACTTGGAG3′; Reverse primer: 5′ CTGAGATTCCTTTGCGTCTTCTA 3′).

Protein Expression, Purification, and Binding Kinetics of Protein Interaction

The full-length mouse *sNASP* cDNA (encoding 448 amino acids) was prepared from B6.lpr mouse using RT-PCR and then inserted into the pET30a expression vector to obtain a pET30a-WT sNASP protein expression vector. The mutated bases of the *rec1c sNASP* allele were introduced into the WT sNASP protein expression vector using the Q5® Site-Directed Mutagenesis Kit (NEB, Ipswich, MA) to generate a pET30a-*rec1c sNASP* allele protein expression vector. All *sNASP* constructs were confirmed by DNA sequencing. WT and mutated expression vectors were transformed into *E. coli* BL21(DE3)and protein expression was induced by Isopropyl β-D-1-thiogalactopyranoside (IPTG). Ion-exchange chromatography and size exclusion chromatography were used to purify proteins from the bacterial lysate. The protein purity was verified using SDS-PAGE electrophoresis. Western-blotting was used to identify mouse sNASP protein using anti-mouse NASP mAb (A-7, Santa Cruz Biotechnology, Inc., Dallas, TX).

Mouse histones H1a, H3.1, H4 were purchased from Lifespan Biosciences (Seattle, WA). The H3.1/H4 tetramer complex was prepared by incubating a mixture of mouse H3.1 and H4 overnight at room temperature followed by purification with size exclusion chromatography. The binding affinity of sNASP for histones was determined using biolayer interferometer Octet K2 system (Pall Fortebio Corp., Menlo Park, CA) at 30′C, following the instrument user guide. Briefly, aminopropylsilane (APS) biosensors were rinsed in assay buffer for 120 s to obtain an initial baseline. Next, mouse sNASP WT and mutant proteins were immobilized on the APS biosensors for 110 s to get a loading curve. Third, the sNASP-immobilized-APS biosensors were dipped into assay buffer for 120 s to acquire another baseline. Fourthly, the sNASP-immobilized-APS biosensors were exposed to various concentrations of histone H1a, H3.1, H4, and H3.1/H4 tetramer complex in assay buffer for 240 s to obtain association curves ($K_{on}/M^{-1}s^{-}1$). Finally, the sNASP-immobilized-APS biosensors were again dipped into assay buffer without histones to get disassociation curves (K_{off}/s^{-1}). The interaction of mouse sNASP and mouse histones was expressed as layer thickness (nm) over time (second). The binding affinity (K_D) was calculated by dividing K_{on} by K_{off}. The protein expression, purification and measurements of binding kinetics were performed by Detai Biologics Company (Nanjing, China).

IgG Autoantibody Detection

IgG anti-dsDNA and anti-chromatin IgG were measured by ELISA as previously described (6). Briefly, mBSA-coated plates were coated overnight with 50 mg/ml dsDNA for anti-dsDNA autoantibody detection. 10 mg/ml of histone H1, H2A, H2B, H3, and H4 were added to the dsDNA-coated plate for anti-chromatin autoantibody measurement. Test sera at 1:100 dilution was added to the plates and bound autoantibodies were detected using alkaline phosphatase-conjugated goat anti-mouse IgG and pNPP substrate. Raw optical densities were converted to units per milliliter, using a standard curve derived from pooled MRL/*lpr* serum, arbitrarily setting the reactivity of a 1:100 dilution of this serum to 100 U/ ml.

Flow Cytometry

Cell subsets and activation status in spleen and lymph nodes were determined by flow cytometry as previously described (8).

In brief, single-cell suspensions were prepared and depleted of red blood cells with 0.83% NH_4Cl Tris-buffer. Cells were blocked with saturating amounts of anti-CD16/CD32 (2.4G2) and stained with fluorochrome-conjugated antibodies against CD3e (145-2C11), CD4 (RM4-5), CD69 (H1.2F3), CD44 (IM7). All antibodies were purchased from BD Pharmingen (San Jose, CA, USA) or eBioscience (San Diego, CA, USA). At least 50,000 events were acquired per sample using a FACSCalibur cytometer (BD Biosciences, San Jose, CA, USA).

Kidney, Lung, and Liver Pathology

Tissues from 4 to 5-months-old mice were fixed and stained with hematoxylin and eosin (H&E). In addition, kidneys were also stained with periodic acid Schiff (PAS). Renal lesions were scored in a blinded manner following the previous report (7), and briefly speaking: grade 0, normal glomeruli, and evident capillary loops and unexpanded mesangium; grade 1, evident capillary loops, and widened mesangium with mild hypercellularity; grade 2, evident capillary loops, and expanded mesangium with more than moderate hypercellularity; grade 3, diminished capillary loops, swollen glomeruli, and more than 50% of all glomeruli with diffuse endocapillary proliferation; grade 4, no capillary loops, and basement membrane thickening and significant mesangial proliferation, more than 90% of all glomeruli with diffuse endocapillary proliferation. Lung pathology alterations were evaluated semi-quantitatively following the protocols in our publication (15), to briefly summarize: grade 0, normal lung architecture; grade 1, 1–10% of alveolar in lung has the pathological alterations of exudates, atelectasis and increased inflammatory cell number; grade 2, 10–25% of alveolar in lung shows the above pathological alterations and mild infiltrate of inflammatory cells around arteries and veins; grade 3, 25–50% alveolar in lung displays the above pathological alterations and moderate infiltrate of inflammatory cells around arteries and veins; grade 4, >50% alveolar in lung demonstrates the above pathological alterations and heavy infiltrate of inflammatory cells around arteries and veins.

The presence of immune complexes in the kidneys were evaluated on 5 μm frozen sections stained with FITC-conjugated rat anti-mouse C3 (SC-58926, Santa Cruz Biotechnology, Dallas, TX) and IgGκ BP-CFL 488 (SC-516176, Santa Cruz Biotechnology, Dallas, TX). Staining intensity was evaluated by examining sections with Olympus BX53 fluorescence microscope and DP80 camera (Diagnostic Instruments). Average 20 glomeruli for each sample was recorded as semi quantitative 0–4 scale using Image J software (NIH).

Statistical Analysis

Data were analyzed with GraphPad Prism 5.0 software with the statistical tests indicated in the text. Non-parametric tests were used when data were not distributed normally.

RESULTS

Fine-Mapping of the *rec1c* Sublocus

Since the *rec1c* interval is of NZB origin (8), we refined its map and defined its ends by genotyping all available markers that are polymorphic between the NZB and B6 genomes (**Figure 1**), including microsatellite Mit and single-nucleotide polymorphisms (SNPs) markers collected from the Mouse Genome Informatics (MGI), the National Center for Biotechnology Information (NCBI) or identified through our own genomic sequencing. The *rec1c* interval includes D4Mit278 at the centromeric end and rs27480282 at the telomeric end, but excludes the Novel5 marker and rs27513842, defining *rec1c* as a 1.39–2.99 Mb interval (**Figure 1**). The *rec1c* and *rec1d1* subloci do not overlap, but together cover the entire *rec1d* sublocus. The *rec1c* is in a gene-rich region, which contains 44 protein-coding genes, including those in the intersection area of B6 and NZB genomes (**Figure 1**).

The *rec1c* Sublocus Promotes End Organ Inflammation in the rec1c.lpr Mouse

We analyzed the autoimmune pathology of the rec1c.lpr strain by comparing with control B6.lpr mice at the age of 4–6 months. The spleen sizes of rec1c.lpr mice were similar as that of B6.lpr mice, but the rec1c.lpr mice presented larger pooled lymph nodes (469 ± 46 mg), about 2 times larger than that of B6.lpr mice (292 ± 16 mg) (**Figure 2A**). The rec1c.lpr mice showed the same percentage of $CD3^+$ T cells in spleen and lymph nodes (**Figure 2B**) and similar frequencies of $CD4^+$ T cell expressing the early activation marker CD69 (**Figure 2C**) as B6.lpr mice. A small but significant increased frequency of $CD44^+CD4^+$ effector T cells was however observed in rec1c.lpr mice (**Figure 2D**).

The rec1c.lpr mice produced the same amount of serum anti-dsDNA and anti-chromatin IgG as the B6.lpr mice (**Figure 3A**). As the rec1c.lpr mice displayed a milder lymphadenopathy than rec1a.lpr or rec1d.lpr mice, the pathology of their kidneys and lungs was not examined in our previous report (7). Unexpectedly, we found that rec1c.lpr mice developed significantly more severe renal and lung inflammation than age-matched B6.lpr mice (**Figures 3B,C**). B6.lpr mice showed a mild mesangial expansion, but the rec1c.lpr mice displayed a markedly proliferative kidney pathology with glomerular cell proliferation and inflammatory cell infiltrates in addition to mesangial expansion (**Figure 3B**). Most of B6.lpr mice exhibited normal blood vessels in their lungs, thin inter-alveolar septum, or a low degree of inflammatory infiltrates. In contrast, the rec1c.lpr lungs showed obvious histopathological alterations, including the presence of numerous congested blood vessels, large peribronchiolar and perivascular inflammatory cell infiltrates (**Figure 3C**). We also examined liver tissues and skin appearance. Most of B6.lpr or rec1.lpr mice displayed normal liver histology, although a few of them had perivascular inflammatory cell infiltrations without a difference between strains. Neither rec1c.lpr nor B6.lpr mice develop skin disease. These results indicated that the *rec1c* sublocus contains some potential disease-causing allele(s), which promotes inflammation of end organs.

A *sNASP* Variant Allele Was Identified in the *rec1c* Interval

To uncover potentially pathogenic genetic variants in the *rec1c* interval, we sequenced all exons of its 44 protein-coding genes using whole exome sequencing (WES). As a result, we identified a variant of somatic nuclear autoantigenic sperm protein gene

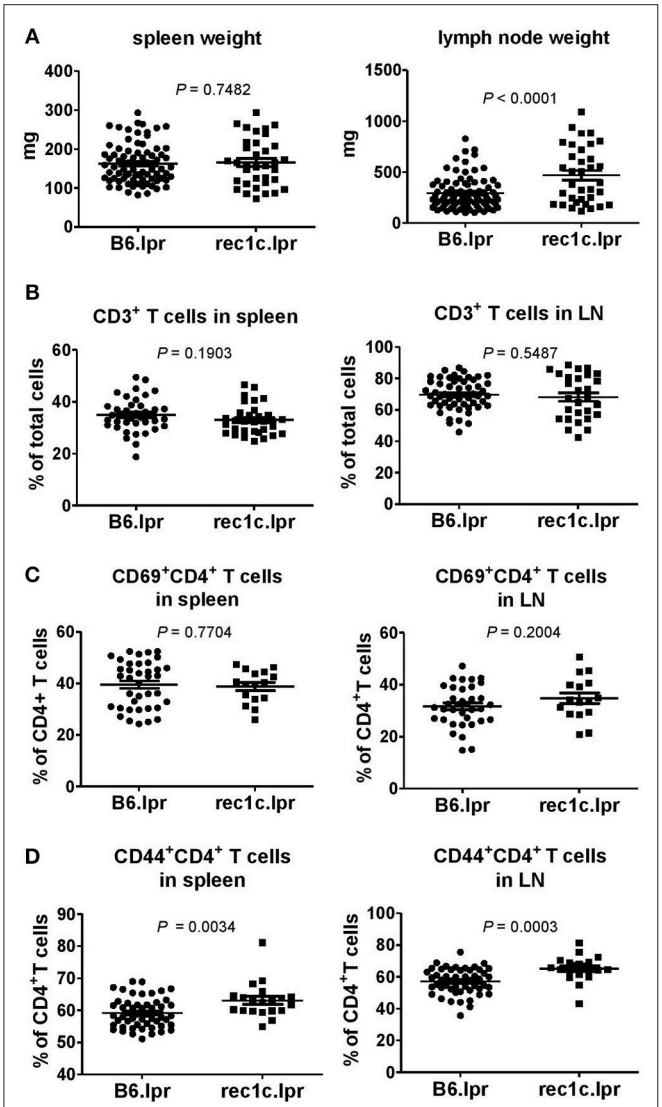

FIGURE 2 | The rec1c.lpr mice show mild immune activation. Weight of spleen and lymph nodes **(A)**, and percentages of $CD3^+$ T cells **(B)** as well as $CD69^+CD4^+$ **(C)** and $CD44^+CD4^+$ **(D)** T cell subsets in spleen and lymph nodes in B6.lpr and rec1c.lpr mice at age of 4–5 months. Statistical analysis was performed using two-tailed Mann-Whitney tests.

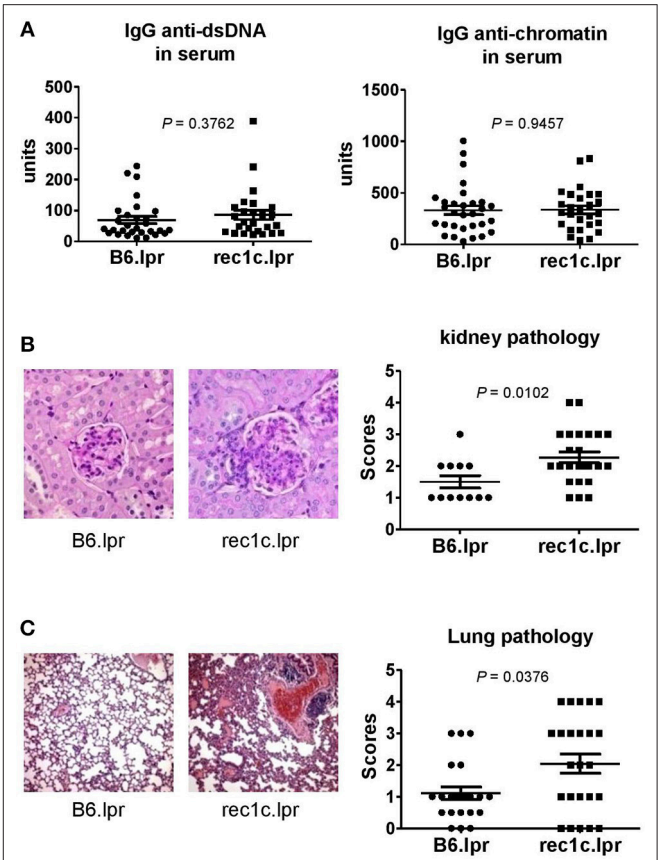

FIGURE 3 | The re1c.lpr mice develop glomerulonephritis and lung inflammation. **(A)** Serum levels of IgG anti-dsDNA and anti-chromatin autoantibodies. **(B)** Representative PAS-stained kidney section (× 400 magnification) and renal histopathology scores. **(C)** Representative H&E-stained lung section (× 100 magnification) and pulmonary histopathology scores. All samples were harvested from B6.lpr and rec1c.lpr mice at age of 4–5 months. Data analysis was performed using two-tailed Mann-Whitney tests.

(*sNASP*) with two mutations in exon 10: Chr4:g116,276,661 G>A and Chr4:g116,276,664 C>T (NCBI m37 assembly), which correspond to 841G>A and 844C>T, respectively, in the *sNASP* cDNA sequence (**Figure 4A**). Consequently, the *rec1c* allele of the sNASP protein has a substitution of two consecutive amino acid residues, V281I and L282F, in its putative histone-binding motif (19). We therefore anticipate that the *rec1c* sNASP protein may have an altered binding to histones. Sequencing of *sNASP* exon 10 in the NZB, NZW, NZM2410, MRL/lpr, and BXSB lupus-prone mice showed the *rec1c* mutations in the NZB and NZM2410 genomes, as expected, also in the NZW and MRL/lpr strains, but not in the BXSB strain (**Figure 4B**). B6.lpr and rec1c.lpr mice produced comparable amount of *sNASP* mRNA in their skin, thymus, bone marrow, and spleen (**Figure 4C**). Overall, these results identify the *sNSAP* allele as a candidate gene for the *rec1c* interval through its possibly altered binding to histones, and show that this allele is shared among several lupus-prone mouse genomes.

The *rec1c sNASP* Protein Is Dysfunctional in Binding Histones

We next investigated the histone-binding function of the *rec1c* sNASP protein function. WT sNASP and *rec1c* sNASP proteins were expressed in *E. coli* and purified by ion-exchange chromatography and size exclusion chromatography with more than 90% purity (**Figure 5A**). Quantitative binding studies of the sNASP protein interacting with mouse histones H1a, H3.1, H4, and the H3.1/H4 tetramer were measured using biolayer interferometry (BLI). A representative BLI assay graph in **Figure 5B** shows the interaction of WT sNASP binding H4 histone as expressed by layer thickness (nm) over time (second). **Table 1** lists the binding constants of the WT sNASP and *rec1c* sNASP proteins interacting with histones H1a, H3.1, H4, and

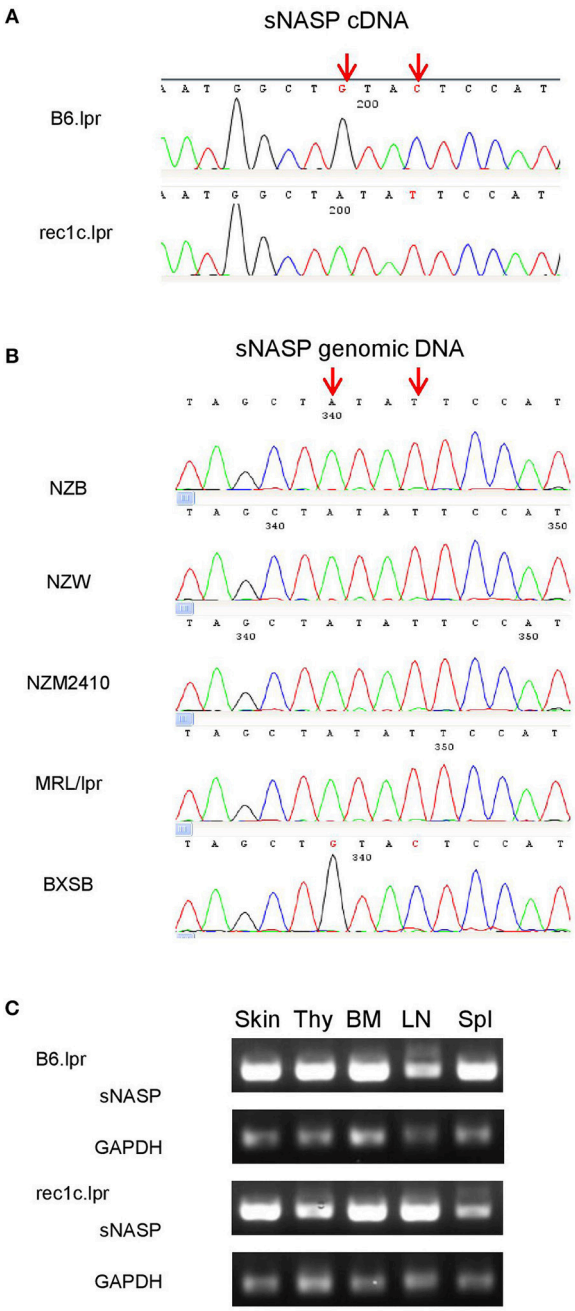

FIGURE 4 | A *sNASP* variant is identified in the *rec1c* interval. DNA sequencing was performed using the Sanger method. The mutated bases of the *sNASP* allele (red arrows) are present in the rec1c.lpr cDNA **(A)** and in the exon 10 of the NZB, NZW, NZM2410, and MRL/*lpr sNASP* gene **(B)**. **(C)** *sNASP* mRNA expression in skin (Ski), thymus (Thy), bone marrow (BM), lymph node (LN), and spleen (Spl) was detected by RT-PCR. *Gapdh* was used as a control.

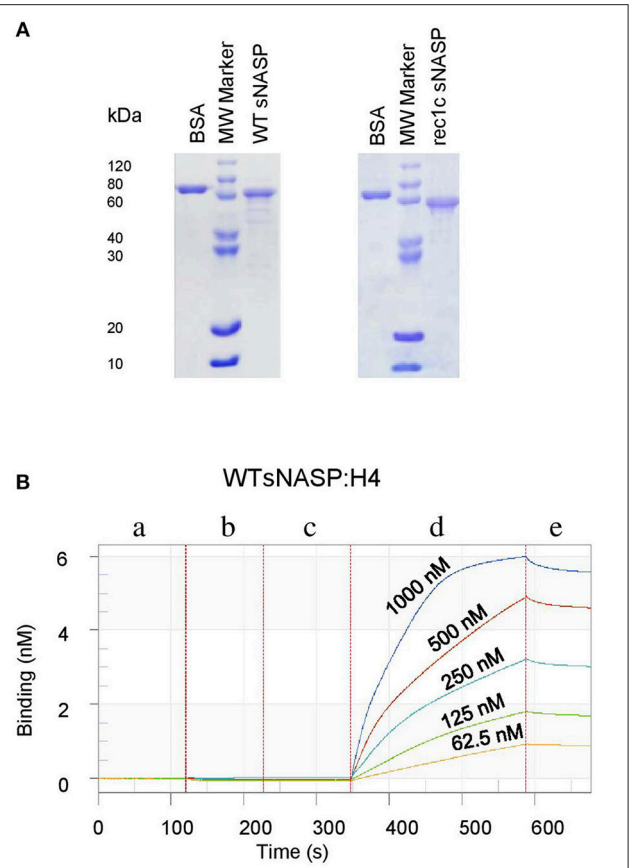

FIGURE 5 | Expression, purification, and detection of histone-binding affinity of the mouse sNASP protein. Proteins were expressed in *E. coli* and purified using ion-exchange chromatography and size exclusion chromatography. **(A)** The purity of recombinant WT sNASP and *rec1c* sNASP proteins was more than 90% as confirmed by SDS-PAGE gel. Biolayer interferometer was used to detect the affinity of WT sNASP and *rec1c* sNASP proteins binding mouse histones H1a, H3.1, H4, and H3.1/H4 tetramer. **(B)** A graph of a representative assay shows the interaction of WT sNASP binding histone 4 at the indicated concentrations from 62.5 to 1,000 nM. Each experiment is represented by an initial baseline (a), a sNASP immobilization curve (b), another baseline (c), an association curve (d), and a disassociation curve (e).

H3.1/H4 tetramer. Both WT and *rec1c* sNASP proteins showed a stronger binding affinity for H3.1 than for H1a histone, with almost a 40-fold difference. However, the WT and rec1c sNASP proteins did not show any different affinity in binding these two histones. sNASP also showed a strong binding affinity for H4 histone or H3.1/H4 tetramer in comparison with its binding to H1a histone (**Table 1**). The *rec1c* sNASP showed significantly lower K_d values for binding to H4 histone or H3.1/H4 tetramer than WT sNASP. This indicated that the *rec1c* sNASP protein has a significantly stronger affinity for binding H4 histone or H3.1/H4 tetramer than WT sNASP protein. These data demonstrate that the substitution of two consecutive amino acid residues in the *rec1* sNASP protein leads to an increased affinity of binding mouse H4 histone or H3.1/H4 tetramer.

The *rec1c sNASP* Allele Promotes Autoimmunity and Exacerbates End Organ Inflammation in a Transgenic ΔsNASP.lpr Model

To test the hypothesis that the *rec1c* sNASP protein, which displays an increased affinity for H4 histone and H3.1/H4 tetramer, is involved in autoimmune diseases, the most reliable

TABLE 1 | Binding kinetics and affinities for the interactions of mouse WT sNASP and *rec1c* variant sNASP proteins with mouse histones H1a, H3.1, H4, and H3.1/H4 tetramer.

	K_{on} (1/Ms)		K_{off} (1s)		K_d (nM)		
	Mean	**SEM**	**Mean**	**SEM**	**Mean**	**SEM**	***P*-value**
H1a BINDING							
WT sNASP	1.006×10^4	0.0281×10^4	3.89×10^{-4}	0.337×10^{-4}	387	11.3	$p > 0.05$
sNASP variant	0.959×10^4	0.0281×10^4	3.95×10^{-4}	0.353×10^{-4}	412	12.6	
H3.1 BINDING							
WT sNASP	0.869×10^4	0.0088×10^4	1.181×10^{-4}	0.105×10^{-4}	13.6	1.21	$p > 0.05$
sNASP variant	0.895×10^4	0.0094×10^4	0.755×10^{-4}	0.144×10^{-4}	8.45	1.61	
H4 BINDING							
WT sNASP	0.199×10^4	0.0010×10^4	0.81×10^{-4}	0.054×10^{-4}	40.7	3.6	$p < 0.01$
sNASP variant	1.587×10^4	0.0147×10^4	3.68×10^{-4}	0.123×10^{-4}	23.2	0.81	
H3.1/H4 TETRAMER BINDING							
WT sNASP	2.44×10^4	0.076×10^4	9.78×10^{-4}	0.700×10^{-4}	40.2	3.14	$p < 0.01$
sNASP variant	3.72×10^4	0.117×10^4	5.39×10^{-4}	0.549×10^{-4}	14.5	1.54	

Quantitative binding studies of the interactions of mouse WT sNASP and rec1c variant sNASP proteins with mouse histones H1a, H3.1, H4, and H3.1/H4 tetramer were measured using biolayer interferometer. The binding kinetic parameters were determined from four separate experiments (n = 4). Values in the table indicate mean and SEM (standard error of mean). Calculated $K_d = k_{off} / k_{on}$.

approach is to construct a transgenic model with the mutated bases of the *rec1c sNASP* allele on the B6 background. Following the targeting strategy shown in **Figure 6A**, we used DNA homologous recombination to substitute the guanine at 4:116276661 and cytosine at 4:116276664 in the B6 genome with the corresponding adenine and thymine present in the *rec1c sNASP* allele. This transgenic model was called B6.ΔsNASP. DNA sequencing confirmed that B6.ΔsNASP mouse has the mutated bases of the *rec1c* allele in *sNASP* cDNA sequence (**Figure 6B**), which indicates that the *rec1c sNASP* allele was correctly introduced into B6 genome. Western blotting revealed that both B6 and B6.ΔsNASP strains express similar amounts of sNASP protein in the skin, spleen, and thymus (**Figure 6C**), indicating that the sNASP protein expression was not affected in the B6.ΔsNASP model. Moreover, similar to B6.rec1c mouse, the B6.ΔsNASP mouse displayed a normal growth and procreation, and did not develop any detectable autoimmune phenotypes (data not shown). Adopting the same strategy as we used with B6.rec1c.lpr, we introduced the *lpr* mutation into the B6.ΔsNASP model to generate B6.ΔsNASP.lpr (ΔsNASP.lpr) mice.

We comprehensively evaluated the autoimmune phenotypes and organ pathology of the ΔsNASP.lpr as compared to B6.lpr mice at the age of 4–6 months. The ΔsNASP.lpr mice developed an enhanced lymphadenopathy with an average weight of the spleen or lymph nodes about twice and triple that of B6.lpr mice, respectively (**Figure 7A**). Total cell numbers in spleen and lymph node of ΔsNASP.lpr mice significantly increased in comparison with B6.lpr mice (**Figure 7B**). The percentages of $CD3^+$ T cells (**Figure 7C**) and $CD19^+$ B cells (**Figure 7D**) in spleen and lymph nodes were comparable between B6.lpr and ΔsNASP.lpr mice. However, ΔsNASP.lpr mice have more absolute numbers of splenic and LN T cells (**Figure 7E**) as well as splenic B cells (**Figure 7F**) than B6.lpr mice. In addition, ΔsNASP.lpr mice showed higher percentages of activated $CD69^+CD4^+$ T cells (**Figure 7G**) and effector $CD44^+CD4^+$ T cells (**Figure 7H**) than B6.lpr mice in spleen and lymph nodes.

The ΔsNASP.lpr mice produced modestly elevated levels of serum anti-chromatin and anti-dsDNA IgG as compared with B6.lpr mice (**Figure 8A**). The immune complexes in kidney were detected using the indirect immunofluorescence technique. Although a small amount of mouse IgG was present in glomeruli, ΔsNASP.lpr mice showed significantly more IgG deposits in glomeruli than B6.lpr mice (**Figure 8B**). The ΔsNASP.lpr mice showed trace C3 deposit in glomeruli (**Figure 8C**). B6.lpr mice seemed to have less C3 accumulation in glumeruli than ΔsNASP.lpr mice. However, there were no statistical difference for C3 deposit in glomeruli between ΔsNASP.lpr and B6.lpr mice (**Figure 8C**). Pathological examination showed that the ΔsNASP.lpr mice, in addition to mild mesangial expansion, develop an enhanced proliferative renal pathology with an increased glomerular cell number and an infiltration of inflammatory cells in comparison with B6.lpr mice (**Figure 8D**). The renal pathology scores of the ΔsNASP.lpr mice were significantly higher than that of B6.lpr mice. However, both sNASP.lpr and B6.lpr mice at age of 4–6 months have trace proteinuria, without a significant difference between these two strains. Moreover, the ΔsNASP.lpr mice also showed significantly a more severe lung inflammation than B6.lpr mice (**Figure 8E**). The lung pathological characteristics of ΔsNASP.lpr mice were similar to what we observed in the rec1c.lpr mice. On the other hand, the ΔsNASP.lpr mice did not develop liver inflammation and dermatitis. In summary, the ΔsNASP.lpr mice not only reproduced all autoimmune phenotypes and organ pathology alterations of rec1c.lpr mice, but also developed additional autoimmune phenotypes, including increased sizes of spleen and lymph nodes, lymphocyte increase, expansion of activated or effector $CD4^+$ T cells, IgG autoantibody elevation, and more IgG deposit in glomeruli. The characterization of the ΔsNASP.lpr

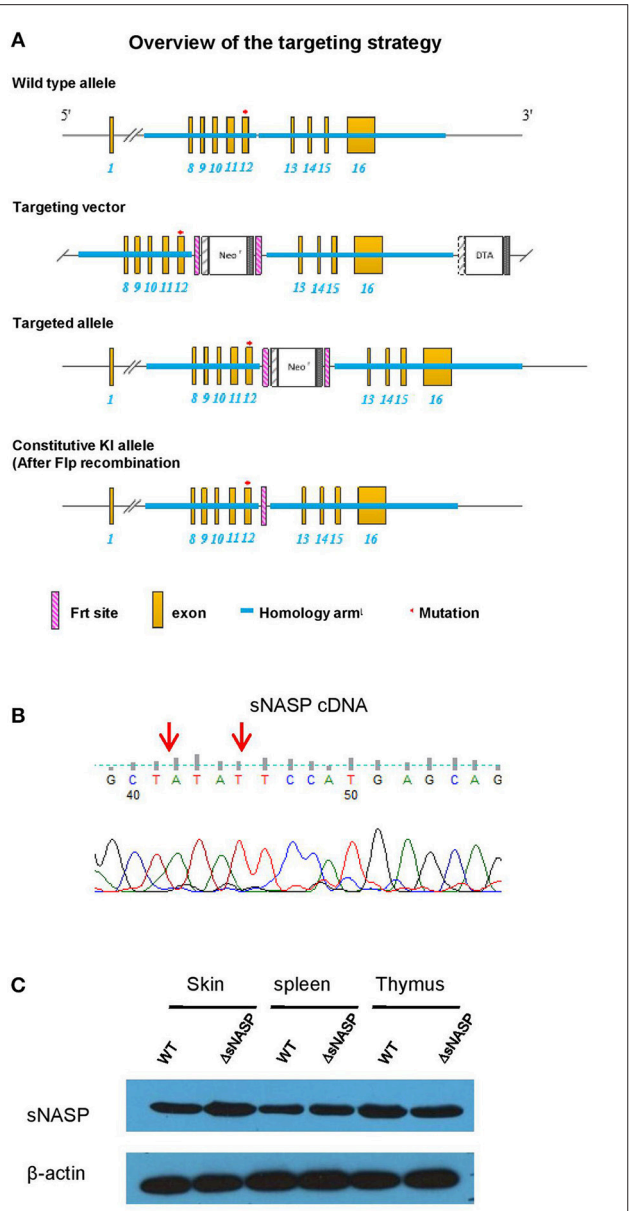

FIGURE 6 | Generation of a transgenic mouse model B6.ΔsNASP expressing the *rec1c sNASP* allele. **(A)** Targeting strategy used to construct a transgenic mouse model B6.ΔsNASP in which the mutated bases of the *rec1c sNASP* allele were introduced into the B6 genome. **(B)** The *sNASP* cDNA sequence of B6.ΔsNASP mouse was verified to have the mutated bases (red arrows) of *rec1c sNASP* allele. **(C)** The sNASP protein expression was determined by Western blotting in tissues and compared between WT B6 and transgenic B6.ΔsNASP mice, and mouse β-actin was used as control.

model demonstrates that the *sNASP* allele is responsible for pathogenic contribution of the *rec1c* sublocus to mouse lupus.

DISCUSSION

The rec1c.lpr mice exhibited a normal spleen size and a modest lymphadenopathy in comparison with control B6.lpr mice, but they developed more significant kidney and lung inflammation, two end-organ manifestations of SLE. These results suggest that the *rec1c* sublocus seemingly is not involved in systemic autoimmunity, but is rather aggravating its consequences. This is a contrast to the adjacent rec1d1 sublocus since the rec1d1.lpr mice showed 3-fold expanded spleen or even 10-fold enlarged lymph node relative to B6.lpr mice, and this expansion was largely accounted for T cells, suggesting that *red1d1* contributes to lupus by targeting T cells (15). We have proposed a model for the genes involved in lupus pathogenesis with a first group of genes breaking tolerance, such as *Ly108* in *Sle1b* (23), a second group amplifying/ polarizing autoimmune activation, such as *Pbx1* in *Sle1a* (24), and a third group of genes modulating disease severity in target organs, such as the kallycrein gene family in *Sle3* (25) in the NZM2410 lupus model (26). We propose that the *Skint6* allele in *rec1d1* belong to group 2 while *sNASP* variant in *rec1c* belongs to the third group. The detailed analysis of the *Sle2c* locus revealed a complex architecture with a total of four genes so far associated with lupus susceptibility: *Cdkn2c*, which regulates B1a cell expansion, the original selecting phenotype for *Sle2c* (8), a protective allele of *Csf3r* (11), a variant of *Skint6* associated with T cell activation (15) and now a variant of *sNASP* that amplifies autoimmunity and aggravate tissue pathology. The presence of these two latter variants may explain why *Sle2*, which is not associated by itself to any end-organ pathology (27), was mapped in association with glomerulonephritis when it interacts with other NZM2410 loci (4) or with *lpr* (7).

Exon sequencing of the *rec1c* interval identified the substitution of two consecutive amino acid residues in the *NASP* gene. *NASP* contains two isoforms, a longer testis-specific *tNASP* and a shorter somatic *sNASP*. However, both isoforms often occur in transformed cell lines (28). It is well known that the sNASP functions as a histone chaperone to perform their vital role in genome maintenance by interacting with soluble histones, driving the accurate assembly and disassembly of nucleosomes (9). The substitution of two consecutive amino acid residues in the *rec1c* sNASP variant protein occurs in the histone-binding domain. We demonstrated that this variant has an increased binding affinity for histone H4 and the H3.1/H4 tetramer, suggesting that the amino acid substitutions alter its three-dimensional structure and dysfunction.

To test the functional significance of the *rec1c sNASP* variant, we introduced the corresponding two mutations into the B6 genome to generate a transgenic B6.ΔsNASP mouse and its derived ΔsNASP.lpr strain. The B6.ΔsNASP mice did not develop any detectable autoimmunity. However, the ΔsNASP.lpr mice produced more IgG autoantibodies, had bigger spleen and lymph nodes along with lymphocyte elevation, displayed mild increase of activated and effector $CD4^+$ T cells in peripheral lymph organs, and more IgG deposit in glomeruli in comparison to B6.lpr mice. These phenotypes of ΔsNASP.lpr mice are a sign of autoimmunity. The ΔsNASP.lpr mice developed more severe kidney and lung inflammation than the control B6.lpr mice. Therefore, the ΔsNASP.lpr mice reproduced most of the autoimmune-pathological phenotypes of the rec1c.lpr mice. These findings establish that the *sNASP* mutant allele is responsible for the contribution of the *rec1c* interval to lupus pathogenesis. On

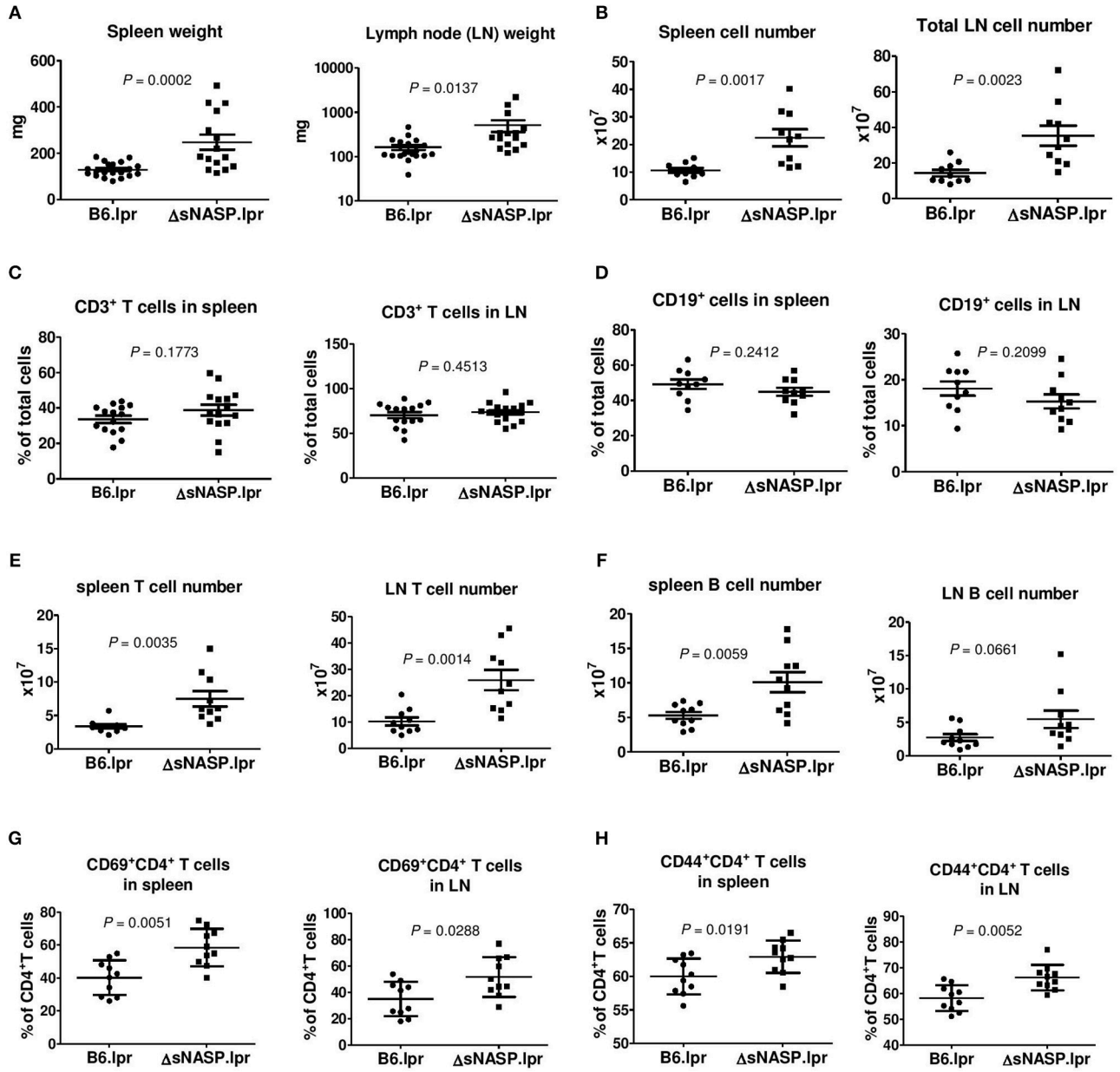

FIGURE 7 | The ΔsNASP.lpr mice present activated immune phenotypes. Weight of spleen and lymph nodes **(A)** of B6.lpr and B6.ΔsNASP.lpr mice at age of 4–5 months. Total cell number of spleen and lymph nodes **(B)**. Percentages of $CD3^+$ T cells **(C)** and $CD19^+$ B cells **(D)**, absolute T cell number **(E)** and absolute B cell number **(F)** as well as $CD69^+CD4^+$ T cells **(G)** and $CD44^+CD4^+$ T cells **(H)** in spleen and lymph node of ΔsNASP.lpr and B6.lpr mice**.** Statistical analysis was performed using two-tailed Mann-Whitney tests.

the other hand, as the ΔsNASP.lpr mice did not develop significant proteinuria, their exacerbated kidney inflammation was not sufficient to result in renal dysfunction. As for the reason why ΔsNASP.lpr mice presented some autoimmune phenotypes different that were not found in rec1c.lpr mice, we speculate it most likely due to unlinked NZM2410 genetic contamination carried over in the rec1c.lpr congenic genome that may interfere with the *sNASP* allele. Such contamination has been documented in other NZM2410-derived congenics [(24) and Morel unpublished].

The MRL/*lpr* strain develops a rapid onset of lupus due to the *lpr* mutation in the *Fas* gene on chromosome 19. A *lpr* modifier locus, *Lprm1*, has been mapped to chromosome 4 in a genomic location close to the *rec1c* sublocus (29). We found that the MRL/*lpr* genome shares the same *sNASP* allele with the *rec1c* NZM2410 allele, suggesting that it may be responsible for the *Lprm1* phenotypes. Our study demonstrated that the *sNASP* mutant allele with higher binding affinity for histone interacts with the *lpr* mutation to modestly enhance lymphadenopathy and autoimmunity and greatly promote tissue inflammation in

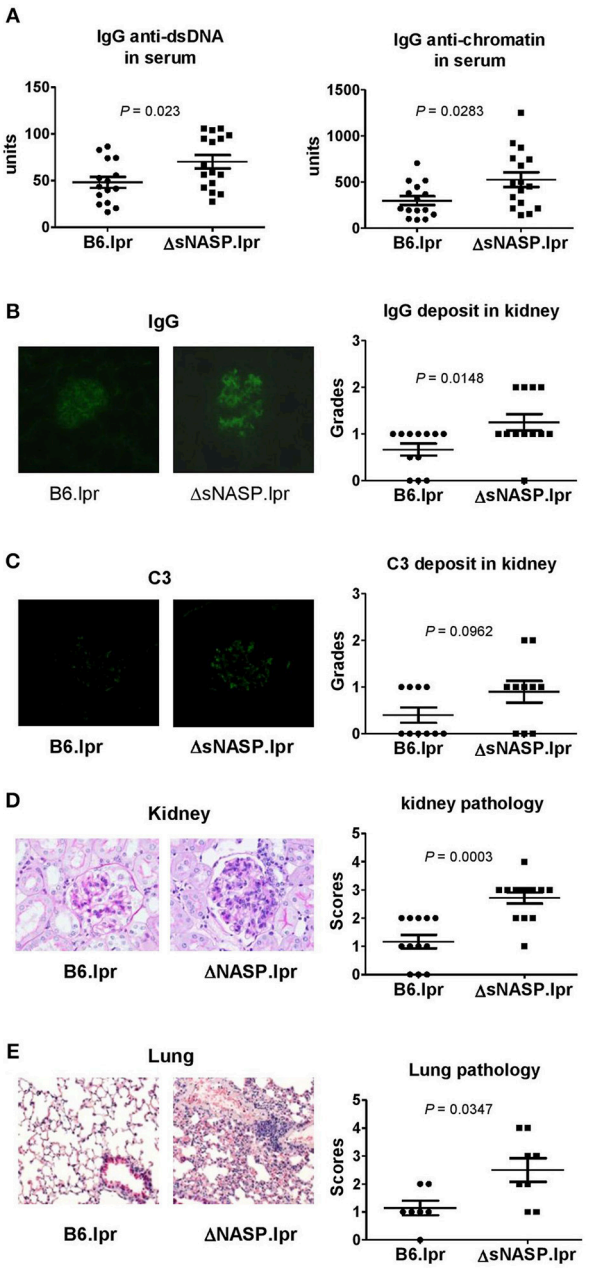

FIGURE 8 | The ΔsNASP.lpr mice exhibit severe inflammatory lesions in the kidneys and lungs. Serum levels of IgG anti-dsDNA and anti-chromatin autoantibodies **(A)**. Representative images of mouse IgG **(B)** and C3 **(C)** deposit in glomeruli from B6.lpr and ΔsNASP.lpr mice (× 400 magnification) and their respective fluorescence intensity grades. Representative PAS-stained kidney section (× 400 magnification) and renal histopathology scores **(D)**. Representative H&E-stained lung section (× 100 magnification) and pulmonary histopathology scores **(E)**. All samples were harvested from B6.lpr and B6.ΔsNASP mice at age of 4–6 months. Data analysis was performed using two-tailed Mann-Whitney tests.

the ΔsNASP.lpr model. Therefore, it is reasonable to hypothesize that the interaction of the *sNASP* mutant allele and the *lpr* mutation represents an important contribution to autoimmune pathogenesis in the MRL/lpr model.

How the *sNASP* allele in the *rec1c* sublocus promotes inflammation needs to be elucidated in the future studies. We hypothesize that the increased histone-binding affinity of the *sNASP* allele may enhance the transcription of inflammatory cytokines, either by immune cells or local cells in target organs. A recent study has reported that sNASP maintains homeostasis of the innate immune response as a negative regulator of TLR signaling by binding TRAF6 and preventing its auto-ubiquitination in unstimulated macrophages (30). Following LPS stimulation, CK2 binds and phosphorylates sNASP protein at serine 158, allowing sNASP protein to dissociate from TRAF6. Free TRAF6 is then auto-ubiquitinated and participates in TLR signaling to trigger the transcription of inflammatory cytokines (30). We speculate that the sNASP variant protein in the *rec1c* sublocus may have a decreased binding affinity for TRAF6, or be more easily phosphorylated by CK2 in innate immune cells following TLR stimulation, leading to excessive TRAF6 auto-ubiquitination and inflammatory cytokine release. The *rec1c sNASP* allele may also enhance the production of inflammatory cytokines directly by facilitating access of transcriptional site or through long-range chromatin alterations. Indeed, NASP regulates chromatin accessibility by maintaining a pool of H3K9me1 methylated histones (21), an epigenetic mark associated with active transcription sites (22). Abnormal histone modification patterns have been reported in the $CD4^+$ T cells of lupus patients (31). Epigenetic factors play a pivotal role in regulating cytokine expression, and hence effector functions, in lupus T cells (32). Specifically, CREMa increases IL-17A transcription (33) and the transcription factor RFX1 regulates the expression of CD11a and CD70 (34) through histone modifications in lupus $CD4^+$ T cells. The critical and complex role of epigenetic regulations in lupus T cells was demonstrated by showing that specifically demethylating either $CD4^+$ or $CD8^+$ T cells had beneficial effects while systemic demethylation worsened disease in MRL/lpr lupus-prone mice (35). A complex pattern of DNA methylation profiles has been revealed in twins discordant for lupus with hypo-and hyper-methylation differences, including some that were cell-specific (36). Defining the mechanisms by which the histone-binding protein NASP variant contributes to lupus pathogenesis using the mouse models that we have generated, either through epigenetic alterations, or other processes such as TRAF6 activation will benefit our understanding of lupus and the regulation of inflammation in autoimmune diseases.

DATA AVAILABILITY

All datasets generated for this study are included in the manuscript and/or the supplementary files.

AUTHOR CONTRIBUTIONS

JJ supervised the construction, genotyping, and husbandry of the transgenic B6.ΔsNASP and B6.ΔsNASP.lpr mice,

and performed some experiments on B6.ΔsNASP.lpr mice. JX performed multiple pathological examinations of kidney and lung tissues of all mouse strains. YZ performed some genotyping and experiments on B6.ΔsNASP.lpr mice. XF performed recombinant vector construction and some flow cytometry experiments on B6.ΔsNASP.lpr mice. LM participated in some experimental designs, interpreted data, and wrote the manuscript. ZX designed and supervised whole project, performed experiments on rec1c.lpr mouse, and was responsible for data analysis, interpretation, and manuscript writing.

FUNDING

This project was supported by the National Natural Science Foundation of China (Grant No. 81373185) and National Institutes of Health Grant K01AR056725 to ZX, and the Natural Science Foundation of Shandong, China (ZR2018MH014) to JJ.

ACKNOWLEDGMENTS

We thank Jianye Zhang, Peng Xie, Shujuan Liang, Yuqing Liu, Wentong Li, Yuewen Li, Kai Zheng, and Gaohang Mu for their technical assistance and discussion.

REFERENCES

1. Li W, Titov AA, Morel L. An update on lupus animal models. *Curr Opin Rheumatol.* (2017) 29:434–41. doi: 10.1097/BOR.0000000000000412
2. Morel L. Genetics of SLE: evidence from mouse models. *Nat Rev Rheumatol.* (2010) 6:348–57. doi: 10.1038/nrrheum.2010.63
3. Mohan C. The long (and sometimes endless) road to murine lupus genes. *J Immunol.* (2015) 195:4043–6. doi: 10.4049/jimmunol.1501963
4. Morel L, Rudofsky UH, Longmate JA, Schiffenbauer J, Wakeland EK. Polygenic control of susceptibility to murine systemic lupus erythematosus. *Immunity.* (1994) 1:219–29. doi: 10.1016/1074-7613(94)90100-7
5. Mohan C, Morel L, Yang P, Wakeland EK. Genetic dissection of systemic lupus erythematosus pathogenesis - Sle2 on murine chromosome 4 leads to B cell hyperactivity. *J Immunol.* (1997) 159:454–65.
6. Xu Z, Butfiloski EJ, Sobel ES, Morel L. Mechanisms of peritoneal B-1a cells accumulation induced by murine lupus susceptibility locus Sle2. *J Immunol.* (2004) 173:6050–8. doi: 10.4049/jimmunol.173.10.6050
7. Xu Z, Cuda CM, Croker BP, Morel L. The NZM2410-derived lupus susceptibility locus Sle2c1 increases TH17 polarization and induces nephritis in Fas-deficient mice. *Arthritis Rheum.* (2011) 63:764–74. doi: 10.1002/art.30146
8. Xu Z, Duan B, Croker BP, Wakeland EK, Morel L. Genetic dissection of the murine lupus susceptibility locus Sle2: contributions to increased peritoneal B-1a cells and lupus nephritis map to different loci. *J Immunol.* (2005) 175:936–43. doi: 10.4049/jimmunol.175.2.936
9. Xu Z, Potula HH, Vallurupalli A, Perry D, Baker H, Croker BP, et al. Cyclin-dependent kinase inhibitor Cdkn2c regulates B cell homeostasis and function in the NZM2410-derived murine lupus susceptibility locus Sle2c1. *J Immunol.* (2011) 186:6673–82. doi: 10.4049/jimmunol.1002544
10. Potula HH, Xu Z, Zeumer L, Sang A, Croker BP, Morel L. Cyclin-dependent kinase inhibitor *Cdkn2c* deficiency promotes B1a cell expansion and autoimmunity in a mouse model of lupus. *J Immunol.* (2012) 189:2931–40. doi: 10.4049/jimmunol.1200556
11. Xu Z, Vallurupalli A, Fuhrman C, Ostrov D, Morel L. An NZB-derived locus suppresses chronic graft versus host disease and autoantibody production through non-lymphoid bone-marrow derived cells. *J Immunol.* (2011) 186:4130–9. doi: 10.4049/jimmunol.1003512
12. Lantow M, Sivakumar R, Zeumer L, Wasserfall C, Zheng YY, Atkinson MA, et al. The granulocyte colony stimulating factor pathway regulates autoantibody production in a murine induced model of systemic lupus erythematosus. *Arthritis Res Ther.* (2013) 15:R49. doi: 10.1186/ar4208
13. Sivakumar R, Abboud G, Mathews CE, Atkinson MA, Morel L. Protective role of myeloid cells expressing a G-CSF receptor polymorphism in an induced model of lupus. *Front Immunol.* (2018) 9:1053. doi: 10.3389/fimmu.2018.01053
14. Xu Z, Croker BP, Morel L. The combination of two Sle2 lupus-susceptibility loci and Cdkn2c deficiency leads to T-cell-mediated pathology in B6.Fas mice. *Genes Immun.* (2013) 14:373–9. doi: 10.1038/gene.2013.28
15. Xu Z, Xu J, Ju J, Morel L. A Skint6 allele potentially contributes to mouse lupus. *Genes Immun.* (2017) 18:111–7. doi: 10.1038/gene.2017.8
16. Cook AJ, Gurard-Levin ZA, Vassias I, Almouzni G. A specific function for the histone chaperone NASP to fine-tune a reservoir of soluble H3-H4 in the histone supply chain. *Mol Cell.* (2011) 44:918–27. doi: 10.1016/j.molcel.2011.11.021
17. Alekseev OM, Bencic DC, Richardson RT, Widgren EE, O'Rand MG. Overexpression of the Linker histone-binding protein tNASP affects progression through the cell cycle. *J Biol Chem.* (2003) 278:8846–52. doi: 10.1074/jbc.M210352200
18. Richardson RT, Alekseev OM, Grossman G, Widgren EE, Thresher R, Wagner EJ, et al. Nuclear autoantigenic sperm protein (NASP), a linker histone chaperone that is required for cell proliferation. *J Biol Chem.* (2006) 281:21526–34. doi: 10.1074/jbc.M603816200
19. Finn RM, Browne K, Hodgson KC, Ausio J. sNASP, a histone H1-specific eukaryotic chaperone dimer that facilitates chromatin assembly. *Biophys J.* (2008) 95:1314–25. doi: 10.1529/biophysj.108.130021
20. Tachiwana H, Miya Y, Shono N, Ohzeki J, Osakabe A, Otake K, et al. Nap1 regulates proper CENP-B binding to nucleosomes. *Nucleic Acids Res.* (2013) 41:2869–80. doi: 10.1093/nar/gks1464
21. Kang X, Feng Y, Gan Z, Zeng S, Guo X, Chen X, et al. NASP antagonize chromatin accessibility through maintaining histone H3K9me1 in hepatocellular carcinoma. *Biochim Biophys Acta.* (2018) 1864:3438–48. doi: 10.1016/j.bbadis.2018.07.033
22. Barski A, Cuddapah S, Cui K, Roh TY, Schones DE, Wang Z, et al. High-resolution profiling of histone methylations in the human genome. *Cell.* (2007) 129:823–37. doi: 10.1016/j.cell.2007.05.009
23. Kumar KR, Li LN, Yan M, Bhaskarabhatla M, Mobley AB, Nguyen C, et al. Regulation of B cell tolerance by the lupus susceptibility gene Ly108. *Science.* (2006) 312:1665–9. doi: 10.1126/science.1125893
24. Choi SC, Hutchinson TE, Titov AA, Seay HR, Li S, Brusko TM, et al. The lupus susceptibility gene Pbx1 regulates the balance between follicular helper T cell and regulatory T cell differentiation. *J Immunol.* (2016) 197:458–69. doi: 10.4049/jimmunol.1502283
25. Liu K, Li QZ, Delgado-Vega AM, Abelson AK, Sánchez E, Kelly JA, et al. Kallikrein genes are associated with lupus and glomerular basement membrane-specific antibody-induced nephritis in mice and humans. *J Clin Invest.* (2009) 119:911–23. doi: 10.1172/JCI36728
26. Wakeland EK, Liu K, Graham RR, Behrens TW. Delineating the genetic basis of systemic lupus erythematosus. *Immunity.* (2001) 15:397–408. doi: 10.1016/S1074-7613(01)00201-1
27. Morel L, Mohan C, Yu Y, Croker BP, Tian N, Deng A, et al. Functional dissection of systemic lupus erythematosus using congenic mouse strains. *J Immunol.* (1997) 158:6019–28.
28. Richardson RT, Batova IN, Widgren EE, Zheng LX, Whitfield M, Marzluff WF, et al. Characterization of the histone H1-binding protein, NASP, as a cell cycle-regulated somatic protein. *J Biol Chem.* (2000) 275:30378–86. doi: 10.1074/jbc.M003781200
29. Wang Y, Nose M, Kamoto T, Nishimura M, Hiai H. Host modifier genes affect mouse autoimmunity induced by the lpr gene. *Amer J Path.* (1997) 151:1791–8.

30. Yang FM, Zuo Y, Zhou W, Xia C, Hahm B, Sullivan M, et al. sNASP inhibits TLR signaling to regulate immune response in sepsis. *J Clin Invest.* (2018) 128:2459–72. doi: 10.1172/JCI95720
31. Hu N, Qiu X, Luo Y, Yuan J, Li Y, Lei W, et al. Abnormal histone modification patterns in lupus CD4+ T cells. *J Rheumatol.* (2008) 35:804–10.
32. Hedrich CM, Crispin JC, Tsokos GC. Epigenetic regulation of cytokine expression in systemic lupus erythematosus with special focus on T cells. *Autoimmunity.* (2014) 47:234–41. doi: 10.3109/08916934.2013.801462
33. Rauen T, Hedrich CM, Juang YT, Tenbrock K, Tsokos GC. cAMP-responsive element modulator (CREM)alpha protein induces interleukin 17A expression and mediates epigenetic alterations at the interleukin-17A gene locus in patients with systemic lupus erythematosus. *J Biol Chem.* (2011) 286:43437–46. doi: 10.1074/jbc.M111.299313
34. Zhao M, Sun Y, Gao F, Wu X, Tang J, Yin H, et al. Epigenetics and SLE: RFX1 downregulation causes CD11a and CD70 overexpression by altering epigenetic modifications in lupus CD4+ T cells. *J Autoimmun.* (2010) 35:58–69. doi: 10.1016/j.jaut.2010.02.002
35. Li H, Tsokos MG, Bickerton S, Sharabi A, Li Y, Moulton VR, et al. Precision DNA demethylation amelioratesdisease in lupus-prone mice. *JCI Insight.* (2018) 3:120880. doi: 10.1172/jci.insight.120880
36. Ulff-Møller CJ, Asmar F, Liu Y, Svendsen AJ, Busato F, Grønbæk K, et al. Twin DNA methylation profiling reveals flare-dependent interferon signature and B cell promoter hypermethylation in systemic lupus erythematosus. *Arthr Rheumatol.* (2018) 70:878–90. doi: 10.1002/art.40422

Conflict of Interest Statement: The authors declare that the research was conducted in the absence of any commercial or financial relationships that could be construed as a potential conflict of interest.

frontiers in Immunology

ORIGINAL RESEARCH
published: 07 May 2019
doi: 10.3389/fimmu.2019.00885

Opposite Profiles of Complement in Antiphospholipid Syndrome (APS) and Systemic Lupus Erythematosus (SLE) Among Patients With Antiphospholipid Antibodies (aPL)

Stephanie L. Savelli[1,2,3]*, *Robert A. S. Roubey*[4]*, *Kathryn J. Kitzmiller*[1,3], *Danlei Zhou*[1,3,5], *Haikady N. Nagaraja*[6], *Evan Mulvihill*[3,5], *Fatima Barbar-Smiley*[3,5], *Stacy P. Ardoin*[3,5], *Yee Ling Wu*[1,3,7]* and *Chack-Yung Yu*[1,3,5]*

[1] The Research Institute at Nationwide Children's Hospital, Columbus, OH, United States, [2] Division of Hematology/Oncology, Nationwide Children's Hospital, Columbus, OH, United States, [3] Department of Pediatrics, College of Medicine, The Ohio State University, Columbus, OH, United States, [4] Division of Rheumatology, Allergy and Immunology, The University of North Carolina at Chapel Hill, Chapel Hill, NC, United States, [5] Division of Rheumatology, Nationwide Children's Hospital, Columbus, OH, United States, [6] Division of Biostatistics, College of Public Health, The Ohio State University, Columbus, OH, United States, [7] Department of Microbiology and Immunology, Loyola University Chicago, Maywood, IL, United States

OPEN ACCESS

Edited by:
José Carlos Crispín, Instituto Nacional de Ciencias Médicas y Nutrición Salvador Zubirán (INCMNSZ), Mexico

Reviewed by:
Kenji Oku, Hokkaido University, Japan
Gabriela Hernandez-Molina, Instituto Nacional de Ciencias Médicas y Nutrición Salvador Zubirán (INCMNSZ), Mexico

***Correspondence:**
Stephanie L. Savelli
ssavelli@akronchildrens.org
Robert A. S. Roubey
robert_roubey@med.unc.edu
Yee Ling Wu
ywu24@luc.edu
Chack-Yung Yu
chack-yung.yu@nationwidechildrens.org

Specialty section:
This article was submitted to Autoimmune and Autoinflammatory Disorders, a section of the journal Frontiers in Immunology

Received: 11 December 2018
Accepted: 05 April 2019
Published: 07 May 2019

Citation:
Savelli SL, Roubey RAS, Kitzmiller KJ, Zhou D, Nagaraja HN, Mulvihill E, Barbar-Smiley F, Ardoin SP, Wu YL and Yu C-Y (2019) Opposite Profiles of Complement in Antiphospholipid Syndrome (APS) and Systemic Lupus Erythematosus (SLE) Among Patients With Antiphospholipid Antibodies (aPL). Front. Immunol. 10:885. doi: 10.3389/fimmu.2019.00885

APS is the association of antiphospholipid antibodies (aPL) with thromboses and/or recurrent pregnancy loss (RPL). Among patients with SLE, one-third have aPL and 10–15% have a manifestation of secondary APS. Animal studies suggested that complement activation plays an important role in the pathogenesis of thrombosis and pregnancy loss in APS. We performed a cross-sectional study on complement proteins and genes in 525 patients with aPL. Among them, 237 experienced thromboses and 293 had SLE; 111 had both SLE and thromboses, and 106 had neither SLE nor thrombosis. Complement protein levels were determined by radial immunodiffusion for C4, C3 and factor H; and by functional ELISA for mannan binding lectin (MBL). Total *C4*, *C4A* and *C4B* gene copy numbers (GCN) were measured by TaqMan-based realtime PCR. Two to six copies of *C4* genes are frequently present in a diploid genome, and each copy may code for an acidic C4A or a basic C4B protein. We observed significantly (a) *higher* protein levels of total C4, C4A, C4B, C3, and anticardiolipin (ACLA) IgG, (b) increased frequencies of lupus anticoagulant and males, and (c) decreased levels of complement factor H, MBL and ACLA-IgM among patients with thrombosis than those without thrombosis ($N = 288$). We also observed significantly *lower* GCNs of total *C4* and *C4A* among aPL-positive patients with both SLE and thrombosis than others. By contrast, aPL-positive subjects with SLE had significantly reduced protein levels of C3, total C4, C4A, C4B and ACLA-IgG, and higher frequency of females than those without SLE. Patients with thrombosis but *without* SLE ($N = 126$), and patients with SLE but *without* thrombosis ($N = 182$) had the greatest differences in mean protein levels of C3 ($p = 2.6 \times 10^{-6}$), C4 ($p = 2.2 \times 10^{-9}$) and ACLA-IgG ($p = 1.2 \times 10^{-5}$). RPL occurred in 23.7% of female patients and thrombotic SLE patients had the highest frequency of RPL (41.0%; $p = 3.8 \times 10^{-10}$). Compared with non-RPL females, RPL had significantly

higher frequency of thrombosis and elevated C4 protein levels. Female patients with homozygous C4A deficiency *all* experienced RPL ($p = 0.0001$) but the opposite was true for patients with homozygous C4B deficiency ($p = 0.017$). These results provide new insights and biomarkers for diagnosis and management of APS and SLE.

Keywords: C3 and C4, C4A and C4B, Copy number variation, Factor H, Lupus anticoagulant, Mannan binding lectin, Recurrent pregnancy loss, Thrombosis

INTRODUCTION

Antiphospholipid syndrome (APS) is characterized by vascular thrombosis and/or pregnancy morbidity such as recurrent fetal loss in the persistent presence of antiphospholipid antibodies (aPL) (1–7). aPL are a heterogeneous group of autoantibodies that include antibodies against phospholipid binding protein β_2-glycoprotein I (β_2GPI), anticardiolipin antibodies (ACLA), and lupus anticoagulant (LAC) (8). Human subjects with triple positivity for all three groups of aPL appeared to be at high risk to experience recurrent thromboembolic events (9). A majority of clinical tests for aPL detects antibodies against β_2GPI. β_2GPI is a plasma protein consisting of five structural domains known as short consensus repeats that are characteristic features of controlling proteins for the complement system (10–12).

SLE is a common autoimmune disease associated with APS. SLE features the generation of autoantibodies against nuclear antigens including double-stranded DNA (13, 14). In a study of European APS patients, over 40% were found to have SLE or a lupus-like disease (15). Among the general SLE population, between 30 and 40% have aPL; and 10–15% of patients with SLE also have clinical manifestations of APS (15–20). In addition to the presence of autoantibodies, *hypo*complementemia is another hallmark of human SLE (21–25). Low serum complement levels for C4 and C3 in patients with SLE can be triggered by a combination of heritable and acquired factors: genetic deficiencies, low copy number of complement *C4* genes, robust consumption caused by immune complex-mediated complement activation, or the presence of inhibitors that inactivate or prevent accessibility. A complete genetic deficiency in any one of the early components specific for the classical complement activation pathway *almost always* lead to pathogenesis of human SLE, inferring that an intact classical pathway of the complement system is essential for the protection against systemic autoimmunity (26–28).

Activations of complement C3 and C5 in the presence of antigen-antibody complexes occur via the formation of the C1 complex (C1q-C1r_2-C1s_2), followed by the activations of C4 and C2 to form C4b and C2a, respectively (29). C4b and C2a are subunits of the C3 and C5 convertases, essential for the classical and lectin activation pathways (26). There are two isotypes of native C4 proteins. C4A is the acidic isotype believed to play an essential role in immune clearance and immunotolerance. C4B is the basic isotype that is capable of rapid propagation of complement activation (30–34). In a diploid genome, complement *C4* gene copy number varies among different individuals. Two to eight copies of *C4* genes are generally present in a diploid genome among most human subjects (35, 36). Each *C4* gene either codes for a C4A or a C4B protein. Such gene copy number variation contributes to quantitative and qualitative diversities in C4 protein levels and function, and therefore different intrinsic strengths for effector functions of innate and adaptive immune responses (25, 34, 36–40). Among European and East-Asian subjects, low copy number of total *C4* or *C4A* is a risk factor for SLE, while high copy number of total *C4* or *C4A* is protective against susceptibility to SLE (22, 38, 41, 42).

An injection of human aPL into animal models including wild-type *mice* induced an increase in thrombus size (43, 44). An injection of human aPL into pregnant mice resulted in fetal resorption. (45, 46). Mice *deficient* in complement C3 or C5, as well as mice injected with a monoclonal antibody against C5, did *not* exhibit an increase in thrombus size in the presence of aPL. Blockade of complement activation by genetic deletion of C3 or C4, or with transgenic insertion of complement regulatory protein Crry-Ig, a soluble inhibitor of mouse C3 convertase, *protected* mice, rats or hamsters from pregnancy complications induced by injections of human aPL (45, 47–56). These phenomena suggest that complement proteins or their activated products are engaged in the pathogenesis of APS, as they probably provide immune effectors for aPL-mediated thromboses, tissue injury and/or fetal loss in mouse models. The generation of immune complexes between aPL and ligands (such as β_2GPI binding to phospholipids) leads to activation of the complement classical pathway, release of C5a and C3a anaphylatoxins (50, 57, 58), which may attract neutrophils and other granulocytes to the site of complement activation, increase vascular permeability, and elicit inflammatory response that contributes to tissue injuries including pregnancy morbidity. Culmination of complement activation pathways leads to the assembly of the membrane attack complex (C5b-9) and provides the "second-hit" to trigger vascular thrombosis (53). Consistent with this notion, it was shown that C3, C5, or C6-deficient rodents were protected from aPL induced thrombosis (56, 59). Such protective effects of complement deficiency in APS-associated disorders observed in

Abbreviations: ANOVA, analysis of variance; aPL, antiphospholipid antibodies; APS, antiphospholipid syndrome; CNV, copy number variation; GCN, gene copy number; LAC, lupus anticoagulant; MBL, mannan binding lectin; NS, no SLE; NT, no thrombosis; NTS, no thrombosis and no SLE; RMSE, root mean square error; RPL, recurrent pregnancy loss; S, SLE; S_o, SLE without thrombosis; SLE, systemic lupus erythematosus; T, thrombosis, T_o, thrombosis without SLE; TS, thrombosis and SLE.

animal models are opposite to the causal effects of deficiencies in early components for the classical complement pathway in human lupus (26, 60). Among human patients with APS, elevated levels of complement activation products (C4a, C3a, C5a, C5b-9) have been demonstrated (55, 61, 62). However, systematic and meticulous studies on how complement proteins and genes contribute to the pathology of human APS (recurrent vascular thrombosis or pregnancy morbidity) and the concurrence of SLE and APS were scarce or limited by small sample size.

Here we performed a cross-sectional study on 525 human subjects with aPL from the Antiphospholipid Syndrome Collaborative Registry. Based on clinical presentations of thrombosis and SLE, these subjects were categorized to four groups: patients with thrombosis only (T_o), with thrombosis and SLE (TS), with SLE only (S_o), and without thrombosis and without SLE (NTS). Plasma protein concentrations for complement total C4, C4A, C4B, C3, factor H, and functional mannan binding lectin (MBL) were measured. Total *C4*, *C4A* and *C4B* gene copy numbers were elucidated. The results reveal substantial phenotypic differences for complement protein concentrations among patients with thromboses or recurrent pregnancy loss, and SLE. There was also a significant difference in *C4* gene copy number variations between patients with both thrombosis and SLE, and patients without SLE and thrombosis.

PATIENTS AND METHODS

Study Population

This study was approved by the Institutional Review Board at Nationwide Children's Hospital. Peripheral blood plasma and matched genomic DNA samples without personal identifiers from 525 patients with aPL and clinical status were provided by the APS Core at University of North Carolina (8, 63). These aPL-positive patients were recruited with written informed consent. Of these patients, 444 (84.57%) were female and 81 (15.43%) were male. The mean age (±SD) was 45.01 ± 12.97 years old. Among these aPL-positive patients, 184 (35.05%) met the Sapporo criteria for definite APS (1); an additional 175 subjects (33.33%) met the extended definition of APS, and 166 asymptomatic subjects (31.6%) who had aPL but no manifestations of thrombosis or pregnancy morbidity. Patients with definite APS as defined by the preliminary or modified Sapporo criteria (1, 6) must have one or more clinical episodes of vascular thrombosis and/or pregnancy morbidity as well as ACLA, anti-β_2GPI IgG and/or IgM or LAC present on two or more occasions at least 6 weeks apart. The expanded APS group was defined by institutions participating in APSCORE and include those patients with one or more clinical manifestations characteristic of APS but not fulfilling the strict definition and either the Sapporo laboratory criteria or one of a group of APS-associated autoantibodies. Asymptomatic patients fulfill the Sapporo laboratory criteria but have no clinical manifestations related to APS.

To perform refined analyses based on clinical presentations, we segregated the aPL subjects based on the presence and absence of thrombosis, SLE and recurrent pregnancy loss. Among the study cohort, 237 subjects had a history of thrombosis and 288 subjects did not have thrombosis. A total of 293 subjects were diagnosed with SLE according to the American College of Rheumatology criteria (64) and 232 subjects did not have a diagnosis of SLE at the time of recruitment. Of the 444 female subjects with aPL, 106 (23.87%) experienced recurrent pregnancy loss.

Quantifications of Total *C4*, *C4A*, and *C4B* Genes by Real-Time PCR

A series of real-time PCR assays was applied to determine the copy number variations of total *C4*, *C4A*, and *C4B* genes (35). All real time PCR assays used the TaqMan MGB probes (ABI). The target probes (*C4*, *C4A*, and *C4B*) were VIC-labeled. The endogenous control probe, which targeted an invariant exon 4 of the *RP1* gene, was FAM-labeled. Each reaction consisted of 0.5 to 1 μM of both forward and reverse primers for the target and control amplicons, 100 nM of the target and endogenous control probes, 25 ng of sample DNA and TaqMan Universal PCR master mix (ABI, PN 4323018). All assays were performed in triplicates using the ABI 7500 RT-PCR system per manufacturer's recommendations. The relative standard curve method was utilized to calculate the copy number of each target gene. The accuracy of *C4A* and *C4B* gene copy number assignments for each sample was cross-confirmed as the gene copy number of total *C4* equals the sum of *C4A* and *C4B*.

Complement C3, C4, Factor H (CFH) and Mannan Binding Lectin (MBL) Protein Concentrations in Citrate-Plasma

Platelet poor plasma samples were processed with a consistent protocol. Briefly, blood samples in citrate tubes were centrifuged at 1,500 *g* for 10 min, at 4–8°C. Plasma samples were transferred to microcentrifuge tubes and spun again at 2,000 *g* for 5 min. Aliquots were kept frozen at −80°C. Plasma protein concentrations of complement C3 and C4 were determined by single radial immunodiffusion assays using commercial kits from The Binding Site (Birmingham, United Kingdom). A comparison of C4 protein concentrations of (a) SLE patients without thrombosis from this study and (b) an *independent* cross-sectional study of Ohio SLE (38) revealed that protein concentrations of complement C4 assayed from platelet-poor citrate plasma, which were subjected to two rounds of centrifugation, were ∼14.5% *lower* than that of EDTA-plasma C4 harvested after a single round of centrifugation.

Complement factor H plasma protein concentrations were measured using homemade RID plates according to a standard protocol (65). Plasma concentrations for MBL were determined using a functional assay kit from the Antibody Shop (Denmark).

Complement C4 Protein Allotyping

Plasma C4A and C4B protein allotypes were determined by immunofixation and immunoblot techniques, as described previously (66–68). The relative band intensities of C4A and C4B allotypes from each sample were quantified by ImageQuant Software. The corresponding plasma C4A and C4B protein concentrations were calculated from the total C4 protein concentrations.

TABLE 1 | Demographics of study populations: aPL patients with definite APS, extended APS and non-APS.

	Definite APS	Extended APS	Non-APS	p^*
n (%)	184 (35.1)	175 (33.3)	166 (31.6)	
Sex, F/M (ratio)	147/37 (4.20:1)	152/23 (6.61:1)	145/21 (6.90:1)	0.099
Age ± SD; years old	44.40 ± 12.54	46.82 ± 13.09	43.78 ± 13.19	0.071
Race: White/Black/Others,‖ *n* (% in each group)	81/24/79 (44.0/13.0/42.9)	67/27/81 (38.3/15.4/46.3)	80/23/63 (48.2/13.9/38.0)	0.44
BMI	28.66 ± 6.86	28.94 ± 7.58	28.22 ± 6.57	0.64
Thrombosis, Y/N, *n* (%)	154/30 (83.7)	83/92 (47.4)	0/166 (0)	$\mathbf{1.4 \times 10^{-69}}$
Pregnancy loss, female, Y/N, *n* (%)	80/67 (54.4)	26/126 (17.1)	0/166 (0)	$\mathbf{1.7 \times 10^{-32}}$
SLE, Y/N, *n* (%)	89/95 (48.4)	99/76 (56.6)	105/61 (63.3)	**0.019**
Complement C3 ± SD; mg/dL	124.1 ± 36.0	128.4 ± 37.8	118.8 ± 33.4	**0.048**
Complement C4 ± SD; mg/dL	22.9 ± 10.9	20.0 ± 9.2	16.6 ± 8.8	$\mathbf{2.6 \times 10^{-8}}$
Correlations between C3 and C4, r^2	0.217 ($p = \mathbf{3.0 \times 10^{-11}}$)	0.310 ($p = \mathbf{2.7 \times 10^{-15}}$)	0.321 ($p = \mathbf{4.0 \times 10^{-15}}$)	

r, coefficient of correlation.

**p values obtained by χ^2 analyses for categorical data, or by ANOVA (analysis of variance) for continuous data; ‖others: other racial and multi-racial groups; p- <0.05 are in bold fonts.*

Statistical Analyses

Descriptive statistics, including means, standard deviations (SD), and 95% confidence intervals (95% CI) were computed for numeric data, and frequency distributions were determined for categorical variables, using statistical software JMP13 (SAS Institute) and GraphPad Prism6 software. Two group comparisons were based on *t*-tests that accounted for unequal variances if appropriate. Specifically, Tukey HSD test with an alpha set at 0.05 was applied, and was followed by pairwise Student's *t*-tests that yielded *p*-values. Dunnett's test with an alpha of 0.05 was applied for comparing study groups to controls. Categorical data were compared by χ^2 analyses and odds ratios were calculated whenever appropriate.

To allow a standardized comparison of all continuous parameters contributing to thrombosis without SLE, SLE without thrombosis, SLE with thrombosis, and no thrombosis and no SLE, we determined the root mean square error (RMSE) of each parameter in these four groups by analysis of variance (ANOVA). The difference in the mean protein levels for each protein between any two groups divided by its RMSE to give the effect size index (69). The mean values of parameters in the NTS group were used as references and the *effect size indices* for T_o, S_o, and TS groups were graphically plotted. This enabled a uniform depiction on effects of all continuous parameters under different clinical conditions.

Stepwise multiple logistic regression analyses were used to identify independent parameters significant for clinical outcomes: thrombosis, arterial thrombosis, venous thrombosis, pregnancy loss, and SLE. Such analyses allowed controlled studies for continuous and categorical parameters. For analyses of a clinical presentation as a response, we first put all parameters studied [i.e., C3 or C4, factor H, MBL, ACLA-IgM, ACLA-IgG, BMI, age, gender (F/M), LAC (presence or absence), SLE (presence or absence)] into the regression model. Those that did not give a *p*-value smaller than 0.1 were removed from the subsequent analyses. The last best model with parameters represented by *p*-values smaller than 0.05 was maintained and presented. Unit Odds Ratio (OR) and range OR were computed. Parameters that could not coexist in the regression model because of strong correlation (e.g., C3 and C4) were put into the regression models separately and the stronger parameter was kept. When C4 was identified as a significant parameter in a model, we further asked whether C4A or C4B or both C4 isotypes were playing a major role.

RESULTS

The study population consisted of 525 human subjects with antiphospholipid antibodies (aPL), recruited through the APSCORE. The mean age of subjects at the time of recruitment was 45.0 ± 13.0 (mean ± SD) years old. These study subjects were initially segregated into three groups: definite APS, extended APS, and non-APS based on clinical manifestations associated with APS, which included vascular thromboses and pregnancy morbidity. Results for an initial characterization for these three groups of patients are shown in **Table 1**. One remarkable feature emerged was the steady and highly significant increase in the mean protein concentration of complement C4 from non-APS (16.6 ± 8.8 mg/dL), to extended APS (20.0 ± 9.2 mg/dL), and definitive APS (22.9 ± 10.0 mg/dL) ($p = 2.6 \times 10^{-8}$). These three groups of patients had different frequencies of SLE, thromboses and pregnancy morbidities. Thus, we set to examine quantitative variations of plasma complement proteins among aPL subjects with different clinical manifestations for thrombosis and/or SLE in both female and male patients, and recurrent pregnancy loss among female patients. The demographic and clinical features for these aPL-positive subjects are shown in **Table 2**.

Variations of Plasma Complement Protein and ACLA Levels in aPL-Positive Subjects With and Without Thromboses

Among the aPL-positive subjects, 45.1% had a past history of thrombosis, and 55.8% were diagnosed with SLE at the time of recruitment. When the mean plasma complement

TABLE 2 | Demographic data and disease status of aPL-positive subjects.

A. Thrombosis status					
	T	**NT**	***p***		
N	237	288			
Age	46.4 ± 13.4	43.9 ± 12.5	**0.029**		
Sex			**7.2×10^{-6}**		
F	182 (0.768)	262 (0.910)			
M	55 (0.232)	26 (0.090)			
F/M ratio	3.21	10.1			
BMI	29.6 ± 7.6	27.8 ± 6.4	**0.0033**		
Race			0.72		
White	107 (0.452)	121 (0.420)			
Black	31 (0.131)	43 (0.149)			
Others	99 (0.418)	124 (0.431)			
B. SLE status					
	S	**NS**			
N	293	232			
Age	44.6 ± 12.4	45.5 ± 13.7	0.42		
Sex			**0.0031**		
F	260 (0.884)	184 (0.793)			
M	33 (0.113)	48 (0.207)			
F/M ratio	7.88	3.83			
BMI	28.7 ± 7.3	28.5 ± 6.7	0.76		
Race, *n* (frequency in each group)			**7.0×10^{-7}**		
White	107 (0.365)	121 (0.522)			
Black	60 (0.205)	14 (0.060)			
Others	126 (0.430)	97 (0.418)			
C. Thrombosis and SLE status					
	T_O	**TS**	**S_O**	**NTS**	**p**
N	126	111	182	106	
Age	47.7±13.9	44.9 ± 12.8	44.4 ± 12.1	43.0 ± 13.1	**0.041**
Sex					**1.2×10^{-7}**
F	85 (0.675)	97 (0.874)	163 (0.896)	99 (0.934)	
M	41 (0.325)	14 (0.126)	19 (0.104)	7 (0.066)	
F/M ratio	2.07	6.93	8.58	14.1	
BMI	29.7 ± 7.2	29.5 ± 8.0	28.2 ± 6.7	27.0 ± 5.8	**0.014**
Race					**2.9×10^{-6}**
White	60 (0.476)	47 (0.423)	60 (0.330)	61 (0.576)	
Black	11 (0.087)	20 (0.180)	40 (0.220)	3 (0.028)	
Others	55 (0.436)	44 (0.396)	82 (0.451)	42 (0.396)	
Pregnancy loss					**2.0×10^{-10}**
yes	24 (0.282)	44 (0.448)	14 (0.086)	24 (0.242)	
no	61 (0.718)	53 (0.552)	149 (0.914)	75 (0.758)	
Correlations between C3 and C4					
r^2	0.167	0.212	0.320	0.352	
p	**2.0×10^{-6}**	**5.3×10^{-7}**	**2.5×10^{-16}**	**2.5×10^{-11}**	

Key: BMI, body mass index; NS, no SLE; NT, no thrombosis; NTS, no thrombosis and no SLE; S, SLE; S_O, SLE without thrombosis; T, thrombosis; T_O, thrombosis without SLE; TS, thrombosis and SLE; frequency in each group is shown in parenthesis. p-values of statistical significance are in bold fonts.

protein concentrations and aPL between thrombotic and non-thrombotic groups were compared, highly significant phenotype differences for total C4, C4A, C4B, MBL, ACLA-IgM, and ACLA-IgG were observed (**Table 3**). The mean protein level (and 95% confidence interval) for total C4 was 22.7 (21.3–24.0) mg/dL in the thrombotic group, and 17.7 (16.6–18.7) mg/dL in the non-thrombotic group, which represented a difference of 28.2% ($p = 1.3 \times 10^{-8}$).

Parallel increases in complement C4A and C4B were observed in the thrombotic group. Mean concentration of plasma C4A in

TABLE 3 | Mean plasma complement and ACLA protein levels in aPL-positive subjects with (T) and without thrombosis (NT).

	n	Mean ± SD	95% CI	*p* (NT vs. T)
C3 protein (mg/dL)				**0.013**
NT	284	120.2 ± 35.1	116.1–124.3	
T	236	128.1 ± 36.6	123.4–132.8	
C4 protein (mg/dL)				**1.3×10^{-8}**
NT	282	17.7 ± 9.0	16.6–18.7	
T	235	22.7 ± 10.6	21.3–24.0	
C4A protein (mg/dL)				**8.2×10^{-6}**
NT	273	9.6 ± 5.6	8.9–10.3	
T	233	12.1 ± 6.7	11.2–12.9	
C4B protein (mg/dL)				**6.7×10^{-6}**
NT	283	8.3 ± 5.0	7.8–8.9	
T	234	10.5 ± 6.0	9.8–11.3	
CFH protein (mg/dL)				0.057
NT	249	52.3 ± 15.0	50.5–54.2	
T	207	49.9 ± 12.1	48.2–51.5	
MBL protein				**0.0007**
NT	242	0.167 ± 0.173	0.145–0.189	
T	214	0.117 ± 0.129	0.100–0.135	
ACLA IgM protein (MPL)				**0.0022**
NT	254	29.9 ± 37.5	25.3–34.6	
T	202	19.5 ± 33.2	14.9–24.1	
ACLA IgG protein (GPL)				**0.0043**
NT	254	29.6 ± 46.7	23.9–35.4	
T	206	45.1 ± 68.4	35.7–54.5	
			Odds ratio (95% CI)	***p***
LAC-Positivity (freq.)			2.63 (1.76–3.94)	**1.3×10^{-6}**
NT	260	0.531		
T	199	0.749		
Sex (F/M ratio)			0.33 (0.20–0.54)	**7.2×10^{-6}**
NT	288 (262/26)	10.0		
T	237 (182/55)	3.23		

CI, confidence interval. Odds ratios were calculated for T vs. NT. p-values of statistical significance are in bold fonts.

the thrombotic group was 12.1 (11.2–12.9) mg/dL, and 9.6 (8.9–10.3) mg/dL in the non-thrombotic group ($p = 8.2 \times 10^{-6}$). Plasma C4B mean protein concentration in the thrombotic group was 10.5 (9.8–11.3) mg/dL, and 8.3 (7.8–8.9) mg/dL in the non-thrombotic group ($p = 6.7 \times 10^{-6}$). For complement C3, moderately higher mean protein level was observed in the thrombotic group than the non-thrombotic group (T: 128.1 mg/dL; NT: 120.2 mg/dL; $p = 0.013$).

By contrast, mean plasma protein level for functional MBL among thrombotic subjects was significantly *lower* than that of non-thrombotic subjects, which were 0.117 (0.100–0.135) mg/dL and 0.167 (0.145–0.189) mg/dL, respectively ($p = 0.0007$). Slightly lower levels of factor H protein were also observed in the thrombotic group (T: 49.9 mg/dL; NT: 52.3 mg/dL; $p = 0.057$).

The mean values of anticardiolipn antibodies among thrombotic subjects were 19.5 (14.9–24.1) units for ACLA-IgM and 45.1 (35.7–54.5) units for ACLA-IgG. In non-thrombotic subjects, the corresponding values were 29.9 (25.3–34.6) and 29.6 (23.9–35.4) units ($p = 0.0022$ for ACLA-IgM; $p = 0.0043$ for ACLA-IgG). Thrombotic subjects had lower levels of ACLA-IgM but higher levels of ACLA-IgG. Three-quarters (74.9%) of thrombotic subjects tested positive for the presence of lupus anticoagulant (LAC), compared to slightly over one-half (53.3%) among non-thrombotic subjects ($p = 1.7 \times 10^{-6}$).

Thrombotic subjects had significantly lower female to male ratio (3.23 to 1) when compared with non-thrombotic subjects (10.0 to 1; $p = 7.2 \times 10^{-6}$).

Plasma Complement Protein and ACLA Levels in aPL-Positive Subjects With and Without SLE

Quantitative variations of complement and ACLA plasma protein were compared between the aPL-positive patients with and without SLE (**Table 4**). The mean C3 concentrations were 118.3 (114.2–122.4) mg/dL in SLE and 130.8 (126.2–135.4) mg/dL in non-SLE, which represented a *reduction*

TABLE 4 | Mean plasma protein concentrations of complement and ACLA in aPL-positive subjects with (S) and without (NS) SLE.

	n	Mean ± SD	95% CI	*p* (NS vs. S)
C3 protein (mg/dL)				**8.0×10^{-5}**
NS	230	130.8 ± 35.4	126.2–135.4	
S	290	118.3 ± 35.6	114.2–122.4	
C4 protein (mg/dL)				**0.0006**
NS	230	21.6 ± 9.6	20.4–22.9	
S	287	18.6 ± 10.3	17.4–19.8	
C4A protein (mg/dL)				**0.0038**
NS	228	11.6 ± 5.8	10.9–12.4	
S	278	10.0 ± 6.5	9.2–10.8	
C4B protein (mg/dL)				**0.005**
NS	230	10.1 ± 5.4	9.4–10.8	
S	287	8.7 ± 5.7	8.1–9.4	
CFH protein (mg/dL)				**0.02**
NS	203	52.9 ± 14.4	50.9–54.9	
S	253	49.9 ± 13.1	48.3–51.5	
MBL protein				0.29
NS	204	0.135 ± 0.140	0.116–0.154	
S	252	0.151 ± 0.168	0.130–0.172	
ACLA IgM protein (MPL)				0.22
NS	183	22.8 ± 29.6	18.5–27.1	
S	273	27.0 ± 39.7	22.3–31.8	
ACLA IgG protein (GPL)				**0.0002**
NS	187	48.8± 70.1	38.7–59.0	
S	273	28.2 ± 46.1	22.7–33.7	
			Odds ratio (95% CI)	**p**
LAC-positivity (freq)			0.79 (0.54–1.16)	0.22
NS	190	0.658		
S	269	0.602		
Sex (F/M ratio)			2.06 (1.27–3.33)	**0.0031**
NS	232 (184/48)	3.81		
S	293 (260/33)	7.62		

LAC, lupus anticoagulant. Odds ratios were calculated for S vs. NS. p-values of statistical significance are in bold fonts.

of 9.6% of mean C3 level in SLE ($p = 8 \times 10^{-5}$). The mean total C4 concentrations were 18.6 (17.4–19.8) mg/dL in SLE and 21.6 (20.4–22.9) mg/dL in non-SLE, which corresponded to a reduction of 13.9% of total C4 in SLE ($p = 0.0006$). The mean C4A and C4B concentrations were 10.0 (9.2–10.8) mg/dL and 8.7 (8.1–9.4) mg/dL, respectively, in the SLE group; and were 11.6 (10.9–12.4) mg/dL and 10.1 (9.4–10.8) mg/dL, respectively, in the non-SLE group ($p = 0.0038$ for C4A; $p = 0.005$ for C4B). Thus, *lower* plasma levels of complement C3 and C4 were conspicuous in the SLE group.

The mean plasma protein levels of MBL between the SLE and non-SLE groups were *not* significantly different [S: 0.151 (0.130–0.172) mg/dL, NS: 0.135 (0.116–0.154) mg/dL; $p = 0.29$]. The mean plasma protein level of factor H was slightly lower in the SLE group [49.9 (48.3–51.5) mg/dL] than that in the non-SLE group [52.9 (50.9–54.9) mg/dL; $p = 0.02$].

The mean ACLA-IgG level was significantly *lower* in the SLE than non-SLE [S: 28.2 (22.7–33.7) GPL, NS: 48.8 (38.7–59.0); $p = 0.0002$]. By contrast, the mean ACLA-IgM levels and the frequency for the presence of LAC were similar between the SLE and the non-SLE groups.

Among the aPL subjects, SLE patients had a higher female to male ratio (7.62 to 1) than non-SLE patients (3.81 to 1; $p = 0.0031$).

Differential Plasma Protein Levels of Complement and ACLA in aPL-Positive Subjects With Thrombosis, SLE, Both Thrombosis and SLE, and Neither Thrombosis Nor SLE

Our study results revealed *higher* levels of mean plasma complement C4, C3, and ACLA-IgG in aPL-positive subjects

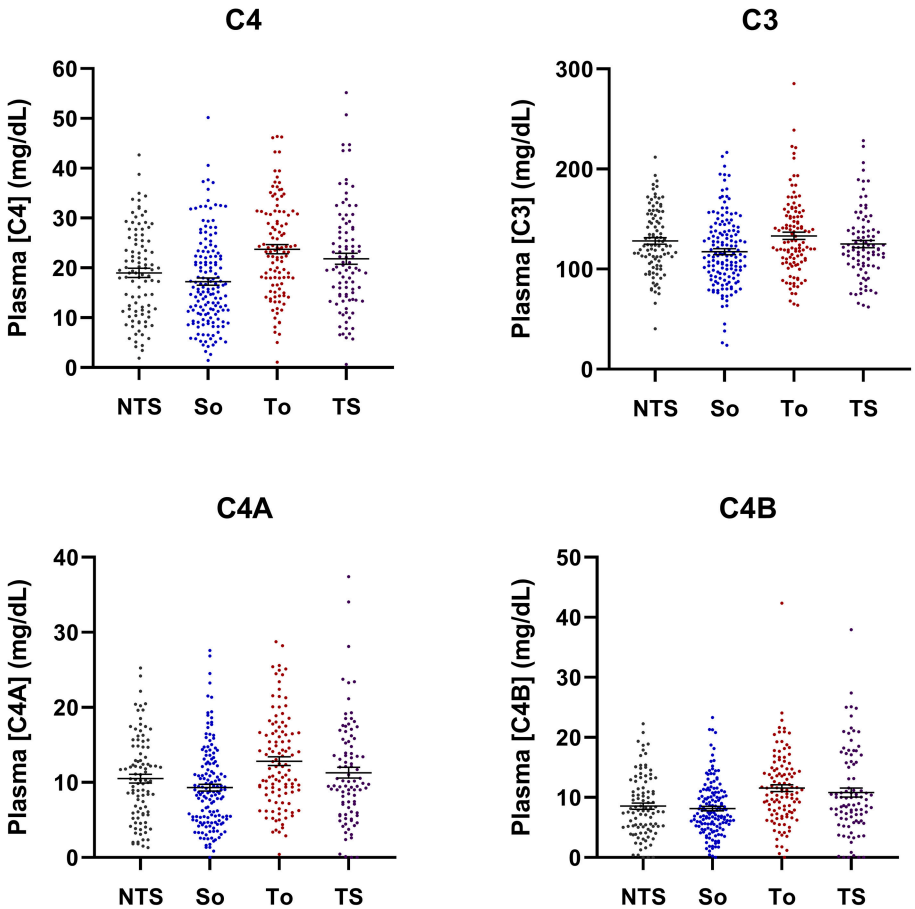

FIGURE 1 | Scattered-plots of complement C4 and C3 plasma protein concentrations in aPL-positive subjects segregated by thrombosis and SLE status and compared. NTS, no thrombosis and no SLE; S_o, SLE only, T_o, thrombosis only; TS, with both thrombosis and SLE. Horizontal bars represent means and standard errors. Overall *p*-values are: 2.8×10^{-7} for C4; 0.0024 for C3; 5.9×10^{-5} for C4A; and 2.7×10^{-6} for C4B.

with a history of thrombosis, but *lower* levels of complement C4, C3, and ACLA-IgG among aPL-positive subjects with SLE. A proportion (37.9%) of aPL-positive subjects diagnosed with SLE also experienced thromboses. To distinguish the roles of complement proteins and ACLA in thromboses and SLE, we segregated the study subjects according to their thrombosis and SLE status: thrombosis only (T_o), thrombotic SLE (TS), SLE only (S_o), and no thrombosis and no SLE (NTS) (**Figure 1**, **Table 5**). Among these four groups, significantly higher mean protein levels were observed for patients with thrombosis only than with SLE only for plasma protein levels of total C4 ($p = 2.2 \times 10^{-9}$), C4A ($p = 1.9 \times 10^{-6}$), C4B ($p = 1.3 \times 10^{-6}$), C3, ($p = 2.6 \times 10^{-5}$), ACLA-IgG ($p = 1.2 \times 10^{-5}$), and in female to male ratio sex ratio ($p = 1.6 \times 10^{-6}$).

For functional MBL and the presence of LAC, main differences were observed between the thrombotic groups and the non-thrombotic groups. Mean MBL protein levels were significantly lower in T_o and TS than in S_o (T_o vs. S_o, $p = 0.0041$; TS vs. S_o, $p = 0.0046$). The mean level of MBL in aPL-positive subjects without thrombosis and SLE (NTS) was slightly higher than those of T_o and TS ($p = 0.078$ and 0.076), and similar to that of S_o ($p = 0.416$). For lupus anticoagulant, 73.5% of patients in T_o and 76.3% of patients in TS were tested positive, compared to 51.2% in S_o (T_o vs. S_o, $p = 0.0002$; TS vs. S_o, $p = 0.000038$) and 56.8% in NTS (T_o vs. NTS, $p = 0.015$; TS vs. NTS, $p = 0.0048$).

Gene Copy Number Variations of Total *C4*, *C4A*, and *C4B* in Patients With aPL

Gene copy numbers (GCN) for total *C4*, *C4A*, and *C4B* from 472 aPL-positive subjects were elucidated by TaqMan based real-time PCR using genomic DNA (35). The copy number of total *C4* genes in this study cohort varied from 2 to 6; *C4A* from 0 to 5; and *C4B* from 0 to 4. The distribution of total *C4*, *C4A*, and *C4B* gene copy number variations among T_o, TS, S_o, and NTS are shown in **Table 6**.

The distribution of GCN groups was analyzed first as categorical data. The distribution of *C4A* genes was statistically different among T_o, TS, S_o, and NTS ($p = 0.034$, χ^2 analysis). Variations of GCNs for total *C4* ($p = 0.088$) and *C4B* ($p = 0.13$)

TABLE 5 | Mean plasma protein levels of complement and ACLA in aPL-positive subjects segregated by thrombosis and SLE status.

	n	Concentrations	95% CI	P T_O: TS	T_O: S_O	T_O: NTS	TS: S_O	TS: NTS	S_O: NTS
C3 protein (RMSE: 35.4)		mg/dL		**0.011**	**2.6×10^{-5}**	0.18	0.19	0.26	**0.011**
1. T_O	126	133.6 ± 37.8	127.0–140.3						
2. TS	110	121.8 ± 34.4	115.3–128.3						
3. S_O	180	116.1 ± 36.2	110.8–121.5						
4. NTS	104	127.3 ± 32.2	121.0–133.6						
C4 protein (RMSE: 9.72)		mg/dL		0.073	**2.2×10^{-9}**	**0.0004**	**0.0001**	0.083	0.056
1. T_O	126	23.7 ± 9.7	22.0–25.4						
2. TS	109	21.4 ± 11.5	19.2–23.6						
3. S_O	178	16.8 ± 9.0	15.5–18.1						
4. NTS	104	19.1 ± 8.8	17.4–20.8						
C4A protein (RMSE: 6.12)		mg/dL		0.247	**1.9×10^{-6}**	**0.017**	**0.0009**	0.23	**0.049**
1. T_O	126	12.5 ± 5.9	11.5–13.5						
2. TS	107	11.6 ± 7.6	10.1–13.0						
3. S_O	171	9.0 ± 5.6	8.2–9.9						
4. NTS	102	10.5 ± 5.6	9.5–11.6						
C4B protein (RMSE: 5.46)		mg/dL		**0.045**	**1.3×10^{-6}**	**0.0008**	**0.012**	0.19	0.31
1. T_O	126	11.2 ± 5.3	10.3–12.2						
2. TS	108	9.8 ± 6.7	8.5–11.0						
3. S_O	179	8.1 ± 4.9	7.4–8.8						
4. NTS	104	8.8 ± 5.2	7.8–9.8						
CFH protein (RMSE:13.7)		mg/dL		0.059	0.78	0.121	0.079	**0.001**	0.053
1. T_O	111	51.5 ± 13.6	49.0–54.1						
2. TS	96	47.9 ± 9.7	46.0–49.9						
3. S_O	157	51.1 ± 14.6	48.8–53.4						
4. NTS	92	54.5 ± 15.4	51.3–57.7						
MBL protein (RMSE: 0.154)		mg/dL		0.95	**0.0041**	0.078	**0.0046**	0.076	0.42
1. T_O	114	0.118 ± 0.140	0.092–0.144						
2. TS	100	0.117 ± 0.115	0.094–0.139						
3. S_O	152	0.173 ± 0.192	0.143–0.204						
4. NTS	90	0.157 ± 0.137	0.128–0.185						
ACLA-IgM protein (RMSE: 35.7)		g/L		0.28	**0.0039**	**0.013**	0.092	0.092	0.95
1. T_O	101	16.8 ± 24.7	11.9–21.7						
2. TS	101	22.3 ± 39.9	14.4–30.1						
3. S_O	172	29.8 ± 39.5	23.9–35.8						
4. NTS	82	30.1 ± 33.4	22.8–37.5						
ACLA-IgG protein (RMSE: 56.9)		g/L		**0.0063**	**1.2×10^{-5}**	0.058	0.17	0.488	**0.041**
1. T_O	103	56.0 ± 87.7	38.9–73.1						
2. TS	103	34.3 ± 38.5	26.7–41.8						
3. S_O	170	24.5 ± 49.9	17.0–32.0						
4. NTS	84	40.1 ± 37.8	31.9–48.3						
LAC-positivity (Frequency)				0.65	**0.0002**	**0.015**	**3.8×10^{-5}**	**0.0048**	0.39
1. T_O	102	0.735							
2. TS	97	0.763							
3. S_O	172	0.512							
4. NTS	88	0.568							
Sex (F/M ratio)				**0.0005**	**1.6×10^{-6}**	**3.4×10^{-7}**	0.43	0.088	0.26
1. T_O	126	2.07							
2. TS	111	6.40							
3. S_O	182	8.58							
4. NTS	106	14.1							

p-values of statistical significance are in bold fonts.

TABLE 6 | Gene copy number variations (CNVs) of total *C4*, *C4A* and *C4B* among aPL-positive subjects.

	T_O (*N* = 109)		TS (*N* = 100)		S_O (*N* = 166)		NTS (*N* = 98)		*p*
GCN	***N***	***f***	***N***	***f***	***N***	***f***	***N***	***f***	
A. C4 CNVs of aPL-positive subjects segregated by thrombosis and SLE status.									
Total C4									0.088
2	1	0.009	6	0.060	5	0.030	2	0.020	
3	29	0.266	35	0.350	51	0.307	29	0.296	
4	72	0.661	57	0.570	96	0.578	57	0.582	
5	7	0.064	2	0.020	14	0.084	8	0.082	
6	0	0	0	0	0	0	2	0.020	
C4A									**0.034**
0	0	0	4	0.040	1	0.006	1	0.010	
1	23	0.211	23	0.230	36	0.217	16	0.163	
2	72	0.661	61	0.610	106	0.639	57	0.582	
3	14	0.128	12	0.120	23	0.139	19	0.194	
4	0	0	0	0	0	0	4	0.041	
5	0	0	0	0	0	0	1	0.010	
C4B									0.13
0	1	0.009	1	0.010	4	0.024	5	0.051	
1	22	0.202	27	0.270	35	0.211	30	0.306	
2	77	0.706	69	0.690	116	0.699	57	0.582	
3	9	0.083	3	0.030	11	0.066	5	0.051	
4	0	0	0	0	0	0	1	0.010	

B. Mean gene copy numbers (±SD) for total C4, C4A and C4B among aPL-positive subjects.

	N	**total *C4* GCN**	***C4A* GCN**	***C4B* GCN**
a. Thrombosis (T) and non-thrombosis (NT)				
NT	263	3.741 ± 0.378	1.989 ± 0.696	1.753 ± 0.633
T	209	3.670 ± 0.613	1.866 ± 0.636	1.804 ± 0.541
	P	0.24	**0.049**	0.36
b. SLE (S) and non-SLE (NS)				
NS	206	3.782 ± 0.637	2.014 ± 0.702	1.767 ± 0.636
S	266	3.654 ± 0.656	1.872 ± 0.643	1.782 ± 0.561
	p	**0.035**	**0.022**	0.79
c. Thrombosis and SLE status				
1. T_O	109	3.780 ± 0.567	1.917 ± 0.579	1.862 ± 0.552
2. TS	100	3.550 ± 0.642	1.810 ± 0.692	1.740 ± 0.524
3. S_O	166	3.717 ± 0.659	1.910 ± 0.611	1.807 ± 0.582
4. NTS	97	3.784 ± 0.710	2.124 ± 0.807	1.660 ± 0.705
T_O vs. TS	*P*	**0.011**	0.25	0.14
T_O vs. S_O	*P*	0.43	0.93	0.45
T_O vs. NTS	*P*	0.97	**0.027**	**0.015**
TS vs. S_O	*P*	**0.042**	0.24	0.37
TS vs. NTS	*P*	**0.012**	**0.001**	0.34
S_O vs. NTS	*P*	0.42	**0.012**	0.052

T_O, thrombosis without SLE; TS, thrombotic SLE; S_O, SLE without thrombosis; NTS, non-thrombosis and non-SLE; f, frequency. GCN, gene copy number. The reference values for mean GCNs of total C4, C4A, and C4B are 3.82 ± 0.75, 2.09 ± 0.79, and 1.74 ± 0.63, respectively, for healthy subjects; and 3.56 ± 0.77, 1.81± 0.89, and 1.76 ± 0.58, respectively, for SLE subjects (38). p values <0.05 were in bold fonts.

had not reached statistical significance. The median GCN groups for total *C4* is 4, and for *C4A* and *C4B* are both 2. Low and high copy number groups are defined as those below and above median GCN groups, respectively. Variations in frequencies were observed for the low and high GCN groups of *C4* genes. For example, 41.0% of the TS group had 2 or 3 copies of total *C4* genes (low GCN), compared to 27.5% in T_o and 31.6% in NTS. By contrast, only 2.0% of the TS group had 5 or 6 copies of total

C4 (high GCN), compared to 10.2% in the NTS group. A similar pattern was observed for *C4A* genes. There was an increase in the frequency of low *C4A* GCN (27.0% in TS, 17.3% in NTS), and a decrease in the frequency of high *C4A* GCN in the TS group (12.0% in TS, 24.5% in NTS).

The GCN values were analyzed as continuous data to compare means by Student's *t*-test. The means for *total C4, C4A*, and *C4B* were 3.67, 1.87, and 1.80, respectively, for the thrombotic subjects; and were 3.74, 1.99, and 1.75, respectively, for the non-thrombotic subjects. Lower mean *C4A* gene copy number was observed in the thrombotic group ($p = 0.049$) (**Table 6**).

The mean GCN for total *C4, C4A, and C4B* were 3.65, 1.87, and 1.78, respectively, for the SLE patients; and were 3.78, 2.01, and 1.77, respectively, for non-SLE subjects. Significantly lower mean GCNs for total *C4* and *C4A* were present in the SLE group ($p = 0.035$ for total *C4*; $p = 0.022$ for *C4A*) (**Table 6B**). The mean *C4B* gene copy numbers were almost identical between patients with and without SLE.

When the aPL subjects were segregated and compared based on both thrombosis and SLE status, it revealed that the NTS group without thrombosis and SLE had the highest mean GCNs for total *C4* and *C4A* (3.78 and 2.12, respectively), but the lowest *C4B* mean GCN (1.66). The thrombotic SLE group (TS) had the lowest values of total *C4* at 3.55 and *C4A* at 1.81.

The mean GCN of total *C4* for NTS was significantly higher than that of TS ($p = 0.012$); of *C4A* for NTS was significantly higher than those of T_o ($p = 0.027$), S_o ($p = 0.012$) and TS ($p = 0.001$); and of *C4B* was significantly lower than that of T_o ($p = 0.015$).

For TS, the mean GCN of total *C4* was significantly lower than those of T_o ($p = 0.011$), S_o ($p = 0.042$), and NTS ($p = 0.012$); and of *C4A* was significantly lower than that of NTS ($p = 0.001$).

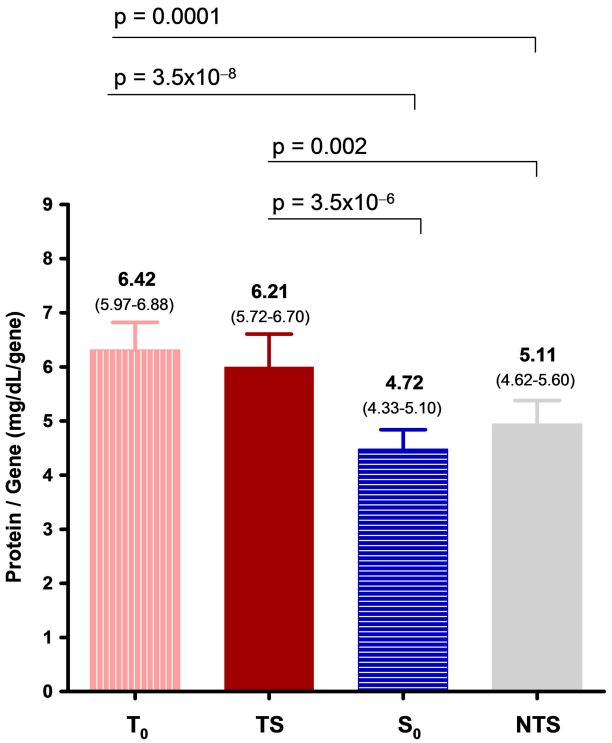

FIGURE 2 | A comparison of mean total plasma C4 protein concentrations per gene-copy (with 95% confidence levels) among aPL-positive subjects categorized by thrombosis and SLE status. Protein concentration per gene-copy allows a comparison of C4 protein levels under various clinical conditions by eliminating the effects of *C4* gene copy number variations among patients.

Plasma C4 Protein Concentrations Per *C4* Gene Copy in Thrombosis and SLE

Both *C4* gene copy number variation and clinical conditions of aPL subjects are important determining factors for C4 plasma protein concentrations. To examine the respective roles of genetic variants and clinical status on plasma protein levels of complement C4, we calculated the C4 protein per gene copy in each study subject by dividing the C4 plasma protein concentration with the *C4* gene copy number. The mean C4 protein concentrations per gene dose among T_o, TS, S_o and NTS were 6.42, 6.21, 4.72, and 5.11 mg/dL, respectively. Thus, the C4 plasma protein yield per gene copy was the highest in aPL subjects with thrombosis only, and the lowest in aPL subjects with SLE only. Highly significant differences were present between the two thrombotic groups (T_o and TS) and the two non-thrombotic groups (S_o and NTS) (**Figure 2**).

Differential Complement and ACLA Plasma Protein Levels and C4 Genetic Deficiencies in aPL-Positive Subjects With and Without Recurrent Pregnancy Loss (RPL)

Of the 444 female aPL-positive subjects, 106 experienced recurrent pregnancy loss (RPL). Thromboses occurred in 63.8% of the RPL patients, compared to 33.7% in non-RPL patients ($p = 5.1 \times 10^{-8}$). SLE were diagnosed in 54.3% of the RPL patients and 59.8% in non-RPL patients ($p = 0.32$). Strikingly, RPL had the highest frequency in patients with both thrombosis and SLE (TS, 41.0%) but lowest in patients with SLE only (S_o, 13.3%); patients of the NTS and T_o groups each had a frequency of 22.9%. The frequencies of RPL are significantly different among aPL-positive patients when segregated into T_o, S_o, TS, and NTS (**Table 6**; $\chi^2 = 46.2$, degree of freedom = 3, $p = 3.8 \times 10^{-10}$). TS patients had an odds ratio (95% confidence interval) of 8.63 (4.37–17.0) over S_o patients to experience recurrent pregnancy loss ($p = 1.6 \times 10^{-11}$).

Lupus anticoagulant was present in 67.1% of patients with RPL and 58.4% of non-RPL female patients ($p = 0.057$). Mean total C4 and ACLA-IgG protein levels were significantly increased, while mean CFH level was reduced (**Table 7**) among RPL patients. The mean total C4 level was 21.8 (19.9 ± 23.7) mg/dL in RPL and 19.1 (18.1 ± 20.2) mg/dL in non-RPL ($p = 0.015$). The ACLA-IgG was 44.2 (35.1 ± 53.3) g/l in RPL and 30.0 (24.2 ± 35.8) g/l in non-RPL ($p = 0.01$). The CFH mean concentrations in RPL were 48.8 (46.6 ± 51.0) mg/dL and 52.1 (50.5 ± 53.7) mg/dL in non-RPL ($p = 0.019$).

Homozygous *C4A* deficiency (GCN of *C4A* = 0) was present in five female aPL patients and all of these five subjects experienced RPL ($p = 0.0001$). On the contrary, homozygous *C4B* deficiency (GCN of *C4B* = 0) was present in 11 female

TABLE 7 | Plasma complement and ACLA levels and risk factors for recurrent pregnancy loss (RPL) in *female* aPL-positive subjects.

a. Continuous data		***n***	**Mean ± SD**	**95% CI**	***P***
C3 Protein, mg/dL	N-RPL	336	123.6 ± 34.0	120.0–127.3	0.23
	RPL	105	131.8 ± 41.8	123.1–140.4	
C4 protein, mg/dL	N-RPL	334	19.2 ± 9.9	18.1–20.2	**0.009**
	RPL	103	22.1 ± 9.6	19.9–23.7	
C4A protein	N-RPL	324	10.3 ± 5.9	9.6–10.91	**0.039**
	RPL	103	11.7 ± 5.5	10.5–12.8	
C4B protein	N-RPL	333	9.1± 5.5	8.5–9.7	0.051
	RPL	104	10.3 ± 5.8	9.2–11.4	
CFH protein, mg/dL	N-RPL	296	52.1 ± 14.2	50.5–53.7	**0.019**
	RPL	87	48.8 ± 10.4	46.6–51.0	
MBL protein, mg/dL	N-RPL	269	0.166 ± 0.164	0.147–0.185	0.051
	RPL	84	0.128 ± 0.130	0.100–0.156	
ACLA-IgM g/L	N-RPL	300	26.8 ± 37.2	22.6–31.0	0.56
	RPL	90	33.6 ± 108.5	10.9–56.4	
ACLA IgG, g/L	N-RPL	301	30.0 ± 51.1	24.2–35.8	**0.01**
	RPL	91	44.2 ± 43.7	35.1–53.3	
b. Categorical data		***Case/total***	***f***	***P***	**Remarks**
C4T, GCN = 2	N-RPL	7/261	0.0269	0.15	
	RPL	5/79	0.0633		
C4A, GCN = 0	N-RPL	0/263	0	**0.0001**	Risk
	RPL	5/81	0.0617		
C4B, GCN = 0	N-RPL	11/261	0.0421	**0.017**	Protective
	RPL	0/75	0		
LAC-Positivity	N-RPL	168/294	0.584	0.057	
	RPL	64/94	0.671		
Thromboses	N-RPL	114/338	0.337	**5.1×10^{-8}**	Risk
	RPL	67/105	0.638		
SLE	N-RPL	136/338	0.414	0.32	
	RPL	48/105	0.467		
c. Subgroup freq.	**T_o**	**S_o**	**TS**	**NTS**	***p***
N-RPL, *n* (%)	61 (18.1)	149 (44.1)	53 (15.7)	75 (22.2)	**3.8×10^{-10}**
RPL, *n* (%)	24 (22.9)	14 (13.3)	43 (40.1)	24 (22.9)	
S_o, *p*	**7.2×10^{-5}**	-			
TS, *p*	**0.021**	**1.6×10^{-11}**	-		
NTS, *p*	0.54	**0.0006**	**0.0024**	-	

f, frequency; N-RPL, no recurrent pregnancy loss; RPL, with recurrent pregnancy loss. p-values of statistical significance are in bold fonts.

aPL patients and *none* of them experienced RPL ($p = 0.017$). Thus, homozygous *C4A* deficiency was a strong risk factor for, and homozygous *C4B* deficiency was a strong protective factor against, recurrent pregnancy loss.

Standardized Comparison of Numeric Parameters Associated With Thrombosis and SLE

To allow a standardized comparison of complement and ACLA protein variations in thrombosis and SLE, we determined the effect size index (69) of each parameter in T_o, S_o, and TS, using the mean protein concentrations or antibody levels of the group without thrombosis and SLE (NTS) as a reference. The difference of mean protein levels for each protein at T_o, S_o, or TS from NTS was divided by its root mean square error (RMSE), which was computed by ANOVA, to yield the effect size index. The effect size indices for complement and ACLA proteins with quantitative variations are depicted in **Figure 3**. In descending order, the greatest intergroup effect size indices are: C4, T_o vs. S_o: 0.709; C4B, T_o vs. S_o: 0.570; C4A, T_o vs. S_o: 0.566; ACLA-IgG, T_o vs. S_o: 0.554; complement factor H, TS vs. NTS: 0.483; ACLA-IgM, T_o vs. NTS: 0.373; and MBL, TS vs. S_o: 0.367.

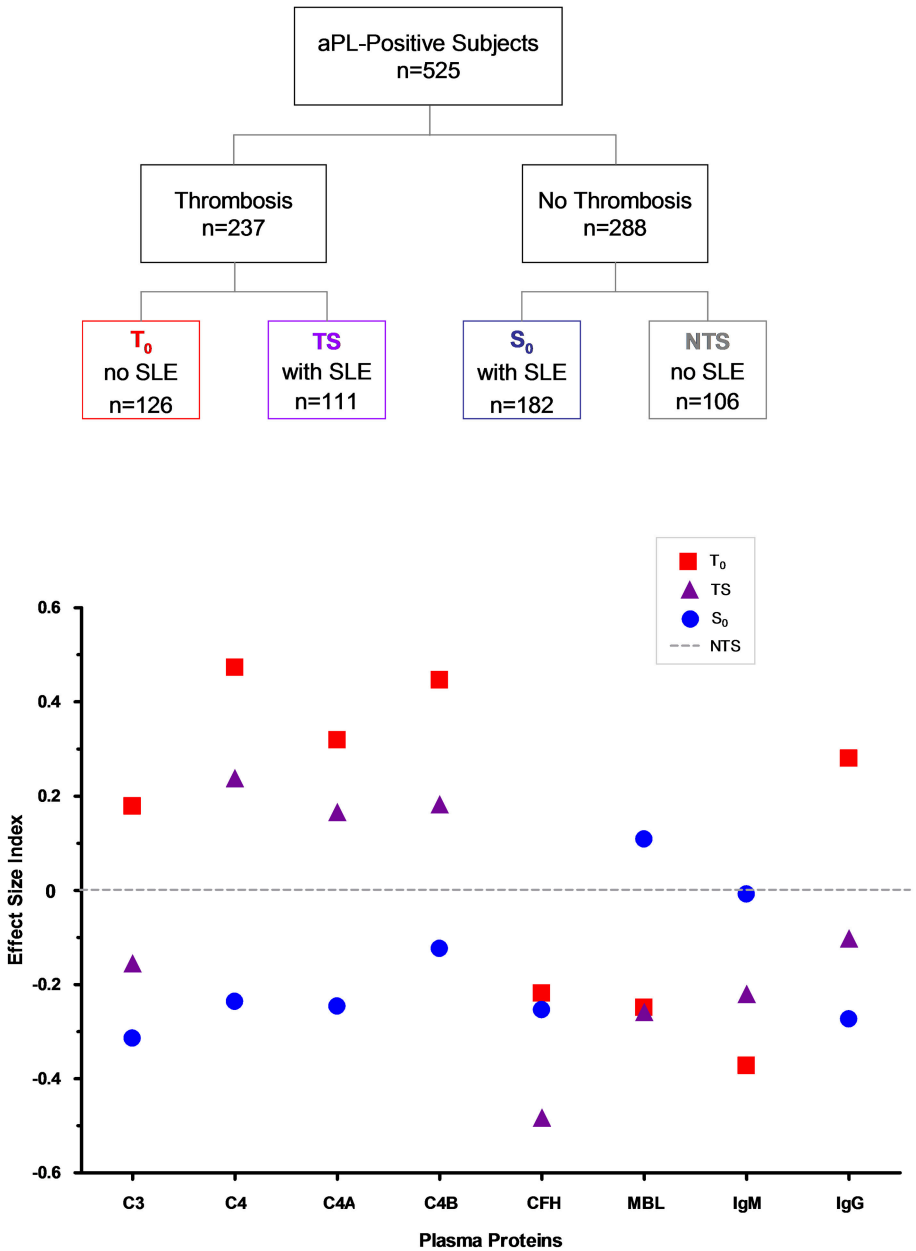

FIGURE 3 | (Upper) Categorization of aPL-positive subjects according to their thrombosis and SLE status. **(Lower)** Standardized differences (effect size index) of mean complement protein levels and ACLA levels among aPL-positive subjects with thrombosis without SLE (T_O), thrombosis and SLE (TS), SLE without thrombosis (S_O) when compared to the non-thrombotic and non-SLE (NTS) group. Root mean square error (RMSE) value for each protein was derived from Oneway ANOVA. Differences of mean protein levels for T_O, TS and S_O from NTS were each divided by their associated RMSE and charted to derive the effect size index. The effect size indices allow a standardized comparison of different parameters under different clinical conditions.

DISCUSSION

This is a cross-sectional study of complement protein profiles and copy number variations of *C4* genes in a relatively large cohort of human subjects with aPL antibodies. These aPL-positive subjects had a variety of clinical presentations: thrombosis, SLE, thrombosis and SLE, no thrombosis and no SLE. Many female aPL-positive subjects also experienced pregnancy morbidity such as recurrent pregnancy losses. Extensive analyses of gene copy number variations for total *C4*, *C4A*, and *C4B*, plasma protein levels of total C4, C4A, C4B, C3, factor H and MBL, and antiphospholipid antibodies revealed distinct patterns of diversity that can be relevant and effective quantitative biomarkers for thrombosis, SLE and recurrent pregnancy loss.

An intriguing aspect of complement *C4* genetics is the *frequent* gene copy number variations (30, 38, 40). Genetic

deficiency (60, 70) or low gene copy numbers of total *C4* or *C4A* has been shown to be a prevalent risk factor for SLE in European and East-Asian Americans (22, 38, 41, 71–73). *C4* gene copy number variations in the aPL-positive subjects were determined and validated by quantitative real-time PCR (35). When SLE and non-SLE subjects were compared, lower total *C4* and *C4A* mean gene copy numbers were found among the SLE subjects, suggesting that aPL-positive subjects with low total *C4* or *C4A* gene copy numbers carried a greater risk of developing SLE, as we reported in earlier studies (22, 38). Among the NTS subjects who were not afflicted with thrombosis and SLE, there were higher mean GCN of *C4A*, which would be protective against SLE; and low GCN of *C4B* that would lead to lower C4B protein levels and thereby reducing the risk of thrombosis.

Using thrombosis as a response, multiple logistic regression analyses suggested that *higher* plasma C4 protein levels and the presence of lupus anticoagulant (LAC) were among the strongest independent biomarkers associated with thrombosis (C4, $p = 6.2 \times 10^{-9}$; LAC, $p = 6.9 \times 10^{-5}$) (**Supplementary Table**). Other relevant parameters for increased risk of thrombosis included male sex and a *reduction* of complement factor H level, which was also observed by Nakamura and colleagues (74). Higher plasma C4 protein levels and the presence of LAC were the two most prominent risk factors for *arterial* thrombosis. The higher level of C4 protein in arterial thrombosis was mainly attributable to higher C4B ($p = 2.1 \times 10^{-5}$). The risk factors identified for *venous* thrombosis also included increased protein level of total C4 ($p = 0.01$) and the presence of LAC ($p = 0.012$). Reduced protein level of functional MBL ($p = 0.0012$) and male gender also had prominent effects.

While the presence of LAC and elevated ACLA-IgG levels have long been recognized for their connections with thrombosis and recurrent pregnancy loss (75), this report provides a firm documentation on the significance of *higher* C4 plasma protein levels among aPL-positive subjects with APS-related clinical manifestations. The presence of LAC and elevated protein level of complement C4 together are predictors for increased risk of thrombosis with values of sensitivity at 0.707 and specificity at 0.664. This study also reveals lower complement factor H protein levels among subjects with SLE and thrombosis. Deficiency, mutation or autoantibody of complement factor H have been linked to atypical hemolytic uremic syndrome that is characterized by thrombotic microangiopathy (76, 77). Along with observations that plasma protein levels of MBL were decreased, evidence for an involvement of complement proteins in human thrombosis or pregnancy loss are compelling and deserve clinical attention (78). High levels of plasma C4 among patients with thrombosis could result in a procoagulation or thromboinflammatory state, which provide large quantities of reagents to fuel the complement cascades, leading to greater extent of complement-mediated tissue injuries. The abundance of the fast-reacting C4B could aggravate the pathogenic process in arterial thrombosis.

Using SLE as a response, multiple logistic regression analysis of plasma protein data suggested that *reduced* levels of C3, C4, and ACLA-IgG, and female gender were strong risk factors for SLE C3 is downstream of C4 in the classical and the MBL activation pathways, the activation and consumption of C3 are amplified by a positive feedback mechanism (79–81). In other words, moderate activation of C4 can lead to large consumption of C3. Thus, fluctuations of serum C3 levels tend to be a more sensitive biomarker for SLE disease activity than C4 does.

Among the female aPL-positive subjects, patients with thrombosis and particularly, thrombotic SLE, had high frequencies of recurrent pregnancy loss. RPL patients had elevated levels of complement C4 and ACLA-IgG, and decreased concentration of factor H. Remarkably, female aPL-positive subjects with homozygous C4B deficiency were *all protected* from RPL, which is consistent with observations in mouse models that complement C4 deficiency or C3 deficiency were protective from RPL induced by injection of human aPL (16). It is also of interest to note that aPL-positive female (human) patients with homozygous C4A deficiency *all* experienced RPL, which underlies the importance of C4A protein in achieving tolerance or defense against autoimmunity and fetal rejections.

It is important to recognize that the direction of changes for plasma protein levels of complement C3, C4, and ACLA-IgG among aPL-positive patients with SLE and with thrombosis or pregnancy morbidity are mostly *opposite* to each other. The highest mean protein levels for these proteins were present in the T_o group (thrombosis without SLE), and the lowest in the S_o group (SLE without thrombosis). Thus, the inter-group differences of these proteins were highly significant (T_o vs. S_o: $p = 2.6 \times 10^{-5}$ for C3; $p = 2.2 \times 10^{-9}$ for C4; $p = 1.2 \times 10^{-5}$ for ACLA-IgG). The resultant effects for these two opposing forces, SLE and thrombosis, are shown in the thrombotic SLE group TS, by which the mean plasma protein levels of C3, C4, C4A, C4B, and ACLA-IgG all fell between those of T_o and S_o groups, and their values were closer to those present in the NTS group. When *standardized* by the gene copy numbers, highly significant differences for mean C4 protein concentrations per gene-copy were observed between the thrombotic subjects and non-thrombotic subjects, and the greatest difference remained between T_o and S_o (6.42 mg/dL/gene for T_o, 4.72 mg/dL/gene for S_o; $p = 3.5 \times 10^{-8}$). The mean C4 protein per gene-copy in TS (6.21 mg/dL/gene) was only slightly lower than that of T_o. This implies the presence of trans-acting factor(s) among patients with thrombosis that *upregulates* C4 protein biosynthesis, and/or reduces its turnover that would have decreased the protein levels. While complement activation is a noted feature for clinical manifestations of APS, such activation likely occurs *locally* that may *not* result in systemic and parallel decline of plasma protein levels for C4 and C3, a phenomenon analogous to what we observed in many patients with juvenile dermatomyositis (82).

The target sites for most aPL appear to be located at the domain D1 or complement controlling protein repeat on β_2GPI. Recombinant antibody recognizing this domain D1 induced fetal loss and coagulation in animal models (83). Interestingly, an engineered β_2GPI antibody without the IgG heavy chain CH_2-domain, which was devoid of the C1q binding site and unable to fix or activate complement, was shown to compete and control the coagulation and abortive effects in animals burgeoned by injection of human aPL (83). Biochemical studies revealed that β_2GPI in its linear conformation can serve as a regulator for the

classical and alternative pathway C3 convertases, as it diminished the activation of C3 (to form C3a) and the assembly of C5b-9 in a dose-dependent manner. Active β_2GPI also enhanced the degradation of C3b in the presence of factor I and factor H (84, 85). The effects of aPL on the functional activities of β_2GPI and plasma complement protein concentrations and activities remain to be elucidated.

The relationships among MBL deficiency, SLE and thrombosis were complex and it was not clear whether MBL deficiency was a risk factor for SLE (86, 87). In a study of 91 SLE patients, Garred et al. demonstrated a near doubling of thrombosis in individuals homozygous for MBL protein structural variants (B,D,C) that led to functional deficiencies of MBL (88). Subsequently, an association was made between MBL deficiency and arterial thrombosis (89). In a study of structural variants and promoter alleles for high and low expression of *MBL2* gene in 114 SLE patients, Font et al. observed that low MBL expression genotypes were associated with venous thrombosis (90). Data from our study further clarifies the role of MBL in SLE and thrombosis: reduced plasma protein concentrations of *functional* MBL were present among aPL-positive patients with thrombosis, regardless of SLE status. Therefore, the link between MBL-deficiency (or low expression of MBL) and SLE could be secondary to *low* functional MBL in SLE patients with APS. As a lectin binding protein that binds to simple carbohydrate (mannose) components on cell membranes, it is possible that MBL could compete with aPL for binding to phospholipids or phospholipid-binding proteins to reduce the risk of aPL on initiating thrombotic events.

Our study population includes multiple racial and ethnic backgrounds but the majority were of Northern European ancestry. When we analyzed the complement and ACLA data on this specific ethnic group, similar conclusions on the contrasting patterns of complement C4 and ACLA in thromboses and SLE can be reached. Results on three clinical studies on stroke or recurrent pregnancy loss were in accord with our observations that *high* C4 and/or *high* C3 plasma protein levels are associated with thrombosis or recurrent pregnancy loss (91–93).

Our observations are consistent with a parallel and independent study that revealed that pediatric SLE patients undergoing a clinical trial (94) with a history of hypertension had persistently higher serum levels of complement C4 and C3 and higher gene copy number of *C4B* (Mulvihill et al, submitted). Here, we further show that patients with both SLE and thrombosis had the lowest mean GCNs for total *C4* (3.55) and *C4A* (1.81), which underscores the importance of C4A deficiency as a genetic risk factor for systemic autoimmune disease. Paradoxically, hypocomplementemia is both a cause and an effect of human SLE. SLE-associated disorders such as lupus nephritis, hemolytic anemia, high titers of anti-dsDNA, and lupus disease flares are notably marked by low serum complement levels due to massive consumption of C3 and C4 (21–23, 25). Systemic and concurrent consumptions of C4 and C3 can be reflected by higher coefficients of correlation (r or r^2) between these two proteins, which are conspicuous among aPL-positive patients in the S_o and NTS groups (**Table 2**) (25). Detailed diagnostic disorders of SLE (64) and triple positivity of aPL autoantibodies (9) were not available for this study to examine the extent of hypocomplementemia in various organ involvement and tissue damage, but these would be relevant topics for future investigations.

This cross-sectional study represents a snapshot of complement and aPL in a population of human subjects with antiphospholipid antibodies. The relatively large study population provided an informative dataset to examine specific patterns of complement and aPL among patients with thrombosis, SLE and recurrent pregnancy loss. Along time courses of patients with chronic, systemic autoimmune disease, plasma or serum complement C3 and C4 levels and their cell-bound products would fluctuate with disease activities. The status of SLE/APS disease activities including flare and remission for each patient at the time of sample collection was not available and therefore not accounted for in our data analyses. The lack of data from longitudinal studies, and blood samples from healthy subjects with and without aPL being processed in parallel with similar methodologies are other limitations of this study. Further studies with large sample size of patients for measurements of complement component protein levels under defined genetic backgrounds, plus determination of activation products C3a, C4a, and C5a, cell-bound and fluid phase levels of C4d and C3d, and membrane attack complexes may provide important insights into mechanism(s) on how complement modulate aPL associated clinical manifestations and disease activities of SLE and APS (55, 58, 61, 62). In addition, effects of complement-mediated tissue damage and thromboses would be more readily demonstrated by immunohistochemical methods.

In conclusion, our results can serve as a foundation for further studies of SLE and APS disease mechanisms, more sensitive disease diagnosis, and possibly better prognosis of disease course and profile. It would be desirable to elucidate the *C4* gene copy numbers among aPL-positive subjects for a prevention purpose, as those with low total *C4* or *C4A* gene copy number would have a higher risk to develop SLE, and high *C4B* GCN would have greater risk for complement-mediated complications such as thrombosis, recurrent pregnancy loss in females, and tissue injuries.

AUTHOR CONTRIBUTIONS

C-YY, SS, YW, and RR designed the research. RR contributed patient samples and clinical data. SS, KK, DZ, YW, and C-YY performed experiments. HN, YW, SS, and C-YY performed statistical analyses. SS, YW, DZ, EM, FB-S, SA, RR, and C-YY analyzed and interpreted data. SS, YW, KK, DZ, EM, FB-S, SA, RR, HN, and C-YY wrote the paper.

ACKNOWLEDGMENTS

We thank Gail Buxton and Bi Zhou for their assistance. This work was supported by grants 1R01 AR050078, 1R21 AR070905, 1R01 AR073311 from the National Institute

of Arthritis, Musculoskeletal and Skin Diseases of the NIH (C-YY), a grant from the General Clinical Research Centers Program of the Division of Research Resources, National Institutes of Health, M01 RR00034 (OSU) and RR00046 (UNC).

SUPPLEMENTARY MATERIAL

The Supplementary Material for this article can be found online at: https://www.frontiersin.org/articles/10.3389/fimmu.2019.00885/full#supplementary-material

REFERENCES

1. Wilson WA, Gharavi AE, Koike T, Lockshin MD, Branch DW, Piette JC, et al. International consensus statement on preliminary classification criteria for definite antiphospholipid syndrome: report of an international workshop. *Arthritis Rheum*. (1999) 42:1309–11. doi: 10.1002/1529-0131(199907)42:7<1309::AID-ANR1>3.0.CO;2-F
2. Levine JS, Branch DW, Rauch J. The antiphospholipid syndrome. *N Engl J Med*. (2002) 346:752–63. doi: 10.1056/NEJMra002974
3. Cervera R. Antiphospholipid syndrome. *Thromb Res*. (2017) 151(Suppl 1):S43–7. doi: 10.1016/S0049-3848(17)30066-X
4. Schur PH. Pathogenesis of antiphospholipid syndrome. In: Pisetsky DS, ed. *Up-To-Date*. (2019). Available online at: https://www.uptodate.com/contents/pathogenesis-of-antiphospholipid-syndrome
5. Schreiber K, Sciascia S, de Groot PG, Devreese K, Jacobsen S, Ruiz-Irastorza G, et al. Antiphospholipid syndrome. *Nat Rev Dis Primers*. (2018) 4:17103. doi: 10.1038/nrdp.2018.5
6. Miyakis S, Lockshin MD, Atsumi T, Branch DW, Brey RL, Cervera R, et al. International consensus statement on an update of the classification criteria for definite antiphospholipid syndrome (APS). *J Thromb Haemost*. (2006) 4:295–306. doi: 10.1111/j.1538-7836.2006.01753.x
7. Viall CA, Chamley LW. Histopathology in the placentae of women with antiphospholipid antibodies: a systematic review of the literature. *Autoimmun Rev*. (2015) 14:446–71. doi: 10.1016/j.autrev.2015.01.008
8. Roubey RA. Antiphospholipid antibodies: immunological aspects. *Clin Immunol*. (2004) 112:127–8. doi: 10.1016/j.clim.2004.02.010
9. Pengo V, Ruffatti A, Legnani C, Gresele P, Barcellona D, Erba N, et al. Clinical course of high-risk patients diagnosed with antiphospholipid syndrome. *J Thromb Haemost*. (2010) 8:237–42. doi: 10.1111/j.1538-7836.2009.03674.x
10. Steinkasserer A, Estaller C, Weiss EH, Sim RB, Day AJ. Complete nucleotide and deduced amino acid sequence of human beta 2-glycoprotein I. *Biochem J*. (1991) 277(Pt 2):387–91. doi: 10.1042/bj2770387
11. Koike T. Antiphospholipid syndrome: 30 years and our contribution. *Int J Rheum Dis*. (2015) 18:233–41. doi: 10.1111/1756-185X.12438
12. Lozier J, Takahashi N, Putnam FW. Complete amino acid sequence of human plasma beta 2-glycoprotein I. *Proc Natl Acad Sci USA*. (1984) 81:3640–4. doi: 10.1073/pnas.81.12.3640
13. Hahn BH. Antibodies to DNA. *N Engl J Med*. (1998) 338:1359–68. doi: 10.1056/NEJM199805073381906
14. Davidson A, Diamond B. Autoimmune diseases. *N Engl J Med*. (2001) 345:340–50. doi: 10.1056/NEJM200108023450506
15. Cervera R, Piette JC, Font J, Khamashta MA, Shoenfeld Y, Camps MT, et al. Antiphospholipid syndrome: clinical and immunologic manifestations and patterns of disease expression in a cohort of 1,000 patients. *Arthritis Rheum*. (2002) 46:1019–27. doi: 10.1002/art.10187
16. Harris EN, Gharavi AE, Boey ML, Patel BM, Mackworth-Young CG, Loizou S, et al. Anticardiolipin antibodies: detection by radioimmunoassay and association with thrombosis in systemic lupus erythematosus. *Lancet*. (1983) 2:1211–4. doi: 10.1016/S0140-6736(83)91267-9
17. Love PE, Santoro SA. Antiphospholipid antibodies: anticardiolipin and the lupus anticoagulant in systemic lupus erythematosus (SLE) and in non-SLE disorders. prevalence and clinical significance. *Ann Intern Med*. (1990) 112:682–98. doi: 10.7326/0003-4819-112-9-682
18. Sestak A, O'Neil KM. Familial lupus and antiphospholipid syndrome. *Lupus*. (2007) 16:556–63. doi: 10.1177/0961203307078071
19. Pons-Estel GJ, Andreoli L, Scanzi F, Cervera R, Tincani A. The antiphospholipid syndrome in patients with systemic lupus erythematosus. *J Autoimmun*. (2017) 76:10–20. doi: 10.1016/j.jaut.2016.10.004
20. de Groot PG, de Laat B. Mechanisms of thrombosis in systemic lupus erythematosus and antiphospholipid syndrome. *Best Pract Res Clin Rheumatol*. (2017) 31:334–41. doi: 10.1016/j.berh.2017.09.008
21. Birmingham DJ, Irshaid F, Nagaraja HN, Zou X, Tsao BP, Wu H, et al. The complex nature of serum C3 and C4 as biomarkers of lupus renal flare. *Lupus*. (2010) 19:1272–80. doi: 10.1177/0961203310371154
22. Chen JY, Wu YL, Mok MY, Wu YJ, Lintner KE, Wang CM, et al. Effects of complement C4 gene copy number variations, size dichotomy, and C4A deficiency on genetic risk and clinical presentation of systemic lupus erythematosus in east asian populations. *Arthritis Rheumatol*. (2016) 68:1442–53. doi: 10.1002/art.39589
23. Schur PH. Complement and lupus erythematosus. *Arthritis Rheum*. (1982) 25:793–8. doi: 10.1002/art.1780250715
24. Ramos-Casals M, Campoamor MT, Chamorro A, Salvador G, Segura S, Botero JC, et al. Hypocomplementemia in systemic lupus erythematosus and primary antiphospholipid syndrome: prevalence and clinical significance in 667 patients. *Lupus*. (2004) 13:777–83. doi: 10.1191/0961203304lu1080oa
25. Wu YL, Higgins GC, Rennebohm RM, Chung EK, Yang Y, Zhou B, et al. Three distinct profiles of serum complement C4 proteins in pediatric systemic lupus erythematosus (SLE) patients: tight associations of complement C4 and C3 protein levels in SLE but not in healthy subjects. *Adv Exp Med Biol*. (2006) 586:227–47. doi: 10.1007/0-387-34134-X_16
26. Lintner KE, Wu YL, Yang Y, Spencer CH, Hauptmann G, Hebert LA, et al. Early components of the complement classical activation pathway in human systemic autoimmune diseases. *Front Immunol*. (2016) 7:36. doi: 10.3389/fimmu.2016.00036
27. Wu YL, Brookshire BP, Verani RR, Arnett FC, Yu CY. Clinical presentations and molecular basis of complement C1r deficiency in a male African-American patient with systemic lupus erythematosus. *Lupus*. (2011) 20:1126–34. doi: 10.1177/0961203311404914
28. Wu YL, Hauptmann G, Viguier M, Yu CY. Molecular basis of complete complement C4 deficiency in two North-African families with systemic lupus erythematosus. *Genes Immun*. (2009) 10:433–45. doi: 10.1038/gene.2009.10
29. Reid KB, Porter RR. The proteolytic activation systems of complement. *Annu Rev Biochem*. (1981) 50:433–64. doi: 10.1146/annurev.bi.50.070181.002245
30. Chung EK, Yang Y, Rennebohm RM, Lokki ML, Higgins GC, Jones KN, et al. Genetic sophistication of human complement components C4A and C4B and RP-C4-CYP21-TNX (RCCX) modules in the major histocompatibility complex. *Am J Hum Genet*. (2002) 71:823–37. doi: 10.1086/342777
31. Yu CY, Chung EK, Yang Y, Blanchong CA, Jacobsen N, Saxena K, et al. Dancing with complement C4 and the RP-C4-CYP21-TNX (RCCX) modules of the major histocompatibility complex. *Prog Nucleic Acid Res Mol Biol*. (2003) 75:217–92. doi: 10.1016/S0079-6603(03)75007-7
32. Isenman DE, Young JR. The molecular basis for the difference in immune hemolysis activity of the chido and rodgers isotypes of human complement component C4. *J Immunol*. (1984) 132:3019–27.
33. Law SK, Dodds AW, Porter RR. A comparison of the properties of two classes, C4A and C4B, of the human complement component C4. *EMBO J*. (1984) 3:1819–23. doi: 10.1002/j.1460-2075.1984.tb02052.x
34. Yu CY, Belt KT, Giles CM, Campbell RD, Porter RR. Structural basis of the polymorphism of human complement components C4A and C4B: gene size, reactivity and antigenicity. *EMBO J*. (1986) 5:2873–81. doi: 10.1002/j.1460-2075.1986.tb04582.x
35. Wu YL, Savelli SL, Yang Y, Zhou B, Rovin BH, Birmingham DJ, et al. Sensitive and specific real-time polymerase chain reaction assays to accurately determine copy number variations (CNVs) of human complement C4A, C4B, C4-long, C4-short, and RCCX modules: elucidation of C4 CNVs in

50 consanguineous subjects with defined HLA genotypes. *J Immunol*. (2007) 179:3012–25. doi: 10.4049/jimmunol.179.5.3012
36. Blanchong CA, Zhou B, Rupert KL, Chung EK, Jones KN, Sotos JF, et al. Deficiencies of human complement component C4A and C4B and heterozygosity in length variants of RP-C4-CYP21-TNX (RCCX) modules in caucasians. the load of RCCX genetic diversity on major histocompatibility complex-associated disease. *J Exp Med*. (2000) 191:2183–96. doi: 10.1084/jem.191.12.2183
37. Yang Z, Mendoza AR, Welch TR, Zipf WB, Yu CY. Modular variations of the human major histocompatibility complex class III genes for serine/threonine kinase RP, complement component C4, steroid 21-hydroxylase CYP21, and tenascin TNX (the RCCX module). A mechanism for gene deletions and disease associations. *J Biol Chem*. (1999) 274:12147–56. doi: 10.1074/jbc.274.17.12147
38. Yang Y, Chung EK, Wu YL, Savelli SL, Nagaraja HN, Zhou B, et al. Gene copy-number variation and associated polymorphisms of complement component C4 in human systemic lupus erythematosus (SLE): low copy number is a risk factor for and high copy number is a protective factor against SLE susceptibility in European Americans. *Am J Hum Genet*. (2007) 80:1037–54. doi: 10.1086/518257
39. Dangel AW, Mendoza AR, Baker BJ, Daniel CM, Carroll MC, Wu LC, et al. The dichotomous size variation of human complement C4 genes is mediated by a novel family of endogenous retroviruses, which also establishes species-specific genomic patterns among old world primates. *Immunogenetics*. (1994) 40:425–36. doi: 10.1007/BF00177825
40. Yang Y, Chung EK, Zhou B, Blanchong CA, Yu CY, Füst G, et al. Diversity in intrinsic strengths of the human complement system: serum C4 protein concentrations correlate with C4 gene size and polygenic variations, hemolytic activities, and body mass index. *J Immunol*. (2003) 171:2734–45. doi: 10.4049/jimmunol.171.5.2734
41. Jüptner M, Flachsbart F, Caliebe A, Lieb W, Schreiber S, Zeuner R, et al. Low copy numbers of complement C4 and homozygous deficiency of C4A may predispose to severe disease and earlier disease onset in patients with systemic lupus erythematosus. *Lupus*. (2018) 27:600–9. doi: 10.1177/0961203317735187
42. Pereira KM, Faria AG, Liphaus BL, Jesus AA, Silva CA, Carneiro-Sampaio M, et al. Low C4, C4A and C4B gene copy numbers are stronger risk factors for juvenile-onset than for adult-onset systemic lupus erythematosus. *Rheumatology (Oxford)*. (2016) 55:869–73. doi: 10.1093/rheumatology/kev436
43. Pierangeli SS, Harris EN. Antiphospholipid antibodies in an *in vivo* thrombosis model in mice. *Lupus*. (1994) 3:247–51. doi: 10.1177/096120339400300408
44. Pierangeli SS, Liu XW, Barker JH, Anderson G, Harris EN. Induction of thrombosis in a mouse model by IgG, IgM and IgA immunoglobulins from patients with the antiphospholipid syndrome. *Thromb Haemost*. (1995) 74:1361–7. doi: 10.1055/s-0038-1649940
45. Branch DW, Dudley DJ, Mitchell MD, Creighton KA, Abbott TM, Hammond EH, et al. Immunoglobulin G fractions from patients with antiphospholipid antibodies cause fetal death in BALB/c mice: a model for autoimmune fetal loss. *Am J Obstet Gynecol*. (1990) 163:210–6. doi: 10.1016/S0002-9378(11)90700-5
46. Blank M, Cohen J, Toder V, Shoenfeld Y. Induction of anti-phospholipid syndrome in naive mice with mouse lupus monoclonal and human polyclonal anti-cardiolipin antibodies. *Proc Natl Acad Sci USA*. (1991) 88:3069–73. doi: 10.1073/pnas.88.8.3069
47. Salmon JE, Girardi G. The role of complement in the antiphospholipid syndrome. *Curr Dir Autoimmun*. (2004) 7:133–48. doi: 10.1159/000075690
48. Holers VM, Girardi G, Mo L, Guthridge JM, Molina H, Pierangeli SS, et al. Complement C3 activation is required for antiphospholipid antibody-induced fetal loss. *J Exp Med*. (2002) 195:211–20. doi: 10.1084/jem.200116116
49. Atkinson JP. Complement system on the attack in autoimmunity. *J Clin Invest*. (2003) 112:1639–41. doi: 10.1172/JCI20309
50. Girardi G, Berman J, Redecha P, Spruce L, Thurman JM, Kraus D, et al. Complement C5a receptors and neutrophils mediate fetal injury in the antiphospholipid syndrome. *J Clin Invest*. (2003) 112:1644–54. doi: 10.1172/JCI200318817
51. Fleming SD, Egan RP, Chai C, Girardi G, Holers VM, Salmon J, et al. Anti-phospholipid antibodies restore mesenteric ischemia/reperfusion-induced injury in complement receptor 2/complement receptor 1-deficient mice. *J Immunol*. (2004) 173:7055–61. doi: 10.4049/jimmunol.173.11.7055
52. Fleming SD, Mastellos D, Karpel-Massler G, Shea-Donohue T, Lambris JD, Tsokos GC. C5a causes limited, polymorphonuclear cell-independent, mesenteric ischemia/reperfusion-induced injury. *Clin Immunol*. (2003) 108:263–73. doi: 10.1016/S1521-6616(03)00160-8
53. Pierangeli SS, Girardi G, Vega-Ostertag M, Liu X, Espinola RG, Salmon J. Requirement of activation of complement C3 and C5 for antiphospholipid antibody-mediated thrombophilia. *Arthritis Rheum*. (2005) 52:2120–4. doi: 10.1002/art.21157
54. Cohen D, Buurma A, Goemaere NN, Girardi G, le Cessie S, Scherjon S, et al. Classical complement activation as a footprint for murine and human antiphospholipid antibody-induced fetal loss. *J Pathol*. (2011) 225:502–11. doi: 10.1002/path.2893
55. Kim MY, Guerra MM, Kaplowitz E, Laskin CA, Petri M, Branch DW, et al. Complement activation predicts adverse pregnancy outcome in patients with systemic lupus erythematosus and/or antiphospholipid antibodies. *Ann Rheum Dis*. (2018) 77:549–55. doi: 10.1136/annrheumdis-2017-212224
56. Tedesco F, Borghi MO, Gerosa M, Chighizola CB, Macor P, Lonati PA, et al. Pathogenic role of complement in antiphospholipid syndrome and therapeutic implications. *Front Immunol*. (2018) 9:1388. doi: 10.3389/fimmu.2018.01388
57. Samarkos M, Mylona E, Kapsimali V. The role of complement in the antiphospholipid syndrome: a novel mechanism for pregnancy morbidity. *Semin Arthritis Rheum*. (2012) 42:66–9. doi: 10.1016/j.semarthrit.2012.01.001
58. Devreese KM, Hoylaerts MF. Is there an association between complement activation and antiphospholipid antibody-related thrombosis? *Thromb Haemost*. (2010) 104:1279–81. doi: 10.1160/TH10-06-0410
59. Fischetti F, Durigutto P, Pellis V, Debeus A, Macor P, Bulla R, et al. Thrombus formation induced by antibodies to beta2-glycoprotein I is complement dependent and requires a priming factor. *Blood*. (2005) 106:2340–6. doi: 10.1182/blood-2005-03-1319
60. Yang Y, Chung EK, Zhou B, Lhotta K, Hebert LA, Birmingham DJ, et al. The intricate role of complement component C4 in human systemic lupus erythematosus. *Curr Dir Autoimmun*. (2004) 7:98–132. doi: 10.1159/000075689
61. Oku K, Atsumi T, Bohgaki M, Amengual O, Kataoka H, Horita T, et al. Complement activation in patients with primary antiphospholipid syndrome. *Ann Rheum Dis*. (2009) 68:1030–5. doi: 10.1136/ard.2008.090670
62. Oku K, Amengual O, Hisada R, Ohmura K, Nakagawa I, Watanabe T, et al. Autoantibodies against a complement component 1 q subcomponent contribute to complement activation and recurrent thrombosis/pregnancy morbidity in anti-phospholipid syndrome. *Rheumatology (Oxford)*. (2016) 55:1403–11. doi: 10.1093/rheumatology/kew196
63. Roubey RA. Antiphospholipid syndrome: antibodies and antigens. *Curr Opin Hematol*. (2000) 7:316–20. doi: 10.1097/00062752-200009000-00010
64. Tan EM, Cohen AS, Fries JF, Masi AT, McShane DJ, Rothfield NF, et al. The 1982 revised criteria for the classification of systemic lupus erythematosus. *Arthritis Rheum*. (1982) 25:1271–7. doi: 10.1002/art.1780251101
65. Giclas PC. Measurement of complement component levels by radial immunodiffusion. *Curr Prot Immunol*. (2003) 13:1.9–1.26. doi: 10.1002/0471142735.im1301s09
66. Sim E, Cross SJ. Phenotyping of human complement component C4, a class-III HLA antigen. *Biochem J*. (1986) 239:763–7. doi: 10.1042/bj2390763
67. Awdeh ZL, Alper CA. Inherited structural polymorphism of the fourth component of human complement. *Proc Natl Acad Sci USA*. (1980) 77:3576–80. doi: 10.1073/pnas.77.6.3576
68. Chung EK, Wu YL, Yang Y, Zhou B, Yu CY. Human complement components C4A and C4B genetic diversities: complex genotypes and phenotypes. *Curr Protoc Immunol*. (2005) Chapter 13:Unit 13 18. doi: 10.1002/0471142735.im1308s68
69. Cohen J. *Statistical Power Analysis for Behavioral Sciences*, 2nd ed. Hillsdale, NJ: Lawrence Earlbaum Associates (1988). p. 20–21.
70. Yang Y, Lhotta K, Chung EK, Eder P, Neumair F, Yu CY. Complete complement components C4A and C4B deficiencies in human kidney diseases and systemic lupus erythematosus. *J Immunol*. (2004) 173:2803–14. doi: 10.4049/jimmunol.173.4.2803

71. Lv Y, He S, Zhang Z, Li Y, Hu D, Zhu K, et al. Confirmation of C4 gene copy number variation and the association with systemic lupus erythematosus in Chinese Han population. *Rheumatol Int*. (2012) 32:3047–53. doi: 10.1007/s00296-011-2023-7
72. Kemp ME, Atkinson JP, Skanes VM, Levine RP, Chaplin DD. Deletion of C4A genes in patients with systemic lupus erythematosus. *Arthritis Rheum*. (1987) 30:1015–22. doi: 10.1002/art.1780300908
73. Fielder AH, Walport MJ, Batchelor JR, Rynes RI, Black CM, Dodi IA, et al. Family study of the major histocompatibility complex in patients with systemic lupus erythematosus: importance of null alleles of C4A and C4B in determining disease susceptibility. *Br Med J (Clin Res Ed)*. (1983) 286:425–8. doi: 10.1136/bmj.286.6363.425
74. Nakamura H, Oku K, Ogata Y, Ohmura K, Yoshida Y, Kitano E, et al. Alternative pathway activation due to low level of complement factor H in primary antiphospholipid syndrome. *Thromb Res*. (2018) 164:63–8. doi: 10.1016/j.thromres.2018.02.142
75. Galli M, Luciani D, Bertolini G, Barbui T. Lupus anticoagulants are stronger risk factors for thrombosis than anticardiolipin antibodies in the antiphospholipid syndrome: a systematic review of the literature. *Blood*. (2003) 101:1827–32. doi: 10.1182/blood-2002-02-0441
76. Ying L, Katz Y, Schlesinger M, Carmi R, Shalev H, Haider N, et al. Complement factor H gene mutation associated with autosomal recessive atypical hemolytic uremic syndrome. *Am J Hum Genet*. (1999) 65:1538–46. doi: 10.1086/302673
77. Kavanagh D, Richards A, Fremeaux-Bacchi V, Noris M, Goodship T, Remuzzi G, et al. Screening for complement system abnormalities in patients with atypical hemolytic uremic syndrome. *Clin J Am Soc Nephrol*. (2007) 2:591–6. doi: 10.2215/CJN.03270906
78. Ekdahl KN, Teramura Y, Hamad OA, Asif S, Duehrkop C, Fromell K, et al. Dangerous liaisons: complement, coagulation, and kallikrein/kinin cross-talk act as a linchpin in the events leading to thromboinflammation. *Immunol Rev*. (2016) 274:245–69. doi: 10.1111/imr.12471
79. Fearon DT. Activation of the alternative complement pathway. *CRC Crit Rev Immunol*. (1979) 1:1–32.
80. Lachmann PJ, Hughes-Jones NC. Initiation of complement activation. *Springer Semin Immunopathol*. (1984) 7:143–62. doi: 10.1007/BF01893018
81. Fearon DT, Daha MR, Weiler JM, Austen KF. The natural modulation of the amplification phase of complement activation. *Transplant Rev*. (1976) 32:12–25. doi: 10.1111/j.1600-065X.1976.tb00226.x
82. Lintner KE, Patwardhan A, Rider LG, Abdul-Aziz R, Wu YL, Lundström E, et al. Gene copy-number variations (CNVs) of complement C4 and C4A deficiency in genetic risk and pathogenesis of juvenile dermatomyositis. *Ann Rheum Dis*. (2016) 75:1599–606. doi: 10.1136/annrheumdis-2015-207762
83. Agostinis C, Durigutto P, Sblattero D, Borghi MO, Grossi C, Guida F, et al. A non-complement-fixing antibody to beta2 glycoprotein I as a novel therapy for antiphospholipid syndrome. *Blood*. (2014) 123:3478–87. doi: 10.1182/blood-2013-11-537704
84. Gropp K, Weber N, Reuter M, Micklisch S, Kopka I, Hallström T, et al. beta(2)-glycoprotein I, the major target in antiphospholipid syndrome, is a special human complement regulator. *Blood*. (2011) 118:2774–83. doi: 10.1182/blood-2011-02-339564
85. Zhu X, Zhang J, Wang Q, Fu H, Chang Y, Kong Y, et al. Diminished expression of beta2-GPI is associated with a reduced ability to mitigate complement activation in anti-GPIIb/IIIa-mediated immune thrombocytopenia. *Ann Hematol*. (2018) 97:641–54. doi: 10.1007/s00277-017-3215-3
86. Garred P, Voss A, Madsen HO, Junker P. Association of mannose-binding lectin gene variation with disease severity and infections in a population-based cohort of systemic lupus erythematosus patients. *Genes Immun*. (2001) 2:442–50. doi: 10.1038/sj.gene.6363804
87. Piao W, Liu CC, Kao AH, Manzi S, Vogt MT, Ruffing MJ, et al. Mannose-binding lectin is a disease-modifying factor in North American patients with systemic lupus erythematosus. *J Rheumatol*. (2007) 34:1506–13.
88. Garred P, Madsen HO, Halberg P, Petersen J, Kronborg G, Svejgaard A, et al. Mannose-binding lectin polymorphisms and susceptibility to infection in systemic lupus erythematosus. *Arthritis Rheum*. (1999) 42:2145–52. doi: 10.1002/1529-0131(199910)42:10<2145::AID-ANR15>3.0.CO;2-#
89. Øhlenschlaeger T, Garred P, Madsen HO, Jacobsen S. Mannose-binding lectin variant alleles and the risk of arterial thrombosis in systemic lupus erythematosus. *N Engl J Med*. (2004) 351:260–7. doi: 10.1056/NEJMoa033122
90. Font J, Ramos-Casals M, Brito-Zerón P, Nardi N, Ibañez A, Suarez B, et al. Association of mannose-binding lectin gene polymorphisms with antiphospholipid syndrome, cardiovascular disease and chronic damage in patients with systemic lupus erythematosus. *Rheumatology (Oxford)*. (2007) 46:76–80. doi: 10.1093/rheumatology/kel199
91. Cavusoglu E, Eng C, Chopra V, Ruwende C, Yanamadala S, Clark LT, et al. Usefulness of the serum complement component C4 as a predictor of stroke in patients with known or suspected coronary artery disease referred for coronary angiography. *Am J Cardiol*. (2007) 100:164–8. doi: 10.1016/j.amjcard.2007.02.075
92. Sugiura-Ogasawara M, Nozawa K, Nakanishi T, Hattori Y, Ozaki Y. Complement as a predictor of further miscarriage in couples with recurrent miscarriages. *Hum Reprod*. (2006) 21:2711–4. doi: 10.1093/humrep/del229
93. Shamonki JM, Salmon JE, Hyjek E, Baergen RN. Excessive complement activation is associated with placental injury in patients with antiphospholipid antibodies. *Am J Obstet Gynecol*. (2007) 196:167 e161–5. doi: 10.1016/j.ajog.2006.10.879
94. Schanberg LE, Sandborg C, Barnhart HX, Ardoin SP, Yow E, Evans GW, et al. Use of atorvastatin in systemic lupus erythematosus in children and adolescents. *Arthritis Rheum*. (2012) 64:285–96. doi: 10.1002/art.30645

Conflict of Interest Statement: The authors declare that the research was conducted in the absence of any commercial or financial relationships that could be construed as a potential conflict of interest.

frontiers in Immunology

ORIGINAL RESEARCH
published: 20 May 2019
doi: 10.3389/fimmu.2019.01066

Mechanistic Characterization of *RASGRP1* Variants Identifies an hnRNP-K-Regulated Transcriptional Enhancer Contributing to SLE Susceptibility

Julio E. Molineros[1†], *Bhupinder Singh*[1†], *Chikashi Terao*[2,3], *Yukinori Okada*[4], *Jakub Kaplan*[1], *Barbara McDaniel*[1], *Shuji Akizuki*[3], *Celi Sun*[1], *Carol F. Webb*[5], *Loren L. Looger*[6] *and Swapan K. Nath*[1*]

[1] *Arthritis and Clinical Immunology Research Program, Oklahoma Medical Research Foundation, Oklahoma City, OK, United States,* [2] *Laboratory for Statistical Analysis, RIKEN Center for Integrative Medical Sciences, Yokohama, Japan,* [3] *Department of Rheumatology and Clinical Immunology, Graduate School of Medicine, Kyoto University, Kyoto, Japan,* [4] *Department of Statistical Genetics, Osaka University Graduate School of Medicine, Osaka, Japan,* [5] *Departments of Medicine, Microbiology and Immunology, University of Oklahoma Health Sciences Center, Oklahoma, OK, United States,* [6] *Howard Hughes Medical Institute, Janelia Research Campus, Ashburn, VA, United States*

OPEN ACCESS

Edited by:
José Carlos Crispín, Instituto Nacional de Ciencias Médicas y Nutrición Salvador Zubirán (INCMNSZ), Mexico

Reviewed by:
Shinsuke Yasuda, Hokkaido University, Japan
Sergio Iván Valdés-Ferrer, Instituto Nacional de Ciencias Médicas y Nutrición Salvador Zubirán (INCMNSZ), Mexico

***Correspondence:**
Swapan K. Nath
swapan-nath@omrf.org

[†] *These authors have contributed equally to this work*

Specialty section:
This article was submitted to Autoimmune and Autoinflammatory Disorders, a section of the journal Frontiers in Immunology

Received: *02 November 2018*
Accepted: *25 April 2019*
Published: *20 May 2019*

Citation:
Molineros JE, Singh B, Terao C, Okada Y, Kaplan J, McDaniel B, Akizuki S, Sun C, Webb CF, Looger LL and Nath SK (2019) Mechanistic Characterization of RASGRP1 Variants Identifies an hnRNP-K-Regulated Transcriptional Enhancer Contributing to SLE Susceptibility. Front. Immunol. 10:1066. doi: 10.3389/fimmu.2019.01066

Systemic lupus erythematosus (SLE) is an autoimmune disease with a strong genetic component. We recently identified a novel SLE susceptibility locus near *RASGRP1,* which governs the ERK/MAPK kinase cascade and B-/T-cell differentiation and development. However, precise causal *RASGRP1* functional variant(s) and their mechanisms of action in SLE pathogenesis remain undefined. Our goal was to fine-map this locus, prioritize genetic variants likely to be functional, experimentally validate their biochemical mechanisms, and determine the contribution of these SNPs to SLE risk. We performed a meta-analysis across six Asian and European cohorts (9,529 cases; 22,462 controls), followed by *in silico* bioinformatic and epigenetic analyses to prioritize potentially functional SNPs. We experimentally validated the functional significance and mechanism of action of three SNPs in cultured T-cells. Meta-analysis identified 18 genome-wide significant ($p < 5 \times 10^{-8}$) SNPs, mostly concentrated in two haplotype blocks, one intronic and the other intergenic. Epigenetic fine-mapping, allelic, eQTL, and imbalance analyses predicted three transcriptional regulatory regions with four SNPs (rs7170151, rs11631591-rs7173565, and rs9920715) prioritized for functional validation. Luciferase reporter assays indicated significant allele-specific enhancer activity for intronic rs7170151 and rs11631591-rs7173565 in T-lymphoid (Jurkat) cells, but not in HEK293 cells. Following up with EMSA, mass spectrometry, and ChIP-qPCR, we detected allele-dependent interactions between heterogeneous nuclear ribonucleoprotein K (hnRNP-K) and rs11631591. Furthermore, inhibition of hnRNP-K in Jurkat and primary T-cells downregulated *RASGRP1* and ERK/MAPK signaling. Comprehensive association, bioinformatics, and epigenetic analyses yielded putative functional variants of *RASGRP1*, which were experimentally validated. Notably, intronic

variant (rs11631591) is located in a cell type-specific enhancer sequence, where its risk allele binds to the hnRNP-K protein and modulates *RASGRP1* expression in Jurkat and primary T-cells. As risk allele dosage of rs11631591 correlates with increased *RASGRP1* expression and ERK activity, we suggest that this SNP may underlie SLE risk at this locus.

Keywords: *RASGRP1*, homology, ERK (extracellular-signal-regulated kinase), genetic variant, luciferase, ChIP-qPCR, EMSA (electrophoretic mobility shift assay)

INTRODUCTION

Systemic lupus erythematosus (SLE) is a complex autoimmune disease that disproportionately affects people of Asian, African, and Hispanic ethnicities and women, in particular, with higher incidence and disease severity (1). Much of SLE etiology remains mysterious. It has been proposed that complex interactions amongst numerous genes and their products with pathogens and other environmental factors promotes dysregulation of both the innate and adaptive immune responses in SLE. Over 80 SLE susceptibility loci have been identified so far across multiple ethnic groups by genome-wide association studies (GWAS) and candidate gene studies (2, 3). However, the precise underlying variants and functional mechanisms associated with disease are largely unidentified for the vast majority of these SLE-associated signals. Understanding SLE pathogenesis requires identification of true causal variants and the target genes and mechanisms by which they contribute to disease.

Previously, we reported a novel SLE susceptibility signal near the RAS guanyl-releasing protein 1 (*RASGRP1*) in Asians (4). We identified several associated variants, the most significant being an intergenic variant (rs12900339) between *RASGRP1* and *C15orf53* (4). However, the actual predisposing variants, target genes, and underlying mechanisms of action for this region are largely unknown. *RASGRP1* belongs to a family of RAS guanyl nucleotide-releasing proteins (RASGRPs) comprising four members (*RASGRP1* through *RASGRP4*), all with a diacylglycerol (DAG)-binding C1 catalytic domain. Upon antigen stimulation, DAG binding and phospholipase C (PLC) signaling drive RASGRPs to the membrane, where they play important roles in RAS activation (5, 6). *RASGRP1*, originally cloned from the brain (7), was later found highly expressed in T-lymphocytes (8); small amounts of *RASGRP1* expression can also occur in B-lymphocytes, neutrophils, mast cells, and natural killer cells (9–11). *RASGRP1* has been shown to be involved in B-cell development, activation and tolerance, in both mice and humans (12, 13). *RASGRP1*$^{-/-}$ mice have been reported for marked deficiency in thymocyte and lymphocyte development, which was associated with impaired proliferation in response to TCR stimulation (14). Deficiency in *RASGRP1* in mice has been associated with CD4+ and CD8+ T cell lymphopenia (8). However, humans deficient in *RASGRP1* show a decrease in CD4+T concurrent with a relative increase in CD8+T cells (15). *RASGRP1* inhibition impairs T-cell expansion and increases susceptibility to Epstein-Barr virus infection, as well as suppressing proliferation of activated T-cells occurring in autoimmune conditions (16). A recent study reported a heterozygous mutation in *RASGRP1* correlated with autoimmune lymphoproliferative syndrome (ALPS)-like disease (17). *RASGRP1* expression in T-cells also correlated negatively with rheumatoid arthritis disease activity (18). Dysregulated expression of *RASGRP1* has been observed in human SLE. The ratio of normal *RASGRP1* isoforms to isoforms missing exon-11 could be linked to defective poly[ADP-ribose] polymerase 1 (*PARP1*) expression and reduced lymphocyte survival in SLE patients (19, 20). Aberrant splice variants accumulate in SLE patients and adversely affect T-cell function (21). There are conflicting reports of the effect of *RASGRP1* on ERK signaling. On one hand, deficiency in *RASGRP1* expression reportedly decreases ERK phosphorylation in B- and T-cells (15). Hydralazine, a drug that causes drug-induced lupus erythematosus, is reported to inhibit ERK signaling, inducing autoimmunity and the production of anti-dsDNA autoantibodies in mice (22). However, some reports found significantly higher levels of pERK and pJNK in SLE patients with active disease vs. controls and inactive SLE patients (23–25), contradicting earlier reports. In spite of these conflicting reports, the consensus is that *RASGRP1* dysfunction is mechanistically associated with autoimmune phenotypes including SLE.

Here, we fine-mapped an SLE locus near *RASGRP1* that we previously identified (4). Using trans-ethnic meta-analysis across six Asian and European cohorts followed by bioinformatic analyses and experimental validation, we identified potential SLE predisposing variants and defined mechanisms by which these functional variants contribute to SLE pathogenicity.

MATERIALS AND METHODS

Patients and Data

We used all associated SNP data at this locus from six cohorts reported previously (**Table 1**). We began with our published Asian cohort report [see Supplementary Table 5 in Sun et al. (4)] and augmented this with two publicly available sets of GWAS summary statistics (26, 27) and a partially published Japanese cohort (28). Our original report contained three Asian cohorts (3AS: Korean, Han Chinese, and Malaya Chinese). Japanese samples included samples (456 cases and 1,102 controls) collected under support of the Autoimmune Disease Study Group of Research in Intractable Diseases, Japanese Ministry of Health, Labor and Welfare, and the BioBank Japan Project (28), and added samples obtained at Kyoto University, Japan. SLE classification followed the

TABLE 1 | Cohorts used in this study.

Population	Cohort	Cases	Controls	Publication
Asian	3AS	2,487	7,620	(4)
HC	Han Chinese	1,659	3,398	(26)
EU	European	4,036	6,958	(27)
JAP	Japanese	1,347	4,486	(28) + new Data
TOTAL		9,529	22,462	

We utilized samples from our previous report (4) (3AS: Korean, Han Chinese and Malaya Chinese) for RASGRP1 SLE association. We added a Han Chinese (HC) and a European (EU) cohort from (26) and a Japanese cohort containing the patients from Okada et al. (28) and additional Japanese samples (JAP).

American College of Rheumatology criteria (29). All sample collections were approved by the Institutional Review Board of the Oklahoma Medical Research Foundation as well as by the collaborating institutions.

Quality Control

SNP quality control for our initial Asian cohort has been described elsewhere (4). Quality control for European, Han Chinese 2, and Japanese samples was described in the original publications (26–28). All SNPs in the study were in Hardy-Weinberg equilibrium ($P > 1 \times 10^{-6}$) and had minor allele frequency >0.5%. Genotypic missingness was <10%. In order to match risk alleles between cohorts, we compared their allele frequencies to the parent populations from the 1,000 Genomes Project. We used the SNP reference dbSNP142 as the SNP-naming convention in common for all variants. SNP imputation for all cohorts was described in their original publications. For this study, SNPs with r^2 and imputation quality information <0.7 were dropped.

Study Design

In order to identify *RASGRP1* functional variants and their mechanisms of action, our analysis followed the workflow presented in **Figure 1**. We first extracted all summary GWAS information in and around *RASGRP1* (118 SNPs) from **Supplementary Table 5** in our previous study of Asian SLE (4). We combined these results with a European (27), an Asian (26), and a partially published Japanese cohort (28), to perform meta-analysis. SNPs that passed the genome-wide significant association threshold ($p = 5 \times 10^{-8}$) were further annotated with functional information. A series of bioinformatics and epigenomic analyses was conducted for each of the candidate SNPs including their effects on gene expression (expression quantitative trait loci, eQTLs), transcription factor binding, promoter/enhancer activities, and chromatin interaction sites. Together, we prioritized and nominated SNPs with stronger association signals and with higher annotated likelihood of being functional (**Supplementary Tables 1, 2**). Finally, we experimentally validated predicted functions of the nominated SNPs in Jurkat and HEK293 cell lines. Following SNP prioritization, we performed electrophoretic mobility shift assays (EMSAs), followed by mass spectrometry, chromatin immuno-precipitation quantitative PCR (ChIP-qPCR), and inhibition-based expression assays.

Association Analysis and Trans-Ethnic Meta-Analysis

Association analysis for all cohorts was performed using PLINK (30) and SNPTEST. Meta-analysis for all cohorts was performed in METAL (31) using cohort sample size correction and standard error correction to estimate the 95% confidence interval for odds ratios. Heterogeneity of odds ratios was estimated and informed the use of P_{meta} values in the study. Variants with $P_{\text{meta}} < 5 \times 10^{-3}$ were selected for further study.

Bioinformatic Analysis

Given that candidate SNPs were located in non-coding regions of the genome, we performed a thorough epigenetic annotation of the variants. Initial annotation of epigenetic features was performed in Haploreg (32). Each SNP in the region was collocated with active and regulatory histone marks including H3K27ac, H3K4me1, and H3K4me3, and DNase hypersensitivity sites (DHS) in GM12878, and CD4+ and CD8+ T cells (**Supplementary Figure 1**). Histone modifications and DHS data were obtained from the ENCODE project (33) and the BLUEPRINT epigenome project (34).

SNP Prioritization

We used a prioritization algorithm to narrow down the large list of SNPs for further validation. Our strategy consisted of two Bayesian algorithms to score each SNP [3dSNP (35) and RegulomeDB (36)], as well as additional expression, epigenetic, and preferential allele-specific information about each SNP. First, we used the 3dSNP (35) tool to assign functional weights based on the presence of enhancers, promoters, experimentally determined (ChIP-seq) transcription factor binding sites (TFBSs), TFBS motif matching, evolutionary conservation, and presence of 3D chromatin interactions. We assigned a 3dSNP weight of 2 to SNPs >2 standard deviations above the mean, a weight of 1 for scores above the mean, and a weight of 0 for the rest. RegulomeDB (36) scores were also assigned for each candidate SNP and converted to an associated weight. Each functional category, i.e., eQTL, enhancer/super-enhancer, rSNP (37), capture Hi-C, TFBS, and allele-specific expression/binding, was assigned a weight of 1 if the SNP had this feature. Finally, we summed all weights for each SNP and nominated the top SNPs for further experimental validation.

Expression Quantitative Trait Loci (eQTLs)

All the candidate SNPs were annotated for the presence of eQTLs changing expression of *RASGRP1* and its surrounding genes in multiple tissues. We used expression databases for whole blood (38, 39), immune cell lines (40), and multiple tissues (41) (GTEx Analysis Release V6p). In order to identify quantitative changes in methylation in blood cell lines, we used the WP10 database from the Blueprint epigenome project (42).

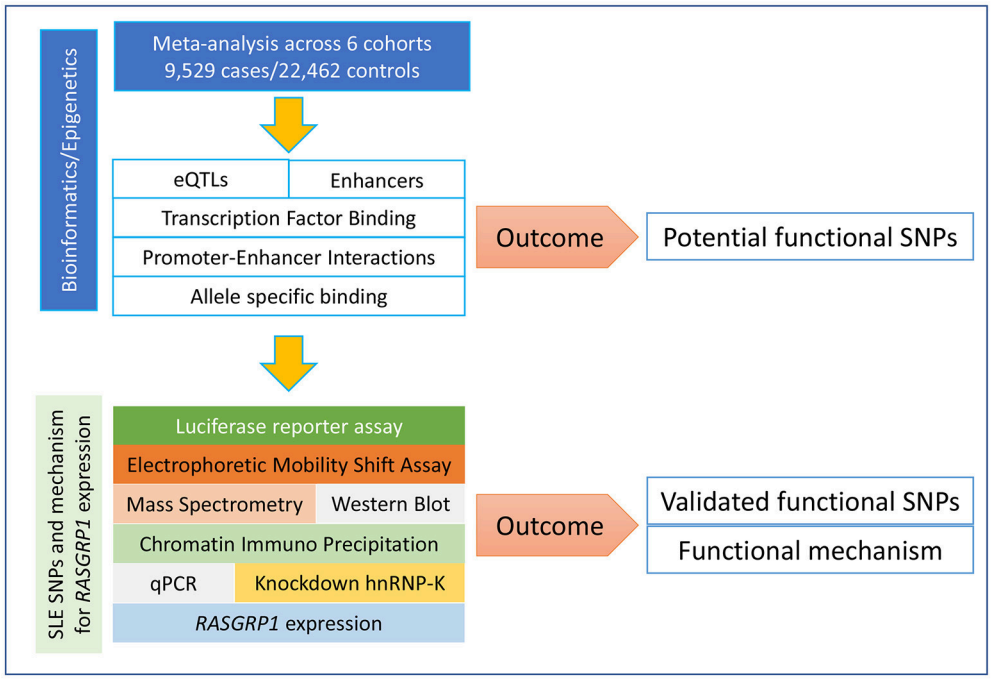

FIGURE 1 | Framework of study design. Our study followed our bioinformatics-prioritized potential functional SNPs with laboratory validation along many different dimensions.

Transcription Factor Binding Sites (TFBSs)

In order to identify allele-specific effects on transcription factor binding (TFBSs), we used the motifBreakr (43) algorithm implemented in R, as well as the PERFECTOS-APE algorithm that identifies fold-changes in binding affinity of SNPs against HOCOMOCO10, HOMER, JASPER, Swiss Regulon, and HT-Selex motif databases. We selected only TFBSs that had at least 5-fold change in affinity.

Assessing SNP Effects on Enhancer/Promoter Sequences

We assessed whether each SNP was located within regulatory (enhancer/promoter) regions across multiple cell lines using active histone marks (H3K27ac, H3K4me1, and H3K4me3) collocation implemented in the 3dSNP application (35). Super-enhancers were annotated using the dbSuper (44), Prestige (45), and EnhancerAtlas (46) databases.

Chromatin Interactions

Chromatin looping was identified using capture Hi-C assays obtained from 3D Genome (47), 3DSNP (35) and CHiCP (48); as well as from Promoter-capture Hi-C (49–52) experiments.

Allele-Specific Binding

Candidate SNPs within the association peaks were further targeted to assess allele-specific binding (ASB) of histone marks H3K4me1 and H3K4me3 in and around them. ASB was calculated using seven heterozygous cell lines (GM10847, GM12890, GM18951, GM19239, GM19240, GM2610, and SNYDER). ASB was implemented in SNPhood (53).

Luciferase Reporter Assays

To test candidate SNP-containing regions for allele-specific enhancer activity, we cloned all three SNPs (rs1163159, rs7173565-rs7173565, and rs9920715) individually into the enhancer reporter plasmid pGL4.26[luc2/minP/Hygro] (Promega, USA). In brief, genomic DNA from the Coriell cell line having different genotypes for the SNP tested (obtained from NIGMS Human Genetic Cell Repository at the Coriell Institute for Medical Research) was amplified using specific primers containing KpnI and HindIII sites (**Supplementary Table 3**). These amplified PCR products surrounding rs11631591 (481 bp), rs7170151 (579 bp), and rs9920715 (455 bp) were digested with KpnI and HindIII restriction enzymes and ligated into the pGL4.26 plasmid. After cloning and transformation, the plasmids generated for each genotype were confirmed by direct Sanger DNA sequencing. To study cell type-dependence, we used two different cell types: human embryonic kidney HEK293 and T-lymphoid Jurkat cell lines. HEK293 cells were seeded in 24-well sterile plastic culture plates at a density of $1x10^5$ cells per well with complete growth medium. The cells were transfected with 500 ng of pGL4.26 (with or without insert) along with 50 ng *Renilla* plasmid as control vector to control for differences in transfection efficiency. LipofectAMINE 3000 (Invitrogen, USA) was used for transfection into HEK293 cells, according to the manufacturer's protocol. For Jurkat transfections, we used the Neon Transfection System (Thermo Fisher Scientific). A total of 5×10^5 Jurkat cells was electroporated with a Neon Transfection System (Invitrogen) under the following conditions: voltage (1,050 V), width (30 ms), pulses (Two), 10-µl tip, and Buffer R. For transfection, we used 2 µg of each plasmid

containing the insert with risk or non-risk allele, along with 50 ng *Renilla* plasmid. Firefly and *Renilla* luciferase activities were measured consecutively at 24 h after transfection using Dual-luciferase assays (Promega), according to the manufacturer's instructions. Luciferase activity was analyzed with Student's *t*-test implemented in GraphPad Prism7. Differences between relative luciferase activity levels were considered significant if Student's *t*-test P-value < 0.05.

Identification of DNA-Binding Proteins

Electrophoretic Mobility Shift Assays (EMSAs) and DNA Pulldown Assays

Jurkat cell lines were obtained from ATCC and maintained in RPMI 1640 medium with 2 mm L-glutamine, 100 μg/ml each of streptomycin and penicillin, and 10% fetal bovine serum at 37°C with 5% CO_2. Cells were harvested at a density of 8 × 10^5 cells/ml, and nuclear extracts were prepared using the NER nuclear extraction kit (Invitrogen) with complete protease inhibitors (Roche Diagnostics). Protein concentrations were measured using a BCA reagent. Biotinylated DNA sequence surrounding the candidate SNPs (rs7170151 and rs11631591) was prepared using a synthetic single-stranded DNA sequence (Integrated DNA Technologies, USA) (**Supplementary Table 3**). Biotinylated DNA sequence with a 5-bp deletion at the SNP region served as a control for the assay. Twenty-five pmol of each DNA product was bound to 1 mg Dynabeads® M-280 Streptavidin (Invitrogen, USA), as per the manufacturer's recommendations. Dynabeads M-280 Streptavidin (Dynal, Inc., Lake Success, NY, USA) were prepared by washing three times in phosphate-buffered saline (pH 7.4) containing 0.1% bovine serum albumin and two times with Tris-EDTA containing 1 M NaCl. Between each wash, beads were pulled down with a Dynal magnetic particle concentrator. Double-stranded, biotinylated oligonucleotides were added to the washed beads, and the mix was rotated for 20–30 min at 21 °C. Equal cpm of proteins translated *in vitro* were diluted to 1× with binding buffer and mixed with ∼100 μg of Dynabeads containing 10 pmol of the individual oligonucleotide probe in a final volume of 250 μl. The mixture was rotated at room temperature for 20 min. Proteins bound to the beads were separated from unbound proteins by successive washes, three times with 0.5× binding buffer and once with 1× binding buffer. Higher stringency washes included two washes with 2× binding buffer. Beads and bound proteins were pulled down with a magnetic concentrator, suspended in 1× sample buffer, boiled for 5 min, and resolved on SDS-PAGE gels, followed by peptide mass fingerprint MALDI-MS analysis of single bands.

Mass Spectrometry Analysis

Mass spectrometry analysis was performed using a Thermo-Scientific LTQ-XL mass spectrometer coupled to an Eksigent splitless nanoflow HPLC system. Bands of interest were excised from the silver nitrate-stained Bis-Tris gel and de-stained with Farmer's reducer (50 mM sodium thiosulfate, 15 mM potassium ferricyanide). The proteins were reduced with dithiothreitol, alkylated with iodoacetamide, and digested with trypsin. Samples were injected onto a 10 cm × 75 mm inner diameter capillary column packed with Phenomenex Jupiter C18 reverse phase resin. The peptides were eluted into the mass spectrometer at a flow rate of 175 nl/min. The mass spectrometer was operated in a data-dependent mode acquiring one mass spectrum and four CID spectra per cycle. Data were analyzed by searching all acquired spectra against the human RefSeq databases using Mascot (Matrix Science Inc., Boston, MA, USA). Minimum identification criteria required two peptides with ion scores >50% and were verified by manual inspection. We verified the identity of the assayed proteins by Western blot.

Confirmation of Identified Protein by Western Blot

Mass spectrometry-identified proteins were confirmed by Western blot. Jurkat nuclear extracts after DNA pulldown assay were lysed in sample buffer [62.5 mM Tris·HCl (pH 6.8 at 25°C), 2% wt/vol SDS, 10% glycerol, 50 mM dithiothreitol, 0.01% wt/vol bromophenol blue]. Equal amounts of protein were loaded onto a 10% SDS-PAGE gel (GTX gel BioRad USA). After it resolved, samples were blotted to Nitrocellulose paper using the Trans-blot Turbo Transfer System (BioRad, USA). Membranes were blocked using LI-COR blocking buffer for 2 h and then incubated with primary antibody 1:1,000 dilution (hnRNP-K, Santa Cruz USA) at 4°C overnight, and with a donkey anti-mouse IR-Dye 800 (LI-COR, USA) secondary antibody for 1 h. The membrane was imaged with a LI-COR Odyssey using Auto-Scan. Background-subtracted signal intensity was quantified using Image Studio 4.0 software.

Chromatin Immuno-Precipitation (ChIP) Assay Followed by qPCR (ChiP-qPCR)

ChIP assays were performed using the MAGnify ChIP system (Life Technologies, NY), according to the manufacturer's protocol. Jurkat cells were fixed for 10 min with 1% formaldehyde to crosslink DNA-protein and protein-protein complexes. The cross-linking reaction was stopped using 1.25 M glycine for 5 min. The cells were lysed, sonicated to shear DNA, and sedimented. Then, their diluted supernatants were incubated with 5 μg hnRNP-K antibody. Ten percent of the diluted supernatants were saved as "input" for normalization. Several washing steps were followed by protein digestion using proteinase K. Reverse crosslinking was carried out at 65°C. DNA was subsequently purified and amplified by quantitative PCR on an SDS 7900 (Applied Biosystems) using specific primers. Because the Jurkat cell line is heterozygous for the SNPs rs11631591 and rs7170151, we performed Sanger DNA sequencing with the ChIP-eluted PCR product.

Isolation of $CD3^+$ T-Cells From Human Blood

We used leukoreduction system chambers (LRS chambers) from human blood donors. LRS chambers were obtained from the Oklahoma Blood Institute (OK, USA) (**Supplementary Table 12**; **Supplementary Figure 9**). LRSCs were sterilized externally using 70% (v/v) ethanol and handled in a class 2 laminar flow cabinet. External tubing was cut, the chamber inverted over a 50 ml sterile

centrifuge tube (Greiner Bio-One), and the contents allowed to drip through. The contents (usually 20 ml) were then diluted to 90 ml in RPMI medium. The peripheral blood mononuclear cells (PBMCs) were isolated by carefully layering 30 ml fractions over 17 ml of histopaque-1077 (Sigma-Aldrich), which was then centrifuged at 340 g for 45 min at 20°C. The PBMC layer was isolated and washed three times with culture medium with cells centrifuged at 340 g for 15 min for the first wash and 10 min for the subsequent two washes. The isolated PBMCs were counted and viability assessed with Trypan blue using a hemocytometer, then centrifuged at 340 g for 10 min. The untouched $CD3^+$ T cells were collected using MojoSort™ Human $CD3^+$ T-Cell Isolation Kit, as per manufacturer instructions (BioLegend, San Diego, CA).

Inhibition of hnRNP-K and ERK Phosphorylation

Inhibition of hnRNP-K was performed in $CD3^+$ T cells from healthy controls, as well as in Jurkat T-cells using 5-Fluorouracil (5-FU) (Sigma Aldrich, USA), as described previously (54). Isolated $CD3^+$ T-cells and Jurkat cells were cultured in RPMI-1640 medium containing 10% heat-inactivated fetal bovine serum (Invitrogen) and kept at 37°C in 5% CO_2 conditions. For 5-FU treatment, the drug was first dissolved in dimethyl sulfoxide (DMSO) and further diluted in medium before use. Cells were treated with 20 ng/μl 5-FU, unless otherwise stated. Next, to examine whether hnRNP-K and/or *RASGRP1* down-regulation by 5-FU led to inhibition of EKR phosphorylation of ERK, Jurkat and $CD3^+$ T-cells were pretreated with PMA 5 μg/μl for 30 min, prior to drug (5-FU) treatment. Inhibition of hnRNP-K and *RASGRP1* was detected using mRNA expression analysis with quantitative PCR (after 48 h) and by Western blot (after 72 h).

RESULTS

Patients and Samples

We used five Asian cohorts and one cohort of European descent; sample sizes for the meta-analysis were 9,529 SLE cases and 22,462 controls (**Table 1**).

Fine-Mapping, Replication and Meta-Analysis of *RASGRP1* Association

First, we probed our previously reported SLE-associated region (chr15: 38.4–39.2 MB, hg19) and extracted association results for six cohorts from the region containing the genes *RASGRP1* (RAS guanyl-releasing protein 1, a diacylglycerol-regulated guanine nucleotide exchange factor) and *C15orf53* [encoding a protein of unknown function linked to alcohol dependence (55)]. The strongest association signal among Asian cohorts localized to intron 2 of *RASGRP1* (**Figure 2**; **Table 2**). Meta-analysis with all cohorts identified the largest signal at intronic SNP rs8032939 [$P_{meta} = 3.2 \times 10^{-11}$, OR (95%CI) = 0.88 (0.85–0.92)]. We identified 17 genome-wide significant (GWS) SNPs ($P_{meta} < 5 \times 10^{-8}$). Our previously reported lead SNP rs12900339 (4) did not reach GWS ($P_{meta} = 9.2 \times 10^{-7}$) (**Table 2**). Analysis of the association signals in the context of linkage disequilibrium (LD) of 1,000 Genome populations (EUR, ASN; **Figure 2**) identified two uncorrelated association signals (**Supplementary Table 1**). The main signal occurred at rs8032939 in intron 2 (**Figure 2**), while the second signal localized to the intergenic region between *RASGRP1* and *C15orf53*: SNP rs9920715 [60 kb 5′ of *RASGRP1*; $P_{meta} = 5.1 \times 10^{-9}$; OR (95%CI) = 0.89(0.86–0.93)]. Many (27 of 118 SNPs) variants were intronic (**Figure 2**). We then examined the 18 GWS SNPs with bioinformatic and epigenomic analysis (**Table 2**). Our top SNP (rs8032939) was previously reported as a rheumatoid arthritis (RA)-associated SNP (56). Within the intronic signal, we also identified rs8035957 ($P_{meta} = 1.3 \times 10^{-10}$), associated with Type I Diabetes (57).

Evaluating Functional SNPs

To identify putative functional SLE SNPs in and around *RASGRP1*, we computed weighted scores for each SNP by integrating multiple sources of functional annotation, including allele-dependent gene expression, overlap with annotated enhancers and promoters, binding affinity to transcription factors, and collocation with anchors in promoter-enhancer-capture Hi-C experiments (**Supplementary Table 2**).

Gene Expression

We then identified allele-dependent changes in gene expression by annotating SNPs using expression quantitative trait locus (eQTL) databases for multiple tissues (**Methods**). All candidate LD SNPs were eQTLs in blood cell lines ($3.2 \times 10^{-3} > P > 1.9 \times 10^{-4}$; **Supplementary Table 4**), as well as in skin, esophagus, and testis (**Table 3**). The intronic (main signal) SNPs affected expression of both *RASGRP1* and *C15orf53*, while the intergenic (secondary) SNPs (in LD with rs9920715) altered expression of only *RASGRP1*. *RASGRP1* SNPs also affected expression of long non-coding RNAs (lncRNAs) *RP11-102L12.2* and *RP11-275I4.2* in non-blood cell lines. All eQTL risk alleles increased expression of *RASGRP1* in multiple cell lines (**Supplementary Table 4**; **Supplementary Figure 2**), but had opposing effects on the neighboring gene *C15orf53* (**Supplementary Table 4**). We also found significant effects of two linked SNPs (rs11073344, rs11631591) on methylation of *RASGRP1* in T-cells and neutrophils, respectively (**Supplementary Table 5**).

Overlap With Enhancers and Super-Enhancers

Then, we investigated the potential of the candidate SNPs to act as enhancers of *RASGRP1* expression. Three GWS SNPs (rs6495979, rs11631591, and rs7173565) overlapped with ENCODE-annotated enhancers for *RASGRP1* in lymphoblastoid cells (GM12878, GM12892) and also in $CD8^+$ T-cells. These three GWS SNPs (all intronic) localized to super-enhancers [i.e., collections of multiple contiguous enhancers (58)] for *RASGRP1* in $CD4^+$ $CD25^-$ $CD45RA^+$ naïve cells, $CD4^+$ $CD25^-$ $CD45RO^+$ memory cells, $CD8^+$ primary cells, $CD4^+$ $CD25^-$ $Il17^+$ phorbol myristate acetate (PMA)-stimulated Th17 cells, and $CD4^+$ $CD25^-$ $Il17^-$ PMA-stimulated Th17 cells (**Supplementary Table 6**). This suggests that these SNPs may regulate *RASGRP1* in T-lymphocytes.

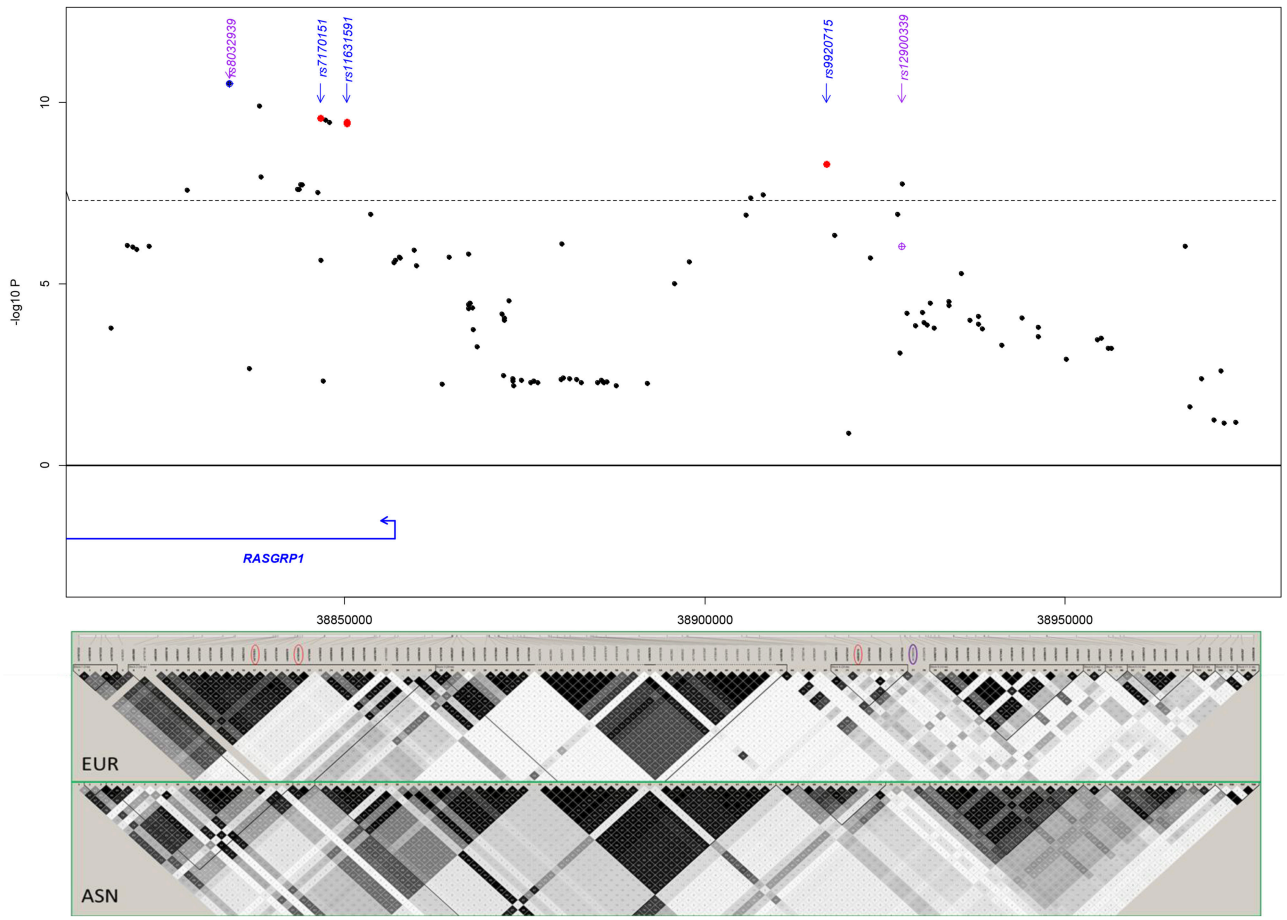

FIGURE 2 | Meta-analysis in the *RASGRP1* region. Blue diamond: lead SNP rs8032939 following initial meta-analysis. Red circles: SNPs chosen for experimental validation. rs11631591-rs7173565 are considered together due to their proximity; only rs11631591 is labeled. Purple diamond: our previously reported (4) lead SNP rs12900339. Linkage disequilibrium in the region (bottom) is notably different between European (EUR) and Asian (ASN) populations.

Chromatin Interactions

Since all candidate SNPs reside outside of the *RASGRP1* promoter, we investigated if the SNPs overlapped with anchors in promoter-enhancer connections through chromatin interactions. We used promoter-capture Hi-C data on blood cell lines, in particular T-cells, to identify physical interactions between the intronic signal and the *RASGRP1* promoter (**Supplementary Table 7**; **Supplementary Figure 3**). We also examined the physical interaction between the intergenic region (represented by rs9920715) and the promoters of *RASGRP1* and *C15orf53*. We identified multiple significant promoter-enhancer interactions between the intronic signal and *RASGRP1, C15orf53*, *FAM98B,* and *SPRED1*, and multiple interactions between the intergenic signal and the promoter of *RASGRP1* (**Supplementary Table 7**).

Effect on Cytokine Production

A critical feature in SLE pathogenicity is cytokine production (59); thus, we investigated if these SNPs alter cytokine abundance. Our candidate SNPs significantly increased expression of interleukins IL6 and IL22 and tumor necrosis factor (TNFα), while SNP rs9920715 exclusively increased IL22 expression (**Supplementary Table 8**).

Allele-Specific Binding

We found that 14 of the candidate GWS SNPs also had allele-specific binding (ASB) to H2K27ac in monocytes, neutrophils, and T-cells (**Supplementary Table 9**), while rs9920715 showed ASB with H3K4me1 in T-cells and neutrophils. To characterize the regulatory mechanisms involved, we assessed ASB of histone marks H3K4me1 and H3K4me3 at and around candidate SNPs (**Supplementary Table 9**; **Table 3**). We identified a significant regulatory region associated with promoter mark H3K4me3 with a higher binding affinity to the extended region (∼1 kb) containing the risk alleles (both C) of intronic SNPs rs11631591-rs7173565 (**Supplementary Figure 4a**). In addition, we identified marginally significant ASB to enhancer mark H3K4me1 at SNPs rs6495979 and rs7170151, which tagged a regulatory region within ∼500 bp (**Supplementary Figure 4b**). These data indicate that allele-specific differences might affect chromatin interactions.

TABLE 2 | Meta-analysis of the *RASGRP1* region.

SNP	Nearby gene	Function	Position	A1	A2	*3AS (4)	CH (26)	EU (27)	JAP (28)	Meta-analysis				
						P-value	*P*-value	*P*-value	*P*-value	*P*-value	OR	95%CI	HetPVal	Direction of OR
rs8043085	RASGRP1	intron 2	38,828,140	T	G	3.91E-03	5.53E-01	1.02E-03	4.52E-05	2.68E-08	1.11	1.1-1.16	0.3072	++++++
rs8032939	RASGRP1	intron 2	38,834,033	T	C	1.40E-04	5.81E-02	1.03E-03	4.35E-05	3.16E-11	0.88	0.85-0.92	0.4913	−−−−−−
rs8035957	RASGRP1	intron 2	38,838,264	T	C	2.52E-04	4.89E-02	1.40E-03	5.14E-05	1.31E-10	0.89	0.85-0.92	0.5035	−−−−−−
rs28536554	RASGRP1	intron 2	38,838,432	T	A	6.37E-03	3.13E-01	9.72E-04	1.72E-05	1.15E-08	0.89	0.9-0.93	0.3438	−−−−−−
rs72727387	RASGRP1	intron 2	38,843,476	A	G	3.43E-03	2.71E-01	3.65E-03	3.92E-05	2.54E-08	1.11	1.07-1.15	0.4756	++++++
rs72727388	RASGRP1	intron 2	38,843,694	C	T	3.36E-03	2.70E-01	3.67E-03	3.92E-05	2.55E-08	0.90	0.9-0.93	0.4756	−−−−−−
rs28582094	RASGRP1	intron 2	38,843,887	G	A	3.77E-03	2.62E-01	2.34E-03	4.16E-05	1.87E-08	0.90	0.87-0.93	0.4971	−−−−−−
rs12593201	RASGRP1	intron 2	38,844,106	A	G	3.25E-03	2.62E-01	2.91E-03	3.92E-05	1.90E-08	1.11	1.1-1.15	0.4893	++++++
rs36027443	RASGRP1	intron 2	38,846,347	A	G	3.79E-03	2.78E-01	2.69E-03	3.63E-05	3.08E-08	1.11	1.07-1.15	0.4629	++++++
rs7170151	RASGRP1	intron 2	38,846,678	C	T	3.36E-04	5.28E-02	2.72E-03	5.93E-05	2.69E-10	1.13	1.1-1.17	0.4429	++++++
rs6495979	RASGRP1	intron 2	38,847,359	C	T	3.21E-04	6.55E-02	3.02E-03	7.01E-05	3.18E-10	1.13	1.09-1.17	0.3495	++++++
rs11348849	RASGRP1	intron 2	38,847,877	I	D	3.30E-04	6.84E-02	3.71E-03	6.20E-05	3.62E-10	1.13	1.07-1.22	0.3029	++++++
rs11631591	RASGRP1	intron 2	38,850,262	T	C	2.53E-04	7.00E-02	3.49E-03	6.51E-05	3.43E-10	0.89	0.9-0.92	0.2393	−−−−−−
rs7173565	RASGRP1	intron 2	38,850,330	T	C	2.83E-04	7.01E-02	3.50E-03	6.51E-05	3.79E-10	0.89	0.9-0.92	0.2677	−−−−−−
rs62006173	RASGRP1-C15orf101	intergenic	38,906,396	T	C	2.06E-04	1.04E-02	1.54E-01	1.94E-03	4.50E-08	0.87	0.8-0.92	0.6036	−−−−−−
rs11073341	RASGRP1-C15orf102	intergenic	38,908,135	G	A	1.38E-04	9.76E-04	1.28E-01	8.25E-04	3.67E-08	1.11	1.1-1.16	0.04208	++++++
rs9920715	RASGRP1-C15orf103	intergenic	38,916,906	T	C	4.21E-05	1.10E-03	5.90E-02	1.34E-03	5.11E-09	0.89	0.86-0.93	0.06495	−−−−−−
rs12900339	RASGRP1-C15orf109	intergenic	38,927,386	G	A	2.75E-06	3.39E-01	3.28E-01	2.69E-04	9.19E-07	1.09	1.1-1.14	0.0166	++++++
rs12324579	RASGRP1-C15orf110	intergenic	38,927,510	C	G	1.20E-05	8.56E-02	3.00E-01	1.09E-05	1.80E-08	0.90	0.9-0.93	0.02404	−−−−−−

*We identified 18 genome-wide significant SNPs in RASGRP1 (intron 2) and between RASGRP1 and C15orf53 (intergenic). *Sun et al. (4)* ***Supplementary Table 5*** *(Korean, Han-Chinese, Malay Chinese, 3AS) was used as the discovery cohort and was replicated in Morris et al. (26) (Han Chinese, HC); and Bentham et al. (27) (European, EU) and in Okada et al. (28) + new samples (Japanese, JAP) cohorts. OR, Odds ratio; 95% CI, 95% confidence interval; HetPVal, P-value for heterogeneity meta-analysis test. Direction of OR is presented as + if OR > 1 and− if OR < 1. Note that all OR directions are consistent for all SNPs.*

TABLE 3 | Relevant epigenetic features of genome-wide significant SNPs.

SNP	Nearby gene	Function	Position	3D_score	RegulomeDB score	Weight 3d score	Weight regulome	eqtl	Enhancer	rSNP	PCHiC	TFBS	ASE/ASB	Total
rs8043085	RASGRP1	intron 2	38,828,140	25.72	5	2	2	1	1	1	1	1	0	9
rs8032939	RASGRP1	intron2	38,834,033	4.67	7	0	0	3	1	1	1	1	1	8
rs8035957	RASGRP1	intron2	38,838,264	1.85	7	0	0	4	1	1	0	1	1	8
rs28536554	RASGRP1	intron2	38,838,432	2.12	6	0	1	2	1	1	0	1	1	7
rs72727387	RASGRP1	intron2	38,843,476	3.55	6	0	1	2	2	1	0	1	1	8
rs72727388	RASGRP1	intron2	38,843,694	3.56	7	0	0	2	2	1	0	1	1	7
rs28582094	RASGRP1	intron2	38,843,887	4.04	6	0	1	2	2	1	0	1	1	8
rs12593201	RASGRP1	intron2	38,844,106	5.49	7	0	0	3	2	1	1	1	1	9
rs36027443	RASGRP1	intron2	38,846,347	11.23	5	1	2	2	2	0	1	1	0	9
rs7170151	RASGRP1	intron2	38,846,678	20.04	3a	2	4	3	2	1	1	1	1	**15**
rs6495979	RASGRP1	intron2	38,847,359	8.79	7	1	0	3	2	1	1	1	1	**10**
rs11348849	RASGRP1	intron2	38,847,877	8.09	7	1	0	0	2	1	1	0	0	5
rs11631591	RASGRP1	intron2	38,850,262	6.86	3a	1	4	2	2	1	1	1	1	**13**
rs7173565	RASGRP1	intron2	38,850,330	8.41	4	1	3	4	2	1	1	1	1	**14**
rs62006173	RASGRP1-C15orf53	intergenic	38,906,396	2.36	6	0	1	0	0	0	0	1	3	5
rs11073341	RASGRP1-C15orf53	intergenic	38,908,135	1.26	5	0	2	3	0	0	0	1	3	9
rs9920715	RASGRP1-C15orf53	intergenic	38,916,906	7.83	3a	1	4	3	0	0	1	1	2	**12**
rs12900339	RASGRP1-C15orf53	intergenic	38,927,386	0.81	6	0	1	3	0	0	0	1	3	8
rs12324579	RASGRP1-C15orf110	intergenic	38,927,510	1	7	0	0	1	0	0	0	0	0	1

We integrated scores from 3dSNP, RegulomeDB and rSNP with blood cell-specific information for eQTLs, enhancer/super-enhancer existence, promoter capture HI-C (PCHiC), transcription factor binding site (TFBS) disruption and allele-specific expression/binding (ASE/ASB) into a weighted score for SNP prioritization. We chose the top three SNPs for further validation (rs11631591 and rs7173565 were used together because of the short distance between them). The top five SNPs are presented in bold.

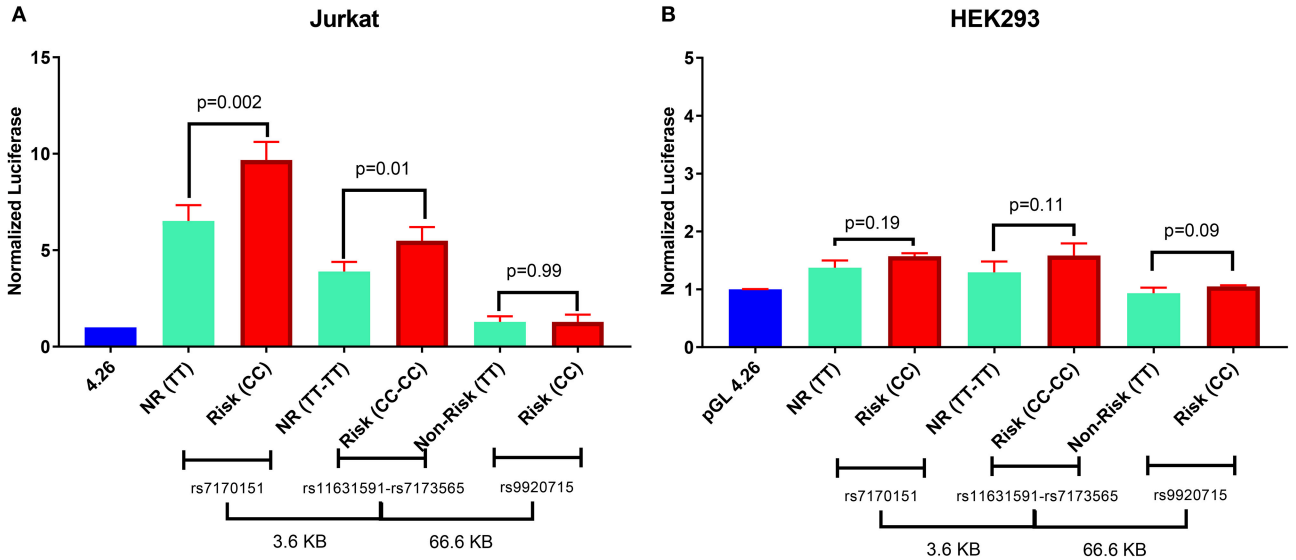

FIGURE 3 | Luciferase reporter assay for rs7170151, rs11631591-rs7173565 and rs9920715. **(A)** Jurkat cells. **(B)** HEK293 cells. Empty vector pGL4.26 was used as reference. NR: non-risk. *P*-values are for Student's *t*-test.

Validation of Enhancer by Luciferase Assays

When testing in a luciferase reporter assay, rs7170151 and rs11631591 showed marked (up to 10-fold over empty vector) enhancer activity in Jurkat cells ($P = 3.0 \times 10^{-4}$, $P = 1.0 \times 10^{-3}$, respectively) and less so (1.6-fold) in HEK293 cells ($P = 4.0 \times 10^{-2}$, $P = 3.0 \times 10^{-3}$); on the other hand rs9920715 functioned as a very weak enhancer only in HEK293 ($P = 4.1 \times 10^{-2}$) (**Figure 3**). Furthermore, rs7170151 and rs11631591 showed dramatic allelic differences in enhancer function. Genomic regions containing homozygous risk alleles of rs7170151 (C) and rs11631591 (C) showed significantly higher enhancer activity (∼50% increase; $P = 1.0 \times 10^{-2}$ and $P = 2.3 \times 10^{-3}$, respectively; **Figure 3A**) compared to non-risk alleles, but only in Jurkat cells. This allele-dependent enhancer activity is consistent with the allele-specific expression we observed in the eQTL data. There were no significant differences in HEK293 cell lines (**Figure 3B**), suggesting that enhancer activity depends on white blood cell-specific factors. The third intergenic SNP (rs9920715) did not show enhancer activity in any assayed cell type (**Figures 3A,B**).

Transcription Factor Binding

We next assessed allele-specific changes in transcription factor binding site (TFBS) affinity using five motif databases (**Methods**). We identified 256 TFBSs significantly affected by ten of our SNPs (**Supplementary Table 10**). Notably, we found 43-fold higher affinity of promoter-specific TF YY1 to the non-risk allele (T) of rs7173565 and 42-fold higher affinity of TF GATA (GATA1..3.p2 motif) to the risk (T) allele of rs6495979. Interestingly, SLE-risk ETS1 (60) binding had 10-fold higher affinity to the risk (C) allele of rs7173565, while SLE-risk IRF5 (61) bound 6-fold more tightly to the non-risk (C) allele of rs6495979.

Identification of DNA-Binding Proteins

We detected DNA-binding protein complexes using electrophoretic mobility shift assays (EMSAs) and DNA pulldown assays using a 41 bp-long dsDNA containing the rs11631591-rs7173565 (homozygous risk, CC; or homozygous non-risk, TT) alleles (**Supplementary Table 11**). We prepared nuclear extracts from Jurkat cells and incubated them with biotin-labeled dsDNA (risk vs. non-risk) bound to magnetic beads coated in streptavidin. EMSA showed multiple bands of DNA-bound proteins (**Supplementary Figure 5**). We observed allele-specific binding of a protein complex at 75 kDa. Although EMSA is not a quantitative assay, we observed in multiple independent experiments that the intensity of the band with the risk (CC) oligo was darker than with the non-risk (TT) oligo, suggesting allele-specific differential binding (**Supplementary Figure 5**). Using mass spectrometry analysis of bound proteins, we identified heterogeneous nuclear ribonucleoprotein K (hnRNP-K) isoform b as the most abundant bound protein (**Supplementary Table 11**). hnRNP-K was also the protein whose binding was most diminished by substitution of the risk CC by non-risk TT nucleotides. We also confirmed that the identified protein bound with the risk oligo for the region of rs11631591 was hnRNP-K through EMSA followed by Western blot (**Supplementary Figure 6**).

SNPs Bind to Different Transcription Factors in an Allele-Specific Manner

Using EMSA and mass spectrometry, we showed that hnRNP-K protein has tighter binding affinity to the risk genotype (CC) of SNP rs11631591-rs7173565. We validated these findings using Jurkat (heterozygous CT at rs11631591-rs7173565) to perform chromatin-immunoprecipitation (ChIP) followed by RT-qPCR (ChIP-qPCR). We observed significant enrichment in binding

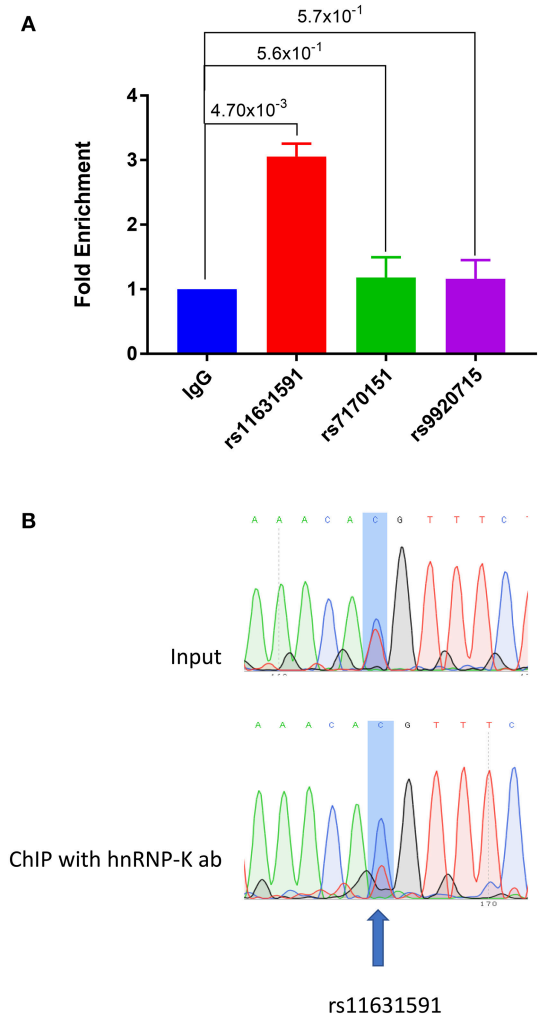

FIGURE 4 | (A) ChIP-qPCR of sequences containing SNPs rs11631591-rs7173565, rs7170151 or rs9920715 in Jurkat cells. SNP rs11631591 showed 3-fold enrichment of hnRNP-K binding over IgG control. No significant enrichment at the other two SNPs was observed. *P*-values are for Student's *t*-test. **(B)** Sequence chromatographs from a heterozygous sample at rs11631591 showing difference in binding between the input (equal binding to the two alleles, above) and the ChIP assay at the risk allele (2–3× more binding to the risk C allele, below).

of the hnRNP-K antibody to the SNP region of rs11631591, but did not observe any binding of hnRNP-K antibody to either rs7170151 or rs9920715 (**Figure 4A**). To determine preferential or allele-specific binding, we performed Sanger sequencing on the region containing rs11631591-rs7173565. Both alleles were present in the original input sample; however, only the risk allele (C) was detected significantly higher than the non-risk allele (T) in chromatograms of the ChIP-eluted PCR product (**Figure 4B**). These data suggest preferential allele-specific binding of the rs11631591-rs7173565 risk locus to hnRNP-K.

hnRNP-K Plays an Important Role in *RASGRP1* Expression

To investigate the role of endogenous hnRNP-K in Jurkat and primary CD3$^+$ T-cells, we transiently inhibited hnRNP-K using 5-fluorouracil (5-FU). After 5-FU treatment (48 h), we observed significantly reduced mRNA expression for both hnRNP-K ($P = 1.4 \times 10^{-3}$; **Figure 5A**) and *RASGRP1* ($P = 3.0 \times 10^{-4}$; **Figure 5B**). 5-FU-induced hnRNP-K downregulation correlated with reduced expression of *RASGRP1* (**Figures 6A,B**). This result suggests that hnRNP-K plays an important role in *RASGRP1* expression in Jurkat cells as well as in primary T-cells. Furthermore, we observed the reduction of ERK phosphorylation with 5-FU after initial induction with PMA in Jurkat and primary T-cells (**Figures 6A–D**). It is of note that stimulation with PMA did not influence cell viability (**Supplementary Figure 7**).

DISCUSSION

In this study, we fine-mapped our previously reported SLE locus near *RAS guanyl-releasing protein 1* (*RASGRP1*), a lynchpin of T-cell development and the RAS/MAP kinase signaling cascade following antigen exposure. We performed a trans-ethnic meta-analysis of the locus with cohorts of Asian and European descent, followed by multiple lines of bioinformatic analysis of its epigenetic context to prioritize SNPs as candidate causal variants. Experimental testing of the top candidates validated them as plausible variants underlying association of this locus with SLE (and perhaps other autoimmune phenotypes).

We identified two independently associated regions correlated with *RASGRP1* regulation and expression. The first signal lies in *RASGRP1* intron 2, represented by SNPs rs11631591-rs7173565 and rs7170151, which regulate *RASGRP1* expression as eQTLs (esophageal mucosa and skin), enhancers (in CD8$^+$ T-cells and thymic and lymphoblastoid cell lines), and as interaction anchors with the nearby *C15orf53* promoter. The SNPs in this region are within a robust enhancer, with the risk alleles (rs7170151-C and rs11631591-C/rs7173565-C) greatly increasing *RASGRP1* expression in multiple tissues (databases) and in Jurkat T-cells (our experiments). Furthermore, this enhancer is targeted by promoter interactions in CD8$^+$ and CD4$^+$ T-cells, B-cells, and monocytes (62) (**Supplementary Figure 3**). We also identified another intergenic signal around 60 kb 5′ of *RASGRP1*, at rs9920715, another SNP within promoter-interacting chromatin that acts as an eQTL for *RASGRP1* in B- and T-cell lines (62). However, this SNP did not show enhancer activity in our assays.

Mammalian gene regulatory elements, especially those that are tissue-specific, show high *in vivo* nucleosome occupancy, which can effectively compete with TF binding (63, 64). This nucleosome-mediated restricted access to regulatory information is a key element for inducible or cell type-specific control of gene expression (65). In the current study, we observed strong enhancer activity at rs11631591-rs7173565 or rs7170151 only in Jurkat but not HEK293 cells. Furthermore, our candidate SNPs show allele-specific *RASGRP1* expression, with the risk alleles driving substantially more (∼50%) expression than the non-risk alleles. Other studies on numerous complex diseases have demonstrated enrichment of disease-associated loci in cell type-specific regulatory regions of corresponding disease-relevant cell types (58, 66–69). Additional studies now document the direct effects of common variation in enhancer elements on enhancer states (70–73), gene expression (70, 74), and disease (75–79). Risk

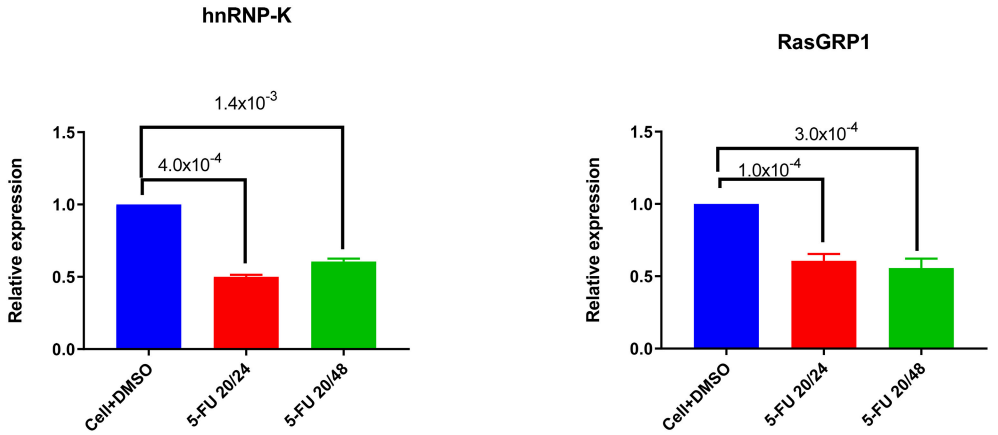

FIGURE 5 | Downregulation of hnRNP-K by 5-FU treatment. 5-FU treatment reduces hnRNP-K expression levels in Jurkat cells. Jurkat cells were treated with DMSO vehicle or 5-FU (20 ng/μl) for 24 or 48 h. *hnRNP-K* **(A)** and *RASGRP1* **(B)** were examined with *GADPH* as loading control.

alleles of rs11631591 also showed significant binding to hnRNP-K protein in an allele-specific manner.

DNA/protein interaction assays demonstrated that hnRNP-K preferentially binds to sequences containing the rs11631591 risk (C) allele. We confirmed this allele-specific binding by EMSA and ChIP DNA sequencing. We only observed allele-specific binding of hnRNP-K at SNP rs116311591-rs7173565, but not at rs7170151 or rs9920715. We also observed that inhibition of hnRNP-K correlates with *RASGRP1* expression and ERK phosphorylation. In fact, expression of *RASGRP1* and hnRNP-K ($P = 9.8 \times 10^{-5}$; $P = 1.4 \times 10^{-2}$, respectively) in spleen (**Supplementary Figure 8**) shows a positive correlation between the risk allele of rs116311591 and both these genes. These data suggest that SNP rs11631591 is a functional SNP and may directly contribute to modulating *RASGRP1* expression. Abnormal expression of *RASGRP1* isoforms will perturb lymphocytes of SLE patients regardless of their clinical disease activity, and may contribute to impaired lymphocyte function and increased apoptosis in SLE patients (19). Abnormal *RASGRP1* expression also induces ERK and JNK phosphorylation in the MAPK pathway, which in turn alters T-cell development, contributes to long-term organ damage, and ultimately increases SLE susceptibility (22, 24, 25). In the present study, we also observed the role of *RASGRP1* expression in the phosphorylation of ERK activity. Altogether, our results indicate increased *RASGRP1* expression correlates with the risk alleles in our functional SLE loci and T-cell dysfunction. However, our study did not examine the differences in *RASGRP1* isoform expression reportedly associated with SLE and correlated with low *RASGRP1* expression (19).

In this study, we characterized the genetic risk of SLE in *RASGRP1*. We also propose a mechanism by which functional SNPs could affect SLE pathogenesis. We identified two functional regions affecting expression and regulation of *RASGRP1* in an intronic region including two SNPs (rs11631591 and rs7170151) and another in an intergenic region harboring SNP rs9920715. All identified SNPs are *RASGRP1* eQTLs and exhibit regulatory potential through enhancer-promoter chromatin interactions. SNP rs11631591 showed T-cell-specific enhancer activity and an allele-specific interaction with hnRNP-K protein. Inhibition of hnRNP-K protein by 5-FU decreased expression of *RASGRP1* in T-cells, suggesting that hnRNP-K plays an important role in *RASGRP1* expression through interactions with the risk genotype of SNP rs11631591. These results are consistent with this SNP being an important factor contributing to SLE pathogenicity.

Heterogeneous nuclear ribonucleoproteins (hnRNPs) represent a large family of nucleic acid-binding proteins implicated in various cellular processes including transcription and translation (24, 80). hnRNP-K is a highly multifunctional protein, with annotated roles in chromatin remodeling, transcription, splicing and translation (80). It is primarily referred to as an RNA-binding protein specific for "poly-C" repeats (81), but it actually prefers single-stranded DNA and can bind to double-stranded DNA (82). hnRNP-K can act as a transcriptional activator or repressor (83); notable examples include transcriptional repression of *CD43* in leukocytes (84) and transcriptional activation of *c-myc* in B-cells (85). Its DNA-binding preference is found to be repeats of the CT motif, separated by several base pairs (82), confirmed by structure determination (86). There are several CT motifs in the immediate environment of rs11631591, whose hnRNP-K binding could be affected by the SNP. It should also be noted that several of the other abundant proteins pulled down by the double-stranded DNA EMSA are primarily annotated as RNA-binding proteins, including hnRNP-M and splicing factor U2AF. Other transcription factors were also abundant, including far upstream element-binding protein 3, supporting the notion that this locus is indeed transcriptionally active.

Taken together, we have identified and mechanistically dissected a lupus risk locus in the 2nd intron of *RASGRP1*, which regulates T- and B-cell development and the MAP kinase pathway. Single SNPs were found to control transcriptional activation and binding to several proteins, including the

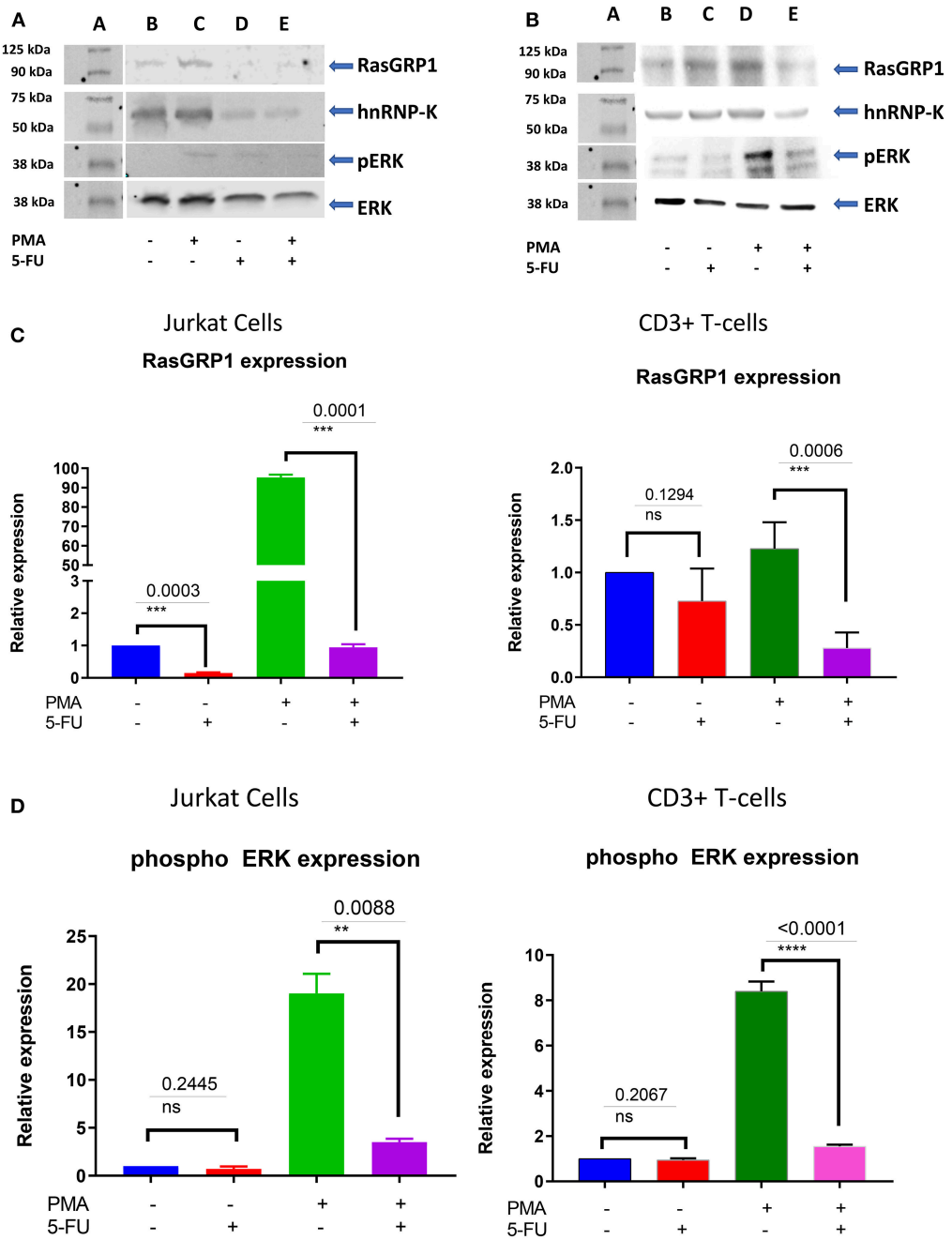

FIGURE 6 | (A) RasGRP1 reduction influences the phosphorylation of ERK. 5-FU treatment reduces hnRNP-K and RasGRP1 expression levels in Jurkat and healthy human $CD3^+$ T cells. Pretreatment with PMA increases levels of RasGRP1 and phospho-ERK. Inhibition of hnRNP-K with 5-FU decreases levels of RasGRP1 and phospho-ERK, even after PMA stimulation. **(B)** 5-FU treatment reduces hnRNP-K as well as RasGRP1 expression level in primary $CD3^+$ T-cells. Pretreatment with PMA induces RasGRP1 expression and leads to phosphorylation of ERK and reduction of RasGRP1; treatment with 5-FU also leads to reduction of phosphorylation of ERK. **(C)** Densitometric analysis for *RASGRP1* normalized to β-actin: primary T-cells and Jurkat cells. Results are presented as relative fold-change following drug treatment with and without stimulation. **(D)** Densitometry analysis for phospho-ERK normalized to β-actin: primary T-cells and Jurkat cells. Results are presented as relative fold-change following drug treatment with and without PMA stimulation. $^{**}P < 0.05$; $^{***}P < 0.005$.

transcription factor hnRNP-K. Experiments confirmed that both the single base-pair risk-to-non-risk substitutions and pharmacological inhibition of hnRNP-K decreased MAPK signaling in T-cells. Systematic refinement of large GWAS peaks to single SNPs, combined with experimental mechanistic analysis, is critical to understand the genetics of highly multigenic diseases and to drive therapeutic interventions to improve human health.

WEB RESOURCES

Bentham and Morris summary SLE GWAS: http://insidegen.com/.

ETHICS STATEMENT

All sample collections were approved by the Institutional Review Board of the Oklahoma Medical Research Foundation as well as by the collaborating institutions.

AUTHOR CONTRIBUTIONS

SN conceived and supervised the project. JM performed the meta-analysis, bioinformatic, and epigenetic analyses, and prepared most of the tables and figures. BS performed most of the experiments and generated experimental figures. CT, YO, and SA ran the association analysis and provided the relevant data for replication of the Japanese samples. JK and BM helped and performed some experiments. CS helped in assembling and analyzing imputed data for association and performed some bioinformatics analysis and also helped in interpreting the results and contributed to the correction of manuscript. CW helped in planning experiments and revising the manuscript. LL provided expertise and helped in interpreting the results. JM, LL, and SN drafted and finalized the manuscript. All authors read and approved the submitted manuscript.

FUNDING

This work was supported by the grants from National Institutes of Health (AR073941, AR060366, AI132532, MD007909) to SN, AI18836 to CW.

ACKNOWLEDGMENTS

The authors thank all of the lupus patients and unaffected controls who participated in this study. We thank the research assistants, coordinators, and physicians who helped in the recruitment of subjects, including the individuals in the coordinating projects.

SUPPLEMENTARY MATERIAL

The Supplementary Material for this article can be found online at: https://www.frontiersin.org/articles/10.3389/fimmu.2019.01066/full#supplementary-material

REFERENCES

1. Alarcon GS, McGwin G Jr., Petri M, Reveille JD, Ramsey-Goldman R, Kimberly RP, et al. Baseline characteristics of a multiethnic lupus cohort: PROFILE. *Lupus*. (2002) 11:95–101. doi: 10.1191/0961203302lu155oa
2. Molineros JE, Yang W, Zhou XJ, Sun C, Okada Y, Zhang H, et al. Confirmation of five novel susceptibility loci for systemic lupus erythematosus (SLE) and integrated network analysis of 82 SLE susceptibility loci. *Hum Mol Genet*. (2017) 26:1205–16. doi: 10.1093/hmg/ddx026
3. Langefeld CD, Ainsworth HC, Cunninghame Graham DS, Kelly JA, Comeau ME, Marion MC, et al. Transancestral mapping and genetic load in systemic lupus erythematosus. *Nat Commun*. (2017) 8:16021. doi: 10.1038/ncomms16021
4. Sun C, Molineros JE, Looger LL, Zhou XJ, Kim K, Okada Y, et al. High-density genotyping of immune-related loci identifies new SLE risk variants in individuals with Asian ancestry. *Nat Genet*. (2016) 48:323–30. doi: 10.1038/ng.3496
5. Carrasco S, Merida I. Diacylglycerol-dependent binding recruits PKCtheta and RasGRP1 C1 domains to specific subcellular localizations in living T lymphocytes. *Mol Biol Cell*. (2004) 15:2932–42. doi: 10.1091/mbc.e03-11-0844
6. Beaulieu N, Zahedi B, Goulding RE, Tazmini G, Anthony KV, Omeis SL, et al. Regulation of RasGRP1 by B cell antigen receptor requires cooperativity between three domains controlling translocation to the plasma membrane. *Mol Biol Cell*. (2007) 18:3156–68. doi: 10.1091/mbc.e06-10-0932
7. Ebinu JO, Bottorff DA, Chan EY, Stang SL, Dunn RJ, Stone JC. RasGRP, a Ras guanyl nucleotide- releasing protein with calcium- and diacylglycerol-binding motifs. *Science*. (1998) 280:1082–6. doi: 10.1126/science.280.5366.1082
8. Dower NA, Stang SL, Bottorff DA, Ebinu JO, Dickie P, Ostergaard HL, et al. RasGRP is essential for mouse thymocyte differentiation and TCR signaling. *Nat Immunol*. (2000) 1:317–21. doi: 10.1038/79766
9. Liu Y, Zhu M, Nishida K, Hirano T, Zhang W. An essential role for RasGRP1 in mast cell function and IgE-mediated allergic response. *J Exp Med*. (2007) 204:93–103. doi: 10.1084/jem.20061598
10. Coughlin JJ, Stang SL, Dower NA, Stone JC. RasGRP1 and RasGRP3 regulate B cell proliferation by facilitating B cell receptor-Ras signaling. *J Immunol*. (2005) 175:7179–84. doi: 10.4049/jimmunol.175.11.7179
11. Shen S, Chen Y, Gorentla BK, Lu J, Stone JC, Zhong XP. Critical roles of RasGRP1 for invariant NKT cell development. *J Immunol*. (2011) 187:4467–73. doi: 10.4049/jimmunol.1003798
12. Bartlett A, Buhlmann JE, Stone J, Lim B, Barrington RA. Multiple checkpoint breach of B cell tolerance in Rasgrp1-deficient mice. *J Immunol*. (2013) 191:3605–13. doi: 10.4049/jimmunol.1202892
13. Guo B, Rothstein TL. RasGRP1 is an essential signaling molecule for development of B1a cells with autoantigen receptors. *J Immunol*. (2016) 196:2583–90. doi: 10.4049/jimmunol.1502132
14. Priatel JJ, Teh SJ, Dower NA, Stone JC, Teh HS. RasGRP1 transduces low-grade TCR signals which are critical for T cell development, homeostasis, and differentiation. *Immunity*. (2002) 17:617–27. doi: 10.1016/S1074-7613(02)00451-X
15. Salzer E, Cagdas D, Hons M, Mace EM, Garncarz W, Petronczki OY, et al. RASGRP1 deficiency causes immunodeficiency with impaired cytoskeletal dynamics. *Nat Immunol*. (2016) 17:1352–60. doi: 10.1038/ni.3575
16. Winter S, Martin E, Boutboul D, Lenoir C, Boudjemaa S, Petit A, et al. Loss of RASGRP1 in humans impairs T-cell expansion leading to Epstein-Barr virus susceptibility. *EMBO Mol Med*. (2018) 10:188–99. doi: 10.15252/emmm.201708292
17. Mao H, Yang W, Latour S, Yang J, Winter S, Zheng J, et al. RASGRP1 mutation in autoimmune lymphoproliferative syndrome-like disease. *J Allergy Clin Immunol*. (2018) 142:595–604 e516. doi: 10.1016/j.jaci.2017.10.026
18. Golinski ML, Vandhuick T, Derambure C, Freret M, Lecuyer M, Guillou C, et al. Dysregulation of RasGRP1 in rheumatoid arthritis and modulation of RasGRP3 as a biomarker of TNFalpha inhibitors. *Arthritis Res Ther*. (2015) 17:382. doi: 10.1186/s13075-015-0894-9
19. Rapoport MJ, Bloch O, Amit-Vasina M, Yona E, Molad Y. Constitutive abnormal expression of RasGRP-1 isoforms and low expression of PARP-1 in patients with systemic lupus erythematosus. *Lupus*. (2011) 20:1501–9. doi: 10.1177/0961203311418790
20. Yasuda S, Stevens RL, Terada T, Takeda M, Hashimoto T, Fukae J, et al. Defective expression of Ras guanyl nucleotide-releasing protein 1 in a subset of patients with systemic lupus erythematosus. *J Immunol*. (2007) 179:4890–900. doi: 10.4049/jimmunol.179.7.4890

21. Kono M, Kurita T, Yasuda S, Kono M, Fujieda Y, Bohgaki T, et al. Decreased expression of Serine/arginine-rich splicing factor 1 in T cells from patients with active systemic lupus erythematosus accounts for reduced expression of RasGRP1 and DNA methyltransferase 1. *Arthritis Rheumatol*. (2018) 70:2046–56. doi: 10.1002/art.40585
22. Deng C, Lu Q, Zhang Z, Rao T, Attwood J, Yung R, et al. Hydralazine may induce autoimmunity by inhibiting extracellular signal-regulated kinase pathway signaling. *Arthritis Rheum*. (2003) 48:746–56. doi: 10.1002/art.10833
23. Molad Y, Amit-Vasina M, Bloch O, Yona E, Rapoport MJ. Increased ERK and JNK activities correlate with disease activity in patients with systemic lupus erythematosus. *Ann Rheum Dis*. (2010) 69:175–80. doi: 10.1136/ard.2008.102780
24. Bloch O, Amit-Vazina M, Yona E, Molad Y, Rapoport MJ. Increased ERK and JNK activation and decreased ERK/JNK ratio are associated with long-term organ damage in patients with systemic lupus erythematosus. *Rheumatology*. (2014) 53:1034–42. doi: 10.1093/rheumatology/ket482
25. Rapoport MJ, Amit M, Aharoni D, Weiss M, Weissgarten J, Bruck N, et al. Constitutive up-regulated activity of MAP kinase is associated with down-regulated early p21Ras pathway in lymphocytes of SLE patients. *J Autoimmun*. (2002) 19:63–70. doi: 10.1006/jaut.2002.0596
26. Morris DL, Sheng Y, Zhang Y, Wang YF, Zhu Z, Tombleson P, et al. Genome-wide association meta-analysis in Chinese and European individuals identifies ten new loci associated with systemic lupus erythematosus. *Nat Genet*. (2016) 48:940–6. doi: 10.1038/ng.3603
27. Bentham J, Morris DL, Cunninghame Graham DS, Pinder CL, Tombleson P, Behrens TW, et al. Genetic association analyses implicate aberrant regulation of innate and adaptive immunity genes in the pathogenesis of systemic lupus erythematosus. *Nat Genet*. (2015) 47:1457–64. doi: 10.1038/ng.3434
28. Okada Y, Shimane K, Kochi Y, Tahira T, Suzuki A, Higasa K, et al. A genome-wide association study identified AFF1 as a susceptibility locus for systemic lupus eyrthematosus in Japanese. *PLoS Genet*. (2012) 8:e1002455. doi: 10.1371/journal.pgen.1002455
29. Hochberg MC. Updating the American College of Rheumatology revised criteria for the classification of systemic lupus erythematosus. *Arthritis Rheum*. (1997) 40:1725. doi: 10.1002/art.1780400928
30. Purcell S, Neale B, Todd-Brown K, Thomas L, Ferreira MA, Bender D, et al. PLINK: a tool set for whole-genome association and population-based linkage analyses. *Am J Hum Genet*. (2007) 81:559–75. doi: 10.1086/519795
31. Willer CJ, Li Y, Abecasis GR. METAL: fast and efficient meta-analysis of genomewide association scans. *Bioinformatics*. (2010) 26:2190–1. doi: 10.1093/bioinformatics/btq340
32. Ward LD, Kellis M. HaploReg: a resource for exploring chromatin states, conservation, and regulatory motif alterations within sets of genetically linked variants. *Nucleic Acids Res*. (2012) 40:D930–4. doi: 10.1093/nar/gkr917
33. Consortium EP. An integrated encyclopedia of DNA elements in the human genome. *Nature*. (2012) 489:57–74. doi: 10.1038/nature11247
34. Pradel LC, Vanhille L, Spicuglia S. The European Blueprint project: towards a full epigenome characterization of the immune system. *Med Sci*. (2015) 31:236–8. doi: 10.1051/medsci/20153103003
35. Lu Y, Quan C, Chen H, Bo X, Zhang C. 3DSNP: a database for linking human noncoding SNPs to their three-dimensional interacting genes. *Nucleic Acids Res*. (2017) 45:D643–9. doi: 10.1093/nar/gkw1022
36. Boyle AP, Hong EL, Hariharan M, Cheng Y, Schaub MA, Kasowski M, et al. Annotation of functional variation in personal genomes using RegulomeDB. *Genome Res*. (2012) 22:1790–7. doi: 10.1101/gr.137323.112
37. Guo L, Du Y, Chang S, Zhang K, Wang J. rSNPBase: a database for curated regulatory SNPs. *Nucleic Acids Res*. (2014) 42:D1033–9. doi: 10.1093/nar/gkt1167
38. Lappalainen T, Sammeth M, Friedlander MR, t Hoen PA, Monlong J, Rivas MA, et al. Transcriptome and genome sequencing uncovers functional variation in humans. *Nature*. (2013) 501:506–11. doi: 10.1038/nature12531
39. Westra HJ, Peters MJ, Esko T, Yaghootkar H, Schurmann C, Kettunen J, et al. Systematic identification of trans eQTLs as putative drivers of known disease associations. *Nat Genet*. (2013) 45:1238–43. doi: 10.1038/ng.2756
40. van der Wijst MGP, Brugge H, de Vries DH, Deelen P, Swertz MA, LifeLines Cohort S, et al. Single-cell RNA sequencing identifies celltype-specific cis-eQTLs and co-expression QTLs. *Nat Genet*. (2018) 50:493–7. doi: 10.1038/s41588-018-0089-9
41. Consortium GT. Human genomics. The Genotype-Tissue Expression (GTEx) pilot analysis: multitissue gene regulation in humans. *Science*. (2015) 348:648–60. doi: 10.1126/science.1262110
42. Chen L, Ge B, Casale FP, Vasquez L, Kwan T, Garrido-Martin D, et al. Genetic drivers of epigenetic and transcriptional variation in human immune cells. *Cell*. (2016) 167:1398–414 e1324. doi: 10.1016/j.cell.2016.10.026
43. Coetzee SG, Coetzee GA, Hazelett DJ. motifbreakR: an R/Bioconductor package for predicting variant effects at transcription factor binding sites. *Bioinformatics*. (2015) 31:3847–9. doi: 10.1093/bioinformatics/btv470
44. Khan A, Zhang X. dbSUPER: a database of super-enhancers in mouse and human genome. *Nucleic Acids Res*. (2016) 44:D164–71. doi: 10.1093/nar/gkv1002
45. Corradin O, Saiakhova A, Akhtar-Zaidi B, Myeroff L, Willis J, Cowper-Sallari R, et al. Combinatorial effects of multiple enhancer variants in linkage disequilibrium dictate levels of gene expression to confer susceptibility to common traits. *Genome Res*. (2014) 24:1–13. doi: 10.1101/gr.164079.113
46. Gao T, He B, Liu S, Zhu H, Tan K, Qian J. EnhancerAtlas: a resource for enhancer annotation and analysis in 105 human cell/tissue types. *Bioinformatics*. (2016) 32:3543–51. doi: 10.1093/bioinformatics/btw495
47. Li R, Liu Y, Li T, Li C. 3Disease Browser: a Web server for integrating 3D genome and disease-associated chromosome rearrangement data. *Sci Rep*. (2016) 6:34651. doi: 10.1038/srep34651
48. Schofield EC, Carver T, Achuthan P, Freire-Pritchett P, Spivakov M, Todd JA, et al. CHiCP: a web-based tool for the integrative and interactive visualization of promoter capture Hi-C datasets. *Bioinformatics*. (2016) 32:2511–3. doi: 10.1093/bioinformatics/btw173
49. Rao SS, Huntley MH, Durand NC, Stamenova EK, Bochkov ID, Robinson JT, et al. A 3D map of the human genome at kilobase resolution reveals principles of chromatin looping. *Cell*. (2014) 159:1665–80. doi: 10.1016/j.cell.2014.11.021
50. Sanborn AL, Rao SS, Huang SC, Durand NC, Huntley MH, Jewett AI, et al. Chromatin extrusion explains key features of loop and domain formation in wild-type and engineered genomes. *Proc Natl Acad Sci USA*. (2015) 112:E6456–65. doi: 10.1073/pnas.1518552112
51. Cairns J, Freire-Pritchett P, Wingett SW, Varnai C, Dimond A, Plagnol V, et al. CHiCAGO: robust detection of DNA looping interactions in Capture Hi-C data. *Genome Biol*. (2016) 17:127. doi: 10.1186/s13059-016-0992-2
52. Taberlay PC, Achinger-Kawecka J, Lun AT, Buske FA, Sabir K, Gould CM, et al. Three-dimensional disorganization of the cancer genome occurs coincident with long-range genetic and epigenetic alterations. *Genome Res*. (2016) 26:719–31. doi: 10.1101/gr.201517.115
53. Arnold C, Bhat P, Zaugg JB. SNPhood. investigate, quantify and visualise the epigenomic neighbourhood of SNPs using NGS data. *Bioinformatics*. (2016) 32:2359–60. doi: 10.1093/bioinformatics/btw127
54. Xiao Z, Ko HL, Goh EH, Wang B, Ren EC. hnRNP K suppresses apoptosis independent of p53 status by maintaining high levels of endogenous caspase inhibitors. *Carcinogenesis*. (2013) 34:1458–67. doi: 10.1093/carcin/bgt085
55. Wang JC, Foroud T, Hinrichs AL, Le NX, Bertelsen S, Budde JP, et al. A genome-wide association study of alcohol-dependence symptom counts in extended pedigrees identifies C15orf53. *Mol Psychiatry*. (2013) 18:1218–24. doi: 10.1038/mp.2012.143
56. Okada Y, Wu D, Trynka G, Raj T, Terao C, Ikari K, et al. Genetics of rheumatoid arthritis contributes to biology and drug discovery. *Nature*. (2014) 506:376-381. doi: 10.1038/nature12873
57. Grant SF, Qu HQ, Bradfield JP, Marchand L, Kim CE, Glessner JT, et al. Follow-up analysis of genome-wide association data identifies novel loci for type 1 diabetes. *Diabetes*. (2009) 58:290–5. doi: 10.2337/db08-1022
58. Hnisz D, Abraham BJ, Lee TI, Lau A, Saint-Andre V, Sigova AA, et al. Super-enhancers in the control of cell identity and disease. *Cell*. (2013) 155:934–47. doi: 10.1016/j.cell.2013.09.053
59. Davis LS, Hutcheson J, Mohan C. The role of cytokines in the pathogenesis and treatment of systemic lupus erythematosus. *J Interferon Cytokine Res*. (2011) 31:781–9. doi: 10.1089/jir.2011.0047
60. Han JW, Zheng HF, Cui Y, Sun LD, Ye DQ, Hu Z, et al. Genome-wide association study in a Chinese Han population identifies nine new susceptibility loci for systemic lupus erythematosus. *Nat Genet*. (2009) 41:1234–7. doi: 10.1038/ng.472

61. International Consortium for Systemic Lupus Erythematosus Group, Harley JB, Alarcon-Riquelme ME, Criswell LA, Jacob CO, Kimberly RP, Moser KL, et al. Genome-wide association scan in women with systemic lupus erythematosus identifies susceptibility variants in ITGAM, PXK, KIAA1542 and other loci. *Nat Genet*. (2008) 40:204–10. doi: 10.1038/ng.81
62. Javierre BM, Burren OS, Wilder SP, Kreuzhuber R, Hill SM, Sewitz S, et al. Lineage-specific genome architecture links enhancers and non-coding disease variants to target gene promoters. *Cell*. (2016) 167:1369–84 e1319. doi: 10.1016/j.cell.2016.09.037
63. Cairns BR. The logic of chromatin architecture and remodelling at promoters. *Nature*. (2009) 461:193–98. doi: 10.1038/nature08450
64. Tillo D, Kaplan N, Moore IK, Fondufe-Mittendorf Y, Gossett AJ, Field Y, et al. High nucleosome occupancy is encoded at human regulatory sequences. *PLoS ONE*. (2010) 5:e9129. doi: 10.1371/journal.pone.0009129
65. Wiench M, John S, Baek S, Johnson TA, Sung MH, Escobar T, et al. DNA methylation status predicts cell type-specific enhancer activity. *EMBO J*. (2011) 30:3028–39. doi: 10.1038/emboj.2011.210
66. Trynka G, Sandor C, Han B, Xu H, Stranger BE, Liu XS, et al. Chromatin marks identify critical cell types for fine mapping complex trait variants. *Nat Genet*. (2013) 45:124–30. doi: 10.1038/ng.2504
67. Pasquali L, Gaulton KJ, Rodriguez-Segui SA, Mularoni L, Miguel-Escalada I, Akerman I, et al. Pancreatic islet enhancer clusters enriched in type 2 diabetes risk-associated variants. *Nat Genet*. (2014) 46:136–43. doi: 10.1038/ng.2870
68. Raj T, Rothamel K, Mostafavi S, Ye C, Lee MN, Replogle JM, et al. Polarization of the effects of autoimmune and neurodegenerative risk alleles in leukocytes. *Science*. (2014) 344:519–23. doi: 10.1126/science.1249547
69. Heinz S, Romanoski CE, Benner C, Glass CK. The selection and function of cell type-specific enhancers. *Nat Rev Mol Cell Biol*. (2015) 16:144–54. doi: 10.1038/nrm3949
70. Degner JF, Pai AA, Pique-Regi R, Veyrieras JB, Gaffney DJ, Pickrell JK, et al. DNase I sensitivity QTLs are a major determinant of human expression variation. *Nature*. (2012) 482:390–4. doi: 10.1038/nature10808
71. Kasowski M, Kyriazopoulou-Panagiotopoulou S, Grubert F, Zaugg JB, Kundaje A, Liu Y, et al. Extensive variation in chromatin states across humans. *Science*. (2013) 342:750–2. doi: 10.1126/science.1242510
72. Kilpinen H, Waszak SM, Gschwind AR, Raghav SK, Witwicki RM, Orioli A, et al. Coordinated effects of sequence variation on DNA binding, chromatin structure, and transcription. *Science*. (2013) 342:744–7. doi: 10.1126/science.1242463
73. McVicker G, van de Geijn B, Degner JF, Cain CE, Banovich NE, Raj A, et al. Identification of genetic variants that affect histone modifications in human cells. *Science*. (2013) 342:747–9. doi: 10.1126/science.1242429
74. Gaffney DJ, Veyrieras JB, Degner JF, Pique-Regi R, Pai AA, Crawford GE, et al. Dissecting the regulatory architecture of gene expression QTLs. *Genome Biol*. (2012) 13:R7. doi: 10.1186/gb-2012-13-1-r7
75. Helgadottir A, Thorleifsson G, Manolescu A, Gretarsdottir S, Blondal T, Jonasdottir A, et al. A common variant on chromosome 9p21 affects the risk of myocardial infarction. *Science*. (2007) 316:1491–3. doi: 10.1126/science.1142842
76. Gaulton KJ, Nammo T, Pasquali L, Simon JM, Giresi PG, Fogarty MP, et al. A map of open chromatin in human pancreatic islets. *Nat Genet*. (2010) 42:255–9. doi: 10.1038/ng.530
77. Kasowski M, Grubert F, Heffelfinger C, Hariharan M, Asabere A, Waszak SM, et al. Variation in transcription factor binding among humans. *Science*. (2010) 328:232–5. doi: 10.1126/science.1183621
78. Cowper-Sal lari R, Zhang X, Wright JB, Bailey SD, Cole MD, Eeckhoute J, et al. Breast cancer risk-associated SNPs modulate the affinity of chromatin for FOXA1 and alter gene expression. *Nat Genet*. (2012) 44:1191–8. doi: 10.1038/ng.2416
79. Bauer DE, Kamran SC, Lessard S, Xu J, Fujiwara Y, Lin C, et al. An erythroid enhancer of BCL11A subject to genetic variation determines fetal hemoglobin level. *Science*. (2013) 342:253–7. doi: 10.1126/science.1242088
80. Bomsztyk K, Denisenko O, Ostrowski J. hnRNP K: one protein multiple processes. *Bioessays*. (2004) 26:629–38. doi: 10.1002/bies.20048
81. Leffers H, Dejgaard K, Celis JE. Characterisation of two major cellular poly(rC)-binding human proteins, each containing three K-homologous (KH) domains. *Eur J Biochem*. (1995) 230:447–53. doi: 10.1111/j.1432-1033.1995.tb20581.x
82. Tomonaga T, Levens D. Heterogeneous nuclear ribonucleoprotein K is a DNA-binding transactivator. *J Biol Chem*. (1995) 270:4875–81. doi: 10.1074/jbc.270.9.4875
83. Choi HS, Hwang CK, Song KY, Law PY, Wei LN, Loh HH. Poly(C)-binding proteins as transcriptional regulators of gene expression. *Biochem Biophys Res Commun*. (2009) 380:431–6. doi: 10.1016/j.bbrc.2009.01.136
84. Da Silva N, Bharti A, Shelley CS. hnRNP-K and Pur(alpha) act together to repress the transcriptional activity of the CD43 gene promoter. *Blood*. (2002) 100:3536–44. doi: 10.1182/blood.V100.10.3536
85. Michelotti GA, Michelotti EF, Pullner A, Duncan RC, Eick D, Levens D. Multiple single-stranded cis elements are associated with activated chromatin of the human c-myc gene *in vivo*. *Mol Cell Biol*. (1996) 16:2656–69. doi: 10.1128/MCB.16.6.2656
86. Braddock DT, Baber JL, Levens D, Clore GM. Molecular basis of sequence-specific single-stranded DNA recognition by KH domains: solution structure of a complex between hnRNP K KH3 and single-stranded DNA. *EMBO J*. (2002) 21:3476–85. doi: 10.1093/emboj/cdf352

Conflict of Interest Statement: The authors declare that the research was conducted in the absence of any commercial or financial relationships that could be construed as a potential conflict of interest.

Advantages of publishing in Frontiers

OPEN ACCESS
Articles are free to read for greatest visibility and readership

FAST PUBLICATION
Around 90 days from submission to decision

HIGH QUALITY PEER-REVIEW
Rigorous, collaborative, and constructive peer-review

TRANSPARENT PEER-REVIEW
Editors and reviewers acknowledged by name on published articles

Frontiers
Avenue du Tribunal-Fédéral 34
1005 Lausanne | Switzerland

Visit us: www.frontiersin.org
Contact us: info@frontiersin.org | +41 21 510 17 00

REPRODUCIBILITY OF RESEARCH
Support open data and methods to enhance research reproducibility

DIGITAL PUBLISHING
Articles designed for optimal readership across devices

FOLLOW US
@frontiersin

IMPACT METRICS
Advanced article metrics track visibility across digital media

EXTENSIVE PROMOTION
Marketing and promotion of impactful research

LOOP RESEARCH NETWORK
Our network increases your article's readership